# Defects and Boundaries in Quantum Field Theories

by

Jingxiang Wu

A thesis

presented to the University of Waterloo

in fulfillment of the

thesis requirement for the degree of

Doctor of Philosophy

in

Physics

Waterloo, Ontario, Canada, 2021

**Examining Committee Membership**

The following served on the Examining Committee for this thesis. The decision of the Examining Committee is by majority vote.

| | |
|---|---|
| Supervisor: | Davide Gaiotto<br>Perimeter Institute for Theoretical Physics |
| Co-supervisor: | Jaume Gomis<br>Perimeter Institute for Theoretical Physics |
| Committee Member: | Ben Webster<br>Department of Pure Mathematics, University of Waterloo |
| Committee Member: | Anton Burkov<br>Department of Physics and Astronomy, University of Waterloo |
| Internal/External Member: | Eduardo Martin-Martinez<br>Department of Applied Mathematics, University of Waterloo |
| External Examiner: | Paul Fendley<br>Peierls Centre for Theoretical Physics, University of Oxford |

## Author's declaration

This thesis consists of material all of which I authored or co-authored: see Statement of Contributions included in the thesis. This is a true copy of the thesis, including any required final revisions, as accepted by my examiners.

I understand that my thesis may be made electronically available to the public.

## Statement of Contributions

Chapter 2 and Chapter 3 of this thesis consist of material from the published paper [1], co-authored with Davide Gaiotto and Ji Hoon Lee.

Chapter 4 of this thesis consists of material from the published paper [2] co-authored with Davide Gaiotto, Ji Hoon Lee and Benoit Vicedo.

Chapter 5 of this thesis consists of material from the published paper [3] co-authored with Lorenzo Di Pietro, Davide Gaiotto and Edoardo Lauria.

**Abstract**

We discuss some aspects of defects and boundaries in quantum field theories (QFTs) and their applications in revealing non-perturbative aspects of QFTs in combination with other techniques, including integrability.

Firstly, we study the Kondo line defects that arise from local impurities chirally coupled to a two-dimensional conformal field theory. They have interesting defect Renormalization Group flows and integrability properties. We give a construction from four-dimensional Chern Simons theory whose two-dimensional compactification leads to a 2d CFT with Kondo line insertion. This construction will provide new perspectives into the surprising integrable properties of Kondo line defects.

Secondly, we study the ODE/IM correspondence, which states a surprising link between conformal field theories and the spectral problems of ordinary differential equations. A direct derivation of the correspondence is still unknown. We study a more refined description by directly relating the expectation values of a Kondo defect line and the generalized monodromy data of an ODE. Thanks to the 4d Chern Simons construction, we conjecture an explicit recipe for constructing the ODE corresponding to a Kondo defect. New examples we discuss include the isotropic/anisotropic Kondo defects in the multichannel $\prod_i SU(2)_{k_i}$ WZW models. We then extend the ODE/IM correspondence we find to the excited states, which provides a full solution to the spectral problems for the affine Gaudin model and the Kondo defects. In particular, by generalizing and applying techniques of exact WKB analysis, we derive the non-perturbative infra-red behaviours and wall-crossing properties of a large class of Kondo line defects.

Finally, we study the conformal boundary conditions of a four-dimensional Abelian gauge field. One starts by coupling a three-dimensional CFT with a $U(1)$ symmetry living on a boundary. This coupling gives rise to a continuous family of boundary conformal field theories (BCFT) parametrised by the gauge coupling $\tau$ in the upper-half plane and by the choice of the 3d CFT in the decoupling limit $\tau \to \infty$. The $SL(2,\mathbb{Z})$ electromagnetic transformations act on the BCFTs and relate different 3d CFTs in the various decoupling limits. We study the general properties of this BCFT and show how to express bulk one and two-point functions, and the hemisphere free-energy, in terms of the two-point functions of the boundary electric and magnetic currents. We propose a new computational scheme that can be used to approximate observables in strongly coupled 3d CFTs. As an example, we consider the 3d CFT to be one Dirac fermion and compute scaling dimensions of various boundary operators and the hemisphere free-energy up to two loops. Using an $S$-duality improved ansatz, we extrapolate the perturbative results and find good approximations to the observables of the $O(2)$ model.

**Acknowledgements**

First and foremost, I owe my deepest gratitude to my supervisor Davide Gaiotto. Through countless stimulating discussions and lectures, he has been very generous in sharing his deep insights and unique ways of thinking, which constantly motivates me to keep sharpening my understanding of physics. I cannot complete my studies without his efforts in providing a carefree atmosphere and his constant support and encouragement for me to push my boundary and pursue my interest. I truly appreciate his patience in teaching me how to do research and guiding me to where I am now.

Special thanks go to Lorenzo Di Pietro. I have been fortunate to have him as a mentor, a collaborator, and a friend. His patient guidance, enthusiasm, and perfectionism have been a critical source of inspiration throughout the entire duration of my Ph.D. studies.

I have benefited greatly from extended discussions and inspiring collaborations with Zohar Komargodski, Benoit Vicedo, and Edoardo Lauria, from whom I have learned so much. I also appreciate innumerable enlightening explanations and conversations with Kevin Costello and Jaume Gomis. I would also like to thank all of my committee memebers Davide Gaiotto, Jaume Gomis, Ben Webster, Anton Burkov, Eduardo Martin-Martinez and Paul Fendley for interesting discussions in numerous meetings and valuable comments on this thesis.

I would like to thank all of my friends and colleagues at Perimeter Institute especially Miroslav Rapcak, Junya Yagi, Lakshya Bhardwaj, Nafiz Ishtiaque, Dalimil Mazáč, Seyed Faroogh Moosavian, Alfredo Guevara, Yilber Fabian Bautista, Yehao Zhou, Yijian Zou, Shan-Ming Ruan, Qi Hu and many others for their kindness and never hesitating to lend a helping hand.

Finally, for their unwavering love and support for all my endeavors, I am grateful to my parents, my brother, and my girlfriend Guohua. Their care, trust, and encouragement make my life immensely rich and enjoyable while pursuing my passion.

# Table of Contents

**List of Figures** xiii

**List of Tables** xviii

**1 Introduction** 1

1.1 Integrable Kondo defect . . . 2
1.2 ODE/IM correspondence . . . 3
1.3 Abelian gauge theory at the boundary . . . 5
1.4 Structure of the thesis . . . 7

**2 Kondo line defect** 9

2.1 Introduction . . . 9
2.2 Generalities of integrable line defects . . . 13
2.2.1 Line defects in 2d CFTs . . . 13
2.2.2 Movable line defects . . . 13
2.2.3 Chiral line defects . . . 14
2.2.4 RG flow of chiral defects and wall-crossing . . . 17
2.2.5 Integrable line defects . . . 18
2.2.6 IR data and wallcrossing . . . 18
2.3 Chiral line defects in the Ising model . . . 19
2.3.1 Fusion relations, TBA, Hirota and full IR behaviour . . . 23

2.4 The $\mathfrak{su}(2)$ Kondo line defects . . . 25
2.4.1 A perturbative analysis of the Kondo defect vevs . . . 26
2.4.2 Perturbative and non-perturbative RG flows . . . 28
2.5 The 4d Chern-Simons construction . . . 31

**3 ODE/IM correspondence** **33**
3.1 Introduction . . . 33
3.2 Opers . . . 33
3.3 ODE/IM correspondence for Ising model . . . 40
3.4 The ODE/IM solution $SU(2)_k$ WZW . . . 43
3.5 Expected generalizations . . . 49
3.5.1 Multichannel Kondo problems . . . 49
3.5.2 Coset Kondo lines . . . 51
3.5.3 WZW vs Kac-Moody . . . 52

**4 Kondo defect, $\lambda$-oper and affine Gaudin model** **55**
4.1 Affine Gaudin models, classical and quantum . . . 55
4.2 Opers, $\lambda$-opers and affine opers . . . 59
4.2.1 $\mathfrak{sl}_2$ opers . . . 60
4.2.2 $\mathfrak{sl}_2$ $\lambda$-opers . . . 61
4.2.3 Miura opers and singularities of trivial monodromy . . . 62
4.2.4 Miura $\lambda$-opers and singularities of trivial monodromy . . . 63
4.2.5 Opers with singularities of trivial monodromy and Bethe equations 65
4.2.6 $\lambda$-Opers with singularities of trivial monodromy and affine Bethe equations . . . 66
4.2.7 Weyl reflections . . . 67
4.2.8 Conjectural count of Bethe solutions . . . 68
4.2.9 Special values of $\alpha_\pm$ . . . 68

4.2.10 WKB expansion and quasi-canonical form . . . 69
4.3 Bethe states and transfer matrices . . . 71
4.3.1 Some Kac-Moody conventions . . . 71
4.3.2 The Bethe equations and Bethe vectors . . . 72
4.3.3 Examples . . . 75
4.4 The UV expansion . . . 80
4.4.1 ODE/IM for primary fields . . . 82
4.4.2 The coset scaling limit . . . 84
4.5 The IR expansion . . . 85
4.5.1 Vacuum state $t(x) = 0$ . . . 86
4.5.2 $t(x) \neq 0$ . . . 91
4.5.3 Physical interpretation . . . 92
4.6 Some comments about the semiclassical limit . . . 94
4.7 Generalizations: $\mathfrak{sl}_3$ . . . 96
4.7.1 Basic Definitions . . . 96
4.7.2 Miura $\lambda$-opers and singularities of trivial monodromy . . . 99
4.7.3 $\lambda$-Opers with singularities of trivial monodromy and affine Bethe equations . . . 102
4.7.4 WKB expansion and quasi-canonical form . . . 103

**5 Conclusions and future directions** **108**

**6 Abelian gauge theory at the boundary** **112**
6.1 Boundary Conditions for 4d Abelian Gauge Field . . . 113
6.1.1 Free Boundary Conditions and $SL(2,\mathbb{Z})$ Action . . . 113
6.1.2 Two-point Function in the Free Theory . . . 116
6.1.3 Coupling to a CFT on the Boundary . . . 118
6.1.4 Boundary Propagator of the Photon . . . 120

6.1.5 Exploring Strong Coupling . . . 123
6.1.6 Two-point Function from the Boundary OPE . . . 126
6.1.7 One-point Functions from the Bulk OPE . . . 128
6.1.8 $c_{ij}(\tau, \bar{\tau})$ in Perturbation Theory . . . 130
6.1.9 Displacement Operator . . . 131
6.1.10 Three-Point Function $\langle \hat{V}_i \hat{V}_j \hat{D} \rangle$ . . . 133
6.2 Free Energy on a Hemisphere . . . 135
6.3 A Minimal Phase Transition . . . 138
6.3.1 Perturbative Calculation of Scaling Dimensions . . . 142
6.3.2 Perturbative $F_\partial$ . . . 145
6.3.3 Extrapolations to the $O(2)$ Model . . . 147
6.4 Other Examples . . . 150
6.4.1 $2N_f$ Dirac fermions at large $N_f$ . . . 150
6.4.2 Complex Scalar . . . 153
6.4.3 $QED_3$ with Two Flavors . . . 158
6.5 Conclusions and future directions . . . 162

**References** **164**

**APPENDICES** **183**

**A Conventions** **184**

**B Perturbative analysis of Ising line defect** **186**

**C Perturbative analysis of WZW line defects** **188**
C.1 Perturbative analysis of WZW line defects . . . 188
C.1.1 Definition of the quantum operator $\hat{T}_{\mathcal{R}}$ . . . 189
C.1.2 Computation of normal-ordered line operator . . . 190

C.1.3 Verification of the commutativity and Hirota relation . . . . . 192
C.1.4 Expectation values . . . . . 193
C.1.5 Beta function and effective coupling . . . . . 194
C.1.6 generalisation to multiple $su(2)$ . . . . . 194

**D WKB analysis** **197**
D.1 Exact solutions of the harmonic oscillator ODE . . . . . 197
D.2 WKB analysis . . . . . 198
D.2.1 WKB asymptotics . . . . . 198
D.2.2 Simple zeroes vs higher order zeroes . . . . . 200
D.2.3 Examples: . . . . . 202
D.2.4 WKB analysis for the WZW ODE/IM . . . . . 207
D.3 Perturbative solutions of ODE . . . . . 210
D.3.1 $SU(2)_k$ vacuum expectation value . . . . . 211
D.3.2 $SU(2)_k$ expectation value between primaries . . . . . 214
D.3.3 Multichannel expectation values . . . . . 216
D.4 Details of UV expansion for excited states . . . . . 220
D.4.1 Examples of UV perturbative matching . . . . . 220
D.4.2 A general perturbative prescription . . . . . 226
D.4.3 nonzero twist $\alpha_+ \neq 0$ . . . . . 228
D.5 WKB analysis . . . . . 229
D.5.1 General remarks and organizations . . . . . 229
D.5.2 Coordinate systems . . . . . 232
D.5.3 Recipe for evaluating Wronskians . . . . . 244
D.5.4 Numerical implementation . . . . . 244
D.5.5 Solutions near zeros and their Wronskians . . . . . 245
D.5.6 Examples: polynomial oper . . . . . 252
D.5.7 Example: chiral WZW . . . . . 258
D.6 Review of the standard ODE/IM correspondance . . . . . 262

**E Boundary QFT** **265**

E.1 Method of Images . . . . . 265

E.2 Defect OPE of $F_{\mu\nu}$ . . . . . 266

E.3 Bulk OPE Limit of $\langle F_{\mu\nu} F_{\rho\sigma} \rangle$ . . . . . 268

E.4 Current Two-Point Functions . . . . . 269

E.5 Calculation of $\langle \hat{V}_i \hat{V}_j \hat{D} \rangle$ . . . . . 272

E.6 Dimension of the Boundary Pseudo Stress Tensor . . . . . 274

E.7 Two-loop Integrals . . . . . 276

# List of Figures

2.1 IR fate of the deformed line defect $L_S[\theta]$ for different $\mathrm{Im}\,\theta$. . . . . 24

2.2 The RG flow pattern over the complex $g$ plane and the complex $1/g$ plane. The top two and he bottom two are plotted using the beta function (2.62) and (2.67) respectively. Note that the lower left figure is the same as Fig. 1 in [4] . . . . . 29

3.1 WKB diagram for the differential equation (3.36) defined in (3.42). Generic flow lines and WKB lines are colored blue and red respectively. . . . . 42

3.2 WKB diagram for $k = 1$ (left) and $k = 2$ (right). Generic flow lines and WKB lines are colored blue and red respectively. $\theta$ is chosen to be 0 and $-i\frac{\pi}{2}$ respectively. We number the WKB lines on large positve $x$ side increasingly from top. There are $k + 2$ WKB lines that are connected to the zero, numbered from $n_0$ to $n_0 + k + 1$. . . . . 48

4.1 Different types of opers: The middle dotted arrows are local gauge transformations by diagonal matrices. The right arrows correspond to working modulo gauge transformations by upper and lower triangular matrices of the form (4.27) and (4.30), respectively. The left arrow corresponds to working modulo gauge transformations by matrices of the form (4.56). . . . . 70

4.2 Blue curves are the Stokes diagram for $k = 3$ and $\vartheta = 0$. There are five special WKB lines connected to the zero of order $k = 3$. The rest of the special WKB lines connect to the negative infinity. Double headed arrows indicate which two solutions are used in the Wronskian $i(\psi_{n_1}, \psi_{n_2})$ with $n_2 - n_1 = n = 2j + 1$ in different scenarios. The lower (upper) end points to the special WKB lines associated to the small solution $\psi_{n_2}$ ($\psi_{n_1}$). Solid lines ($j = 1$) depict scenarios $0 \leq j \leq \frac{k}{2}$. Colors (black, green and red) of the lines indicate three scenarios as we shift $\mathrm{Im}\,\theta$: physical strip ($L_j$ flows to $\mathcal{L}_j$ ), sequence of transitions ($L_j$ flows to $L^{\mathrm{IR}}_{j-\frac{s}{2}} \otimes \mathcal{L}_{\frac{s}{2}}$, $s = 2j-1, \ldots, 1$) and $L^{\mathrm{IR}}_j$. Dashed lines ($j = 2$) depict scenarios $j > \frac{k}{2}$ respectively. Colors (black, green and red) of the lines indicate three scenarios as we shift $\mathrm{Im}\,\theta$: physical strip ($L_j$ flows to $\mathcal{L}_{k/2} \otimes L^{IR}_{j-k/2}$ ), sequence of transitions ($L_j$ flows to $L^{\mathrm{IR}}_{j-\frac{s}{2}} \otimes \mathcal{L}_{\frac{s}{2}}$, $s = k-1, \ldots, 1$) and $L^{\mathrm{IR}}_j$. The dotted burgundy line denotes the unique generic WKB line that gives rise to the local integrals of motion. 93

4.3 The three different types of (Miura) $\mathfrak{sl}_3$ $\lambda$-opers, labelled I, II and III, associated with the three nodes of the Dynkin diagram of $\widetilde{\mathfrak{sl}}_3$. They all share a common $\widetilde{\mathfrak{sl}}_3$ oper which describes the WKB momenta of the third order differential operator (4.134). . . . . 104

6.1 The family of conformal boundary conditions $B(\tau, \bar{\tau})$ labeled by the variable $\tau$ in the upper-half plane and by a 3d CFT $T_{0,1}$ with $U(1)$ global symmetry. At the cusp at infinity the current $\hat{I}^a$ decouples and we are left with the local 3d theory $T_{0,1}$ on the boundary, with $U(1)$ current $\hat{J}^a$. Approaching this cusp from $T$-translations of the fundamental domain amounts to adding a CS contact term to the 3d theory, or equivalently to redefine the current $\hat{J}^a$ by multiples of the current $\hat{I}^a$ that is decoupling. This is the $T$ operation on $T_{0,1}$ in the sense of [5]. In the favorable situation in which no phase transitions occur, the BCFT continuously interpolate to the cusps at the rational points of the real axis $\tau = -q/p$, where again the bulk and the boundary decouple and we find new 3d CFTs $T_{p,q}$. These theories are obtained from $T_{0,1}$ with a more general $SL(2, \mathbb{Z})$ transformation, that involves coupling the original $U(1)$ global symmetry to a 3d dynamical gauge field. . . . . 124

6.2 A cartoon of a possible phase transition at strong coupling. A scalar boundary operator becomes marginal at a certain curve in the $\tau$ plane, i.e. setting $\hat{\Delta}(\tau,\bar{\tau}) = 3$ we find solutions in the upper-half plane. In conformal perturbation theory from a point on the curve, the beta function takes the form (6.51). We might be unable to find real fixed points for the marginal coupling. In such a situation, $B(\tau,\bar{\tau})$ can only be defined as a complex BCFT. Assuming that we were able to define $B(\tau,\bar{\tau})$ as a real BCFT in perturbation theory around $\tau \to \infty$ by continuity such a real BCFT is ensured to exist in the full region above the wall, but we might be unable to continue it beyond the wall without introducing complex couplings (or breaking conformality). 125

6.3 Diagrams for the two-point function of the displacement operator. The leading order contribution $(a)$ is the square of the two-point function of the topological current $\hat{I}$. At next-to-leading order we have the diagrams $(b.1)$-$(b.2)$-$(b.3)$ that are also sensitive to the electric current $\hat{J}$. The shaded blobs denote insertions/correlators of $\hat{J}$ in the undeformed CFT. . . . . 132

6.4 The upper-half plane of the gauge coupling $\tau_{DN}$, i.e. in the duality frame in which at $\tau_{DN} \to \infty$ we find the $O(2)$ model on the boundary. Thanks to particle-vortex duality, the cusp in the origin $\tau_{DN} = 0$ also gives a decoupled $O(2)$ model on the boundary. Thanks to the boson-fermion duality between $U(1)_1$ coupled to a critical scalar and a free Dirac fermion, the cusps at $\tau_{DN} = \pm 1$ give a free Dirac fermion. . . . . 140

6.5 The upper-half plane of the gauge coupling $\tau = \tau_{NN'} - \frac{1}{2}$, i.e. in the duality frame in which at $\tau \to \infty$ we find a free Dirac fermion on the boundary. Thanks to fermionic particle-vortex duality, the cusp in the origin $\tau = 0$ also gives a free Dirac fermion on the boundary. Thanks to the boson-fermion duality between $U(1)_{\frac{1}{2}}$ coupled to a Dirac fermion and the $O(2)$ model, the cusps at $\tau = \pm\frac{1}{2}$ give the $O(2)$ model. . . . . 141

6.6 Feynman rules. $\Pi_{ab}$ is defined in (6.46). . . . . 144

6.7 Feynman rules for the zero-momentum insertions of the composite operators. Note that there are two vertices associated to $O_2$. . . . . 144

6.8 One loop and two loops diagrams. We sum over all possible insertions of the composite operators on the internal fermion lines, and also on vertices in the case of $O_2$. . . . . 145

6.9 Leading corrections to the boundary current two-point function for the Dirac fermion. . . . . 146

6.10 Extrapolations of the scaling dimensions from the Dirac fermion point ($\tan^{-1}(g_s) = 0$) to the $O(2)$ point ($\tan^{-1}(g_s) = \pi/2$). . . . . 150

6.11 Extrapolations of the free energy from the Dirac fermion point ($\tan^{-1}(g_s) = 0$) to the $O(2)$ point ($\tan^{-1}(g_s) = \pi/2$). . . . . 151

6.12 The diagrams that contribute to the boundary propagator of the photon in the limit $N_f \to \infty$ with $\lambda = g^2 N_f$ fixed. . . . . 151

6.13 Feynman rules with the complex scalar on the boundary . . . . . 155

6.14 One loop diagrams that contribute to the wave-function renormalization. . 155

6.15 Diagrams contributing to $\mathcal{O}(g^6)$ in $\beta_\rho$. . . . . 156

6.16 Diagrams contributing to $\mathcal{O}(\rho^2)$ and $\mathcal{O}(\rho g^2)$ in $\beta_\rho$. . . . . 156

6.17 One loop and two loops diagrams . . . . . 157

D.1 WKB diagram for the differential equation (D.28). Generic flow lines and WKB lines are colored blue and red respectively. . . . . 203

D.2 WKB diagram for the differential equation (D.48). Generic flow lines and WKB lines are colored blue and red respectively.On the left, $E > 0$ and there are three simple zeros. On the right, $E = 0$ and there are one simple zero and one second order zero. . . . . 206

D.3 The Stokes diagrams in the local coordinate system around the simple zero and the double zero. The numbers close to the origin label the numbering for the nice local solutions $A_i(y)$ we use in this section, whereas $\psi_\bullet$ label the corresponding small solutions. . . . . 241

D.4 Numerical and analytic evaluation in the local coordinate system around a cubic zero defined at the beginning of Subsection D.5.5. Parameters used are chosen in a rather generic way: $\hbar = \frac{1}{5}$, $a = -\frac{4}{21}$, $b = \frac{1}{2}$. (Top) Various approximate evaluations of $A_{3,0}(y)$. Approximation gets better with higher corrections included. (Bottom) $\Delta_{\text{error}} \equiv \frac{\partial_x^2 \psi(x)}{\psi(x)} - \frac{1}{\hbar^2} P(x)$. We don't show the $\Delta_{\text{error}}$ for the WKB asymptotic solution since the error is too big. The legend of coloring is shared in both diagrams. . . . . 251

D.5 Numerical error $\Delta_{\text{error}} \equiv \frac{\partial_x^2 \psi(x)}{\psi(x)} - \frac{1}{\hbar^2} P(x)$. (Left) $P(x) = x^2 - 2$ and $\hbar = 1$ (Right) $P(x) = x^3 - x^2$ and $\hbar = 1$. This is just to illustrate numerical error is indeed very small. . . . . 254

D.6 Stokes diagram for (Left) $P(x) = x^2 - 2a$, (Right) $P(x) = x^3 - x^2$. . . . . 255

D.7 Evaluations of the Wronskian $i(\psi_{-1}, \psi_2)$. The red dots are the numerical result. The blue line and the red line are the analytic prediction from the local coordinate system around the double zero up to $\hbar^{-1}$ and $\hbar$ order respectively given in (D.249). . . . . 257

D.8 Stokes diagram for $P(x) = e^{2x}$, which corresponds to $SU(2)_0$ trivial theory. There are infinite number of special WKB lines depicted as red paralell lines. 259

D.9 In the top figure, $g$ is assumed to be a some order 1 constant, independent of $\theta$. $x_{-\infty}(\theta)$ is farther away from $-\frac{1}{g}$ as $\theta \to \infty$. $\delta$ is the local variation around $x_{-\infty}(\theta)$ that is complex. So it doesn't have to be on the real axis. In the bottom figures, the red line is an example of $g_{\text{eff}}$ discussed in this section, namely an example of circular RG flow. . . . . 261

E.1 The two-point function of the boundary current $\hat{J}$. The shaded blob represents the one-photon irreducible two-point function $\Sigma(p)$, by which we mean the sum of all the diagrams that cannot be disconnected by cutting a photon line. The full two-point function can be obtained in terms of $\Sigma$, via the geometric sum shown in the figure. . . . . 269

E.2 Relations between the two-point functions involving the current $V_2$ and the two-point function $\langle JJ \rangle$. The relation in the second line is only true up to a contact term. . . . . 270

# List of Tables

6.1 Comparison of the extrapolations with the known data: for the energy operator we are quoting the value from the conformal bootstrap [6], and from the $\epsilon$-expansion [7]. For the sphere free energy we are comparing to the value from the $\epsilon$-expansion in [8]. . . . . 149

# Chapter 1

# Introduction

Quantum field theory (QFT) is a theoretical framework used in almost every discipline of modern physics. In contrast to its importance and ubiquitousness, there is still no canonical and rigorous formulation of what QFT is. Perturbative quantum field theory is arguably the best-understood corner and, despite its great effectiveness, has fundamental limitations: in many physical systems, the important regimes are often non-perturbative, where perturbation theory breaks down. On top of that, perturbative QFT is mostly concerned with what one might colloquially referred to as *local* information, e.g. local operators and their Operator Product Expansion whereas studies in the past decades indicate *global* information is very essential and must be built into a QFT from the very beginning. Notable examples are generalized global symmetries, the global part of the gauge group in gauge theories and the global structure of the spacetime, etc. As they are often hard to access with conventional perturbation theory, we do not yet know a complete list of the information required to define a quantum field theory in general.

One can probe the global aspects of a quantum field theory (QFT) by introducing extended operators like boundaries and defects of various codimensions. Among them, topological defects are the best understood class. In the topological field theories where local degrees of freedoms are trivial, they are the most natural observables and can often be rigorously studied. Notably, their importance in non-topological QFTs is gradually being recognized. For example, invertible topological defects of various dimensions encode the (generalized) global symmetry [9] of the QFTs, and more general topological defects have also been shown to carry properties of category symmetry.

In this thesis, we are mostly interested in the more general defects/boundaries that are *not* topological. In the first part, we will study a class of non-topological line defects called

Kondo line defects. They have the surprising property of being integrable. In the second part, we will study conformal boundary conditions of the four-dimensional free Abelian gauge theories. Despite the fact that the bulk theory is free, we will see its (conformal) boundary conditions are very rich.

## 1.1 Integrable Kondo defect

One of the objectives of this thesis is to study Kondo line defects in two-dimensional conformal field theories (CFT). Physically, Kondo line defects arise from the Kondo model, which was invented to describe a single magnetic impurity in a condensed matter system and now has become a prototypical example of quantum impurity [10, 11, 12, 13, 14, 15, 16]. See e.g. [17, 18] for a detailed account of the historical developments and further references. In the language of quantum field theory (e.g. [19, 20, 21, 22, 23]), such a local impurity coupled to the bulk defines a line defect. Bachas and Gaberdiel [24] showed such a line defect on the quantum level needs a careful renormalization. They studied a particular example where the bulk CFT is $SU(2)_k$ WZW model and found an asymptotically free defect Renormalization Group flow. The renormalized Kondo defect has some nice properties: (1) it is translation invariant along the defect. (2) it is rigid translation invariant perpendicular to the defect. (3) it is invariant under the global symmetry $SU(2)$. (4) it commutes with the entire antichiral sector of $SU(2)_k$ WZW model. The regularization recipe in [24] can be generalized to more general cases in a straightforward way.

More generally, the Kondo line defects that we will consider in this thesis belong to a large class of *chiral* line defects where the impurity is only coupled to the chiral degrees of freedom of the bulk CFT, and more specifically only to the chiral currents in the case of the Kondo line defect. Therefore throughout this thesis, we will only specify the chiral half of the bulk CFT since the Kondo defects are transparent to the anti-chiral sector.

What makes Kondo line defects interesting is that they are expected to be *integrable* in the sense that they give rise to an infinite number of commuting conserved charges. Translation invariance of the line defect in the direction transverse to the defect [25] leads to conserved charges. In particular, a Kondo defect wrapping the spatial circle will commute with the Hamiltonian and define a continuous family of conserved charges, labelled by the RG flow scale. A surprising observation is that in many important examples these conserved charges will commute with each other, which is sometimes referred to as the integrability structure of the underlying CFT [26, 27, 28]. One may trace the origin of the integrability back to the fact that the Kondo impurity model is known to be integrable from the early days of the Kondo model [12, 13, 14, 15, 16, 17]. One advantage of using the line

defect language is that we can succinctly encode the integrability by the commutativity of different Kondo line defects. In many situations, integrability comes with rich extra structures such as Yangian symmetry, Hirota recursion relations, Thermodynamic Bethe Ansatz equations, and more.

Like in most integrable systems, integrability is far from obvious. The requirement of commutativity is highly over-constrained, so the existence of solutions is quite surprising. In this thesis, we will perform an explicit and tedious calculation to verify the commutativity of the Kondo line defects at the first few orders of the perturbation theory in the ultraviolet. However, in general, it is a long-lasting question to understand why there exist integrable systems and how we can construct new integrable systems. In particular, one of the unique features of the integrability is the existence of the spectral parameter, which begs for a unified understanding.

Questions along these lines have been partly answered. Recently, a four-dimensional version of Chern-Simons theory has emerged as a general organizing principle for many integrable problems [29, 30, 31, 32, 33, 34, 35, 36], including integrable field theories. This thesis is part of a multi-pronged exploration of that construction. We will construct the Kondo models in the 4d Chern Simons setup, where the Kondo defects are realized by Wilson lines. The construction of Kondo problems in 4d Chern-Simons theory predicts the existence of a broad class of integrable defect Renormalization Group (RG) flow in the space of couplings for any irrep which can be extended to a representation of the Yangian for $\mathfrak{g}$. Many surprising properties including the commutativity of the Kondo lines can be readily understood.

## 1.2 ODE/IM correspondence

The emergence of the integrability structure is accompanied by other unexpected relations such as the ODE/IM correspondence [37, 38], which refers to the mysterious link[1] between two setups that don't appear to be related in a physical way: conformal field theories and ordinary differential equations in the complex domain. In the standard formulation [37, 38, 39, 40], the statement roughly goes as follows. One can arrive at the same set of functional relations from both setups: one from the transfer matrices $\mathbf{T}$ and Baxter $\mathbf{Q}$ operators associated to a conformal field theory defined in [41, 42, 43], the other one from the spectral determinants of an ordinary differential equation. We emphasize that this ODE is not derived from the CFT, e.g as some version of the equation of motion. In

[1] We will review the original formulation in the appendix D.6.

fact, to our knowledge, a direct derivation of such a differential equation from a conformal field theory is lacking. As a result, all examples we know for now are found in a seashell-collecting style. See e.g. the review [44] for a summary of the historical development and a list of known examples. One of the objectives of this thesis is to explore this surprising coincidence, propose a recipe for constructing new examples, and take some steps towards finding a derivation of the ODE/IM correspondence.

One nice way to organize various spectral determinants of an ODE is to view them as generalized monodromy data. The ODEs in question will have singularities of a prescribed nature. Monodromies of the solutions will encode how we can parallel transport the solutions around singularities. There will also be irregular singularities with the Stokes phenomenon. In general, we will refer to the collection of monodromies, Stokes matrices and other transport coefficients as generalized monodromy data, which typically takes the form of Wronskians. We then propose the following more refined statement of ODE/IM correspondence[2]: for a given Kondo line defect, its vacuum expectation values (VEV) will be exactly given by generalized monodromy data of the corresponding ODE written in terms of Wronskians. This proposal will be checked explicitly in numerous examples.

This concrete physical interpretation of ODE/IM correspondence using Kondo defects allows us to make contact with 4d Chern Simons. It is then natural to ask whether it is possible to derive the ODE/IM correspondence by using the 4d Chern Simons construction of the Kondo model. We will see this is indeed very promising by providing some strong evidence. For example, we will see the central ingredient in the 4d Chern Simons construction, i.e. the meromorphic one form, actually canonically determine an ODE, which in the known examples, exactly coincide with the ones in the literature.

To complete the dictionary, we would like to see if the expectation value for other states, apart from the VEV, of the Kondo defect can be mapped to the generalized monodromy data of certain ODEs. It was first pointed out in [39, 40] that the expectation values for the excited states needs a different ODE, which can be found by slightly modifying the ODE for the vacuum state. More precisely, one needs to add regular singularities of trivial monodromy without changing the asymptotic structures. It turns out to do this systematically is not an easy task since the problem is over-constrained. Fortunately, this has been (at least partially) understood by mathematicians in the studies of (affine) oper. This is because these ODEs are globally defined on a Riemann surface, which formally speaking, belong to a mathematical structure called *oper*. We will see how the theory of opers fits nicely into the story and how it leads to the proposal of the ODEs for excited states.

[2]Earlier proposal in a similar style can also be found in [45]

One can find numerous applications of the ODE/IM correspondence in the line defect interpretation. One of the most important questions in the studies of Kondo line defects is to figure out the properties of the line defects at the infrared fixed points. It is a hard question from the perspective of the ultraviolet as the infrared is strongly coupled. Sometimes when a large $k$ limit can be taken, the infrared fixed point can be brought to be perturbative and observables can be computed in the $\frac{1}{k}$ expansion. In general, one has to resort to numerical methods. In this thesis, we will see how integrability, especially ODE/IM correspondence, can help us analytically compute observables in the strongly coupled region and determine the infrared phase diagram. Interestingly, we find infrared line defects exhibit delicate wall-crossing behaviours.

## 1.3 Abelian gauge theory at the boundary

Another objective of this thesis is to study conformal invariant boundary conditions for free Abelian gauge theory in four dimensions. A striking property of these boundary conformal field theories (BCFTs) is that they are typically well-defined on some open patch in the space of the four-dimensional gauge coupling.

The simplest way to produce such boundary conditions is to couple the four-dimensional gauge fields to a three-dimensional CFT with a $U(1)$ global symmetry. This is sometimes called a "modified Neumann" boundary condition [46]. Assuming that certain mild conditions are satisfied, one obtains a BCFT which is well-defined as long as the four-dimensional gauge coupling is sufficiently small [47, 48, 49, 50, 51, 52, 53]. The conformal data of the BCFT can be computed from the data of the original CFT by perturbation theory in the four-dimensional gauge coupling.

Conversely, there is a general expectation that any BCFT $B$ defined at arbitrarily small 4d gauge coupling will be either a Dirichlet boundary condition or a modified Neumann boundary condition associated with some 3d CFT $T_\infty[B]$ with a $U(1)$ symmetry. Because of electric-magnetic duality, the same statement applies to any other "cusp" $C$ in the space of the complexified gauge coupling, where some dual description of the four-dimensional gauge field becomes arbitrarily weakly coupled. If the BCFT $B$ is defined around the cusp $C$, we can associate to it another 3d CFT $T_C[B]$, which is obtained from $T_\infty[B]$ by applying the $SL(2,\mathbb{Z})$ transformation [5] that maps the cusp at infinity to $C$. Therefore, the theories living at the other cusps can be thought of as 3d Abelian gauge theories obtained by gauging the $U(1)$ global symmetry of $T_\infty[B]$.

In the absence of phase transitions, a given BCFT $B$ can be defined on the whole space of 4d gauge couplings and is thus associated to an infinite family $T_*[B]$ of 3d CFTs. The

conformal data of the BCFT will admit a similar collection of perturbative expansions in the neighbourhood of each cusp.

We start the section by studying the general properties of this family of BCFT's. A universal feature is the presence in the spectrum of boundary operators of two conserved $U(1)$ currents, the electric and the magnetic currents, that arise as a consequence of the electric and magnetic one-form symmetries in the bulk [9]. The endpoints of bulk line operators carry charge under this $U(1) \times U(1)$ symmetry, while all the local boundary operators are neutral. By matching the bulk and boundary OPE expansions of correlators of the bulk field strength, we show that several BCFT observables –including non-local ones such as the free-energy on a hemisphere background– can be obtained in terms of the coefficients $c_{ij}$ in the two-point correlators of these currents, and of the coefficient $C_{\hat{D}}$ of the two-point function of the displacement operator. The latter relations hold for any $\tau$, provided $B$ exists. We also show that the leading perturbative corrections to $c_{ij}$ and $C_{\hat{D}}$ around a cusp are captured universally in terms of the two-point function of the $U(1)$ current of the 3d CFT living at the cusp, in the decoupling limit.

We then turn these abstract considerations into a very concrete computational strategy: if some $T_C$ is simple enough for perturbative computations to be feasible, we may study the properties of other $T_*$ theories by re-summing the perturbation theory. If we happen to know, or conjecture, that there are two cusps $C$ and $C'$ such that $T_C$ and $T_{C'}$ are both simple, we may be able to implement an enhanced re-summation which uses both pieces of data to predict the properties of the other $T_*$ theories.

This approach gives a new approximation scheme, orthogonal to previously known perturbative approaches to 3d Abelian gauge theories such as the $\epsilon$-expansion [54, 55, 56, 57, 58, 59, 60, 61] or the large-$N$ expansion (see e.g. [62, 63, 64, 65, 66, 67, 68] for recent results and the review [69]). We will apply this strategy to a very nice boundary condition for a $U(1)$ gauge theory, which is conjecturally associated with a free Dirac fermion at two distinct cusps and to the $O(2)$ model at two other cusps [70, 71, 72, 73, 74]. The fact that these theories appear at the cusps can be seen as a consequence of the recently discovered 3d dualities [70, 75, 76], and it entails the existence of a $\mathbb{Z}_2$ action on $\tau$ that leaves $B(\tau, \bar{\tau})$ invariant. We will do a two-loop calculation at the free-fermion cusp and then extrapolate to the $O(2)$ cusp, finding good agreement with the known data of the $O(2)$ model.

We also consider other applications: Taking the boundary degrees of freedom to be an even number $2N_f$ of free Dirac fermions, setting the gauge coupling to $g^2 = \lambda/N_f$ and taking $N_f$ to infinity with $\lambda$ fixed, we argue that the theory admits a $1/N_f$-expansion, which interpolates between the free theory at $\lambda = 0$ and large-$N_f$ $\text{QED}_3$ at $\lambda = \infty$. The exact $\lambda$ dependence can be easily obtained order-by-order in the $1/N_f$ expansion. Applying the

general strategy to compute the hemisphere partition function to this case, and taking the limit $\lambda \to \infty$, we obtain the $1/N_f$ correction to the sphere partition function of large-$N_f$ $\text{QED}_3$. Another example with a $\mathbb{Z}_2$ duality acting on $\tau$ is conjecturally obtained in the case where the theory on the boundary is a free complex scalar, or equivalently the $U(1)$ Gross-Neveu model [77, 78]. We consider perturbation theory around the free-scalar cusp and show the existence of a stable fixed point for the classically marginal sextic coupling on the boundary at large $\tau$. We also discuss an example with two bulk gauge fields coupled to two distinct Dirac fermions on the boundary. We show how to obtain $\text{QED}_3$ with 2 fermionic flavors starting with this setup, using the extended electric-magnetic duality group $Sp(4,\mathbb{Z})$ that acts on the two bulk gauge fields.

## 1.4 Structure of the thesis

In chapter 2, we will first review the necessary background on the line defect in two-dimensional quantum field theory and summarize the main properties of chiral defects. Then we perform explicit calculations of the Kondo line defect to verify its integrable properties and other novel feature in 2d CFT, with a particular focus on the Ising model and $SU(2)_k$ WZW model. We give a construction of the Kondo line defect in the four-dimensional Chern Simons theory, with which the surprising properties of the Kondo defect will be manifest. In chapter 3, we give an interpretation of ODE/IM correspondence in terms of Kondo line defects and describe some novel applications of the ODE/IM correspondence.

In chapter 4, we will begin with a quick review of the affine Gaudin model in Section 4.1. We then define $\lambda$-opers with singularities of trivial monodromy and derive the affine Bethe equations in Section 4.2. We analyze the Stokes data at large and small $\lambda$ in Sections 4.4 and 4.5, respectively, and compare it with direct calculations for the Kondo defects. In the large $\lambda$ regime, the Stokes data are obtained with the help of (exact) WKB analysis [79, 80, 81, 82, 83, 84, 85, 86, 87, 88, 89]. The examples under study have some unusual features that require us to generalize the standard WKB analysis in order to evaluate the complete collection of the Stokes data. In order not to clutter the main body, we will only quote the results in Section 4.5 while leaving the detailed review of the WKB analysis and our generalizations in the Appendix D.5.

We will also see that the construction automatically includes integrable defects in coset models $\frac{\prod_i \widehat{\mathfrak{g}}_{k_i}}{\widehat{\mathfrak{g}}_{\sum_i k_i}}$. We discuss briefly some alternative semiclassical limits in Section 4.6. Although we focus on $SU(2)$ examples in the main body of this work, we expect the results to extend to general affine ADE Lie algebras and will comment on that in Section 4.7.

In chapter 5, we will conclude the first part of the thesis and summarize the main findings and future directions.

In chapter 6, we start in section 6.1 by reviewing the non-interacting boundary conditions for a Maxwell field in four dimensions. We then define the family of interacting boundary conditions $B(\tau, \bar{\tau})$. We derive the general relations that we described above for the bulk two- and three-point functions of the field strength and obtain the leading corrections in perturbation theory around the cusps in the $\tau$ plane. In section 6.2 we obtain similar results for a different observable, the hemisphere partition function of $B(\tau, \bar{\tau})$. In particular, we show how to recover the $S^3$ partition function for the 3d CFTs in the decoupling limit. In section 6.3 we put this machinery at work in the example of the boundary condition defined by the $O(2)$ model / a free Dirac fermion. Section 6.4 contains the other applications that we consider: large-$N_f$ fermions, a complex scalar, and two bulk gauge fields coupled to two Dirac fermions. We conclude in section 6.5 by discussing some future directions. Several appendices include the details of calculations, and some supplementary material, e.g. a calculation of the anomalous dimension of the boundary stress-tensor using multiplet recombination in appendix E.6, and an explanation of the technique that we used to evaluate the two-loop integrals in appendix E.7.

# Chapter 2

# Kondo line defect

## 2.1 Introduction

A *chiral line defect* in a 2d CFT is a line defect $L$ which is invariant under translations along the direction of the defect and transparent to the anti-holomorphic part $\bar{T}$ of the stress tensor. All line defects in a chiral CFT are obviously chiral. Deformations of topological line defects by chiral operators also give rise to chiral defects.

In particular, we are interested in a particular class of chiral defects which we will refer to as the Kondo defect. The most basic example comes from the studies of magnetic impurities in condensed matter systems, which we now review.

#### The $\mathfrak{su}(2)_1$ Kondo problem

The prototypical example of a Kondo defect comes from a single qubit impurity coupled to a doublet of chiral complex fermions by an $SU(2)$ invariant local coupling

$$g\,\vec{S}\cdot\vec{J}(t,0) \tag{2.1}$$

Here $\vec{S}$ are the Pauli matrices acting on the qubit impurity and

$$\vec{J}(t,0)\equiv\psi^{\dagger}(t,0)\vec{\sigma}\psi(t,0) \tag{2.2}$$

are the $\mathfrak{su}(2)_1$ WZW currents built out of the complex fermions.

This model provides one of the simplest, best-studied examples of (defect) RG flow. The perturbative coupling $g$ is classically marginal and is marginally relevant for $g > 0$. The deformation thus defines a UV-complete line defect $L_{\frac{1}{2}}[\theta]$ in the chiral CFT, equipped with a dynamically generated non-perturbative scale $\mu \equiv e^{\theta}$ which breaks scale invariance. The IR endpoint of the RG flow is conjecturally known [22, 90]: it is the non-trivial topological defect $\mathcal{L}_{\frac{1}{2}}$ whose Cardy label is the spin $\frac{1}{2}$ primary in the WZW model.

We can define operators $\hat{T}[\theta]$ by Wick-rotating the line defects $L[\theta]$ to wrap a space circle of unit radius. Almost by construction, the $\hat{T}[\theta]$ are operators acting on the Hilbert space of the CFT which commutes with the Hamiltonian. They are renormalized path-ordered exponentials of the chiral currents $\vec{J}$, which were computed at the first few orders of perturbation theory in [90].

The basic integrability claim is that they commute with each other:

$$\left[\hat{T}[\theta], \hat{T}[\theta']\right] = 0 \tag{2.3}$$

We actually expect a stronger statement to be true. Consider Kondo defects of spin $j$ in the same CFT. These are defined in the same manner as the basic Kondo defect, except that $\vec{S}$ are taken to be $\mathfrak{su}(2)$ generators acting on a spin $j$ irreducible representation. Global $SU(2)$ invariance ensures that renormalization can only affect the overall coupling $g$, which is again marginally relevant (when positive) and gives rise to a family of line defects $L_j[\theta]$. Conjecturally, the RG flow ends on IR free line defects, defined as spin $j - \frac{1}{2}$ Kondo defects with negative coupling.

Define "transfer matrix" operators $\hat{T}_j[\theta]$ as above. Then we claim that

$$\left[\hat{T}_j[\theta], \hat{T}_{j'}[\theta']\right] = 0 \tag{2.4}$$

and that in an appropriate renormalization scheme (See Appendix C.1.3,) a Hirota fusion-like relation holds true:[91, 92] (See also the review article [93] and references therein for a more modern exposition.)

$$\hat{T}_j\left[\theta + \frac{i\pi}{2}\right]\hat{T}_j\left[\theta - \frac{i\pi}{2}\right] = 1 + \hat{T}_{j-\frac{1}{2}}[\theta]\hat{T}_{j+\frac{1}{2}}[\theta] \tag{2.5}$$

Combined with general physical considerations, the Hirota relations lead to a TBA framework to compute the $\hat{T}_j[\theta]$ eigenvalues, which is the "conformal limit" of the one for the chiral Gross-Neveu model (See e.g. [94] for a review of the TBA framework).

The Hirota relations also lead us to simple ODE/IM relation[1]: the expectation values of $\hat{T}_j[\theta]$ on a spin $l$ primary state match the transport data for the second order differential equation

$$\partial_x^2 \psi(x) = \left[ e^{2\theta}(1+gx)e^{2x} + \frac{l(l+1)g^2}{(1+gx)^2} \right] \psi(x) \tag{2.6}$$

for $\mathfrak{su}(2)_1$ and a simple modification for twisted sectors and higher WZW levels. We discuss this model in detail in Section 2.4, leaving a full description of the excited state ODE/IM for a separate publication [2].

### Multichannel $\mathfrak{su}(2)$ Kondo problem and generalizations

We can generalize the basic Kondo problem by coupling the impurity to multiple copies of the chiral fermion theory, with a coupling

$$\vec{S} \cdot \sum_i g_i \vec{J}^{(i)}(t,0) \tag{2.7}$$

involving $n$ decoupled $\mathfrak{su}(2)_1$ WZW currents built out of the complex fermions [2].

The RG flow is now potentially much richer, as it takes place in an $n$-dimensional space of couplings. Four-dimensional Chern-Simons considerations suggest an important simplifying feature: in an appropriate RG scheme, the RG flow should preserve the differences $g_i^{-1} - g_j^{-1}$ between the inverse couplings. If we set, say,

$$g_i^{-1} = g^{-1} + z_i, \tag{2.8}$$

say with $\sum_i z_i = 0$, then the RG flow should only change the overall coupling $g$ [3] and the $z_i$ should label RG flow trajectories. We will test this conjecture at the first few orders in perturbation theory.

Furthermore, we conjecture the following integrability relation:

$$\left[ \hat{T}[\theta; z_i], \hat{T}[\theta'; z_i] \right] = 0 \tag{2.9}$$

[1] The vacuum module at $k = 1$ and other related ODEs have been proposed and studied in [95, 96, 97, 98, 99, 100, 101]

[2] If any $k$ couplings coincide, say $g_i = g_{i+1} = \cdots = g_{i+k-1}$, the defect only couples to the diagonal $\mathfrak{su}(2)_k$ WZW current $J^{(i)} + J^{(i+1)} + \cdots J^{(i+k-1)}$. That means this setup includes as a special case the coupling of an impurity to any collection of $\mathfrak{su}(2)_{k_i}$ WZW currents.

[3] This is compatible with the fact that the RG flow must fix the loci $g_i = g_j$, see the previous footnote

which should only hold for line defects in the *same* RG flow trajectory.

We also conjecture that with appropriate labeling of RG trajectories, higher spin impurities will give other commuting transfer matrices $\hat{T}_j[\theta; z_i]$, still satisfying Hirota relations. We will formulate an ODE/IM statement involving the transport data for the second order differential equation

$$\partial_x^2\psi(x) = \left[e^{2\theta}e^{2x}\prod_i(1+g_ix) + \sum_i \frac{l_i(l_i+1)g_i^2}{(1+g_ix)^2} + \sum_{i<j}\frac{2l_il_jg_ig_j}{(1+g_ix)(1+g_jx)}\right]\psi(x) \tag{2.10}$$

for $\prod_i \mathfrak{su}(2)_1$.

We discuss this model in detail in Section 3.5.1.

The ideas of this work can be extended to a wide variety of integrable Kondo problems associated with the four-dimensional Chern-Simons theory. In Section 3.5.2 we look briefly at another well studied example [102], involving integrable deformations of topological line defects in $\frac{\prod_i \mathfrak{su}(2)_{k_i}}{\mathfrak{su}(2)_{\sum_i k_i}}$ coset models, such as Virasoro minimal models.

The corresponding conjectural ODE is a polynomial potential:

$$\partial_x^2\psi(x) = \left[e^{2\theta}\prod_i(x-z_i)^{k_i} + \sum_i \frac{l_i(l_i+1)}{(x-z_i)^2} + \sum_{i<j}\frac{2l_il_j}{(x-z_i)(x-z_j)}\right]\psi(x) \tag{2.11}$$

with RG flow acting as a common rescaling of the $z_i$.

We also briefly comment on further extensions along the direction of the integrable CFTs discussed in [33] and to transfer matrices for integrable deformations of these CFTs. For recent studies of polynomial potentials along the directions of this work, see e.g. [103].

For simplicity, we only discuss models associated with the $SU(2)$ group. Broad generalizations to other groups $G$ are possible and mostly straightforward. The biggest subtlety is that the space of endomorphisms of an irreducible representation may contain multiple copies of the adjoint representation, so that the RG flow may deform $\vec{S}$ away from the generators of the Lie algebra $\mathfrak{g}$ for $G$ even if we impose global $G$ invariance.

4d Chern-Simons theory constructions predict the existence of a specific integrable RG trajectory in the space of couplings for any irrep which can be extended to a representation of the Yangian for $\mathfrak{g}$. It would be very interesting to see how such a restriction arises in the Kondo problem, at least perturbatively.

## 2.2 Generalities of integrable line defects

### 2.2.1 Line defects in 2d CFTs

Let's consider a translation invariant line defect at some point in space, say $x^1 = 0$ and extending along the direction of $x^0$. The translation invariance along $x^0$ direction implies the following energy conservation relation, which controls the discontinuity in energy flux across the defect, is satisfied

$$\left[T - \bar{T}\right]_{x^1=0^+} - \left[T - \bar{T}\right]_{x^1=0^-} = 2i\partial_{x^0} t^{00} \tag{2.12}$$

where $t^{00}$ is the defect stress tensor. Notice that all four summands on the left hand side of the equation are well-defined defect local operators.

The defect would be conformal invariant if and only if $t^{00} = 0$. We are interested in defects that are *not* conformal invariant.

If we act with a more general bulk conformal transformation fixing the $x^1 = 0$ location of the defect, the line defect will thus change. Infinitesimally, the deformation under a conformal transformation which restricts to a vector field $v^0(x^0)$ along the defect is given by the boundary action

$$\int t^{00}\partial_0 v^0 dx^0 \tag{2.13}$$

In particular, $t^{00}$ can be added to the defect action to implement an infinitesimal scaling transformation.

A global rescaling by a factor of $e^\theta$ will map $L$ to a new chiral line defect $L[\theta]$. Shifts of $\theta$ in the positive real direction correspond to the RG flow of the line defect. More general conformal transformations will lead to a line defect with a position-dependent $\theta$ parameter.

### 2.2.2 Movable line defects

It is also possible to consider defects whose correlation functions are invariant under rigid translations in a direction transverse to the line defect. In terms of the bulk stress tensor, this means that

$$\left[T + \bar{T}\right]_{x^1=0^+} - \left[T + \bar{T}\right]_{x^1=0^-} = 2\partial_{x^0} \tilde{t}^{00} \tag{2.14}$$

for some defect operator $\tilde{t}^{00}$. In other words, the "displacement operator" is a total derivative.

This is automatically true for translation-invariant line defects in a chiral CFT, where $\tilde{t}^{00}$ is proportional to $it^{00}$, as we explain in the next section.

Now we can consider an infinitesimal conformal transformation which changes the location of the defect, followed by a displacement back to the original $x^1 = 0$ location. The result is a deformation

$$\int \left[t^{00}\partial_0 v^0 + \tilde{t}^{00}\partial_0 v^1\right] dx^0 \tag{2.15}$$

In particular, a rigid rotation by an angle $\phi$ of the defect followed by a deformation back to the vertical direction allows us to extend the family $L[\theta]$ of integrable line defects from before to a two-parameter family $L[\theta, \phi]$. We can define this deformation directly for $|\phi| < \frac{\pi}{2}$ and then iterate it to reach a broader range of $\phi$. There is no guarantee that this is periodic in $\phi$. In general, $L[\theta, \phi + 2\pi] \neq L[\theta, \phi]$.

If the line defect $L$ is invariant under reflections $x^0 \to -x^0$, $L[\theta, \phi]$ will break that symmetry, as $\tilde{t}^{00}$ is pseudo-real. If we rotate all the way by $\phi = \pi$, though, we should go back to a reflection-symmetric defect.

Movable defects can be naturally fused. Consideration of a U-shaped configuration suggests that the fusion of $L[\theta, \phi + \frac{\pi}{2}]$ and $L[\theta, \phi - \frac{\pi}{2}]$ should include the identity line defect.

### 2.2.3 Chiral line defects

If the defect is chiral, so that $[\bar{T}]_{x^1=0^+} = [\bar{T}]_{x^1=0^-}$, then one has a simpler relation

$$[T]_{x^1=0^+} - [T]_{x^1=0^-} = 2i\partial_{x^0} t^{00} \tag{2.16}$$

which implies that the line defect is also invariant under rigid translations in the $x^1$ direction, i.e. is movable.

Furthermore, $\tilde{t}^{00} = it^{00}$ and a conformal transformation deforms the line defect by

$$\int \left[\partial_0 v^0 + i\partial_0 v^1\right] t^{00} dx^0 \tag{2.17}$$

In particular, $L[\theta, \phi] \equiv L[\theta + i\phi]$ and thus $\theta$ can be taken to be valued in the complex plane.

In general, we expect $\langle |L[\theta]\rangle_R$ to be an entire function of $\theta$. Computing such a function is the typical objective of a calculation in this work. If the line defect $L$ is invariant under

reflections $x^0 \to -x^0$, the asymptotics

$$\langle |L[\theta]| \rangle_R \sim e^{-2\pi R e^\theta E_0} \tag{2.18}$$

will hold in a whole open strip of width $\frac{\pi}{2}$ around the positive real $\theta$ axis.

As we deform all the way to $\mathrm{Im}\,\theta = \pi n$, we will reach a collection of other unitary line defects, with nice RG flow and asymptotics

$$\langle |L[\theta]| \rangle_R \sim e^{-(-1)^n 2\pi R e^\theta E_0^{(n)}} \tag{2.19}$$

which will hold in a whole open strip of width $\frac{\pi}{2}$ around the $\mathrm{Im}\,\theta = \pi n$, $\mathrm{Re}\,\theta \gg 0$ lines. At $\mathrm{Im}\,\theta = \pi(n + \frac{1}{2})$ we will have wall-crossing phenomena as the IR physics of the line defect jumps. In the opposite limit of large negative $\theta$ we explore the UV definition of the defect.

A chiral defect does *not* have to preserve conformal symmetry or scale invariance. Indeed, a conformal invariant chiral line defect would be actually topological. We are interested in chiral line defects which are not topological, and thus must depend on some intrinsic scale $\mu$. We will write $\mu = \mu_0 e^\theta$ and label the corresponding RG flow family of line defects as $L[\theta]$. Although $\theta$ starts its life as a real positive parameter, it makes sense to analytically continue $L[\theta]$ to general complex $\theta$, as discussed above. This deformation breaks reflection positivity but will unlock important features.

A useful perspective[4] on the analytic continuation is that infinitesimal variations of $\theta$ are implemented by an exactly marginal local operator: the defect stress tensor $t^{00}$. This operator enters the local energy conservation law for the defect

$$T^{01}|_{x^1=0^+} - T^{01}|_{x^1=0^-} = \partial_{x^0} t^{00} \tag{2.20}$$

and measures the local violation of scale invariance for a chiral line defect placed along $x^0$.

Analytic continuation in $\theta$ is thus achieved infinitesimally by adding $t^{00}$ to the defect action with a complex coefficient. It is important to observe that the line defect $L[\theta]$ is generically *not* periodic under shifts $\theta \to \theta + 2i\pi$. It is an entire function of the $\theta$ plane.

A chiral line defect can be freely translated in a direction perpendicular to the defect.

[4] Another nice perspective is studied in [4]. Essentially, complexifying $\theta$ is equivalent to complexifying the Kondo coupling $g$. The resulting non-Hermitian extension of the Kondo problem has been studied in [4] to model the inelastic scattering and atom losses, where some neat physical interpretations of the wall-crossing behaviors we discuss in Section 3.4 are given. We thank Masaya Nakagawa for the correspondence on this point.

Such a translation is implemented infinitesimally by

$$\frac{1}{2i}\int dx^0 \left[T-\bar{T}\right]|_{x^1=0^+} - \left[T-\bar{T}\right]|_{x^1=0^-} \tag{2.21}$$

The argument inside the integral equals

$$\left[T+\bar{T}\right]|_{x^1=0^+} - \left[T+\bar{T}\right]|_{x^1=0^-} \tag{2.22}$$

which is proportional to the total derivative $\partial_{x^0} t^{00}$ and integrates by parts to zero for a rigid rotation. [5]

A chiral line defect wrapping a space circle gives rise to a conserved charge, as it commutes with time translations. We denote the corresponding operator on the Hilbert space of the theory as $\hat{T}_L[\theta]$.

Before moving on, we would like to clarify a notational issue. The vev of the line defect depends also on the radius of the space circle. As $\mu$ and $R^{-1}$ are the only energy scales in the problem, the operator $\hat{T}_L[\theta]$ can only depend on the combination $2\pi R\mu \equiv 2\pi R\mu_0 e^{\theta}$. Without loss of generality, we can thus do calculations either at fixed $R$ or at fixed $\mu$. In most of the expressions below we will do the former: fix the radius to a convenient value $2\pi R = \mu_0^{-1} = 1$ and write answers as a function of $e^{\theta}$. However in explicit calculations, for example in Appendix B and C.1, it is often useful to keep $R$ generic and set $\theta = 0$. The $\theta$ dependence can be easily restored.

In perturbative situations, where the line defect is labelled by some renormalized coupling(s) $g$, one can also absorb the $\theta$ dependence into an effective coupling $g_{\text{eff}}(\theta)$, so that

$$\langle L_g \rangle_{e^{\theta}R} \equiv \langle L_g[\theta] \rangle_R \equiv \langle L_{g_{\text{eff}}(\theta)} \rangle_R \tag{2.23}$$

For example, in the WZW case below we define the renormalized coupling through a dimensionally transmuted scale $\mu_0 = g^{\frac{k}{2}} e^{-\frac{1}{g}}$ and the operator $\hat{T}_g[\theta]$ is a function of

$$2\pi R g^{\frac{k}{2}} e^{-\frac{1}{g}} e^{\theta} \equiv 2\pi R g_{\text{eff}}(\theta)^{\frac{k}{2}} e^{-\frac{1}{g_{\text{eff}}(\theta)}}. \tag{2.24}$$

The ground state of the theory is automatically an eigenstate of $\hat{T}_L[\theta]$ (not to be confused with the stress tensor!), with an eigenvalue we can denote as $T_L[\theta]$. This can be

[5] We also see that a more general deformation of the defect will be possible at the price of introducing a position-dependent $\theta$ along the defect. This is analogous to the "framing anomaly" encountered in [31], which plays an important role in understanding the shifts of $\theta$ which occur in Hirota-like relations.

identified with the (exponential of the) "g-function" of the defect [104]. For real $\theta$, when the line defect is unitary/reflection positive, $T_L[\theta]$ varies monotonically along the RG flow [105].

More generally, $\hat{T}_L[\theta]$ only mixes states in the CFT within the same chiral algebra module and with the same $L_0$ eigenvalues. The corresponding $\hat{T}_L[\theta]$ eigenvalues will be also studied below.

### 2.2.4 RG flow of chiral defects and wall-crossing

In the far IR, a chiral line defect should flow to a conformal invariant chiral line defect and thus become topological. In a given renormalization scheme, the IR topological defect will be dressed by a constant local counterterm, the ground state energy $E_L$ of the line defect. In an Euclidean setting, that appears as a prefactor $e^{-2\pi R e^{\theta} E_L}$ in front of $\hat{T}_L[\theta]$. In particular, we learn the asymptotic behavior of $\hat{T}_L[\theta]$ for large real positive $\theta$:

$$T_L[\theta] \sim e^{-2\pi R E_L e^{\theta}} g_{IR} \tag{2.25}$$

Here we denote as $g_{IR}$ the (exponential of the) $g$-function of the topological line defect in the IR. [6]

The IR behavior of the line defects $L[\theta]$ is obviously invariant under real shifts of $\theta$. As we explore the imaginary $\theta$ direction, though, or as we vary other continuous parameters, the IR behavior may jump at walls of first-order phase transitions. At the level of the vevs $T_L[\theta]$, two exponential contributions will exchange dominance at these walls. This can happen when $(E_L - E'_L)e^{\theta}$ is purely imaginary, which typically means that the imaginary part of $\theta$ is $(n + \frac{1}{2})\pi$ with integer $n$.

Such wall-crossing behavior is not only possible. It is necessary in order to have some interesting physics. Indeed, an entire function $T_L[\theta]$ with uniform asymptotics of the form above for large positive real part of $\theta$ and arbitrary imaginary part, and reasonable behavior at negative real $\theta$, would have to essentially coincide with the far IR answer $e^{-2\pi R E_L e^{\theta}} g_{IR}$.

Interesting line defects will instead have a distinct asymptotic behavior

$$T_L[\theta] \sim e^{-2\pi R E_L^{(n)} e^{\theta}} g_{IR}^{(n)} \tag{2.26}$$

[6] More precisely, $g$-function is originally[104] defined to a boundary state $|B\rangle$ in CFT $\otimes$ $\overline{\text{CFT}}$ via the folding trick. And $\log g$ is referred to as the boundary entropy of $|B\rangle$. However the notion is naturally extended to defect lines. See, for example [106, 107] for related discussions.

in each strip

$$(n-\frac{1}{2})\pi < \mathrm{Im}\,\theta < (n+\frac{1}{2})\pi \tag{2.27}$$

We will see some concrete examples momentarily.

### 2.2.5 Integrable line defects

Finally, we can call a chiral line defect (or a collection of line defects) *integrable* if

- Close line defects $L[\theta]$ for different $\theta$'s give commuting operators.
- The identification between the compositions of line defects $L[\theta]$ and $L[\theta']$ in opposite order can be implemented by a R-matrix $R[\theta-\theta']$, i.e. a topological local operator interpolating between $L[\theta]L[\theta']$ and $L[\theta']L[\theta]$.
- The R-matrix satisfies Yang-Baxter relations.

### 2.2.6 IR data and wallcrossing

A typical observable of interest would be the expectation value $\langle|L[\theta]|\rangle_R$ of the line defect on a cylinder, with some choices of states at the two ends of the cylinder, as a function of the radius $R$ of the cylinder. The expectation value will be a function of the combination $Re^\theta$ and we can set $R=1$ without loss of generality.

If the line defect $L$ is invariant under reflections $x^0 \to -x^0$, upon Wick rotation it will map to a defect that preserves unitarity. This property is obviously preserved by the above global rescaling for real $\theta$, so the whole $L[\theta]$ family is unitary.

A unitary line defect should have a nice, monotonic RG flow landing onto some conformal-invariant line defect in the far IR. The expectation value on a large cylinder should thus behave as

$$\langle|L[\theta]|\rangle_R \sim e^{-2\pi R e^\theta E_0} \tag{2.28}$$

where $E_0$ is the energy of groundstate of the line defect. Subleading corrections should be suppressed by similar exponentials with a larger real energy.

## 2.3 Chiral line defects in the Ising model

Chiral line defects in Virasoro minimal models are a canonical example of integrable line defects [26]. The Ising model is a particularly nice case, because the Kondo problem is exactly solvable in the free fermion description of the model [108]. We will discuss it in this section.

The integrable minimal model Kondo problems involve relevant deformations of topological line defects which support chiral local operators. The solvable Ising model examples involve the deformation by the chiral local operator $\psi(z)$ which is the free fermion in disguise.

Recall that the Ising model has three irreducible topological line defects [109, 110, 106]:

- The trivial line defect $I$, with Cardy label 1 and $g_I = \langle 0|I|0\rangle = 1$
- The $\mathbb{Z}_2$ symmetry defect $P$, with Cardy label $\epsilon$ and $g_\epsilon = \langle 0|P|0\rangle = 1$
- The Kramers-Wannier duality defect $S$, with Cardy label $\sigma$ and $g_\sigma = \langle 0|S|0\rangle = \sqrt{2}$

where we also list their $g$-values $g(L_k) = S_{k0}/S_{00}$ and the vacuum expectation values. They form an Ising fusion category, with $P \times P = I$, $S \times S = I + P$, $S \times P = S$. They are Verlinde lines with the action on the primary state given as follows,

$$\hat{L}_k \, |\phi_i\rangle = \frac{S_{ki}}{S_{0i}} \, |\phi_i\rangle \tag{2.29}$$

which reads explicitly

$$\begin{array}{lll} \hat{P}|1\rangle = |1\rangle, & \hat{P}|\epsilon\rangle = |\epsilon\rangle, & \hat{P}|\sigma\rangle = -|\sigma\rangle \\ \hat{S}|1\rangle = \sqrt{2}|1\rangle, & \hat{S}|\epsilon\rangle = -\sqrt{2}|\epsilon\rangle, & \hat{S}|\sigma\rangle = 0 \end{array} \tag{2.30}$$

By evaluating the partition function twisted by topological line defects, one can find the Hilbert space of defect fields living on a topological line defect with Kac label $k$ [107, 111].

$$\mathcal{H}_k^{\text{defect}} = \bigoplus_{i,j} \left(R_i \otimes \bar{R}_j\right)^{\oplus \sum_x N_{ij}^x N_{kk}^x} \tag{2.31}$$

where $R_i(\bar{R}_j)$ are irreps of Virasoro $\text{Vir}(\overline{\text{Vir}})$ and $N_{ij}^k$ are the fusion rule coefficients. In

particular, the only irreducible line defect which supports $\psi(z)$ as a local operator is $S$.[7] We thus define a Kondo problem by deforming $S$ by the relevant deformation $\psi$ [107]:

$$g \int \psi(x^0, 0) dx^0 \tag{2.32}$$

The deformation is clearly transparent to the anti-chiral stress tensor. The result is a chiral line defect $L_S$. As $\psi$ has dimension $\frac{1}{2}$, in natural renormalization schemes the RG flow will simply rescale $g$ by $e^{\frac{\theta}{2}}$. We can simply set $g = 1$ and parameterize the RG flow by $\theta$. If needed, we can restore $g$ by a shift of $\theta$.

The line defect $L_S[\theta]$ should coincide with $L_S[\theta + 4\pi i n]$ up to the only available counterterm, which is a constant. [8]

Due to the $g$ theorem [104], the RG flow can only end on topological line defects with a lower $g$ function than $S$. The only possibilities are $I$ and $P$. The sign of the coupling $g$ is expected to determine if the flow ends on $I$ or $P$ [107, 112]. Up to some convention ambiguities, we can say that a positive deformation will flow to $I$.

We define the operator $\hat{T}_S[\theta]$ by wrapping the deformed line defect $L_S[\theta]$ along a space circle. As $\hat{T}_S[\theta]$ commutes with the Hamiltonian, the vacuum is an eigenvector of $\hat{T}_S[\theta]$. The expectation value of $\hat{T}_S[\theta]$ on the vacuum is of particular interest. We will denote it as

$$T_S(\theta) \equiv \langle 0 | \hat{T}_S[\theta] | 0 \rangle_{2\pi R = \mu_0^{-1}} \tag{2.33}$$

It is instructive to start with a perturbative UV calculation. We can set $\theta = 0$ and restore it later on, but keep the radius $R$ generic. The leading order answer is the quantum dimension $\sqrt{2}$ of $S$. The first subleading correction appears at second order, as the vev of $\psi$ vanishes. The $\psi(s)\psi(s')$ two-point function on the cylinder with vacuum states at the two ends is

$$\frac{1}{2R \sin \frac{s-s'}{2R}} \tag{2.34}$$

As a consequence, the leading perturbative correction to the vev has a log divergence

$$2\pi R g^2 \log \cot \frac{\epsilon}{4R} \tag{2.35}$$

[7] One can also consider the superposition $I + P$, where $\psi$ appears as a boundary-changing operator. The corresponding RG flow can be obtained from the RG flow for $S$ by fusion with a second, topological $S$ line.

[8] Using RCFT technology one can also see that $L_S[\theta + 2\pi i]$ should coincide with $L_S[\theta] \times P$ up to a constant counterterm.

which requires a constant counterterm $2\pi R g^2 \log \epsilon$ in a minimal subtraction scheme.

In a more general renormalization scheme, we have

$$\langle L_S \rangle_R = \sqrt{2} \left(1 + 2\pi R g^2 \log(2\pi R) + 2\pi R g^2 c + \cdots\right) \tag{2.36}$$

We can adjust $c$ to that the answer is a function of $2\pi R g^2$ only. Recall that the only renormalization ambiguity in the definition of $L_S$ is a constant counterterm $\delta \int dx_0$, which rescales the above correlator by $e^{2\pi R \delta}$.

Restoring $\theta$ and setting $2\pi R g^2 = 1$, we write

$$T_S[\theta] = \sqrt{2} \left(1 + \theta e^\theta + c' e^\theta + \cdots\right) \tag{2.37}$$

for some arbitrary $c'$.

The full answer for $T_S[\theta]$ can be obtained by mapping the problem to the free fermion realization of the Ising model. Recall that the Ising model is obtained as the GSO projection of a free fermion (spin-)CFT, inverting the Jordan-Wigner transformation. See [113] for a recent review.

On the other side of the $S$ defect, we have Kramers Wannier dual of the Ising model which can be obtained by the GSO projection of stacking the free fermion theory with an Arf topological field theory (aka Majorana chain) is defined on half of the space-time and then GSO project the combined system.

The Arf theory is trivial on the bulk but supports a single Majorana mode $\gamma$ at the boundary. The bilinear combination $\gamma\psi$ survives the GSO projection and becomes the "$\psi$" operator on the S defect. We employ this description for a straightforward one-loop calculation of $T_S[\theta]$, reviewed in Appendix B.

The unregularized one loop determinant would give $\prod_{n\geq 0}(n + \frac{1}{2} + 2\pi R g^2)$. Restoring $\theta$ and setting $2\pi R g^2 = 1$, we write the regularized expression as

$$T_S(\theta) = \frac{\sqrt{2\pi} e^{\theta e^\theta - e^\theta}}{\Gamma(\frac{1}{2} + e^\theta)} \tag{2.38}$$

This interpolates nicely between the perturbative answer in the UV for $e^\theta \ll 1$ and an infrared expansion

$$T_S(\theta) \sim 1 + \frac{1}{24} e^{-\theta} + \cdots \tag{2.39}$$

valid for $e^\theta \gg 1$ as long as the phase of $\theta$ lies strictly between $-\pi$ and $\pi$. [9]

This agrees with the expectation that $L_S$ flows to $I$ or $P$, which both have vev 1 acting on the vacuum. The leading correction in the IR is a deformation of $I$ or $P$ by the least irrelevant operator, i.e. the stress tensor. The coefficient $\frac{1}{24}$ is $-2$ times the vacuum energy, and we will now test the statement further for excited states. According to integrability lore, [26], higher-order terms in the IR expansion of $\hat{T}_S(\theta)$ should correspond to the higher "quantum KdV" charges hidden in the Ising CFT.

If we compute the vev of $L_S$ in a different state $|n_i\rangle$, obtained from the vacuum by acting with chiral fermion momentum modes of momentum $n_i+\frac{1}{2}$ with $n_i \geq 0$ (and any anti-chiral fermions) we obtain a similar one-loop determinant but with some signs switched, leading to

$$\hat{T}_S(\theta)|n_i\rangle = \prod_i \frac{e^\theta - n_i - \frac{1}{2}}{e^\theta + n_i + \frac{1}{2}} \frac{\sqrt{2\pi} e^{\theta e^\theta - e^\theta}}{\Gamma(\frac{1}{2} + e^\theta)} |n_i\rangle \tag{2.40}$$

In the UV, the correction factor goes as

$$\prod_i \left( -1 + \frac{2}{n_i + \frac{1}{2}} e^\theta + \cdots \right) \tag{2.41}$$

The leading term gives the sign of the action of $S$ on the vacuum module/$\epsilon$ modules, which is $\sqrt{2}$ /$-\sqrt{2}$. This agrees with (2.30).

In the IR, we have

$$\langle n_i|\hat{T}_S(\theta)|n_i\rangle \sim 1 + \frac{1}{24} e^{-\theta} - \sum_i (2n_i + 1) e^{-\theta} \cdots \tag{2.42}$$

which shows clearly that the leading correction to the identity line defect is the integral of the stress tensor along the defect, giving a $-2L_0 e^{-\theta}$.

Similarly, in the Ramond ground state/$\sigma$ module for the Ising model we get the regularized determinant

$$\langle \sigma|\hat{T}_S(\theta)|\sigma\rangle \equiv T_{S;\sigma}[\theta] = \frac{\sqrt{2\pi e^\theta} e^{\theta e^\theta - e^\theta}}{\Gamma(1 + e^\theta)} \tag{2.43}$$

In the UV this goes as

$$T_{S;\sigma}[\theta] \sim \sqrt{2\pi e^\theta} + \cdots \tag{2.44}$$

[9] We choose our $c'$ counter-term in such a way that the IR ground state energy is 0.

which arises at the leading order from a one-point function of $\psi$. Note that $T_{S;\sigma} = 0 = \langle\sigma|S|\sigma\rangle$ at the UV fixed point, as expected, since duality line $S$ annihilate $|\sigma\rangle$. (2.30). In the IR, we have

$$T_{S;\sigma}[\theta] \sim 1 - \frac{1}{12}e^{-\theta} + \cdots \tag{2.45}$$

which agrees again at leading order with $1 - 2L_0 e^{-\theta}$. For excited states, we modify that to

$$\langle\sigma; n_i|\hat{T}_S(\theta)|\sigma; n_i\rangle = \prod_i \frac{e^\theta - n_i}{e^\theta + n_i} \frac{\sqrt{2\pi e^\theta} e^{\theta e^\theta - e^\theta}}{\Gamma(1 + e^\theta)} \tag{2.46}$$

### 2.3.1 Fusion relations, TBA, Hirota and full IR behaviour

Before the deformation, the $S$ line defects have a nice fusion relation:

$$S \times S = I + P \tag{2.47}$$

with $P$ being the $Z_2$ symmetry line of the Ising model.

After the deformation, we claim that the fusion is deformed to something like

$$L_S\left[\theta - i\frac{\pi}{2}\right] L_S\left[\theta + i\frac{\pi}{2}\right] = 1 + e^{-2\pi\int dx^0} P \tag{2.48}$$

meaning that there is a ground state energy difference of $2\pi$ between the superselection sectors associated to the identity and $P$ lines. [10]

The claim is supported by the fusion relation

$$T_{S;0}\left[\theta - i\frac{\pi}{2}\right] T_{S;0}\left[\theta + i\frac{\pi}{2}\right] = 1 + e^{-2\pi e^\theta} \tag{2.49}$$

which leads to the integral formula

$$\log T_{S;0}(\theta) = \frac{1}{2\pi}\int_{-\infty}^{\infty} d\theta' \, \frac{1}{\cosh[\theta - \theta']} \log\left[1 + e^{-2\pi e^{\theta'}}\right] \tag{2.50}$$

valid on a strip of width $\pi$ around the real axis.

The fusion relation holds equally well for excited states, which have extra sources in

[10] This statement can in principle be checked with the RCFT tools from [28], as long as renormalization is treated carefully.

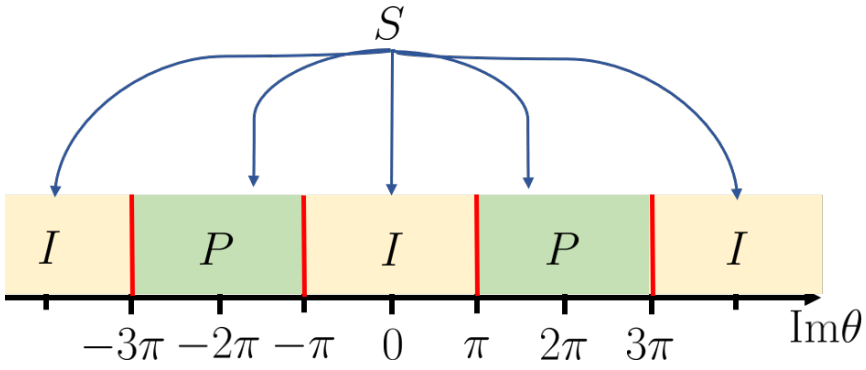


Figure 2.1: IR fate of the deformed line defect $L_S[\theta]$ for different $\mathrm{Im}\,\theta$.

the integral equation due to the zeroes in the strip:

$$\log T_{S;\{n_i\}}(\theta) = \sum_i \log \frac{e^\theta - n_i - \frac{1}{2}}{e^\theta + n_i + \frac{1}{2}} + \frac{1}{2\pi}\int_{-\infty}^{\infty} d\theta' \, \frac{1}{\cosh[\theta - \theta']} \log\left[1 + e^{-2\pi e^{\theta'}}\right] \tag{2.51}$$

Furthermore, we have

$$T_{S;\sigma}\left[\theta - i\frac{\pi}{2}\right] T_{S;\sigma}\left[\theta + i\frac{\pi}{2}\right] = 1 - e^{-2\pi e^\theta} \tag{2.52}$$

and

$$\log T_{S;\sigma}(\theta) = \frac{1}{2\pi}\int_{-\infty}^{\infty} d\theta' \, \frac{1}{\cosh[\theta - \theta']} \log\left[1 - e^{-2\pi e^{\theta'}}\right] \tag{2.53}$$

valid on a strip of width $\pi$ around the real axis.

The fusion relation suggests that if $e^\theta$ has a positive real part, the identity summand dominates and $L_S\left[\theta - i\frac{\pi}{2}\right]$ and $L_S\left[\theta + i\frac{\pi}{2}\right]$ will both flow to the same line, either $I$ or $P$, in accordance with $I \times I = P \times P = I$. If $e^\theta$ has a negative real part, the $P$ summand dominates and $L_S\left[\theta - i\frac{\pi}{2}\right]$ and $L_S\left[\theta + i\frac{\pi}{2}\right]$ will flow to an opposite choice of line, in accordance with $I \times P = P \times I = P$.

In conclusion, the prediction is that $L_S[\theta]$ will flow to the identity line in the range $|\,\mathrm{Im}\,\theta| < \pi$, but will flow to a $P$ line (with renormalized ground state energy) in the ranges $\pi < \mathrm{Im}\,\theta < 3\pi$ and $-3\pi < \mathrm{Im}\,\theta < -\pi$, etcetera, with periodicity $4\pi$ and sharp transitions at $\mathrm{Im}\,\theta = \pm\pi$ where the line flows to a direct sum of 1 and $P$ with the same real part of the ground state energy.

Another sanity check of this prediction Fig.2.1 is that it is compatible with $P \times S = S$.

The fusion of $S$ with $P$ must map $\psi$ to a multiple of itself [114], so $P$ must act on $L_S[\theta]$ as a shift of $\theta$, up to a constant counterterm shifting the defect Hamiltonian[11]. This obviously agrees with Fig.2.1, where upon fusing $S$ with $P$, $\mathrm{Im}\,\theta$ is shifted by $2\pi$, $P \to I$ and $I \to P$.

The fusion relation is the simplest example of $\mathfrak{su}(2)$ Hirota dynamics:

$$T_s\left[\theta - i\frac{\pi}{2}\right] T_s\left[\theta + i\frac{\pi}{2}\right] = 1 + T_{s-1}T_{s+1} \tag{2.54}$$

with $T_2 = T_S$, $T_1 = 1$, $T_3 = e^{-2\pi e^{\theta}}$, $T_0 = T_4 = 0$. Compare with (2.56).

## 2.4 The $\mathfrak{su}(2)$ Kondo line defects

Consider any CFT equipped with some level $k$ chiral $\widehat{\mathfrak{su}}(2)$ WZW currents $J^a$. This implies that the CFT is a modular-invariant combination of an $\widehat{\mathfrak{su}}(2)_k$ chiral WZW model and some other degrees of freedom [12]. The line defects we will discuss momentarily only interact with the chiral WZW degrees of freedom and are transparent to everything else.

We define the Kondo line defects by coupling the theory to a spin $j$ (half integer) quantum-mechanical system by the natural $\mathfrak{su}(2)$-invariant marginally relevant coupling [90]

$$g \int \sigma_a J^a dx^0 \tag{2.55}$$

with $\sigma_a$ being the matrices representing $\mathfrak{su}(2)$ in the spin $j$ quantum-mechanical system. Dimensional transmutation converts the coupling $g$ into a scale, which we can absorb in the $\theta$ dependence. The result is a family of chiral line defects $L_j[\theta]$.

Gleaning information from the vast literature on integrability, including [90, 28, 115, 116, 117, 88, 118] and more, and adding some judicious guesses one is presented with the following conjectures:

- The Kondo line defects give commuting transfer matrices $\hat{T}_{2j+1}[\theta]$. These operators commute with the Hamiltonian and act within primary towers for the WZW currents.

[11] Here we are using the standard observation that fusion with topological defects does not affect the local RG flow dynamics. See [114] for applications of this principle to conformal boundary conditions.

[12] The obvious choice is an anti-chiral WZW model, but many alternatives are possible. A nice possibility is a $\widehat{\mathfrak{u}}(k)_2$ chiral WZW model, which would combine with $\widehat{\mathfrak{su}}(2)_k$ to give a theory of $2k$ complex chiral fermions, by level-rank duality. Of course, a universally valid choice is a 3d $SU(2)_k$ Chern-Simons TFT defined on a half-space.

- The Kondo line defects fuse in a manner analogous to representations of the $\mathfrak{su}(2)$ Yangian:
$$\hat{T}_{2j+1}\left[\theta - i\frac{\pi}{2}\right]\hat{T}_{2j+1}\left[\theta + i\frac{\pi}{2}\right] = 1 + \hat{T}_{2j}[\theta]\hat{T}_{2j+2}[\theta] \tag{2.56}$$

- Expectation values in a generic WZW primary state $|l\rangle$
$$\langle l|\hat{T}_{2j+1}[\theta]|l\rangle_{2\pi R=1} \equiv T_{2j+1;l}(\theta) \tag{2.57}$$
or eigenvalues of $\hat{T}_{2j+1}[\theta]$ acting on descendants give solutions of the Hirota dynamics. The vacuum expectation value $T_{2j+1;0}(\theta)$ will just be referred to as $T_{2j+1}(\theta)$

- The expectation values can be computed as transport coefficients of an auxiliary Schröedinger equation
$$\partial_x^2\psi(x) = \left[e^{2\theta}e^{2x}(1+gx)^k + \frac{l(l+1)}{(x+1/g)^2}\right]\psi(x) \tag{2.58}$$
in the spirit of the ODE/IM correspondence.

- The $\hat{T}_{2j+1}[\theta]$ expectation values on the vacuum or other eigenstates are also expected to satisfy certain TBA equations, which are the conformal limit of the TBA equations for chiral Gross-Neveu models, i.e. the deformation of a non-chiral WZW model by a $J^a\bar{J}^a$ marginally relevant interaction.

These claims are hard to prove or even justify in a concise manner directly in 2d. In the remaining part of this section, we study the Kondo defect perturbatively in preparation for the ODE/IM correspondence (2.58) discussed in section 3.4. The last two claims should really hold for all common sets of eigenvalues of the $\hat{T}_{2j+1}[\theta]$, with a slight modification according to the states, which is the main goal in chapter 4.

### 2.4.1 A perturbative analysis of the Kondo defect vevs

Using the definition of the line defects, one can compute in perturbation theory
$$\hat{T}_n = n + g^2\hat{t}_{n,2} + g^3\hat{t}_{n,3} + g^4\hat{t}_{n,4} + \cdots, \tag{2.59}$$
where $n = 2j+1$. The linear term is missing because $\operatorname{Tr}\sigma_a = 0$.

The calculation requires some careful renormalization, which dimensionally transmutes the coupling into a scale $\mu_0(g)$. The RG flow rescales that to $\mu = \mu_0 e^\theta$ and the coupling runs as

$$\mu_0(g)e^\theta = \mu_0\left(g_{\text{eff}}(\theta)\right) \tag{2.60}$$

The only counter-terms are a constant counterterm and the renormalization of the coupling, which first appears at order $g^3$.

Up to a rescaling of coupling, the perturbative RG flow equation takes the form [13]

$$\partial_\theta g_{\text{eff}}(\theta) = g_{\text{eff}}(\theta)^2 + c g_{\text{eff}}(\theta)^3 + \cdots \tag{2.61}$$

where we normalize the coupling such that the leading coefficient is 1. In this sign convention, a small positive UV coupling will grow in the IR and our line defect will be asymptotically free, with a typical IR mass scale which is exponentially suppressed at small positive $g_{\text{eff}}$. This is the microscopic definition of the $L_n$ line defects we are interested in. A negative coupling, instead, flows to 0. Such IR free line defects will appear later on as IR outcomes of some of the RG flows we consider, with a typical UV mass scale which is exponentially large at small negative $g_{\text{eff}}$.

The coefficient $c$ cannot be re-defined away. An explicit calculation in Appendix C.1 shows that it is independent of $n$ and equals $-\frac{k}{2}$. The ellipses indicate terms that can be arbitrarily adjusted by a perturbative redefinition of the coupling. This can be checked rather easily.

We choose to fix the renormalization ambiguities by imposing

$$\partial_\theta g_{\text{eff}}(\theta) = \frac{g_{\text{eff}}(\theta)^2}{1 + \frac{k}{2} g_{\text{eff}}(\theta)} \tag{2.62}$$

i.e.

$$e^{-\frac{1}{g_{\text{eff}}(\theta)}} g_{\text{eff}}(\theta)^{\frac{k}{2}} \equiv e^{-\frac{1}{g}} g^{\frac{k}{2}} e^\theta \tag{2.63}$$

or $\mu_0(g) = e^{-\frac{1}{g}} g^{\frac{k}{2}}$. This choice of RG scheme has the advantage that $0 < g_{\text{eff}} < \infty$ parameterizes the full range of scales. It will also agree with the RG scheme implicit in the Hirota relations, ODE/IM correspondence, etc. See Appendix C.1.3 and D.3 for more details. Other choices of RG scheme are of course possible and sometimes useful.

The defect vevs will depend only on the combination $2\pi R e^{-\frac{1}{g}} g^{\frac{k}{2}} e^\theta$. Perturbatively, that

[13] The right-hand side is the negative of the beta function.

means the $\theta$ dependence of $\hat{T}_n[\theta]$ is captured by

$$\hat{T}_n[\theta] = n + g_{\text{eff}}(\theta)^2 \hat{t}_{n,2} + g_{\text{eff}}(\theta)^3 \hat{t}_{n,3} + g_{\text{eff}}(\theta)^4 \hat{t}_{n,4} + \cdots \tag{2.64}$$

with

$$g_{\text{eff}}(\theta) = g + \theta g^2 + \theta(\theta - \frac{k}{2}) g^3 + \theta(\theta^2 - \frac{5}{4} k\theta + \frac{k^2}{4}) g^4 + \cdots \tag{2.65}$$

The $\hat{t}_{n,m}$ are complicated expressions of the Fourier modes of WZW currents. In Appendix C.1 we compute the explicit form of $\hat{T}_n$ up to order $g^4$. Strikingly, the $\hat{t}_{n,m}$ we computed all commute with each other, confirming that the $\hat{T}_n[\theta]$ behave as commuting transfer matrices.

Even more strikingly, we find that our choice of renormalization scheme is such that the $\hat{T}_n[\theta]$ satisfy Hirota fusion relations as long as we fix the reference coupling $g$ to be the same for all defects, at least at the order we could compute. Perturbatively, that requires the relations

$$\begin{aligned} 2n\hat{t}_{n,2} &= (n+1)\hat{t}_{n-1,2} + (n-1)\hat{t}_{n+1,2} \\ 2n\hat{t}_{n,3} &= (n+1)\hat{t}_{n-1,3} + (n-1)\hat{t}_{n+1,3} \\ 2n\hat{t}_{n,4} + \hat{t}_{n,2}^2 &= (n+1)\hat{t}_{n-1,4} + (n-1)\hat{t}_{n+1,4} + \hat{t}_{n+1,2}\hat{t}_{n-1,2} + \frac{3}{2} n\pi^2 \hat{t}_{n,2} \end{aligned} \tag{2.66}$$

### 2.4.2 Perturbative and non-perturbative RG flows

For physical values of the parameters, perturbation theory is only useful in the UV and non-perturbative dynamics kick in at low energy. If we analytically continue $\theta$ sufficiently away from the real axis, though, we get a surprise: under RG flow the effective coupling $g_{\text{eff}}(\theta)$ grows a bit but then swings back to be small and negative. The imaginary part of $\frac{1}{g_{\text{eff}}(\theta)}$ decreases by a finite amount in absolute value, changing by $-\frac{k}{2}\pi$ as the real part flows to large negative values.

That means that the line defects remain perturbative all along the RG flow as long as the initial imaginary part of $\frac{1}{g}$ is sufficiently large! The analytically continued line defects are not unitary, so the non-monotonic RG flow is not a contradiction, but it is still a bit surprising.

These perturbative IR limits for large positive and large negative imaginary part of $\frac{1}{g}$ differ, as the two branches of $\frac{1}{g_{\text{eff}}(\theta)}$ differ by $k\pi$. The two perturbative regimes are separated by some intermediate phases, where the RG flow is non-perturbative.

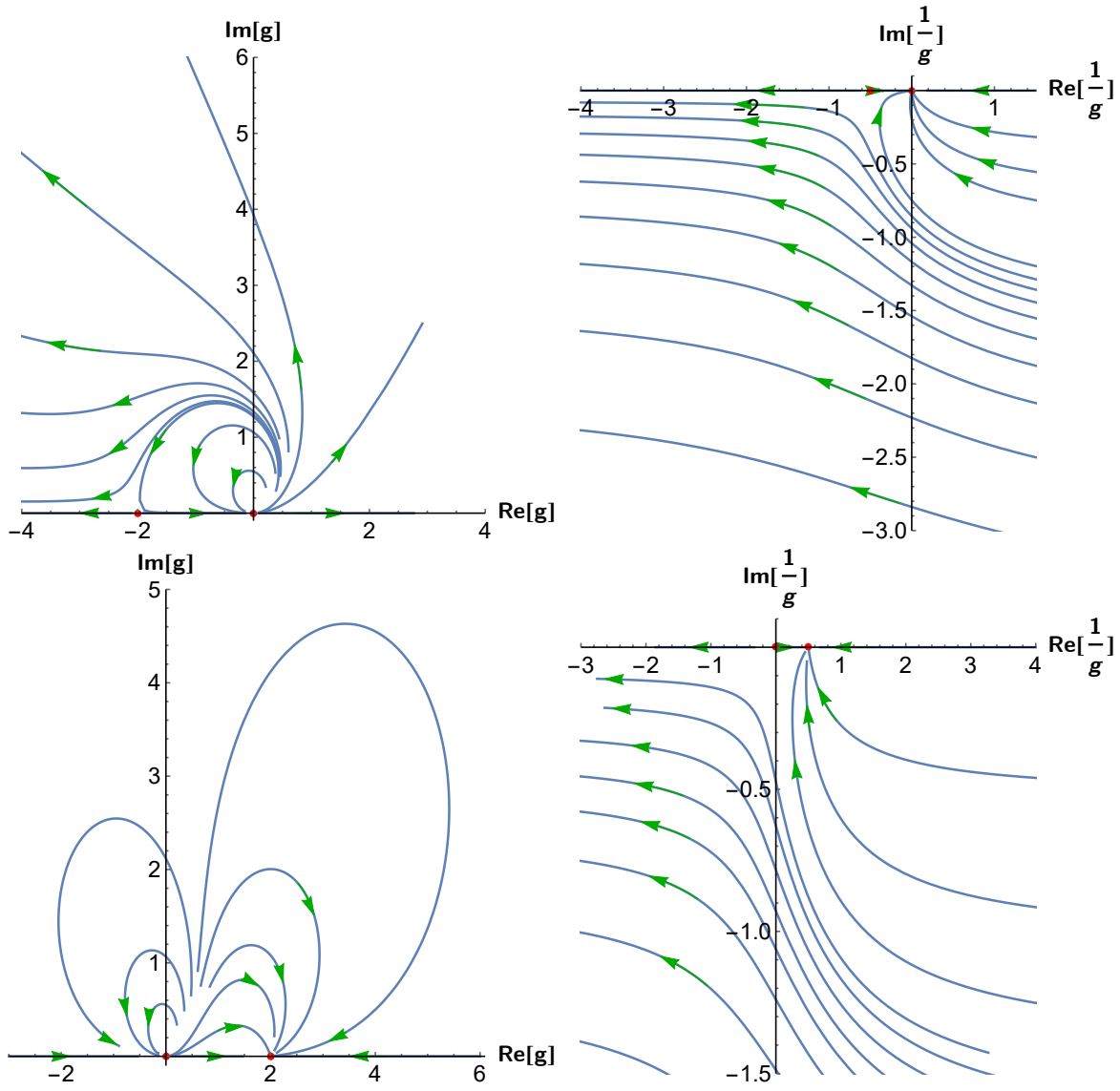


Figure 2.2: The RG flow pattern over the complex $g$ plane and the complex $1/g$ plane. The top two and he bottom two are plotted using the beta function (2.62) and (2.67) respectively. Note that the lower left figure is the same as Fig. 1 in [4]

Another important situation where perturbation theory is applicable is large $k$, at least at finite $j$. If we use an alternative RG scheme where

$$\partial_\theta g'_{\text{eff}}(\theta) = g'_{\text{eff}}(\theta)^2 - \frac{k}{2} g'_{\text{eff}}(\theta)^3 \tag{2.67}$$

we get a perturbative zero for the $\beta$ function at $g'_r = \frac{2}{k}$.

That means the RG flow for large $k$ and fixed $j$ must lower the $g$ function by an amount of order $k^{-1}$. The leading correction actually comes at order 3 in perturbation theory and is proportional to $j(j+1)(2j+1)$.

For $j = \frac{1}{2}$ our hands are tied: the only topological line defect with quantum dimension slightly lower than 2 is the topological line $\mathcal{L}_{\frac{1}{2}}$ whose Cardy label is the spin $\frac{1}{2}$ primary field and whose quantum dimension is $2\cos\frac{\pi}{k+2}$. The leading correction is consistent with this. This is a standard result [22, 90].

The RG flow of $g'_{\text{eff}}(\theta)$ as a function of the imaginary part of $\theta$ is quite interesting. As we increase the imaginary part to large values of order $k$, we hit a thin region where the flow reaches strong coupling, and beyond that, the perturbative flow back to the spin $\frac{1}{2}$ IR Kondo line discussed before. We interpret this as a phase transition from the flow to $\mathcal{L}_{\frac{1}{2}}$ to the flow to $L^{IR}_{\frac{1}{2}}$. This will indeed happen in the exact solution proposed below.

In a similar manner, for sufficiently small $j$, the physical flow of $L_j[\theta]$ should end on the topological line $\mathcal{L}_j$ of quantum dimension

$$d^{(k)}_{2j+1} \equiv \frac{\sin(2j+1)\frac{\pi}{k+2}}{\sin\frac{\pi}{k+2}} \tag{2.68}$$

while for sufficiently large imaginary part of $\theta$ it should go back to $L^{IR}_j[\theta]$. Recall that $\mathcal{L}_j$ is the topological line with Cardy label given by the primary field of spin $j$, where $j = 0, \frac{1}{2}, 1, \ldots, \frac{k}{2}$.

We can anticipate here the conjectural behaviour of the physical RG flows for all $k$ and $j$ is that (up to constant counterterms) supported by the ODE/IM solution:

- For $j \leq \frac{k}{2}$, $L_j[\theta]$ flows to $\mathcal{L}_j$.
- For $j > \frac{k}{2}$, $L_j[\theta]$ flows to $\mathcal{L}_{\frac{k}{2}} \times L^{IR}_{j-\frac{k}{2}}[\theta]$

These statements are conjecturally valid on a strip of width $2\pi$ around the real $\theta$ axis.

Hirota recursion relations determine the IR behavior of all lines beyond that strip. One finds all sort of combinations of the form $\mathcal{L}_{j'} \times L^{IR}_{j-j'}[\theta]$, with $j'$ jumping by $\pm\frac{1}{2}$ across phase transitions.

## 2.5 The 4d Chern-Simons construction

The four dimensional Chern Simons theory is a recently proposed approach to integrable models. Original articles are very nicely written[29, 30, 31, 32, 33]. The relation with some old ideas are explained in an introductory article [119]. Other more recent development can be found here [34, 35, 36].

The action can be given by

$$S = \frac{1}{\hbar}\int_{\mathbb{R}^2\times C} \omega \wedge \mathrm{CS}(A) \tag{2.69}$$

where we take the four-dimensional spacetime to be $\mathbb{R}^2 \times C$ with $C$ being a complex curve. The theory is topological in the direction of $\mathbb{R}^2$ with the coordinates $x, y$, and holomorphic along the curve $C$ with the local coordiante $z$. Here we mostly focus on the case $C = \mathbb{C}$. $\mathrm{CS}(A)$ is the usual Chern Simons three form

$$\mathrm{CS}(A) := \mathrm{Tr}\left(A \wedge dA + \frac{2}{3}A \wedge A \wedge A\right) \tag{2.70}$$

Classically, the 4d Chern-Simons gauge theory on $\mathbb{C} \times \mathbb{R}^2$ can be minimally coupled to a 2d chiral WZW model, sitting at a point $z = 0$ in the holomorphic plane and wrapping the $\mathbb{R}^2$ topological directions. The coupling to the 4d CS theory does not induce any deformation of the two-dimensional WZW theory, simply because there is no spin 0 operator in the WZW theory which could describe such a deformation.

The only effect of the coupling is that it allows the WZW model to interact with Wilson lines $W_j[z]$ of the 4d CS theory, lying parallel to the surface defect at some separate point in the holomorphic plane. An important property of the 4d CS theory is that the interactions are local on the topological plane so that the Wilson line will appear as a 2d local line defect to the 2d degrees of freedom. The leading classical interaction takes the form

$$\int \sigma^a r_{ab}(z) J^b(t) dt \tag{2.71}$$

where $r_{ab}(z)$ is the classical rational R-matrix which takes the role of a propagator in the 4d theory. This is simply the Kondo interaction, with a coupling $g = \frac{\hbar}{i\pi z}$.

An important quantum correction to this statement is due to the 2d gauge anomaly of the WZW model. This can be cured by a perturbative modification of the 1-form $\omega(z)dz$ in the 4d CS action

$$\int \omega(z)dz \wedge \Omega_{CS}[A] \tag{2.72}$$

which adds a pole at $z = 0$:

$$\frac{dz}{\hbar} \to \frac{dz}{\hbar} + \frac{k}{2\pi i z}dz \tag{2.73}$$

The 4d CS perturbation theory is essentially an expansion in inverse powers of $z$, so this is a sub-leading correction to the classical action.

The Wilson lines of the 4d CS theory automatically satisfy the Yangian fusion relations and, when wrapped along a compact direction in the topological plane, should give vevs which satisfy the $\mathfrak{su}(2)$ Hirota dynamics. In particular, the one form $\omega(z)dz$ controls the precise form of the line defects fusion: when $\omega(z) = 1$ it involves shifts of $z$ by multiples of $i\frac{\pi}{2}$, but for general $\omega(z)$ one has to compute the primitive

$$\theta = -i\pi\frac{z}{\hbar} - \frac{k}{2}\log z = -\frac{1}{g} + \frac{k}{2}\log g \tag{2.74}$$

such that $d\theta = \omega(z)dz$. Then the fusion relations involve shifts of $\theta$ by multiples of $i\frac{\pi}{2}$.

We, therefore, identify $\theta$ as the "spectral parameter" of the Wilson lines, which is exactly what we found in the purely 2d analysis!

Our analysis is compatible with yet unpublished work [120] demonstrating the existence of a renormalization scheme for 4d CS theory coupled to 2d chiral matter, with the property that the $g = \frac{\hbar}{i\pi z}$ is not renormalized, and RG flow only affects the position of Wilson line defects by a uniform shift of the $\theta$ local coordinate, i.e. the beta function for $z$ is proportional to $\omega(z)^{-1}$.

# Chapter 3

# ODE/IM correspondence

## 3.1 Introduction

Of all the surprising structures integrability comes with, ODE/IM correspondence is one of the most mysterious relations. For completeness, we will briefly review the standard formulation in section D.6. In the language of the Kondo defect we studied in the previous section, it can be phrased as the following conjecture: in the simplest setting $\mathfrak{su}(2)_1$, the expectation values of Kondo line $\hat{T}_j[\theta]$ on a spin $l$ primary state match the Stokes data for the second order differential equation

$$\partial_x^2\psi(x) = \left[e^{2\theta}(1+gx)e^{2x} + \frac{l(l+1)g^2}{(1+gx)^2}\right]\psi(x) \tag{3.1}$$

and simple modifications for twisted sectors and higher WZW levels.

In this section, we will first review some necessary background in order to properly state the correspondence. We then investigate this conjectured relation and perform explicit calculations to verify the proposal.

## 3.2 Opers

In precise mathematical terms, the ODE like (3.1) is encoded in a particular mathematical structure called *oper* first introduced by A. Beilinson and V. Drinfeld [121]. The term

"oper" is motivated by the fact that for most of the classical $G$ one can interpret G-opers as differential operators between certain line bundles.

Here in this section we review some of the relevant mathematical background. [122, 123, 124, ?]

### Projective connection

Consider a Riemann surface $C$ (equipped with a spin structure), a *projective connection* is a second order differential operator that acts between the sheaves of sections of the following line bundles

$$K_C^{-1/2} \to K_C^{3/2} \tag{3.2}$$

which can be locally written in a trivialization to be

$$\partial_{x_a}^2 - T(x_a) \tag{3.3}$$

where $x_a$ is the coordinate in an open subset $U_a \subset C$. $K_C$ is the canonical line bundle on $C$. $T$ is referred to as a classical stress tensor, which, on the overlap $U_a \cap U_b$, is required to transform as

$$T_b(x_b) = \left(\frac{\partial x_a}{\partial x_b}\right)^2 T_a(x_a) - \frac{1}{2}\{x_a, x_b\} \tag{3.4}$$

where the Schwarzian derivative is defined to be

$$\{z, x\} = \frac{z'''(x)}{z'(x)} - \frac{3}{2}\left(\frac{z''(x)}{z'(x)}\right)^2 \tag{3.5}$$

Consequently, the difference of two classical stress tensors is a quadratic differential.

A classical stress tensor, or equivalently a projective connection (3.3) can be used to define globally a Schröedinger equation

$$\left(\partial_{x_a}^2 - T_a(x_a)\right)\psi_a(x_a) = 0 \tag{3.6}$$

which behaves well under coordinate transformations if $\psi$ transforms appropriately:

$$\psi_a(x_a) = \left(\frac{dx_b}{dx_a}\right)^{-\frac{1}{2}} \psi_b(x_b) \tag{3.7}$$

This has two-dimensional space of solutions, spanned by $\psi_{a;1}$ and $\psi_{a;2}$. The Wronskian of

two solutions

$$W(\psi_{a;1}, \psi_{a;2}) = \psi_{a;1}\partial_{x_a}\psi_{a;2} - \psi_{a;2}\partial_{x_a}\psi_{a;1} \tag{3.8}$$

is constant and invariant under coordinate transformations.

If we know a solution $\psi(x)$, we can get a second independent solution by quadrature:

$$\psi'(x) = \psi(x)\int^x \frac{dx'}{\psi(x')^2} \tag{3.9}$$

**Special coordinates**

Let's choose the covering $\{U_a\}$ of $C$ to be fine enough so that the solution $\psi_2$ is never 0, and we normalize the solutions in such a way that the ratio of two solutions has Wronskian 1.

$$W\left(\psi_{a;1}, \psi_{a;2}\right) = 1 \tag{3.10}$$

Define

$$s_a(x) = \frac{\psi_{a;1}(x)}{\psi_{a;2}(x)} : U_a \to \mathbb{C} \tag{3.11}$$

gives a map $C \to \mathbb{C}P^1$ defined up to monodromies in $\mathrm{SL}(2,\mathbb{C})$. It is also a local *complex* coordinate such that the Schröedinger operator reduces to $\partial^2_{s_a}$. Notice that

$$\partial_{x_a} s_a(x_a) = \frac{1}{\psi_{a;2}(x_a)^2} \tag{3.12}$$

so never zero and thus the map is non-singular.

Recall that the Schwarzian derivative $\{z, x\}$ is 0 if and only if $z(x)$ is a Möbius transformation

$$z(x) = \frac{ax+b}{cx+d}, \quad \begin{pmatrix} a & b \\ c & d \end{pmatrix} \in PGL_2(\mathbb{C}) \tag{3.13}$$

So once we assign the differential operator to be $\partial^2_{s_a}$ with $T_a(s_a)$ in one open subset $U_a$, it will be preserved different and $s_a$ are related by Möbius transformation.

Formally speaking, if we have a projective connection on $C$, we can associate to each overlapping $U_a \cap U_b$ a *constant* map

$$U_a \cap U_b \to PSL_2(\mathbb{C}) \tag{3.14}$$

**Flat connection**

The constant map (3.14) tells us all the transition functions are constant, which gives rise to a *flat* $PSL_2(\mathbb{C})$ bundle. Let's represent this as a holomorphic $PSL_2(\mathbb{C})$ bundle $\mathcal{F} \to C$ with a holomorphic connection $\mathcal{D}_z$, which is automatically flat.

From this perspective, we can think of the coordinate $s_a : U_a \to \mathbb{CP}^1$ as a *global* section of an associated $\mathbb{CP}^1$-bundle

$$\mathbb{P}^1_{\mathcal{F}} = \mathcal{F} \times_{PGL_2(\mathbb{C})} \mathbb{CP}^1 \tag{3.15}$$

with the following *oper* condition:

- the global section has a nowhere vanishing derivative with respect to $\mathcal{D}_z$

There is an equivalent way of rephrasing this *oper* condition[125]. Let $E \to C$ be a flat rank two complex vector bundle over the Riemann surface $C$, with a holomorphic line sub-bundle $L \subset E$ that satisfies the following property:

- $L$ is nowhere invariant under parallel transport by $\mathcal{D}_z$

More explicitly, if $\sigma$ is a local nonzero holomorphic section of $L$, then the statement that $L$ is nowhere invariant is the same as

- $\sigma \wedge \mathcal{D}_z \sigma$ is nowhere zero

We then have the definition for a $PGL_2$-oper on $C$: it is a flat principal $PSL_2(\mathbb{C})$-bundle $\mathcal{F} \to C$ with

- a holomorphic connection $\mathcal{D}_z$
- a sub-bundle $\mathcal{F}_B$ which is $B$-reduction of $\mathcal{F}$,

where the Borel subgroup $B \subset PSL_2(\mathbb{C})$ is the group of upper triangular matrices.

It is easy to see the $PSL_2(\mathbb{C})$-oper is the same as the projective connection we defined in the previous section, where the datum of the principal $B$-bundle $\mathcal{F}_B$ is equivalent to the datum of a section of the associated $\mathbb{CP}^1$-bundle $\mathbb{P}^1_{\mathcal{F}}$. To see this, recall that

$$\mathbb{CP}^1 = PSL_2(\mathbb{C})/B \tag{3.16}$$

so each point in $\mathbb{CP}^1$ defines a copy of subgroup $B \subset G$. As a result, a section of $\mathbb{P}^1_{\mathcal{F}}$ defines a principal $B$ sub-bundle.

How do we then interpret the oper condition from this perspective? Intuitively, we would like to say the nowhere does the flat connection $\mathcal{D}_z$ preserve the principal $B$-subbundle. To see this more clearly, we might want to choose a local coordinate $z$ on an open subset $U \subset C$, and trivialize the holomorphic bundle $\mathcal{F}$, then the connection $\mathcal{D}_z$ can be written as

$$\mathcal{D}_z = \partial_z + \begin{pmatrix} a(z) & b(z) \\ c(z) & -a(z) \end{pmatrix} \tag{3.17}$$

which, under changes of trivialization of $\mathcal{F}$, transforms like a gauge transformation for the group $G = PSL_2(\mathbb{C})$. So if we gauge transform to the *horizontal* trivialization where $\mathcal{D}_z = \partial_z$, then the oper condition is just

$$\blacksquare \quad \partial_z s \neq 0, \quad \forall z \tag{3.18}$$

by thinking of the global section as a function $U \to \mathbb{CP}^1$.

However, clearly, this is not very useful since we just went back to our starting point. One practical and ingenious way to proceed is to only allow a partial gauge fixing. More precisely, we choose a trivialization of $\mathcal{F}$ on $U \subset C$ that is induced by a trivialization of $\mathcal{F}_B$ on $U$. In other words, we only allow gauge transformation in $B$, the group of upper triangular matrices.

The the oper condition of nonvanishing derivative just means intuitively that moving the point $x \in U$ maps a nonzero change in $\mathfrak{sl}_2/\mathfrak{b}$. So we conclude that

■ the oper condition simply means $c(z)$ is nowhere vanishing,

which is a gauge invariant statement for the group $B$, since performing gauge transformation of the group $B$ will change $c(z) = 0$ to $c(z) \neq 0$ or vice versa. On the other hand, it would not be a gauge invariant statement in the trivialization (3.17).

Having realized this, we can then use the gauge transformation to bring the connection to the standard form

$$g\mathcal{D}_z g^{-1} = \partial_z + \begin{pmatrix} 0 & b + a^2 + \partial_z a \\ 1 & 0 \end{pmatrix} \tag{3.19}$$

where the gauge transformation is

$$g = \begin{pmatrix} 1 & -a \\ 0 & 1 \end{pmatrix} \cdot \begin{pmatrix} c^{1/2} & 0 \\ 0 & c^{-1/2} \end{pmatrix} \tag{3.20}$$

Denote $t(z) = b(z) + a(z)^2 + \partial_z a(z)$. Then trivialize the rank two bundle $E \to C$ by $\psi$ and $\partial_z \psi$, where the differential equaiton take the form

$$\left(\partial_z + \begin{pmatrix} 0 & b + a^2 + \partial_z a \\ 1 & 0 \end{pmatrix}\right) \begin{pmatrix} \partial_z \psi(z) \\ -\psi(z) \end{pmatrix} = \begin{pmatrix} \partial_z^2 \psi - t(z)\psi \\ 0 \end{pmatrix} = 0 \tag{3.21}$$

is thus equivalent to the second order differential operator we consider in the previous section

$$\left(\partial_z^2 - t(z)\right)\psi = 0 \tag{3.22}$$

Under a change of coordinate, $z = z(x)$, the connection becomes

$$\partial_x + z'(x) \begin{pmatrix} 0 & t(z(x)) \\ 1 & 0 \end{pmatrix} \tag{3.23}$$

which can be brought back to the standard form via appropriate gauge transformation

$$\partial_x + \begin{pmatrix} 0 & t_x(x) \\ 1 & 0 \end{pmatrix} \tag{3.24}$$

where

$$t_x(x) = \left(\frac{\partial z}{\partial x}\right)^2 t_z(z(x)) - \frac{1}{2}\{z, x\} \tag{3.25}$$

This is precisely the transformation rule we require for the projective connection (3.4).

We can re-write (3.25) to be

$$\partial_x^2 - t_x(x) = (\partial_x z)^{\frac{3}{2}} \Big(\partial_z^2 - t_z(z)\Big)(\partial_x z)^{\frac{1}{2}}. \tag{3.26}$$

which implies it is an differential operator that acts between

$$K_C^{-1/2} \to K_C^{3/2} \tag{3.27}$$

**Stokes data**

The Stokes data of a Schröedinger equation are defined as the point in an appropriate space of flat $\mathrm{SL}(2, \mathbb{C})$ connections defined by parallel transport of the solutions. The data of the flat connections depend on the types of singularities of $T(x)$:

- If $T(x)$ is holomorphic, the Stokes data encode the monodromy of the solutions

around cycles of $C$.

- If $T(x)$ has regular singularities, at which

$$T(x) \sim \frac{m^2 - \frac{1}{4}}{(x - x_0)^2} \tag{3.28}$$

then one also has monodromies around the regular punctures. For generic $m$, one can define monodromy eigenvectors $\psi_{\pm}^{x_0}(x)$ and express the Stokes data in terms of Wronskians between eigenvectors transported along various paths on $C$.

- If $T(x)$ has irregular singularities, at which

$$T(x) \sim \frac{c}{(x - x_0)^{r+2}} \tag{3.29}$$

then one also has $r$ Stokes matrices at the irregular puncture. One can define $r$ special solutions $\psi_i^{x_0}(x)$ which decay exponentially fast along appropriate rays towards $x_0$. The Stokes data can be expressed in terms of Wronskians between such solutions transported along various paths on $C$.

- We will also be interested in exponential singularities, at which

$$T(x) \sim e^{\frac{c}{x - x_0}} \tag{3.30}$$

We will see that at such a singularity one can define an infinite sequence of special solutions $\psi_i^{x_0}(x)$.

### Classical limit of BPZ equation

One can find the appearance of opers in many physical settings. One of such arises from the semiclassical limit of a conformal block for correlation functions of degenerate Virasoro primary fields [125], which we will review below.

Primary fields of Virasoro are associated with the highest weight representations of the Virasoro algebra. Of special importance, a *degenerate* primary field is a primary field of Virasoro algebra whose descendant at a certain level is null, i.e. a highest weight vector. They will be labelled by two integers $\Phi_{r,s}$, for $r, s = 1, 2, 3, \ldots$. A correlation function with an insertion of a degenerate field will satisfy a certain differential equation due to the null-ness condition, called Belavin–Polyakov–Zamolodchikov (BPZ) equation.

For now, we will only focus on a special case $r = 2, s = 1$. BPZ equation for degenerate field $\Phi_{2,1}$ reads

$$\partial^2 \Phi_{2,1}(x) + b^2 : T(x)\Phi_{2,1}(x) := 0 \tag{3.31}$$

where $b$ parametrize the central charge

$$c = 13 - 6(b^2 + \frac{1}{b^2}) \tag{3.32}$$

In the semi-classical limit $b \to 0$, normal ordering is irrelevant and we define the classical stress tensor $t(x) = b^2 T(x)$, whose transformation under change of coordinate is deduced from

$$T(x) = \left(\frac{d\tilde{x}}{dx}\right)^2 \tilde{T}(\tilde{x}) + \frac{c}{12}\{\tilde{x}, x\} \tag{3.33}$$

and reads

$$t(x) = \left(\frac{d\tilde{x}}{dx}\right)^2 \tilde{t}(\tilde{x}) - \frac{1}{2}\{\tilde{x}, x\} \tag{3.34}$$

The conformal dimension of $\Phi_{2,1}(x)$ is

$$h_{2,1} = -\frac{1}{2} - \frac{3}{4}b^2 \tag{3.35}$$

Therefore, in the limit $b \to 0$, it transforms as a section of $K_C^{-1/2}$

## 3.3 ODE/IM correspondence for Ising model

We are now ready to explain our proposed interpretation of ODE/IM correspondence using the Kondo defect. As an instructive toy example, we study ODE/IM correspondence for the Ising model.

The main object we are interested in is the expectation value of the Kondo line defect $T_S(\theta)$ defined in (2.33). We claim that the function $T_S(\theta)$ coincides with a basic Stokes datum for the harmonic oscillator Schröedinger equation [115]

$$e^{-2\theta}\partial_x^2 \psi(x) = (x^2 - 2)\psi(x) \tag{3.36}$$

This equation has four *small* solutions $\psi_n$, uniquely characterized by their exponentially

fast decrease along rays of direction $e^{-\frac{\theta}{2}-\frac{in\pi}{2}}$. We can normalize $\psi_0$ so that

$$\psi_0 \sim \frac{1}{\sqrt{2x}}(\sqrt{2e}x)^{e^\theta} e^{-\frac{\theta}{2}-\frac{e^\theta x^2}{2}} \tag{3.37}$$

and define

$$\psi_n(x;\theta) = \psi_0(x;\theta + i\pi n) \tag{3.38}$$

The definition can be extended to all integer $n$, with $\psi_{n+4} = -e^{-2\pi i(-1)^n e^\theta}\psi_n$.

In the current case, the Schrodinger equation (3.36) can be solved explicitly. In particular, the function $\psi_0$ can be given in terms of parabolic cylinder functions:

$$\psi_0 = \frac{e^{\frac{1}{4}\left(-2e^\theta(\theta-1)-\theta\right)} D_{\frac{1}{2}\left(-1+2e^\theta\right)}\left(\sqrt{2}e^{\theta/2}x\right)}{\sqrt[4]{2}} \tag{3.39}$$

Details can be found in Appendix D.1. Importantly, since the equation (3.36) is regular everywhere on the complex plane, the solution $\psi_0$ is an entire function.

The Wronskian $(\psi_n, \psi_{n+1}) \equiv \psi_n \partial_x \psi_{n+1} - \psi_{n+1}\partial_x \psi_n$ of consecutive solutions is $-i$. Because of the periodicity, we also have $i(\psi_{-1}, \psi_2) = e^{-2\pi i e^\theta}$. We have

$$T_S(\theta) = i(\psi_{-1}, \psi_1) \tag{3.40}$$

The simplest proof of this fact is that the two functions satisfy the same Riemann-Hilbert problem in the $\theta$ plane.

The Hirota recursion (2.54) follows from the Plücker relation[1] between the Wronskians:

$$(\psi_{-1}, \psi_1)(\psi_0, \psi_2) = (\psi_{-1}, \psi_0)(\psi_1, \psi_2) + (\psi_0, \psi_1)(\psi_{-1}, \psi_2) \tag{3.41}$$

A standard WKB analysis as reviewed in Appendix D.2 controls the IR asymptotics. The WKB analysis employs the WKB network, namely the union of flow lines[2], along which the WKB differential

$$\sqrt{x^2 - 2}e^\theta dx \tag{3.42}$$

is real, shown in Fig. 3.1. In contrast to the generic flow lines which end on singularities,

[1] This simply follows from the fact that any three vectors $a$, $b$, $c$ in a two dimensional vector space must satisfy a linear relation in the form of $(a,b)c+(b,c)a+(c,a)b = 0$, where brackets denote exterior product.

[2] Various names are used in the literature. The WKB network is often called spectral network or Stokes diagram in the literature, where the WKB line goes under the name of Stokes line or anti-Stokes line.

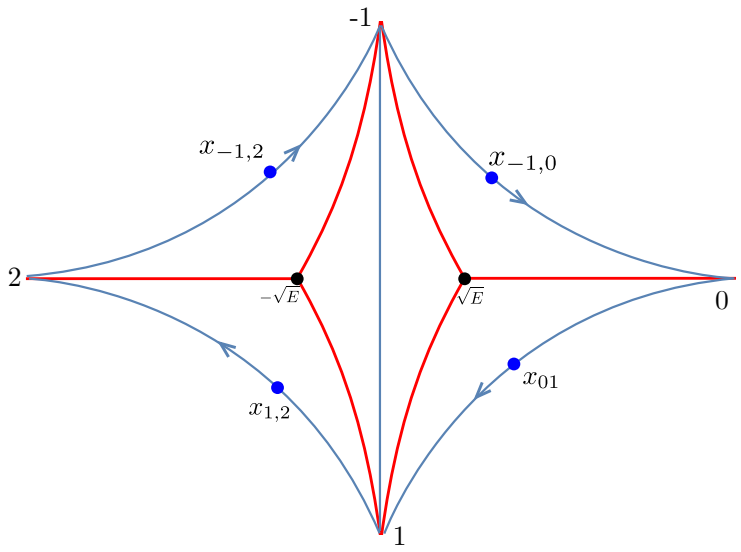


Figure 3.1: WKB diagram for the differential equation (3.36) defined in (3.42). Generic flow lines and WKB lines are colored blue and red respectively.

there are special lines emanating from a zero of the differential, which we will refer to as WKB lines.

The cross-ratio

$$\frac{(\psi_0,\psi_1)(\psi_{-1},\psi_2)}{(\psi_{-1},\psi_0)(\psi_1,\psi_2)} = e^{-2\pi i e^{\theta}} \tag{3.43}$$

is controlled by the period of $\sqrt{x^2-2}\,dx$ around a contour wrapping around the cut, while the IR asymptotics of the Wronskian are controlled by a (vanishing) regularized period of $\sqrt{x^2-2}\,dx$ from $-i\infty$ to $i\infty$, where the regularization subtracts the reference asymptotics in (3.37)

$$T_S(\theta) \equiv i(\psi_{-1},\psi_1) \sim 1 + \dots \tag{3.44}$$

The UV asymptotics can be obtained by dropping the constant term on the right-hand side of the Schröedinger equation. Indeed, we can rescale the $x$ variable to get

$$e^{-2\theta}\partial_x^2\psi(x) = (x^2 - 2g^2)\psi(x) \tag{3.45}$$

which is amenable to a perturbative expansion in the UV.

## 3.4 The ODE/IM solution $SU(2)_k$ WZW

Having tested the techniques in the toy example, we now turn to the main example: the ODE/IM correspondence for the chiral $SU(2)$ WZW model.

Following the same recipe, we propose to identify the expectation value of the Kondo defect $T_n[\theta]$ defined in (2.57) with the Stokes data of the Schröedinger equation

$$\partial_x^2\psi(x) = e^{2\theta}e^{2x}(1+gx)^k\psi(x) \tag{3.46}$$

The first immediate observation is that the shift $x \to x - \frac{1}{g}$ maps the equation to

$$\partial_x^2\psi(x) = e^{2\theta}e^{-\frac{2}{g}}g^k e^{2x}x^k\psi(x) \tag{3.47}$$

so that the Stokes data is only a function of the combination $e^{\theta}e^{-\frac{1}{g}}g^{\frac{k}{2}}$, as in (2.63).

### ODE definition of $T_n$

We can define the solution $\psi_0(x;\theta)$ of

$$e^{-2\theta}\partial_x^2\psi(x) = (1+gx)^k e^{2x}\psi(x) \tag{3.48}$$

for real positive $g$ as the solution which decreases asymptotically fast along the line of large real positive $x+\theta$. If we analytically continue in $g$, the imaginary part of $x+\theta$ has to be accordingly adjusted to keep $e^{\theta}(1+gx)^{\frac{k}{2}}e^x dx$ real and positive.

We can normalize $\psi_0$ so that it agrees with WKB asymptotics in that region, as before:

$$\psi_0(x;\theta) \sim \frac{1}{\sqrt{2(1+gx)^{\frac{k}{2}}e^{x+\theta}}}e^{-e^{\theta}f_k(x;g)} \tag{3.49}$$

for large positive real $x+\theta$. Here $f_k(x;g)$ is a function defined by

$$f_k(x;g) = \int_{-\frac{1}{g}}^{x} e^y(1+gy)^{\frac{k}{2}}dy = e^{-\frac{1}{g}}g^{\frac{k}{2}}\int_0^{x+\frac{1}{g}} e^y y^{\frac{k}{2}}dy \tag{3.50}$$

We then define again an infinite sequence of other solutions

$$\psi_n(x;\theta) \equiv \psi_0(x;\theta + i\pi n) \tag{3.51}$$

which have the above asymptotics for large positive real $x+\theta+i\pi n$.

The Stokes coefficients of this Schröedinger equation consist of the Wronskians $i(\psi_0,\psi_n)$. The large positive $x$ asymptotics guarantee $i(\psi_0,\psi_1)=1$, but the other Wronskians are non-trivial functions of $\theta$.

Adjusting the shifts to match the quantum determinants and Hirota relations in a standard form, we can propose

$$T_{n;l}(\theta)=i\left(\psi_0(x;\theta-\frac{i\pi n}{2}),\psi_0(x;\theta+\frac{i\pi n}{2})\right) \tag{3.52}$$

At large negative $x$, the right hand side of the Schröedinger equation decreases exponentially and thus we must have

$$\psi_0(x;\theta)\sim -Q(\theta)(x+\frac{1}{g})-\tilde{Q}(\theta) \tag{3.53}$$

up to exponential corrections. We included the $\frac{1}{g}$ shift so that both $Q(\theta)$ and $\tilde{Q}(\theta)$ are functions of $e^{\theta}e^{-\frac{1}{g}}g^{\frac{k}{2}}$ only. [3]

The $T$-functions $T_n$ take the form of quantum determinants built from $Q$ and $\tilde{Q}$,

$$T_{n;l}(\theta)=iQ(\theta+\frac{i\pi n}{2})\tilde{Q}(\theta-\frac{i\pi n}{2})-i\tilde{Q}(\theta+\frac{i\pi n}{2})Q(\theta-\frac{i\pi n}{2}) \tag{3.54}$$

which can be naturally interpreted as the two $Q$-functions for the system. [4]

### The UV fixed point $g=0$

If we turn off the coupling, we have the simpler equation

$$e^{-2\theta}\partial_x^2\psi(x)=e^{2x}\psi(x) \tag{3.55}$$

[3] Notice that there is an interesting spectral problem where one requires $\psi$ to be finite at large negative $x$ and asymptotically decreasing at large positive $x$. The zeroes of the $Q(\theta)$ functions are the solutions of that spectral problem

[4] Finding a direct 2d CFT physical interpretation for the $Q$ functions, or $\psi_0(x;\theta)$ itself, is a long standing problem, which we do not address in this work.

This has a unique solution

$$\psi_0(x;\theta) = \frac{1}{\sqrt{\pi}} K_0(e^{x+\theta}) \tag{3.56}$$

which behaves as

$$\psi_0(x;\theta) \sim \frac{1}{\sqrt{2e^{x+\theta}}} e^{-e^{x+\theta}} \tag{3.57}$$

for large positive real $x+\theta$.

On the other hand, at large negative real part of $x+\theta$ we have

$$\psi_0(x;\theta) \sim -\frac{1}{\sqrt{\pi}}(x+\theta+\gamma-\log 2) \tag{3.58}$$

up to exponentially small corrections.

We can obtain an infinite sequence of other solutions

$$\psi_n(x;\theta) \equiv \psi_0(x;\theta+i\pi n) = \frac{1}{\sqrt{\pi}} K_0(e^{x+\theta}) - \pi i n \frac{1}{\sqrt{\pi}} I_0(e^{x+\theta}) \tag{3.59}$$

which have the above asymptotics for large positive real $x+\theta+i\pi n$. Clearly, at large negative real part of $x+\theta$ we have

$$\psi_n(x;\theta) \sim -\frac{1}{\sqrt{\pi}}(x+\theta+i\pi n+\gamma-\log 2) \tag{3.60}$$

so that the Wronskian of two such solutions is exactly

$$i(\psi_0,\psi_n) = n \tag{3.61}$$

which is the expected UV value of $T_n$.

**Weak-coupling expansion**

When $g$ is sufficiently small and positive, it is reasonable to attempt a perturbative expansion of the solution $\psi_0$ around the $g=0$ solution

$$\psi_0^{(0)}(x;\theta) = \frac{1}{\sqrt{\pi}} K_0(e^{x+\theta}) \tag{3.62}$$

The perturbative expansion should be valid for $x \ll \frac{1}{g}$ and match smoothly with the expansion of the asymptotic expression 3.49 in positive powers of $g$.

At each order of the perturbative expansion we solve a Schröedinger equation with a source that decreases exponentially at large positive $x$ and select the solution $\psi_0^{(n)}(x;\theta)$ which also decreases exponentially and matches the expansion of the asymptotic expression 3.49 in positive powers of $g$.

At large negative $x$, the perturbative corrections will systematically correct the Q functions to some

$$\begin{aligned} Q(\theta) &= \frac{1}{\sqrt{\pi}}\left(1 + q_1 g_{\text{eff}}(\theta) + \cdots\right) \\ \tilde{Q}(\theta) &= \frac{1}{\sqrt{\pi}}\left(-\frac{1}{g_{\text{eff}}} + \tilde{q}_0 + \tilde{q}_1 g_{\text{eff}}(\theta) + \cdots\right) \end{aligned} \tag{3.63}$$

where the $g$ and $\theta$ dependence combine into a power series in $g_{\text{eff}}(\theta)$.

The Wronskian relation $i(\psi_0, \psi_1) = 1$ should hold automatically. It actually determines the expansion coefficients of $Q$ in terms of these of $\tilde{Q}$.

When we plug the expansion of the $Q$ functions into the quantum determinant expression for $T_n(\theta)$, the result only depends on the $\tilde{q}_n$ starting from the order $g^4$. The lower orders are fixed uniquely. We have

$$T_n \sim n - \frac{\pi^2}{2} k I_R g^3 + \frac{\pi^2}{4} I_R g^4 \left[3k^2 + 2k(-\tilde{q}_0 - 3\theta) + 8\tilde{q}_1\right] \cdots \tag{3.64}$$

where $I_R = \frac{1}{6} n\left(-1 + n^2\right)$ and $\tilde{q}_0 = -\frac{k}{4} + (\gamma - \log 2)$. In particular, in order to match with the explicit line defect calculations we only need the first sub-leading coefficient $\tilde{q}_1$ in the expansion of $\tilde{Q}$, which can be found in Appendix D.3.

### WKB IR expansion

The WKB analysis of the Schröedinger equation, valid in the IR limit $e^\theta \to \infty$, requires a slightly more refined analysis than the Voros/GMN-style one applicable to meromorphic potentials with simple zeroes [81, 88]. In Appendix D.2, we review the standard analysis and extend it to the case of zeroes of higher degree or exponential singularities.

A crucial role is played by the WKB/spectral network, which depicts the structure of

the WKB lines, along which the leading WKB differential

$$(1+gx)^{\frac{k}{2}}e^{x+\theta}dx \tag{3.65}$$

is real. The main property of WKB lines is that the WKB solutions which are asymptotically growing along the WKB lines can be trusted as an approximation for the parallel transport of true solutions.

A GMN-style analysis focuses on generic WKB lines, which join asymptotic directions where some small solutions have been defined. The Wronskian of the small solutions at the endpoints of a WKB line can be estimated reliably as the Wronskian of the corresponding WKB approximants. The asymptotic approximation is valid in a whole half-plane in the $e^{\theta}$ plane centered around the ray used to draw the WKB network. [5]

For Schröedinger equation with a meromorphic potential and simple zeroes and generic $\theta$, the generic WKB lines give estimates for exactly enough "WKB" Wronskians to fully determine the full Stokes data. All other Wronskians and monodromies can be reconstructed as Laurent polynomials in the WKB Wronskians.

In more general situations we need to work a bit harder, and use WKB lines which join an asymptotic direction and matching regions near zeroes of higher order or where the potential is exponentially small. The WKB lines can still be used to reliably transport the small solutions to the matching regions, where they can be compared with an appropriate basis of local solutions. The case at hand is a beautiful example of the generalized analysis. We will present the results here and a more detailed discussion in Appendix D.2.2. For a generic phase of $e^{\theta}$ one has that

- $k+2$ consecutive asymptotic lines at large positive real $x+\theta+i\pi n$ are connected by special WKB lines to the order $k$ zero at $x=-\frac{1}{g}$. Say that $n_0 \leq n \leq n_0+k+1$ for some $n_0$ which can be easily determined. This allows a WKB estimate of the Wronskians of pairs of $\psi_n$'s in this interval. With our conventions, it is just $d^{(k)}_{n'-n}$. These Wronskians compute certain $T_{n'-n}$ functions in a specific range of $\mathrm{Im}\theta$. We learn that the corresponding $L_{\frac{n'-n}{2}}[\theta]$ likely flow to $\mathcal{L}_{\frac{n'-n}{2}}$ topological defects. This expectation will be further solidified by the analysis of the $T_{n'-n;l}$ asymptotics.

- The remaining asymptotic lines get connected by special WKB lines to the asymptotic region at large negative real part of $x+\theta$, but the imaginary part of $x+\theta$ gets shifted by $\pm\frac{\pi}{2}k$. Say that the imaginary part increases by $\frac{\pi}{2}k$ for $n \geq n_0+k+1$ and decreases

[5] If WKB network is defined by $(1+gx)^{\frac{k}{2}}e^{x+\theta_0}dx \in \mathbb{R}^+$, then the formal WKB series is an asymptotic series as $e^{-\theta} \to 0$ within a closed half plane $\mathbb{H}_{\theta_0} = \{\mathrm{Re}(e^{\theta-\theta_0}) \geq 0\}$.

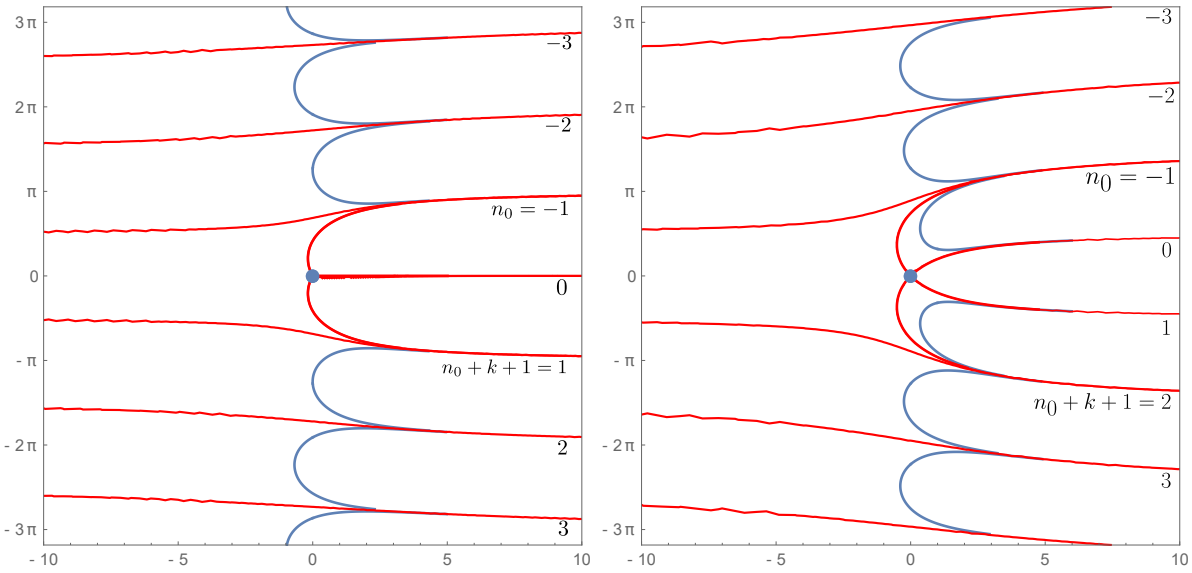


Figure 3.2: WKB diagram for $k = 1$ (left) and $k = 2$ (right). Generic flow lines and WKB lines are colored blue and red respectively. $\theta$ is chosen to be 0 and $-i\frac{\pi}{2}$ respectively. We number the WKB lines on large positve $x$ side increasingly from top. There are $k+2$ WKB lines that are connected to the zero, numbered from $n_0$ to $n_0 + k + 1$.

by $\frac{\pi}{2}k$ for $n \leq n_0$. With our conventions, up to factors of the form $e^{m_{n,n'}e^{\theta}}$ for some $m_{n,n'}$, one gets WKB estimates $n'-n$ for pairs of lines which are on the same side of $n_0$, $n'-n-k$ otherwise. These WKB estimates help us predict RG flows ending on $L^{IR}_{n'-n} \otimes \mathcal{L}_{\frac{k}{2}}$ or $L^{IR}_{n'-n-k} \otimes \mathcal{L}_{\frac{k}{2}}$ defects.

This is enough to reconstruct the RG flows near the real $\theta$ axis. The Wronskians that do not fall into these two types can be related to these two types via Plücker formulae. This is the same as using Hirota relations to explore general $\theta$.

We refer to Appendix D.2.4 for details.

## 3.5 Expected generalizations

### 3.5.1 Multichannel Kondo problems

The simplest generalization of the Kondo defects is to consider a theory with multiple $\mathrm{su}(2)_{k_i}$ WZW currents and couple them all to the same line defect by a coupling

$$\int \sigma_a \sum_i g_i J_i^a dx^0 \tag{3.66}$$

which, in 4d CS setup, corresponds to taking multiple chiral WZW surface defects of levels $k_i$ at positions $z_i$. This results in a classical coupling of the schematic form

$$\int \sigma_a \sum_i \frac{1}{z-z_i} J_i^a dx^0 \tag{3.67}$$

Assuming the classical couplings are not corrected, we get an immediate prediction: two such line defects should give commuting transfer matrices if the couplings can be written as $g_i = \frac{1}{z-z_i}$ and $g'_i = \frac{1}{z'-z_i}$.

A second prediction is that this one-parameter family of commuting defects would be connected by RG flow, with the RG flow translating the $z$ parameter according to the 1-form

$$dz + \sum_i \frac{k_i}{2(z-z_i)} dz \tag{3.68}$$

This gives RG flow equations

$$\mu\partial_\mu g_i = -\frac{g_i^2}{1+\sum_j \frac{k_j}{2} g_j} \tag{3.69}$$

which can be checked against explicit 2d perturbative calculations. Details can be found in Appendix C.1.6. We should stress that the perturbative match of the RG flow equations is rather non-trivial in the multi-channel case, as redefinitions of the couplings leave invariant infinitely many combinations of beta function coefficients, rather than the single "$c$" we found in the single coupling case.

There is a simple proposal for an ODE/IM solution for the expectation values of the line defect: they should coincide with the Stokes data for the equation

$$\partial_x^2\psi(x) = \left[e^{2\theta+2x}\prod_i (1+g_i x)^{k_i} + u(x)^2 - u'(x)\right]\psi(x) \tag{3.70}$$

where

$$u(x) = \sum_i \frac{l_i}{x+1/g_i} \tag{3.71}$$

We can define an overall scaling parameter $g \equiv 1/z$ and set $g_i = g/(1+z_i g)$ where, say, $\sum_i z_i = 0$. Performing a translation of $x$, we can rewrite the equation as

$$\partial_x^2\psi(x) = \left[e^{2\theta}e^{-2/g}g^{\sum_i k_i}\prod_i (1+gz_i)^{-k_i}e^{2x}\prod_i (x+z_i)^{k_i} + \Big(\sum_i \frac{l_i}{x+z_i}\Big)^2 + \sum_i \frac{l_i}{(x+z_i)^2}\right]\psi(x) \tag{3.72}$$

and the Stokes data will only depend on $\{z_i\}$ and the combination

$$e^{-1/g_{\text{eff}}(\theta)} g_{\text{eff}}(\theta)^{\sum_i k_i/2} \equiv e^{\theta}e^{-1/g}g^{\sum_i k_i/2}\prod_i (1+gz_i)^{-k_i/2} \tag{3.73}$$

where we define the effective coupling $g_{\text{eff}}$, analogous to (2.63).

The Stokes data can be defined as before in Section 3.4. A primary state $|l_1, l_2, \dots\rangle$ is labeled by a list of half integers, one for each $\mathfrak{su}(2)$ factor. We therefore make the following identification

$$\langle l_1, l_2, \dots|\hat{T}_n|l_1, l_2, \dots\rangle \equiv T_{n;l_i}(\theta) = i\left(\psi_0(x;\theta - \frac{i\pi n}{2}), \psi_0(x;\theta+\frac{i\pi n}{2})\right) \tag{3.74}$$

In the UV, it will have a perturbative expansion in $g_i$ around $T_{n;l_i} \sim n$. We perform the calculation in detail in Appendix D.3.3. The result matches nicely with the direct 2d perturbative calculations.

In the IR, the WKB analysis can be done in a straightforward way, with relatively simple answers for real values of the $g_i$.

An entertaining check is that if two $g_i$'s coincide, the equation is the same as for a model with one fewer WZW factors. This is reasonable: a coupling involving a sum $J_i^a + J_j^a$ with equal coefficients naturally factors through the WZW model of level $k_i + k_j$ defined by the total currents $J_i^a + J_j^a$, with the remaining coset model decoupling from the line defect.

Notice that the Schröedinger equation seems to take a universal form

$$\partial_x^2 \psi(x) = \left[e^{2\theta} e^{2p(x)} + u(x)^2 - u'(x)\right] \psi(x) \tag{3.75}$$

where $\partial_x p(x) = \omega(x)$. We will see momentarily that this statement holds for other examples as well. We expect it to hold universally for any purely chiral 4d $SU(2)$ CS setup. We will explore this point further, as well as relations to affine Gaudin models and affine Geometric Langlands, in a future publication.[2]

### 3.5.2 Coset Kondo lines

A well studied class of examples of ODE/IM correspondence involves polynomial potentials

$$\partial_x^2 \psi(x) = e^{2\theta} P_n(x) \psi(x) \tag{3.76}$$

where $P_n$ is a polynomial of degree $n$, say with $m$ zeroes of order $k_i$.

Based on the various examples in the literature e.g. [102], it is easy to guess that this differential equation should control the vacuum expectation values of Kondo lines in coset models of the form

$$\frac{\prod_{i=1}^m \mathrm{su}(2)_{k_i}}{\mathrm{su}(2)_{\sum_i k_i}} \tag{3.77}$$

The integrable Kondo defects are deformations of certain topological line defects by the chiral coset primary fields with coset labels $[1;3]$. These are the primary fields $\Phi^{(i)}$ which appear in the coset decomposition of the $\mathrm{su}(2)_{k_i}$ currents $J_a^{(i)}$:

$$J_a^{(i)} = \Phi^{(i)} \otimes \phi^a + \cdots \tag{3.78}$$

with $\phi^a$ being the spin 1 primary of the diagonal $\mathrm{su}(2)_{\sum_i k_i}$. There are $m-1$ such coset fields, so the Kondo defects have $m-1$ couplings of the same scaling dimension. They are mapped to the relative positions of the zeroes of $P_n(x)$.

The basic topological line defects which support $\phi^a$ local operators are these labeled by primary fields of $\mathrm{su}(2)_{\sum_i k_i}$. There are $n-1$ of them, as the identity line or the spin $\frac{n}{2}$ do not support non-trivial primaries. They match nicely the possible Wronskians built from the $n+2$ small solutions for the ODE.

The RG flows admit a perturbative UV description if at least one of the levels is large so that the scaling dimension of the $\phi^a$ is close to 1. For example, if one of the levels $\kappa$ is large while the others are kept finite, so that we study the coset

$$\frac{\mathfrak{su}(2)_\kappa \times \prod_i \mathrm{su}(2)_{k_i}}{\mathfrak{su}(2)_{\kappa+\sum_i k_i}} \tag{3.79}$$

and the ODE will be

$$\partial_x^2 \psi(x) = \left[\prod_i (1+g_i x)^{k_i}\right] x^\kappa \psi(x) \tag{3.80}$$

We expect this to be a "trigonometric" 4d CS setup, where the holomorphic direction is a $\mathbb{C}^*$ with local coordinate $z = e^w$ and the classical differential is

$$\omega = \frac{\kappa}{2z} dz \tag{3.81}$$

corrected by the coupling to 2d WZW models to

$$\omega = \frac{\kappa}{2z} dz + \sum_i \frac{k_i}{2(z-z_i)} dz \tag{3.82}$$

We remark that (3.80) takes the same form as the ODE for anisotropic Kondo model [126, 127]. See the discussion in [127] for more details. We leave this for future investigations.

### 3.5.3 WZW vs Kac-Moody

At the expense of ruining unitarity, we can replace the WZW currents at integral level $k$ with Kac-Moody currents at some generic level $\kappa$. At the level of perturbation theory,

there is no difference. Non-perturbatively, there must be deep differences, as most of the RG statements we made for integral $k$ do not have a natural extension to non-integral $\kappa$.

For large $\kappa$ and finite $j$, the perturbative considerations still indicate the RG flow $L_j^{UV} \to \mathcal{L}_j$. The topological lines $\mathcal{L}_j$ in Kac-Moody exist for all $j$, but non-perturbative effects should kick in as $j \simeq \kappa$.

As the spin $j$ is integral, one cannot make sense directly of "$\mathcal{L}_{\frac{\kappa}{2}}$" which appears in the RG flows at integral $k$. The spin $\frac{\kappa}{2}$ primary in WZW models, though, has another interpretation: it is the image of the vacuum module under a spectral flow operation. This suggests that the large $j$ RG flow in the Kac-Moody theory may land on topological lines associated with spectral flowed modules.

Another interesting new wrinkle is that once we compute the $\hat{T}_j$, we can subject the Kac-Moody current modes in them to a spectral flow operation. As the $\hat{T}_n$ commute both with $L_0$ and $J_0^3$, the image under $w$ units of spectral flow will also give a conserved operator $\hat{T}_{n;w}$. This suggests we should be able to define spectral flow images $L_{j;w}[\theta]$ of the usual $L_j[\theta]$ defects. The UV definition may be a bit subtle, but the notion should be well-defined.

We will now propose an ODE/IM interpretation of the $T_{n;w}[\theta]$, which suggests how one may compute the IR image of $L_{j;w}[\theta]$ or postulate new sets of Hirota equations controlling their fusion.

The ODE for general $\kappa$

$$e^{-2\theta}\partial_x^2\psi(x) = (1+gx)^\kappa e^{2x}\psi(x) \tag{3.83}$$

has a branch cut from $x \to -\infty$ to $x = -\frac{1}{g}$. Consequently, one can take some small solution $\psi_n(x;\theta)$, defined in the usual way, analytically continue it $w$ times around $x = -\frac{1}{g}$ to obtain a solution of

$$e^{-2\theta-2\pi i\kappa w}\partial_x^2\psi(x) = (1+gx)^\kappa e^{2x}\psi(x) \tag{3.84}$$

and take a Wronskian with some $\psi_{n'}(x;\theta+\pi\kappa w)$.

Up to picking some convention for the shifts of $\theta$, this gives a possible definition of $T_{n'-n;w}[\theta]$. Plücker relations give a slew of new Hirota-like formulae controlling the fusion of $T_{n,w}$ functions with all sort of spectral flow amounts and $\theta$ shifts by multiples of $i\pi$ and $i\pi\kappa$.

The WKB analysis of the ODE is straightforward, although the details depend somewhat sensitively on choices such as the sign of the real part of $\kappa$, etc. The main novelty

is that some of the WKB lines will go across the cut so that the collection of Wronskians with "good" WKB asymptotics may include some $T_{n;w}[\theta]$ with $w \neq 0$.

# Chapter 4

# Kondo defect, $\lambda$-oper and affine Gaudin model

The purpose of this section is to explore the connections between three topics:

1. Integrable Kondo defects in products of chiral $SU(2)$ WZW models $\prod_i \widehat{\mathfrak{sl}}(2)_{k_i}$ [1, 10, 11, 13, 19, 128, 129, 20, 21, 130, 22, 4, 14, 15, 23, 131, 16, 132, 90]. These are families of mutually commuting line defects parameterized by a conformal symmetry-breaking scale $e^{\theta} \equiv \lambda^{-1}$.

2. Bethe equations for an affine $SU(2)$ Gaudin model [133, 134, 135]. The Kondo lines can be identified with a renormalized version of the quantum transfer matrices for the affine Gaudin model. The corresponding Bethe equations (and Bethe vectors) should thus control the spectrum of the transfer matrices.

3. Solutions of the affine $\widehat{\mathfrak{sl}}(2)$ Bethe equations can be used to produce $PSU(2)$ $\lambda$-*opers with singularities of trivial monodromy* [133, 134, 136, 137, 138]. We identify the spectrum of the transfer matrices with the Stokes data of the $\lambda$-opers. This provides a complete ODE/IM correspondence for integrable Kondo problems.

## 4.1 Affine Gaudin models, classical and quantum

Given a finite dimensional simple Lie algebra $\mathfrak{g}$, highest weight $\lambda$, irrep $V_\lambda$. A $N$-site Gaudin model is defined by

- a collection of integral dominant weights $\underline{\lambda} = \{\lambda_1, \ldots, \lambda_N\}$. Then the Hilbert space is given by $V_{\underline{\lambda}} = V_{\lambda_1} \otimes \cdots \otimes V_{\lambda_N}$.
- a set $\underline{z} = \{z_1, \ldots, z_N\}$

The algebra of observables is $U(\mathfrak{g})^{\otimes N}$. There is a large commutative subalgebra called Gaudin subalgebra, which in particular contains the quadratic Gaudin Hamiltonian

$$H_i = \sum_{k \neq i} \frac{t_i^a t_k^a}{z_i - z_k} \tag{4.1}$$

where $t^a$ are a set of orthonormal basis of $\mathfrak{g}$. One can easily check that $H_i$ commute with each other. Other elements in the Gaudin subalgebra are referred to as higher Gaudin Hamiltonians, which are more complicated unknown in general. In the case of $\mathfrak{g} = \mathfrak{gl}_2$, there are no higher Gaudin Hamiltonian and $H_i$ are all we need.

The Hilbert space is $\otimes_{i=1}^N M_i$, where $M_i$ are a collection of $\mathfrak{g}$-modules. Since Gaudin algebra commutes with the diagonal action of $\mathfrak{g}$, the eigenvectors are organized into $\mathfrak{g}$ irreps. Then the natural question is the diagonalization of the commuting charges acting on $\otimes_{i=1}^N M_i$. Finding both eigenvectors and eigenvalues is achieved partially using Bethe ansatz.

A more powerful result is its surprising relation with $G^\vee$ oper, where $G^\vee$ is the Langlands dual to $G$. Gaudin algebra is isomorphic to the algebra of functions on the space of $\mathfrak{g}^\vee$ oper on $\mathbb{P}^1$ with regular singularities at $z_1, \ldots, z_N, \infty$ of trivial monodromy. In particular, since we are mostly focusing on $\mathfrak{g} = \mathfrak{sl}_2$, its dual group is $G^\vee = PGL_2$.

More precisely, for any $N$-tupe of distinct point $z_1, \ldots, z_N$, we consider a particular type of $PGL_2$-oper

$$\partial_z^2 - t(z) = (\partial_z + a(z))(\partial_z - a(z)) \tag{4.2}$$

where $t(z) = a(z)^2 + \partial a(z)$ and

$$a(z) = -\sum_{i=1}^N \frac{l_i}{z - z_i} + \sum_{j=1}^m \frac{1}{z - w_j}, l_i \in \frac{1}{2}\mathbb{Z}_{\geq 0} \tag{4.3}$$

The positions of $w_j$ are determined by the Bethe Ansatz

$$-\sum_{i=1}^N \frac{l_i}{w_a - z_i} + \sum_{j=1, j\neq a}^m \frac{1}{w_a - w_j} = 0 \tag{4.4}$$

It turns out, as a result of the Bethe Ansatz equation (4.4), $w_j$ are only apparantly singularities, namely $t(z)$ is non-singular there despite the singular behaviors of $a(z)$.

On the other hand, it can shown that [124] $z_1, \ldots, z_N, \infty$ are regular singularities with trivial monodromy. Let's write

$$t(z) = \sum_{i=1}^{N} \frac{c_i}{(z-z_i)^2} + \frac{\mu_i}{z-z_i} \tag{4.5}$$

The surprising relation between Gaudin model and opers is that

$$\left\{ c_i, \mu_i, i = 1, \ldots, N \,\middle|\, \sum_{i=1}^{N} \mu_i = 0 \right\} \tag{4.6}$$

is precisely the spectrum of the Gaudin algebra: $c_i$ are the eigenvalues of the Casimir operators $C_i = \frac{1}{2}\sum_a t_a^{(i)} t^{a(i)}$ for $i = 1, \ldots, N$ and $\mu_i$ are the eigenvalues of the Gaudin Hamiltonians $H_i$. Explicitly they are

$$c_i = l_i(l_i+1) \tag{4.7}$$

$$\mu_i = l_i \left( \sum_{j \neq i} \frac{2l_j}{z_i - z_j} - \sum_{j=1}^{m} \frac{1}{z_i - w_j} \right) \tag{4.8}$$

Note that the condition $\sum_{i=1}^{N} \mu_i = 0$ has its meaning on both sides. On the opers side, it comes from the requirement that $\infty$ is a *regular* singularity, which is automatically satisfied due to the construction $t(z) = a^2 + \partial a$ and the Bethe Ansatz equation. On the Gaudin model side, the condition $\sum_{i=1}^{N} \mu_i = 0$ has to be true since the sum of all quadratic Gaudin Hamiltonians $\sum_i H_i = 0$.

The affine Gaudin model first studied in [134], is a somewhat conjectural integrable system that quantizes the classical affine Gaudin model, in a manner analogous to the relation between the classical and quantum KdV integrable systems [139, 140, 26][1].

The classical affine Gaudin model is defined by a collection of Poisson-commuting Hamiltonians built from classical currents $\mathcal{J}_i^a$ with Kac-Moody Poisson brackets. The

[1] We will actually find that the quantum KdV integrable system can be recovered in a certain decoupling limit from the affine Gaudin model, adjusting parameters in such a way that the total Kac-Moody currents decouple and leave behind a coset model.

latter are organized into a Lax matrix

$$\varphi(z)\mathcal{L}^a(z;\sigma) = \sum_{i=1}^{N} \frac{\mathcal{J}_i^a(\sigma)}{z - z_i} \tag{4.9}$$

where the $z_i$ are couplings and we use the auxiliary 1-form

$$\varphi(z)dz = \left(1 + \frac{1}{2}\sum_{i=1}^{N} \frac{k_i}{z - z_i}\right)dz \tag{4.10}$$

where $k_i$ are the levels for the currents $\mathcal{J}_i^a$.

The Lax matrix is used to define both the Poisson-commuting transfer matrices

$$\mathcal{T}[z] = \mathrm{Tr}\,\mathcal{P}\exp\left(\oint \mathcal{L}^a(z;\sigma)t_a d\sigma\right), \tag{4.11}$$

and families of local Hamiltonian densities $\mathcal{H}_u^{(n)}(\sigma)$ labelled by exponents $n$ of the affine Kac-Moody algebra and zeros $\zeta_u$ of the twist function (4.10). In classical types, the $\mathcal{H}_u^{(n)}$ are given by specific homogeneous polynomials [141, 142, 143, 144] in

$$\mathrm{Tr}\big(\varphi(z)\mathcal{L}^a(z;\sigma)t_a\big)^r\big|_{z=\zeta_u}, \tag{4.12}$$

of total degree $n+1$ in the currents $\mathcal{J}_i^a$.

One of our main proposals is that the correct quantization of the affine Gaudin model involves Kondo line defects defined by coupling a spin to a collection of quantum Kac-Moody currents $J_i^a$. These Kondo lines are defined in the UV in the same manner as the classical transfer matrices:

$$T[z] = \mathrm{Tr}\,\mathcal{P}\exp\left(\oint \sum_i g_i[z]J_i^a(\sigma)t_a d\sigma\right). \tag{4.13}$$

The couplings $g_i[z]$ need to be renormalized and acquire a scale dependence. It was conjectured in [1] that the RG flow factors through a flow of the spectral parameter, so that the spectral parameter may be identified with the (complexified) renormalization scale $e^\theta$ via dimensional transmutation. In other words, the RG flow defines a one-parameter family of commuting line defects. The specific functional form of the couplings $g_i[z]$ along the commuting family depends on the chosen renormalization scheme.

The RG flow is physically rich and depends sensitively on the spin of the auxiliary $\mathfrak{sl}_2$ generators $t^a$ and on the relative UV couplings. The endpoint is some IR-free line defect whose nature can be predicted with the help of the ODE/IM correspondence. For special choices of spin and couplings, the endpoint is an irrelevant deformation of a single identity line defect. Such a deformation must take the form

$$\mathrm{Tr}\,\mathcal{P}\exp\left(\oint\sum_n e^{-n\theta}\mathcal{O}_u^{(n)}(\sigma)d\sigma\right) \tag{4.14}$$

for some collection of bulk quasi-primaries $\mathcal{O}_u^{(n)}(\sigma)$ of dimension $n+1$.

Now we denote with $u$ the choice of UV line defect flowing to the identity line. We will see that this generalizes naturally the choice of a zero $\zeta_u$ for $\varphi(z)$ above. A special property of such deformations by bulk chiral currents is that there exists a renormalization scheme where the path-ordered exponential becomes effectively an integration along separate contours. Therefore the path-ordered exponential is essentially Abelian, and reduces to the exponential of the zero-modes of the $\mathcal{O}_u^{(n)}(\sigma)$.

These IR effective line defects commute with the transfer matrices by construction and thus the zero-modes of $\mathcal{O}_u^{(n)}$ can be identified with the quantum version of the classical Hamiltonians $\mathcal{H}_u^{(n)}$. With the help of a WKB analysis of the ODE/IM solution, we will match the vevs of the zero-modes of $\mathcal{O}_u^{(n)}$ on eigenstates with the conjectural eigenvalues of the quantum version of the $\mathcal{H}_u^{(n)}$ proposed in [145].

## 4.2 Opers, $\lambda$-opers and affine opers

In this section, for simplicity, we specialize to the case of $\mathfrak{sl}_2$. The generalisation to $\mathfrak{sl}_3$ will be discussed in section 4.7. The main objective of this section is to introduce the family of Schrödinger operators which provides the conjectural full ODE/IM solution of the Kondo defects spectrum problem:

$$\partial_x^2 - \lambda^{-2}P(x) - t(x), \tag{4.15}$$

where $P(x) = e^{2\alpha x}\prod_{a=1}^N (x-z_a)^{k_a}$ and $t(x)$ is an auxiliary meromorphic classical stress tensor which will be determined by a solution of the Bethe equations.

We will motivate some of our definitions in analogy to the well-known correspondence between the (non-affine) Gaudin model and opers with singularities of trivial monodromy [146, 147, 148]. The latter is one of the most basic manifestations of the Geometric Langlands correspondence and can be investigated with the help of supersymmetric gauge theory

[149, 150]. It would be very nice to give a similar derivation of the ODE/IM proposal based on gauge theory or string theory constructions.

### 4.2.1 $\mathfrak{sl}_2$ opers

An $\mathfrak{sl}_2$ *oper* is a complexified Schrödinger operator

$$\partial_x^2 - t(x) \tag{4.16}$$

with a natural transformation law under a change of coordinate

$$\partial_x^2 - t(x) = (\partial_x \tilde{x})^{\frac{3}{2}} \Big( \partial_{\tilde{x}}^2 - \tilde{t}(\tilde{x}) \Big) (\partial_x \tilde{x})^{\frac{1}{2}}. \tag{4.17}$$

This implies that $t(x)$ transforms as a classical stress tensor

$$t(x) = (\partial_x \tilde{x})^2 \tilde{t}(\tilde{x}) + \frac{3}{4} \left( \frac{\partial_x^2 \tilde{x}}{\partial_x \tilde{x}} \right)^2 - \frac{1}{2} \frac{\partial_x^3 \tilde{x}}{\partial_x \tilde{x}}. \tag{4.18}$$

We will always consider $\mathfrak{sl}_2$ opers for which $t(x)$ is a rational function and only allow coordinate transformations which preserve this property.

We will typically denote a solution/flat section of the Schrödinger equation as $\psi(x)$:

$$\partial_x^2 \psi(x) = t(x) \psi(x) \tag{4.19}$$

and the (constant) Wronskian of two solutions as

$$(\psi, \psi') = \psi(x) \partial_x \psi'(x) - \psi'(x) \partial_x \psi(x). \tag{4.20}$$

The data of an $\mathfrak{sl}_2$ oper (4.16) is equivalent to that of a flat connection

$$\partial_x + \begin{pmatrix} 0 & t(x) \\ 1 & 0 \end{pmatrix}. \tag{4.21}$$

More generally, see for instance [151], an $\mathfrak{sl}_2$ oper can be described as a flat connection of the form

$$\partial_x + \begin{pmatrix} a(x) & b(x) \\ 1 & -a(x) \end{pmatrix} \tag{4.22}$$

where $a(x)$ and $b(x)$ are rational functions, modulo gauge transformations by unipotent

upper-triangular matrices whose entries are rational functions. We can fix the gauge invariance completely by bringing (4.22) to its unique *canonical form* (4.21) with stress tensor given by

$$t(x) = b(x) + \partial_x a(x) + a(x)^2. \tag{4.23}$$

### 4.2.2 $\mathfrak{sl}_2$ $\lambda$-opers

An $\mathfrak{sl}_2$ $\lambda$-*oper*, or simply $\lambda$-*oper*, is a complexified Schrödinger operator with standard dependence on a quantization parameter $\hbar$, here denoted as $\lambda$, namely

$$\partial_x^2 - \frac{P(x)}{\lambda^2} - t(x). \tag{4.24}$$

The coordinate transformations act in the same way as for an $\mathfrak{sl}_2$ oper so that $t(x)$ is a classical stress tensor and $P(x)$ is a quadratic differential. We will always work with $\lambda$-opers for which $t(x)$ is a rational function on $\mathbb{C}$ but allow $P(x)$ to be a more general analytic function, typically with branch points or an essential singularity at infinity, but whose logarithmic derivative is a rational function.

The data of a $\lambda$-oper can be encoded in a flat connection of the form

$$\partial_x + \begin{pmatrix} 0 & P(x)\lambda^{-1} + t(x)\lambda \\ \lambda^{-1} & 0 \end{pmatrix}. \tag{4.25}$$

More generally, an $\mathfrak{sl}_2$ $\lambda$-oper is a flat connection

$$\partial_x + \begin{pmatrix} a(x) & P(x)\lambda^{-1} + b(x)\lambda \\ \lambda^{-1} & -a(x) \end{pmatrix}, \tag{4.26}$$

where $a(x)$ and $b(x)$ are rational functions, modulo gauge transformations by upper-triangular matrices of the form

$$\begin{pmatrix} 1 & v(x)\lambda \\ 0 & 1 \end{pmatrix}. \tag{4.27}$$

for some rational function $v(x)$. Every $\lambda$-oper admits a unique *canonical form* as in (4.25) with stress tensor as in (4.23).

Of course, we could equally describe a $\lambda$-oper using a flat connection of the form

$$\partial_x + \begin{pmatrix} 0 & \lambda^{-1} \\ P(x)\lambda^{-1} + t(x)\lambda & 0 \end{pmatrix}. \tag{4.28}$$

This leads to another (equivalent) way of describing $\lambda$-opers, namely as a flat connection

$$\partial_x + \begin{pmatrix} a(x) & \lambda^{-1} \\ P(x)\lambda^{-1} + b(x)\lambda & -a(x) \end{pmatrix} \tag{4.29}$$

modulo gauge transformations by lower-triangular matrices of the form

$$\begin{pmatrix} 1 & 0 \\ v(x)\lambda & 1 \end{pmatrix}. \tag{4.30}$$

### 4.2.3 Miura opers and singularities of trivial monodromy

A *Miura* $\mathfrak{sl}_2$ *oper*, or simply *Miura oper* for short, is a connection of the form (4.22) with $b(x) = 0$, namely

$$\partial_x + \begin{pmatrix} a(x) & 0 \\ 1 & -a(x) \end{pmatrix}. \tag{4.31}$$

Its equivalence class modulo gauge transformations by unipotent upper-triangular matrices defines an oper, with stress tensor $t(x) = a(x)^2 + \partial_x a(x)$, which we refer to as the oper underlying (4.31). The corresponding Schrödinger operator (4.16) factorises as $(\partial_x + a(x))(\partial_x - a(x))$ and has an obvious solution $\psi(x) = e^{\int a(x)dx}$ which is an eigenline of the monodromy around each singularity of $t(x)$.

It is useful to allow the Miura oper to have apparent singularities where the monodromy eigenline $\psi(x)$ has a simple zero but where $t(x)$ is regular. At such an apparent singularity, $a(x)$ behaves as

$$a(x) = \frac{1}{x-w} + O(x-w). \tag{4.32}$$

Another important type of singularity is one of the form

$$a(x) = -\frac{l}{x-z} + O(1) \tag{4.33}$$

for a non-negative half integer $l$. Then

$$t(x) = \frac{l(l+1)}{(x-z)^2} + \cdots \tag{4.34}$$

and the Schrödinger operator (4.16) has a local solution with $\pm 1$ monodromy around $z$, of

the form

$$\psi(x) \sim (x-z)^{-l} + \cdots \tag{4.35}$$

The Miura condition then gives a second local solution with $\pm 1$ monodromy around $z$, of the form

$$\psi'(x) \sim (x-z)^{l+1} + \cdots \tag{4.36}$$

It follows that the monodromy of any flat section around $z$ must be $\pm 1$. Therefore $z$ is a regular singularity of trivial monodromy for $t(x)$. One can also see this by noting that the Miura oper (4.31) is gauge equivalent to the connection

$$\partial_x + \begin{pmatrix} r(x) & 0 \\ (x-z)^{2l} & -r(x) \end{pmatrix} \tag{4.37}$$

where $r(x) = a(x) + \frac{l}{x-z}$, which is manifestly regular at $z$ for non-negative $l$.

A quick discussion of the term "trivial monodromy" is in order here. If $l$ is allowed to be half-integral, we have to consider the monodromy as living in $PSL(2)$, so that $\pm 1$ is a trivial monodromy. If $l$ is restricted to be integral, then we can take the monodromy to be valued in $SL(2)$, and will still be trivial. This binary choice is a manifestation of Geometric Langlands duality: $PSL(2)$ opers are dual to the $SL(2)$ Gaudin model, and vice versa.

### 4.2.4 Miura $\lambda$-opers and singularities of trivial monodromy

A *Miura* $\mathfrak{sl}_2$ *$\lambda$-oper*, or simply *Miura $\lambda$-oper*, is a connection of the form

$$\partial_x + \begin{pmatrix} a_+(x) & P(x)\lambda^{-1} \\ \lambda^{-1} & -a_+(x) \end{pmatrix}. \tag{4.38}$$

This is of the general form (4.26) and therefore a Miura $\lambda$-oper defines a $\lambda$-oper with stress tensor $t(x) = a_+(x)^2 + \partial_x a_+(x)$. We refer to this as the $\lambda$-oper underlying (4.38). It can be described as a complex Schrödinger operator

$$(\partial_x + a_+(x))(\partial_x - a_+(x)) - \frac{P(x)}{\lambda^2}. \tag{4.39}$$

Crucially, the connection (4.38) is locally gauge equivalent (in $PSL(2)$) to a connection

of the following alternative form

$$\partial_x + \begin{pmatrix} -a_-(x) & \lambda^{-1} \\ P(x)\lambda^{-1} & a_-(x) \end{pmatrix} \tag{4.40}$$

where $a_+(x) + a_-(x) = -\frac{1}{2}\frac{\partial_x P(x)}{P(x)}$. We refer to this connection as the *dual* of the Miura $\lambda$-oper (4.38). Since it is of the general form (4.28) it also defines a $\lambda$-oper, which we call the *dual* $\lambda$*-oper* underlying (4.38), with stress tensor $\tilde{t}(x) = a_-(x)^2 + \partial_x a_-(x)$. The latter can also be described as a complex Schrödinger operator of the same form as in (4.39) with $a_+(x) \to a_-(x)$.

Since the Miura $\lambda$-oper (4.38) and its dual (4.40) are gauge equivalent, we therefore identify a crucial property of $\lambda$-opers: the pair of $\lambda$-opers with stress tensors built from $a_\pm(x)$, i.e. the $\lambda$-oper and the dual $\lambda$-oper underlying a given Miura $\lambda$-oper, have the same monodromy (in $PSL(2)$, unless $P(x)$ is a perfect square).

If at some generic point $w$ we have

$$a_+(x) = \frac{1}{x-w} + O(z-w) \tag{4.41}$$

then it follows by the above arguments for singularities of Miura opers that the Miura $\lambda$-oper built from $a_+(x)$ has an apparent singularity at $w$ while the other Miura $\lambda$-oper built from $a_-(x)$ has a regular singularity at $w$, which must necessarily have trivial monodromy (in $PSL(2)$). The same argument applies if at a point $w'$ we have

$$a_-(x) = \frac{1}{x-w'} + O(z-w') \tag{4.42}$$

with the roles of the two Miura $\lambda$-opers (4.38) and (4.40) interchanged.

If at a zero $z$ of order $k$ of $P(x)$ we have

$$a_+(x) = -\frac{l}{x-z} + O(1) \tag{4.43}$$

then

$$a_-(x) = -\frac{\frac{k}{2} - l}{x-z} + O(1). \tag{4.44}$$

As long as $0 \leq l \leq \frac{k}{2}$, the pair of Miura $\lambda$-opers both have trivial monodromy around $z$.

Indeed, the Miura $\lambda$-oper (4.38) is gauge equivalent to the connection

$$\partial_x + \begin{pmatrix} r(x) & (x-z)^{k-2l} q(x) \lambda^{-1} \\ (x-z)^{2l} \lambda^{-1} & -r(x) \end{pmatrix}$$

where we wrote $P(x) = (x-z)^k q(x)$ with $q(z) \neq 0$ and $r(x) = a_+(x) + \frac{l}{x-z}$, which is manifestly regular at $z$ when $0 \leq l \leq \frac{k}{2}$.

A quick discussion of the term "trivial monodromy" is again in order here. If $l$ is allowed to be half-integral and $k$ integral, we have to consider the monodromy as living in $PSL(2)$, so that $\pm 1$ is a trivial monodromy and gauge transformations can have a sign ambiguity. If $l$ is restricted to be integral and $k$ even, then we can take the monodromy to be valued in $SL(2)$. This binary choice is presumably a manifestation of an affine Geometric Langlands duality: $PSL(2)$ $\lambda$-opers are dual to the affine $SL(2)$ Gaudin model, and vice versa.

### 4.2.5 Opers with singularities of trivial monodromy and Bethe equations

For a general oper, the condition for a regular singularity to have trivial monodromy is an intricate polynomial constraint on the coefficients of the expansion of $t(x)$ near the regular singularity.

Given a Miura oper on $\mathbb{C}$ with a rank 1 irregular singularity at infinity and whose other singularities are all regular with trivial monodromy, we can write

$$a(x) = -\alpha - \sum_a \frac{l_a}{x - z_a} + \sum_i \frac{1}{x - w_i}. \tag{4.45}$$

The condition that each $w_i$ is an apparent singularity reduces to the Bethe equations

$$-\sum_a \frac{l_a}{w_i - z_a} + \sum_{j \neq i} \frac{1}{w_i - w_j} = \alpha. \tag{4.46}$$

These are the Bethe equations for a $\mathfrak{sl}_2$ quantum Gaudin model with sites of spectral parameters $z_a$, supporting $\mathfrak{sl}_2$ irreps of dimension $2l_a + 1$.

We call the overall residue of $a(x)$ at infinity the *weight at infinity* of the Miura oper. Since the underlying oper has trivial monodromy at all the $z_a$ and $w_i$ we refer to it as an *oper with singularities of trivial monodromy*. The eigenvalues of the quantum Gaudin Hamiltonians can be extracted from the expression of $t(x)$.

### 4.2.6 $\lambda$-Opers with singularities of trivial monodromy and affine Bethe equations

We are interested in the class of Miura $\lambda$-opers on $\mathbb{C}$ for which $a_\pm(x)$ take the same form

$$a_+(x) = -\alpha_+ - \sum_a \frac{l_a}{x - z_a} + \sum_i \frac{1}{x - w_i} - \sum_i \frac{1}{x - w'_i}, \tag{4.47a}$$

$$a_-(x) = -\alpha_- - \sum_a \frac{\frac{k_a}{2} - l_a}{x - z_a} + \sum_i \frac{1}{x - w'_i} - \sum_i \frac{1}{x - w_i} \tag{4.47b}$$

and satisfy the Bethe equations

$$-\sum_a \frac{l_a}{w_i - z_a} + \sum_{j \neq i} \frac{1}{w_i - w_j} - \sum_j \frac{1}{w_i - w'_j} = \alpha_+, \tag{4.48a}$$

$$-\sum_a \frac{\frac{k_a}{2} - l_a}{w'_i - z_a} + \sum_{j \neq i} \frac{1}{w'_i - w'_j} - \sum_j \frac{1}{w'_i - w_j} = \alpha_-. \tag{4.48b}$$

These ensure that the (dual) Miura $\lambda$-oper built from $a_+(x)$ (resp. $a_-(x)$) has apparent singularities at each $w_i$ (resp. $w'_i$). The *weight at infinity* of the Miura $\lambda$-oper is the pair of residues of $a_\pm(x)$ at infinity.

These are the Bethe equations for an affine $\mathfrak{sl}_2$ quantum Gaudin model with sites of spectral parameters $z_a$, supporting $\widetilde{\mathfrak{sl}}_2$ Weyl representations induced from $\mathfrak{sl}_2$ irreps of dimension $2l_a + 1$, for WZW current algebras of level $k_a$.

The $\lambda$-oper (resp. the dual $\lambda$-oper) underlying a given Miura $\lambda$-oper has regular singularities with trivial monodromies at the zeroes $z_a$ of $P(x)$ as well as at $w'_i$ (resp. $w_i$), for all values of $\lambda$. We, therefore, refer to the $\lambda$-oper and its dual as a *pair of $\lambda$-opers with singularities of trivial monodromy*. They have interesting Stokes data at $x = \infty$ which we call the *monodromy data* of the pair of $\lambda$-opers.

The eigenvalues of the affine $\mathfrak{sl}_2$ quantum Gaudin model transfer matrices, as well as the quantum local Hamiltonians, can be extracted from the Stokes data in a manner described in the remainder of the work.

### 4.2.7 Weyl reflections

Given some $\mathfrak{sl}_2$ oper with trivial monodromy $t(x) = a(x)^2 + \partial_x a(x)$ and $\alpha \neq 0$, there must be two canonical solutions which at infinity behave like $e^{\pm\alpha x}$ times some analytic functions. The one behaving as $e^{-\alpha x}$ is the Miura eigenline, with logarithmic derivative $a(x)$. The other gives a second rational solution $\tilde{a}(x)$ of $t(x) = \tilde{a}(x)^2 + \partial_x \tilde{a}(x)$, namely

$$\tilde{a}(x) = \alpha - \sum_a \frac{l_a}{x - z_a} + \sum_i \frac{1}{x - \tilde{w}_i} \tag{4.49}$$

with opposite weight at infinity to $a(x)$. This gives an action of the Weyl group of $\mathfrak{sl}_2$ on the collection of Miura opers with the same stress tensor $t(x)$. In particular, it acts as a Weyl transformation on the weight at infinity of the Miura oper.

In terms of connections of the form (4.31), the above transformation $a(x) \to \tilde{a}(x)$ is implemented as a gauge transformation by a unipotent upper-triangular matrix which preserves the Miura form of the connection. Explicitly, a gauge transformation of the Miura oper (4.31) by

$$\begin{pmatrix} 1 & f(x) \\ 0 & 1 \end{pmatrix} \tag{4.50}$$

transforms it as $a(x) \to \tilde{a}(x) = a(x) + f(x)$ provided $f(x)$ is a (rational) solution of the Riccati equation

$$\partial_x f(x) + f(x)^2 + 2a(x)f(x) = 0. \tag{4.51}$$

If we have a Miura $\lambda$-oper with trivial monodromy, such that $\alpha_\pm$ are sufficiently generic, then we have two transformations, $\alpha_+ \to -\alpha_+$ or $\alpha_- \to -\alpha_-$, which map it to a different Miura $\lambda$-oper, with the same $P(x)$ and the same monodromy data, as either one of the $\lambda$-opers is fixed by the transformations.

Explicitly, on a Miura $\lambda$-oper (4.38) or its dual Miura $\lambda$-oper (4.40) we can perform a gauge transformation by, respectively,

$$\begin{pmatrix} 1 & f_+(x)\lambda \\ 0 & 1 \end{pmatrix} \qquad \text{or} \qquad \begin{pmatrix} 1 & 0 \\ f_-(x)\lambda & 1 \end{pmatrix}. \tag{4.52}$$

This produces a new pair of Miura $\lambda$-opers with $a_+(x) \to \tilde{a}_+(x) = a_+(x) \pm f_\pm(x)$ and $a_-(x) \to \tilde{a}_-(x) = a_-(x) \mp f_\pm(x)$ provided that the functions $f_\pm(x)$ are (rational) solutions of the Riccati equation

$$\partial_x f_\pm(x) + f_\pm(x)^2 + 2a_\pm(x)f_\pm(x) = 0. \tag{4.53}$$

These two reflections can be iterated to generate an interesting group: the Weyl group of $\widetilde{\mathfrak{sl}}_2$. It acts as a Weyl transformation on the weight at infinity of the Miura affine oper. More precisely, repeated reflections act as

$$\begin{aligned}\cdots \longleftrightarrow (\alpha_+ + 2\alpha_-, -\alpha_-) \longleftrightarrow (\alpha_+, \alpha_-) \longleftrightarrow (-\alpha_+, 2\alpha_+ + \alpha_-) \\ \longleftrightarrow (3\alpha_+ + 2\alpha_-, -2\alpha_+ - \alpha_-) \longleftrightarrow \cdots \end{aligned} \tag{4.54}$$

and similarly on the weight at infinity.

### 4.2.8 Conjectural count of Bethe solutions

For generic values of $\alpha$, the relation between opers with singularities of trivial monodromy and the Gaudin model suggests that the number of solutions of the Bethe equations should coincide with the graded dimension of the Gaudin Hilbert space, which is the product of $\mathfrak{sl}_2$ irreps of dimension $2l_a + 1$, graded by total weight. A priori, this statement is rather not obvious.

We expect a similar statement for the affine opers with singularities of trivial monodromy: for generic values of $\alpha$ the number of solutions of the Bethe equations should coincide with the graded dimension of the affine Gaudin Hilbert space, which is the product of $\widetilde{\mathfrak{sl}}_2$ Weyl representations induced from $\mathfrak{sl}_2$ irreps of dimension $2l_a + 1$, for WZW current algebras of level $k_a$.

### 4.2.9 Special values of $\alpha_\pm$

The Weyl reflection is not well-defined for an oper with singularities of trivial monodromy when $\alpha = 0$, essentially because there isn't a canonical choice of a second solution. Any choice of solution will do, so we really get a $\mathbb{CP}^1$ family of opers with singularities of trivial monodromy. Only one of these solutions is special, in the sense that it decreases at infinity faster than the others, and will thus have a special weight.

In the dual Gaudin model, we are turning off a parameter that breaks the global $\mathfrak{sl}_2$ symmetry. A whole $\mathfrak{sl}_2$ irrep of eigenstates is represented by a single special oper with singularities of trivial monodromy.

Something similar happens if $\alpha_+ = n(\alpha_+ + \alpha_-)$ for any integer $n$. One of the Weyl reflections in the chain breaks down, and instead, we get a continuous family of solutions. In the dual affine Gaudin model, we are restoring one of the $\mathfrak{sl}_2$ subgroups of the total affine

$\widetilde{\mathfrak{sl}}_2$ symmetry. A whole $\mathfrak{sl}_2$ irrep of eigenstates is represented by a single special affine oper with singularities of trivial monodromy.

If we set both $\alpha_\pm = 0$, the whole Weyl chain breaks down and we get an intricate continuous family of solutions. In the dual affine Gaudin model, we are restoring the whole total affine $\widetilde{\mathfrak{sl}}_2$ symmetry. Essentially, the transfer matrices commute with the total Kac-Moody currents and thus secretly live in the coset CFT.

### 4.2.10 WKB expansion and quasi-canonical form

The Miura $\lambda$-oper (4.38) and its dual (4.40) are locally gauge equivalent to a connection of the more symmetric form

$$\partial_x + \begin{pmatrix} a_0(x) & \sqrt{P(x)}\lambda^{-1} \\ \sqrt{P(x)}\lambda^{-1} & -a_0(x) \end{pmatrix} \tag{4.55}$$

where $a_0(x) = a_+(x) + \frac{\partial_x P(x)}{4P(x)}$. Following [133, 134], we will refer to this as a *Miura* $\widetilde{\mathfrak{sl}}_2$ *oper*. We can consider the equivalence class of such a connection under gauge transformations by matrices of the form

$$\exp \begin{pmatrix} u(x;\lambda) & v_+(x;\lambda) \\ v_-(x;\lambda) & -u(x;\lambda) \end{pmatrix} \tag{4.56}$$

for some formal power series

$$u(x;\lambda) = \sum_{n=0}^{\infty} P(x)^{-n} u_n(x) \lambda^{2n}, \qquad v_\pm(x;\lambda) = \sum_{n=0}^{\infty} P(x)^{-n-\frac{1}{2}} v_n^\pm(x) \lambda^{2n+1} \tag{4.57}$$

where $u_n(x)$ and $v_n^\pm(x)$ are rational functions. This defines an *affine* $\mathfrak{sl}_2$ *oper*, or more precisely an $\widetilde{\mathfrak{sl}}_2$ *oper* for the untwisted affine Kac-Moody algebra $\widetilde{\mathfrak{sl}}_2$ associated with $\mathfrak{sl}_2$. We are working in the loop realisation of $\widetilde{\mathfrak{sl}}_2$ associated with the principal $\mathbb{Z}$-gradation.

The relationship between the different opers described above is depicted in Fig. 4.1. Note that the notions of $\lambda$-oper and dual $\lambda$-oper are naturally associated with the two roots of the Dynkin diagram of $\widetilde{\mathfrak{sl}}_2$.

By allowing gauge transformations as in (4.56) one can bring the connection (4.55) to a *quasi-canonical form* [145]

$$\partial_x + \begin{pmatrix} 0 & p(x;\lambda) \\ p(x;\lambda) & 0 \end{pmatrix} \tag{4.58}$$

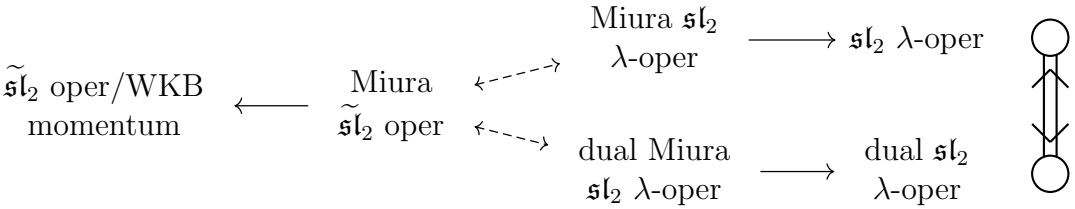


Figure 4.1: Different types of opers: The middle dotted arrows are local gauge transformations by diagonal matrices. The right arrows correspond to working modulo gauge transformations by upper and lower triangular matrices of the form (4.27) and (4.30), respectively. The left arrow corresponds to working modulo gauge transformations by matrices of the form (4.56).

for some formal Laurent series

$$p(x;\lambda) = \frac{\sqrt{P(x)}}{\lambda} + \sum_{n=1}^{\infty} P(x)^{-n+\frac{1}{2}} p_n(x) \lambda^{2n-1}. \tag{4.59}$$

Unlike the canonical form (4.21) of an $\mathfrak{sl}_2$ oper as in (4.22), however, the quasi-canonical form (4.58) of an affine $\mathfrak{sl}_2$ oper is not unique. Indeed, the quasi-canonical form is preserved by residual gauge transformations of the form (4.56) with $u(x;\lambda) = 0$ and $v_-(x;\lambda) = v_+(x;\lambda)$, the effect of which is

$$p(x;\lambda) \longmapsto p(x;\lambda) + \partial_x v_+(x;\lambda). \tag{4.60}$$

Now the quasi-canonical form (4.58) can be transformed to

$$\partial_x + \begin{pmatrix} -\frac{1}{2}\frac{\partial_x p(x;\lambda)}{p(x;\lambda)} & \lambda p(x;\lambda)^2 \\ \lambda^{-1} & \frac{1}{2}\frac{\partial_x p(x;\lambda)}{p(x;\lambda)} \end{pmatrix} \tag{4.61}$$

and by a further gauge transformation we can bring it back to the form

$$\partial_x + \begin{pmatrix} 0 & \lambda\Big(p(x;\lambda)^2 + \frac{3}{4}\Big(\frac{\partial_x p(x;\lambda)}{p(x;\lambda)}\Big)^2 - \frac{1}{2}\frac{\partial_x^2 p(x;\lambda)}{p(x;\lambda)}\Big) \\ \lambda^{-1} & 0 \end{pmatrix}. \tag{4.62}$$

In particular, by comparing this with the expression (4.25) for the $\lambda$-oper underlying the

Miura $\lambda$-oper we started with, we recognize the equation for the WKB momentum

$$\frac{P(x)}{\lambda^2} + t(x) = p(x;\lambda)^2 + \frac{3}{4}\left(\frac{\partial_x p(x;\lambda)}{p(x;\lambda)}\right)^2 - \frac{1}{2}\frac{\partial_x^2 p(x;\lambda)}{p(x;\lambda)} \tag{4.63}$$

which is used to study the $\lambda \to 0$ limit of the transport data of the $\lambda$-oper.

In particular, the contour integrals

$$\oint p(x;\lambda)dx \tag{4.64}$$

control the WKB asymptotics of certain transport coefficients. They are also known to match the eigenvalues of local integrals of motion for the affine Gaudin model [136, 145, 152].

## 4.3 Bethe states and transfer matrices

### 4.3.1 Some Kac-Moody conventions

We follow the convention from [1]. Our normalization convention for the spin basis of $\mathfrak{sl}_2$ is

$$t^{\pm} = \frac{1}{\sqrt{2}}(t^1 \pm it^2), \quad t^0 = \frac{1}{\sqrt{2}}t^3, \tag{4.65}$$

which satisfy the relations

$$[t^0, t^{\pm}] = \pm t^{\pm}, \quad [t^+, t^-] = 2t^0. \tag{4.66}$$

The relations in the corresponding untwisted affine Kac-Moody algebra $\widetilde{\mathfrak{sl}}_2$ read

$$\left[J_n^0, J_m^0\right] = \frac{\kappa n}{2}\delta_{n+m,0} \tag{4.67}$$

$$\left[J_n^0, J_m^{\pm}\right] = \pm J_{n+m}^{\pm} \tag{4.68}$$

$$\left[J_n^+, J_m^-\right] = 2J_{n+m}^0 + \kappa n \delta_{n+m,0}, \tag{4.69}$$

for $n, m \in \mathbb{Z}$. Let $|l, \kappa\rangle$ denote the ground state in the spin $l$ module at level $\kappa$.

**Action of the spectral flow**

Spectral flow [153, 154] is an automorphism of $\widehat{\mathfrak{sl}}_2$ given, for $\alpha \in \mathbb{R}$, by

$$\mathrm{U}_\alpha : \quad J_n^+ \mapsto J_{n+\alpha}^+, \quad J_n^- \mapsto J_{n-\alpha}^-, \quad J_n^0 \mapsto J_n^0 + \frac{k}{2}\alpha\delta_{n,0}, \tag{4.70a}$$

$$L_0 \mapsto L_0 + \alpha J_0^0 + \frac{k}{4}\alpha^2. \tag{4.70b}$$

There is also an involutive automorphism induced by the Weyl group $\mathrm{W}(\mathfrak{sl}_2) = \mathbb{Z}_2$

$$w_1 : \quad J_n^+ \mapsto J_n^-, \quad J_n^- \mapsto J_n^+, \quad J_n^0 \mapsto -J_n^0 \tag{4.71}$$

which satisfy

$$\mathrm{U}_\alpha \mathrm{U}_{\alpha'} = \mathrm{U}_{\alpha+\alpha'}, \quad \mathrm{U}_0 = w_1^2 = 1, \quad \mathrm{U}_\alpha w_1 = w_1 \mathrm{U}_{-\alpha}. \tag{4.72}$$

We therefore have $\mathrm{Aut}(\widehat{\mathfrak{sl}}_2) = \mathbb{R} \rtimes \mathbb{Z}_2$. In particular, the even part is inner and corresponds to the affine Weyl group $\mathrm{W}(\widehat{\mathfrak{sl}}_2) = (2\mathbb{Z}) \rtimes \mathbb{Z}_2$. Consequently, the induced action by $\mathrm{U}_{2\mathbb{Z}}$ maps each integral highest weight representation into itself, whereas more general $\mathrm{U}_\alpha$ maps between the (twisted) modules. For example,

$$\mathrm{U}_1 : j \mapsto \frac{k}{2} - j, \quad j = 0, \frac{1}{2}, 1, \ldots, \frac{k}{2}. \tag{4.73}$$

### 4.3.2 The Bethe equations and Bethe vectors

Let us take the quadratic differential $P(x) = e^{2x}x^\kappa$. This should correspond to an affine Gaudin model with a single site, i.e. an integrable Kondo problem in the $SU(2)_\kappa$ WZW model. A generic state in the spin $l$ module of the $SU(2)_\kappa$ WZW model which is singular under the zero-mode $\mathfrak{sl}_2$ subalgebra can be described by a pair of Miura $\lambda$-opers of the form

$$a_+(x) = -\frac{l}{x} + \sum_i \frac{1}{x - w_i} - \sum_i \frac{1}{x - w_i'}, \tag{4.74a}$$

$$a_-(x) = -1 - \frac{\frac{\kappa}{2} - l}{x} + \sum_i \frac{1}{x - w_i'} - \sum_i \frac{1}{x - w_i} \tag{4.74b}$$

with the Bethe roots $w_i$ and $w'_i$ satisfying the Bethe equations

$$-\frac{l}{w_i}+\sum_{j\neq i}\frac{1}{w_i-w_j}-\sum_j\frac{1}{w_i-w'_j}=0, \tag{4.75a}$$

$$-1-\frac{\frac{\kappa}{2}-l}{w'_i}+\sum_{j\neq i}\frac{1}{w'_i-w'_j}-\sum_j\frac{1}{w'_i-w_j}=0. \tag{4.75b}$$

It is useful to denote the set of all Bethe roots $\{w_i\}\cup\{w'_i\}$ collectively as $\{t_i\}$. To each Bethe root $w_i$ we associate the lowering operator $F_{w_i}=J_0^-$ in $\widetilde{\mathfrak{sl}}_2$ and to each Bethe root $w'_i$ the lowering operator $F_{w'_i}=J_{-1}^+$. By analogy with the finite-dimensional case [155] and based on the expression for the Bethe vector in affine Gaudin models with regular singularities [156], we then conjecture that, associated with each solution of the Bethe equations (4.75) with $m$ Bethe roots, there is a corresponding Bethe vector in the spin $l$ module given by

$$|\{t_i\}\rangle=\sum_{\sigma\in S_m}\frac{F_{t_{\sigma(1)}}F_{t_{\sigma(2)}}\dots F_{t_{\sigma(m)}}|l,\kappa\rangle}{\big(t_{\sigma(1)}-t_{\sigma(2)}\big)\big(t_{\sigma(2)}-t_{\sigma(3)}\big)\dots\big(t_{\sigma(m-1)}-t_{\sigma(m)}\big)t_{\sigma(m)}}. \tag{4.76}$$

This state is singular under the zero-mode $\mathfrak{sl}_2$ subalgebra. Moreover, its Virasoro level is equal to the number $\#w'$ of Bethe roots $w'_i$ and its spin is $l+\#w'-\#w$.

The leading non-trivial term in the UV expansion of the transfer matrix is proportional to the zero-mode quadratic Casimir $T^{(2)}=J_0^aJ_0^a$. Since (4.76) has definite spin it is an eigenvector of $T^{(2)}$ with eigenvalue $2(l+\#w'-\#w)(l+1+\#w'-\#w)$. From the subleading term in the UV expansion we obtain the operator

$$T^{(3)}=\sum_{n>0}\frac{i}{2n}f_{abc}J_{-n}^aJ_0^bJ_n^c+\sum_{n>0}\frac{2}{n}J_{-n}^aJ_n^a. \tag{4.77}$$

We checked that this non-trivial operator is indeed diagonalized by the examples of Bethe vectors in Subsection 4.3.3. It would be very nice to derive the Bethe equations directly from the diagonalization of $T^{(3)}$ with the Bethe vector ansatz (4.76). Moreover, we conjecture that the expectation value of $T^{(3)}$ in the generic eigenstate (4.76) is

$$\langle\{t_i\}|T^{(3)}|\{t_i\}\rangle=-2(l+1+\#w'-\#w)\bigg(\sum_i w'_i-\sum_j w_j\bigg). \tag{4.78}$$

A similar conjecture was made in [135] for the eigenvalue of the first non-local integral of

motion of the affine $\widetilde{\mathfrak{sl}}_2$ Gaudin model describing quantum KdV theory as a coset CFT. We also expect from the UV expansion of the corresponding $\lambda$-oper in Appendix D.4.2 that the eigenvalues of all the higher-order UV expansion coefficients $T^{(n)}$ of the transfer matrix are given by supersymmetric polynomials in the Bethe roots $\{w_i\} \cup \{w'_j\}$. This was conjectured in [135] for the higher non-local charges of quantum KdV theory.

The expression for the next subleading term $T^{(4)}$ is much more complicated. We did check in Appendix D.4 that the Bethe vector expectation value of the UV expansion of transfer matrices matches the Stokes data of the corresponding $\lambda$-opers.

The multichannel case can be treated similarly. For the product of WZW model we take the quadratic differential $P(x) = e^{2x} \prod_a (x - z_a)^{\kappa_a}$. We can then describe a generic state in the tensor product of spin $l_a$ modules which is singular under the total zero-mode $\mathfrak{sl}_2$ subalgebra using a pair of Miura $\lambda$-opers of the form

$$a_+(x) = -\sum_a \frac{l_a}{x - z_a} + \sum_i \frac{1}{x - w_i} - \sum_i \frac{1}{x - w'_i}, \tag{4.79a}$$

$$a_-(x) = -1 - \sum_a \frac{\frac{\kappa_a}{2} - l_a}{x - z_a} + \sum_i \frac{1}{x - w'_i} - \sum_i \frac{1}{x - w_i} \tag{4.79b}$$

where $w_i$ and $w'_i$ are the Bethe roots satisfying the Bethe equations

$$-\sum_a \frac{l_a}{w_i - z_a} + \sum_{j \neq i} \frac{1}{w_i - w_j} - \sum_j \frac{1}{w_i - w'_j} = 0, \tag{4.80a}$$

$$-1 - \sum_a \frac{\frac{\kappa_a}{2} - l_a}{w'_i - z_a} + \sum_{j \neq i} \frac{1}{w'_i - w'_j} - \sum_j \frac{1}{w'_i - w_j} = 0. \tag{4.80b}$$

If we denote the set of all Bethe roots collectively as $\{t_i\}$ then we conjecture that the corresponding Bethe vector in the tensor product of spin $l_i$ modules is given by

$$|\{t_i\}\rangle = \sum_{\{t_{i,j}\}} \bigotimes_a \frac{F_{t_{a,1}} F_{t_{a,2}} \dots F_{t_{a,m_a}} |l_a, \kappa_a\rangle}{(t_{a,1} - t_{a,2})(t_{a,2} - t_{a,3}) \dots (t_{a,m_a - 1} - t_{a,m_a})(t_{a,m_a} - z_a)} \tag{4.81}$$

where the sum is over all partitions of the set $\{t_i\}$ into $N$ ordered subsets $(t_{a,1}, \dots t_{a,m_a})$ with $m_1 + \dots + m_N = m$. It has Virasoro level $\#w'$ and spin $\sum_a l_a + \#w' - \#w$.

In the two-point case, the leading term in the UV expansion of the transfer matrix is proportional to the total zero-mode quadratic Casimir $(J^a_{0,1} + J^a_{0,2})^2$ with eigenvalue $2(l_1 + l_2 + \#w' - \#w)(l_1 + l_2 + 1 + \#w' - \#w)$ on the Bethe vector (4.81). The next term

in the UV expansion is proportional, in a suitable renormalization scheme, to

$$T^{(3)} = \sum_{n>0} \frac{i}{2n} f_{abc}(J^a_{-n,1} + J^a_{-n,2})(J^b_{0,1} + J^b_{0,2})(J^c_{n,1} + J^c_{n,2}) \\ + \sum_{n>0} \frac{2}{n}(J^a_{-n,1} + J^a_{-n,2})(J^a_{n,1} + J^a_{n,2}) - (z_1 J^a_{0,1} + z_2 J^a_{0,2})(J^a_{0,1} + J^a_{0,2}),$$

We conjecture that its expectation value in the eigenstate (4.81) is given by the supersymmetric polynomial in the Bethe roots

$$\langle\{t_i\}|T^{(3)}|\{t_i\}\rangle = -2(l_1 + l_2 + 1 + \#w' - \#w)\left(z_1 l_1 + z_2 l_2 + \sum_i w'_i - \sum_j w_j\right). \quad (4.82)$$

### 4.3.3 Examples

In this subsection, we study the solutions to the Bethe equation (4.75) in the vacuum and spin $\frac{1}{2}$ WZW modules.

#### Vacuum module

**Level 1 states:**

$\#w' = 1$, $\#w = 0$**:** The Bethe equation (4.75) is just $\frac{\kappa}{w'} + 2 = 0$. This is inconsistent if $\kappa = 0$. When $\kappa \neq 0$ we have $w' = -\frac{\kappa}{2}$ and the corresponding Bethe vector (4.76) is then proportional to

$$|\{w'\}\rangle \propto J^+_{-1}|0,\kappa\rangle.$$

This is singular when $\kappa = 0$, corresponding to the fact that there are no solutions to the Bethe equations in this case.

$\#w' = 1$, $\#w = 1$**:** No solution, as it should be since there is no singlet state at level 1 in the vacuum module: $J^0_{-1}|0,\kappa\rangle = -\frac{1}{2}J^-_0 J^+_{-1}|0,\kappa\rangle$ is a descendant.

**Level 2 states:**

$\#w' = 2$, $\#w = 0$**:** The Bethe equations (4.75) have solutions if and only if $\kappa \neq 0, 1$. The Bethe vector corresponding to the cases $\kappa \neq 0, 1$ is proportional to

$$|\{w_1', w_2'\}\rangle \propto J_{-1}^+ J_{-1}^+ |0, \kappa\rangle.$$

which for $\kappa = 1$ is singular and for $\kappa = 0$ is a descendant of the singular vector $J_{-1}^+|0, 0\rangle$.

$\#w' = 2$, $\#w = 1$**:** The Bethe equations have a solution if and only if $\kappa \neq 0, -1$. The corresponding Bethe vector is given by

$$\begin{aligned}|\{w_1', w_2', w_1\}\rangle = &\left(\frac{1}{w_1' - w_2'}\frac{1}{w_2' - w_1}\frac{1}{w_1} + \frac{1}{w_2' - w_1'}\frac{1}{w_1' - w_1}\frac{1}{w_1}\right) J_{-1}^+ J_{-1}^+ J_0^- |0, \kappa\rangle \\ &+ \left(\frac{1}{w_1' - w_1}\frac{1}{w_1 - w_2'}\frac{1}{w_2'} + \frac{1}{w_2' - w_1}\frac{1}{w_1 - w_1'}\frac{1}{w_1'}\right) J_{-1}^+ J_0^- J_{-1}^+ |0, \kappa\rangle \\ &+ \left(\frac{1}{w_1 - w_1'}\frac{1}{w_1' - w_2'}\frac{1}{w_2'} + \frac{1}{w_1 - w_2'}\frac{1}{w_2' - w_1'}\frac{1}{w_1'}\right) J_0^- J_{-1}^+ J_{-1}^+ |0, \kappa\rangle,\end{aligned}$$

which is proportional to $J_{-2}^+|0, \kappa\rangle = \left(\frac{1}{2} J_{-1}^+ J_0^- + J_{-1}^0\right) J_{-1}^+ |0, \kappa\rangle$. In particular, when $\kappa = 0$ it is a descendant of the singular vector $J_{-1}^+|0, 0\rangle$.

The situation when $\kappa = -1$ is more subtle since we see that the state $J_{-2}^+|0, -1\rangle$ in the spin 0 module of level $-1$ is not described by a solution of the Bethe ansatz. In the limit $\kappa \to -1$ of a solution of the Bethe equations for $\kappa \neq -1$, all the Bethe roots collide with the origin so that the Miura $\lambda$-oper (4.74) becomes

$$a_+(x) = -\frac{1}{x}, \qquad a_-(x) = -1 + \frac{3}{2x}. \tag{4.83}$$

This is no longer of the form (4.74) since the residues at the origin are not given by the pair $(-l, -\frac{\kappa}{2} + l) = (0, \frac{1}{2})$ corresponding to the highest weight of the vacuum module at level $\kappa = -1$. However, the residues of (4.83) do correspond to a shifted Weyl reflection of this highest weight. Indeed, the simple roots of $\widetilde{\mathfrak{sl}}_2$ act by shifted Weyl reflections on the residues at the origin as

$$\cdots \longleftrightarrow (0, \tfrac{1}{2}) \longleftrightarrow (1, -\tfrac{1}{2}) \longleftrightarrow (-1, \tfrac{3}{2}) \longleftrightarrow \cdots$$

Therefore the pair (4.83) describes a generalised Miura $\lambda$-oper in the sense of [133, 148]. We conjecture that the state $J_{-2}^+|0, -1\rangle$ is described by this generalized Miura $\lambda$-oper. This is checked to fourth order in the UV expansion in Appendix D.4.

$\#w' = 2$, $\#w = 2$**:** The Bethe equations admit a solution if and only if $\kappa \neq -2, 0$. The corresponding Bethe vector is proportional to

$$|\{w_1', w_2', w_1, w_2\}\rangle \propto J^a_{-1} J^a_{-1} |0, \kappa\rangle.$$

This is singular when $\kappa = -2$, the critical level, and for $\kappa = 0$ it is a descendant of the singular vector $J^+_{-1}|0, 0\rangle$ since it can be written as

$$J^a_{-1} J^a_{-1} |0, 0\rangle = \big(-\tfrac{1}{2} J^0_{-1} J^-_0 - \tfrac{1}{4} J^+_{-1} J^-_0 J^-_0 + \tfrac{1}{2} J^-_{-1}\big) J^+_{-1} |0, 0\rangle.$$

**Spin $\frac{1}{2}$ module**

**Level 1 states:**

$\#w' = 1$, $\#w = 0$**:** The Bethe equations (4.75) have a solution if and only if $\kappa \neq 1$, in which case the Bethe vector is proportional to

$$|\{w_1'\}\rangle \propto J^+_{-1} |\tfrac{1}{2}, \kappa\rangle.$$

This becomes singular at $\kappa = 1$.

$\#w' = 1$, $\#w = 1$**:** The Bethe equations (4.75) are inconsistent when $\kappa = -2$ and for $\kappa \neq -2$ they have the unique solution $w_1' = -(\kappa + 2)$ and $w_1 = -\frac{1}{3}(\kappa + 2)$. The corresponding Bethe vector reads

$$\begin{aligned} |\{w_1', w_1\}\rangle &= \frac{1}{w_1' - w_1} \frac{1}{w_1} J^+_{-1} J^-_0 |\tfrac{1}{2}, \kappa\rangle + \frac{1}{w_1 - w_1'} \frac{1}{w_1'} J^-_0 J^+_{-1} |\tfrac{1}{2}, \kappa\rangle \\ &= \frac{3}{(\kappa + 2)^2} (J^+_{-1} J^-_0 + J^0_{-1}) |\tfrac{1}{2}, \kappa\rangle. \end{aligned}$$

The vector $(J^+_{-1} J^-_0 + J^0_{-1})|\frac{1}{2}, \kappa\rangle$ becomes singular when $\kappa = -2$.

Note that when $\kappa = 1$ we have the spin $\frac{1}{2}$ state

$$|\{w_1', w_1\}\rangle = \tfrac{2}{3}(J^+_{-1} J^-_0 + J^0_{-1}) |\tfrac{1}{2}, 1\rangle = 2 J^0_{-1} |\tfrac{1}{2}, 1\rangle + \tfrac{2}{3} J^-_0 J^+_{-1} |\tfrac{1}{2}, 1\rangle. \tag{4.84}$$

The second term on the right-hand side is a descendant of the singular vector $J^+_{-1}|\frac{1}{2}, 1\rangle$ and is therefore zero in the spin $\frac{1}{2}$ module at level $\kappa = 1$.

**Level 2 states:**

$\#w' = 2$, $\#w = 0$**:** The Bethe equations (4.75) have no solution unless $\kappa \neq 1, 2$, in which case the corresponding Bethe vector is given by the spin $\frac{5}{2}$ state

$$|\{w'_1, w'_2\}\rangle = \frac{1}{(\kappa-1)(\kappa-2)} J^+_{-1} J^+_{-1} |\tfrac{1}{2}, \kappa\rangle.$$

The state $J^+_{-1}J^+_{-1}|\frac{1}{2},\kappa\rangle$ becomes singular when $\kappa = 2$. When $\kappa = 1$ it is a descendant of the singular vector $J^+_{-1}|\frac{1}{2}, 1\rangle$.

$\#w' = 2$, $\#w = 1$**:** The Bethe equations (4.75) have two inequivalent families of solutions:

($i$) The first family is valid for $\kappa \neq -\frac{1}{2}$ and the Bethe vector is proportional to

$$w_+ = -\tfrac{1}{6}\Big(3 + 8\kappa + \sqrt{41 + 64\kappa + 64\kappa^2}\Big) J^+_{-1}(J^0_{-1} + J^+_{-1}J^-_0)|\tfrac{1}{2}, \kappa\rangle + \tfrac{1}{3}(\kappa+2) J^+_{-2}|\tfrac{1}{2}, \kappa\rangle.$$

This is singular for $\kappa = -\frac{1}{2}$. Moreover, it vanishes for $\kappa = -2$.

($ii$) The second family is valid for $\kappa \neq 1, -2$ with Bethe vector proportional to

$$w_- = -\tfrac{1}{6}\Big(3 + 8\kappa - \sqrt{41 + 64\kappa + 64\kappa^2}\Big) J^+_{-1}(J^0_{-1} + J^+_{-1}J^-_0)|\tfrac{1}{2}, \kappa\rangle + \tfrac{1}{3}(\kappa+2) J^+_{-2}|\tfrac{1}{2}, \kappa\rangle.$$

When $\kappa = 1$ we can rewrite this vector as $w_- = \frac{1}{3}\big(5J^0_{-1} + J^-_0 J^+_{-1}\big)J^+_{-1}|\frac{1}{2}, 1\rangle$ which is thus a descendant of the singular vector $J^+_{-1}|\frac{1}{2}, 1\rangle$. Likewise, when $\kappa = -2$ we obtain the state $w_- = \frac{13}{3} J^+_{-1}(J^0_{-1} + J^+_{-1}J^-_0)|\frac{1}{2}, -2\rangle$ which is a descendant of the singular vector $(J^0_{-1} + J^+_{-1}J^-_0)|\frac{1}{2}, -2\rangle$.

In conclusion, we have the following cases:

- For $\kappa \neq -2, -\frac{1}{2}, 1$ we have two spin $\frac{3}{2}$ Bethe vectors $w_\pm$.
- For $\kappa = 1$ we have just one spin $\frac{3}{2}$ Bethe vector

$$w_+ = J^+_{-2}|\tfrac{1}{2}, 1\rangle - 4J^+_{-1}(J^0_{-1} + J^+_{-1}J^-_0)|\tfrac{1}{2}, 1\rangle.$$

- For $\kappa = -\frac{1}{2}$ we also have just one spin $\frac{3}{2}$ Bethe vector

$$w_- = \tfrac{1}{2}J^+_{-2}|\tfrac{1}{2},1\rangle + J^+_{-1}(J^0_{-1} + J^+_{-1}J^-_0)|\tfrac{1}{2},1\rangle.$$

- For $\kappa = -2$ there are no spin $\frac{3}{2}$ Bethe vectors.

<u>$\#w' = 2$, $\#w = 2$:</u> There are again two inequivalent families of solutions:

($i$) The first family is valid for $\kappa \neq -2, -\frac{7}{3}$ and the corresponding Bethe vector is proportional to

$$\begin{aligned} w_+ = \Big( & (\kappa+2)\big(\kappa+2+\sqrt{\kappa^2+16\kappa+32}\big)J^+_{-2}J^-_0 \\ & + \big(5\kappa+12-\sqrt{\kappa^2+16\kappa+32}\big)(J^+_{-1}J^-_{-1} + J^0_{-1}J^0_{-1}) \\ & + \tfrac{1}{2}\big(\kappa+\sqrt{\kappa^2+16\kappa+32}\big)J^+_{-1}J^+_{-1}J^-_0J^-_0 \\ & + \big(\kappa^2-\kappa-8+(\kappa+3)\sqrt{\kappa^2+16\kappa+32}\big)J^-_{-2}\Big)|\tfrac{1}{2},\kappa\rangle. \end{aligned}$$

This vanishes when $\kappa = -2$. On the other hand, when $\kappa = -\frac{7}{3}$ we find

$$w_+ = -J^+_{-1}J^+_{-1}J^-_0J^-_0|\tfrac{1}{2},-\tfrac{7}{3}\rangle$$

which has zero norm.

($ii$) The second family is valid for $\kappa \neq 1$ with Bethe vector proportional to

$$\begin{aligned} w_- = \Big( & \tfrac{1}{2}\big(7\kappa+16-\sqrt{\kappa^2+16\kappa+32}\big)J^+_{-2}J^-_0 \\ & - \tfrac{1}{2}\big(3\kappa+8+3\sqrt{\kappa^2+16\kappa+32}\big)(J^+_{-1}J^-_{-1} + J^0_{-1}J^0_{-1}) \\ & + 2J^+_{-1}J^+_{-1}J^-_0J^-_0 \\ & + \big(5\kappa+12+\sqrt{\kappa^2+16\kappa+32}\big)J^-_{-2}\Big)|\tfrac{1}{2},\kappa\rangle. \end{aligned}$$

For $\kappa = 1$ this vector can be rewritten as

$$w_- = 2\big(J^-_0J^-_0J^+_{-1} - 4J^-_{-1}J^+_{-1} + 8J^0_{-1}J^-_0\big)J^+_{-1}|\tfrac{1}{2},1\rangle$$

which is thus a descendant of the singular vector $J^+_{-1}|\frac{1}{2},1\rangle$.

In conclusion, we have the following cases:

- For $\kappa \neq -\frac{7}{3}, -2, 1$ we have two spin $\frac{1}{2}$ Bethe vectors $w_\pm$.
- For $\kappa = 1$ we have just one spin $\frac{1}{2}$ Bethe vector

$$w_+ = 2\big(10J^0_{-2} + 2J^+_{-1}J^+_{-1}J^-_0J^-_0 + 5J^0_{-1}J^0_{-1} + 5J^+_{-1}J^-_{-1} + 15J^+_{-2}J^-_0\big)|\tfrac{1}{2}, 1\rangle.$$

- For $\kappa = -2$ or $\kappa = -\frac{7}{3}$ we also have just one spin $\frac{1}{2}$ Bethe vector

$$w_- = 2\big(2J^0_{-2} + J^+_{-1}J^+_{-1}J^-_0J^-_0 - 2J^0_{-1}J^0_{-1} - 2J^+_{-1}J^-_{-1}\big)|\tfrac{1}{2}, \kappa\rangle.$$

## 4.4 The UV expansion

Kondo line defects in $\prod_i SU(2)_{k_i}$ WZW models are defined as the trace of the path ordered exponential

$$\hat{T}_{\mathcal{R}}\left(\{g_i\}\right) := \mathrm{Tr}_{\mathcal{R}}\,\mathcal{P}\exp\left(i\int_0^{2\pi}\sum_i g_i t^a J^a_i(\sigma)d\sigma\right) \tag{4.85}$$

where $t^a$ are the generators of the Lie algebra $\mathfrak{su}(2)$ and the trace is taken in an $\mathfrak{su}(2)$ representation $\mathcal{R}$, labeled by its dimension $n$ from now on. The factor $i$ in front of the integral is $\sqrt{-1}$. The WZW currents are denoted as $J^a_i(\sigma)$ for each $SU(2)$ factor. The integration is along the compact direction.

Following [1], we adopt the convention that the physical RG flows start from asymptotically free defects and the couplings grow in the positive real direction approaching the infrared. Therefore the UV expansion is concerned with small positive $g_i$. Perturbatively in $g_i$, we can expand the exponential

$$\hat{T}_n\left(\{g_i\}\right) = n + \sum_{N=1}^{\infty} i^N \hat{T}^{(N)}_n, \tag{4.86}$$

where each $\hat{T}^{(N)}_n$ depend on the set $\{g_i\}$, and perform the loop integral. In doing so, one carries out a careful and lengthy renormalization procedure since the currents don't commute with each other. This was done [1] following the prescription given in [90]. We are interested in the expectation value of the Kondo line operator in a generic state $|\ell\rangle$, with $\ell$ denoting the list of quantum numbers of the state. Details can be found in Appendix D.4.

If the twist $\alpha_+$ is nonzero, the Kondo line defect comes with a twist,

$$\hat{T}_{\mathcal{R}}\left(\{g_i\},\alpha_+\right) := \mathrm{Tr}_{\mathcal{R}}\, e^{i2\pi\alpha_+ t^0}\mathcal{P}\exp\left(i\int_0^{2\pi}\sum_i g_i t^a J_i^a(\sigma)d\sigma\right). \tag{4.87}$$

Therefore the leading order is simply given by the character in the representation $\mathcal{R}$ of dimension $n$, namely

$$\mathrm{Tr}_{\mathcal{R}}\, e^{i2\pi\alpha_+ t^0} = \frac{\sin n\pi\alpha_+}{\sin\pi\alpha_+}. \tag{4.88}$$

Note that in order for (4.87) to make sense, the integrand inside the path ordered exponential has to be single-valued. Therefore, the inclusion of the nonzero twist in the trace forces us to work with the twisted affine Lie algebra. It is easy to see that this twisted affine algebra is precisely the one we get by acting with $\mathrm{U}_{\alpha_+}$ defined in (4.70b) on the untwisted affine algebra $\widehat{\mathfrak{sl}}_2$.

It was proposed[2] in [1] that the expectation values in a state $|\ell\rangle$ of such a Kondo line defect will coincide with the transport coefficients of the Miura $\lambda$-oper, where the quadratic differential is $P(x) = e^{2x}\prod_i (x-z_i)^{k_i}$ for $\prod_i SU(2)_{k_i}$ WZW and where $t(x)$ is constructed from solutions of the Bethe equations for the state $|\ell\rangle$. The corresponding Schrödinger equation reads

$$\partial_x^2\psi(x) = \left(\frac{1}{\lambda^2}e^{2x}\prod_i (x-z_i)^{k_i} + t(x)\right)\psi(x). \tag{4.89}$$

The UV perturbative expansion is available whenever the Stokes data for the Schrödinger equation becomes close to the Stokes data for the simpler equation

$$\partial_x^2\psi(x) = e^{2x}\psi(x). \tag{4.90}$$

In order to study the UV asymptotics ($0 < g_i \ll 1$), we rewrite this as

$$\partial_x^2\psi(x) = \left(e^{2\theta}e^{2x}\prod_i (1+g_i x)^{k_i} + t(x)\right)\psi(x) \tag{4.91}$$

where $e^{2\theta} = \frac{1}{\lambda^2}\prod_i g_i^{-k_i}$ is identified with an RG scale. When $t(x) = 0$, the Miura $\lambda$-oper describes the vacuum state whereas non-trivial $t(x) = a_+(x)^2 + \partial_x a_+(x)$ that we build from

[2]The vacuum module at $k = 1$ and other related ODEs have been proposed and studied in [95, 96, 97, 98, 99, 100, 101].

the solution to the Bethe equations (4.48) describes a more general state $|\ell\rangle$.

Let $\psi(x;\theta)$ be the unique *small solution*, whose precise meaning is defined in the next section, that decays exponentially fast along the ray of large real positive $x+\theta$. The normalization is chosen to match asymptotically the WKB series in (4.106). By the ODE/IM correspondence, we identify

$$T_{n;\ell}(\theta) \equiv \langle \ell | \hat{T}_n | \ell \rangle = i \left( \psi\Big(x; \theta - \frac{i\pi n}{2}\Big), \psi\Big(x, \theta + \frac{i\pi n}{2}\Big) \right). \tag{4.92}$$

As the transfer function $T_{n;\ell}(\theta)$ is independent of $x$, we can evaluate the Wronskian in a convenient region where the explicit form of $\psi$ is accessible. For the case of $SU(2)_k$ chiral WZW model, this region is $1/g \gg -x \gg 0$. For $\prod_{i=1}^m SU(2)_{k_i}$, one can define an overall scaling parameter $g$ defined as $\frac{1}{g} = \frac{1}{m}\sum_{i=1}^m \frac{1}{g_i}$ for which the relevant region is $1/g \gg -x \gg 0$ (see Appendix F.3 of [1] for details). This allows for a systematic expansion in powers of the $g_i$.

In the same vein as in [116, 157], we can also define $Q$-functions, essentially as the coefficients of $\psi(x)$ in an expansion at large negative $x$. If the twist $\alpha_+$ in $a_+(x)$ is zero, then the construction of $Q$-functions is given in [1] and reviewed in Appendix D.4. As a result, (4.92) becomes expressible as a quantum Wronskian

$$T_{n;\ell}(\theta) = \frac{i}{2\ell+1}\left[ Q_\ell\left(\theta + \frac{i\pi n}{2}\right)\widetilde{Q}_\ell\left(\theta - \frac{i\pi n}{2}\right) - Q_\ell\left(\theta - \frac{i\pi n}{2}\right)\widetilde{Q}_\ell\left(\theta + \frac{i\pi n}{2}\right)\right], \tag{4.93}$$

a form that is familiar from the integrability literature.

This turns out to be a useful tool in perturbative calculations as well. We can find the expression for $Q$ and $\tilde{Q}$ to sufficient order in $g$ by comparing to a direct perturbative evaluation of (4.91). For the ground state in a generic spin $l$ module, the above claim has been verified in [1]. In this work, we will present a few examples of the claim for excited states in Appendix D.4.

### 4.4.1 ODE/IM for primary fields

We propose to identify the expectation values $T_{n;l}[\theta]$ on the $\mathfrak{su}(2)$ WZW primary fields $|l\rangle$ with the transport data of the Schröedinger equation

$$\partial_x^2 \psi(x) = \big[e^{2\theta} e^{2x}(1+gx)^k + \frac{l(l+1)}{(x+1/g)^2}\big]\psi(x) \tag{4.94}$$

The second term is the standard angular momentum term [116], which accounts for different highest weight modules. Again, the shift $x \to x - \frac{1}{g}$ maps the equation to

$$\partial_x^2 \psi(x) = \big[e^{2\theta} e^{-\frac{2}{g}} g^k e^{2x} x^k + \frac{l(l+1)}{x^2}\big] \psi(x) \tag{4.95}$$

so that the transport data is only a function of the combination $e^{\theta} e^{-\frac{1}{g}} g^{\frac{k}{2}}$.

An important observation is in order. The above differential equation makes sense for all values of $l$, and one can define small sections $\psi_n$ at positive infinity and their Wronskians $T_{n;l}[\theta]$ as for the $l = 0$ case. The regular singularity at $x = -\frac{1}{g}$, though, generically changes the overall monodromy structure of the differential equation: solutions are not entire functions of $x$, but have a monodromy around $x = -\frac{1}{g}$. The $T_{n;l}[\theta]$ functions do not exhaust the monodromy data of the differential equation.

For applications to an $\mathfrak{su}(2)_k$ WZW model, we are interested in integrable modules only, for which $0 \leq l \leq \frac{k}{2}$ and $2l$ is an integer. It turns out that this is a very special choice for the differential equation as well. Naively, a regular singularity such that $2l$ is an integer will have a logarithmic monodromy. The order $k$ zero of the regular part of the potential, though, forces the monodromy to be simply $(-1)^l$. In other words, the differential equation has a regular singularity of trivial monodromy at $x = -\frac{1}{g}$. This guarantees that the differential equation has the same type of monodromy data as the $l = 0$, captured fully by the $T_{n;l}[\theta]$ functions.

The WKB analysis also proceeds in much the same way as for the $l = 0$ case, except that the local problem around $x = -\frac{1}{g}$ is modified. This has two consequences:

- The local Wronskians $d^{(k)}_{2j+1}$ are replaced by

$$d^{(k)}_{2j+1;l} \equiv \frac{\sin(2j+1)(2l+1)\frac{\pi}{k+2}}{\sin(2l+1)\frac{\pi}{k+2}} \tag{4.96}$$

  which coincide with the expectation values of $\mathcal{L}_j$ in the primary tower of spin $l$.

- An extra $(-1)^l$ sign appears in the IR behaviour of certain Wronskians, which we interpret as the expectation values of $\mathcal{L}_{\frac{k}{2}}$ in the primary tower of spin $l$.

The perturbative analysis requires some extra care, because the angular momentum

term dominates over the exponential for sufficiently negative $x$, leading to a behaviour

$$\psi_0(x) \sim -\frac{Q_l(g_{\text{eff}})}{2l+1}(x+\frac{1}{g})^{l+1} - \frac{\tilde{Q}_\ell(g_{\text{eff}})}{2l+1}(x+\frac{1}{g})^{-l}. \tag{4.97}$$

In the matching region $\frac{1}{g} \gg -x \gg 0$, the asymptotic behavior becomes

$$\psi_0(x) \sim -\frac{Q_l(g_{\text{eff}})}{2l+1}\frac{1}{g^{l+1}}[1+(l+1)gx] - \frac{\tilde{Q}_\ell(g_{\text{eff}})}{2l+1}g^l[1-lgx]. \tag{4.98}$$

Here, we find a perturbative expansion of the two Q-functions:

$$\begin{aligned} Q(\theta) &= \frac{g_{\text{eff}}^l}{\sqrt{\pi}}\left(1+q_1 g_{\text{eff}}(\theta)+\cdots\right) \\ \tilde{Q}(\theta) &= \frac{g_{\text{eff}}^{-l}}{\sqrt{\pi}}\left(-\frac{1}{g_{\text{eff}}}+\tilde{q}_0+\tilde{q}_1 g_{\text{eff}}(\theta)+\cdots\right) \end{aligned} \tag{4.99}$$

and derive a perturbative expansion for $T_{n;l}$:

$$\begin{aligned} T_{n;l} \sim n - I_R\pi^2 l(l+1)g^2 + \frac{\pi^2}{2}\left[k\left(-1+l+2l^2\right) - 4l(\theta+l\theta+\tilde{q}_0)\right]I_R g^3 \\ +\frac{\pi^2}{60}I_R g^4\Big[-45k^2\left(l^2-1\right)+30k(\tilde{q}_0(4l-1)+\theta(l+1)(8l-3)) \\ +\pi^2 l(l+1)\left(3n^2\left(l^2+l+3\right)-(l+2)(7l+13)\right) \\ -60l\left(6\theta\tilde{q}_0+2\tilde{q}_0^2+4\tilde{q}_1+3\theta^2(l+1)\right)+120\tilde{q}_1\Big]\cdots \end{aligned} \tag{4.100}$$

where $I_R = \frac{1}{6}n\left(-1+n^2\right)$ and $\tilde{q}_0 = -\frac{k}{4}+(1+l)(\gamma-\log 2)$. We match it with the explicit line defect calculations in Appendix D.3.

### 4.4.2 The coset scaling limit

We can scale the variable $x$ in the $\lambda$-oper to get a slightly different parameterization

$$\partial_x^2\psi(x) = \left(\frac{\alpha^{2+\sum_i k_i}}{\lambda^2}e^{2\alpha x}\prod_i(x-\alpha^{-1}z_i)^{k_i}+\alpha^2 t(\alpha x)\right)\psi(x). \tag{4.101}$$

A scaling limit $\alpha \to 0$ while keeping $\alpha^{-1} z_i$ and $\frac{\alpha^{2+\sum_i k_i}}{\lambda^2}$ fixed will bring this to a $\lambda$-oper which is naturally associated to integrable lines in a coset model.

Physically, we are sending the $g_i$ to infinity while keeping their ratios fixed and adjusting the RG flow scale. We expect the Kondo lines RG flow in that limit to admit an intermediate regime where the line defects become effectively transparent to the overall WZW currents, so that they can be identified with defect lines in a coset model. It would be nice to explore this limit more carefully.

## 4.5 The IR expansion

The Kondo line defects $L_j[\theta]$, where $j$ is the spin that labels the $SU(2)$ representation and $\theta$ is the spectral parameter, are asymptotically free line defects defined in a product of WZW models. They have a non-trivial, possibly non-perturbative RG flow which can be explored by looking at their action on the circle Hilbert space with the help of the ODE/IM correspondence. In the UV, the action is given perturbatively by the corresponding operator $\hat{T}_j$, defined in (4.85).

In the IR, the defects will flow to conformally-invariant defects. Because of their chiral nature, in the IR they will commute with both holomorphic and anti-holomorphic stress tensor and define topological line defects. A rich CFT such as the product of WZW models can have a very large variety of topological line defects, which commute with the stress tensor but with little else.

The ODE/IM correspondence, though, gives immediate evidence that the IR limit of Kondo defects should be more special than that, and commute with all the Kac-Moody currents. Indeed, we will see that the far IR limit of the ODE/IM solution is controlled by a WKB leading answer which depends very little on the details of $t(z)$, up to the choice of $l_i$. In particular, they are blind to the details of the Bethe roots, which control which current descendants one is taking expectation values on.

Line defects that commute with the whole current algebra of the product of WZW models are referred to as Verlinde line operators. They are labeled by the Kac labels, i.e. same as current algebra primary operator. They are products of individual Verlinde lines in each WZW factor.

Denoted by $\mathcal{L}_j$, with $j = 0, \frac{1}{2}, 1, \ldots, \frac{k}{2}$, their expectation value in the vacuum state,

often called the quantum dimension, is given by

$$\langle \mathcal{L}_j \rangle = d^{(k)}_{2j+1} \equiv \frac{\sin \frac{\pi}{k+2}(2j+1)}{\sin \frac{\pi}{k+2}}. \tag{4.102}$$

In the ground state of spin $l$, or in any descendant of that, their expectation value is

$$\langle l,k|\mathcal{L}_j|l,k\rangle = d^{(k)}_{2j+1;l} \equiv \frac{\sin \frac{\pi}{k+2}(2l+1)(2j+1)}{\sin \frac{\pi}{k+2}(2l+1)}. \tag{4.103}$$

If we go to the IR, but not to the infinitely far IR, the Kondo line defects will be described as IR free deformations of some sums of products of Verlinde lines. The deformation can involve any $SU(2)$-invariant local operators supported on the Verlinde lines. For generic Verlinde lines, there are many such operators, looking like descendants of chiral primary fields of various spins. We will see that the subleading WKB corrections do generically involve fractional powers of the scale $e^{\theta}$ which can be explained by the conformal dimension of these operators.

As we mentioned in Section 4.1, something special happens when the far IR defect is the identity line, or some other Verlinde line which does *not* support non-trivial chiral primaries. In such a situation, the IR free deformation must involve the integral along the line of $SU(2)$-invariant *bulk* chiral operators, starting with the stress tensor. The expectation values of these deformed identity lines are simply the exponential of the zero-modes of these bulk operators, which behave as local Hamiltonians for the affine Gaudin model.

We will see below that the ODE/IM correspondence predicts such IR destiny for line defects associated with pairs of Stokes sectors which are joined by a generic WKB line[3]. The number of such pairs is precisely the same as the number of zeroes for $\varphi(z)$, as expected from the classical affine Gaudin model. The WKB expansion of these reproduces the expectation values of the quantum local Hamiltonians.

### 4.5.1 Vacuum state $t(x) = 0$

Let us first focus on the case of single $SU(2)$ and $t(x) = 0$. The Schrödinger equation takes the form

$$\partial_x^2 \psi(x) = e^{2\theta} e^{2x} (1+gx)^k \psi(x). \tag{4.104}$$

[3]In the case of a single SU(2), there is one generic WKB line; see the end of Section 4.5.1.

In this section, we are interested in the IR limit $\lambda^{-1} = e^{\theta} \to \infty$, where Voros/GMN-style WKB analysis is applicable. The analysis is essentially the same as in [1], except that we are also interested in the sub-leading terms in the $\lambda$ expansion.

We will briefly review the analysis and leave details in Appendix D.5. One starts by reading off the quadratic differential $P(x)dx^2 = e^{2x}(1+gx)^k dx^2$, which has a zero of order $k$ at $x_0 = -1/g$ and an exponential singularity at infinity. For any angle $\vartheta \in \mathbb{R}/2\pi\mathbb{Z}$, *$\vartheta$-WKB lines* are curves in the complex plane where

$$\mathrm{Im}\left[e^{i\vartheta}\sqrt{P(x)}dx \cdot \partial_t\right] = 0, \tag{4.105}$$

where $\partial_t$ is the tangent vector of the curve. One such line passes through any point in the $x$ plane. Generic WKB lines go to positive infinity in both directions, joining two Stokes sectors there. Special WKB lines hit a zero of $P(x)$ such as $x = -\frac{1}{g}$ or flow to negative infinity. [4]

The union of special WKB lines is called the WKB diagram/spectral network. $\vartheta$ is chosen such that $e^{\theta}$ lies in the half-plane centered on $e^{i\vartheta}$, where the WKB approximation gives the correct $e^{-\theta} \to 0$ asymptotics. The structure of the spectral network governs which solutions of the Schrödinger equation have a specific WKB asymptotic expansion.

In our current example, the structure of the WKB diagram is shown in Fig. 4.2. Special WKB lines go towards positive infinity along the positive real $x+\theta+i\pi n$, $n \in \mathbb{Z}$ direction. There are $k+2$ of them that are connected to the order $k$ zero $x_0 = -\frac{1}{g}$. The remaining special WKB lines go towards negative infinity with imaginary part shifted by $\pm\frac{\pi}{2}k$.

Next, one needs to find a set of solutions, referred to as *small solutions*, which decrease exponentially fast along the Stokes lines towards positive infinity (and thus along WKB lines asymptoting to them). In particular, we define $\psi_0(x)$ to be the small solution that decreases fast along the line of large real positive $x+\theta$ and agrees with the WKB asymptotics along this line

$$\psi_0(x;\theta) \sim \frac{1}{\sqrt{2\partial S^{\mathrm{asym}}(x,e^{\theta})}} e^{-S^{\mathrm{asym}}(x,e^{\theta})} \tag{4.106}$$

where $S^{\mathrm{asym}}(x,e^{\theta})$ is the primitive of the WKB momentum, given by an asymptotic series in large $x$ and small $e^{-\theta}$. Although the WKB momentum is uniquely defined, its primitive

[4] Special WKB lines are also sometimes called Stokes lines. In the situation at hand, there are two possible meaning for "Stokes": it may refer to the asymptotic expansion of a solution at large positive $x$, as in defining the Stokes data of the oper, or it may refer to the WKB asymptotic expansion at small $\lambda$. In order to avoid confusion, we use the terms "WKB" exclusively for the latter and "Stokes" for the former.

needs a choice of integration constant. We choose the leading term to be

$$e^{\theta}\int_{-\frac{1}{g}}^{x} e^{y}(1+gy)^{\frac{k}{2}}dy = e^{\theta}e^{-\frac{1}{g}}g^{\frac{k}{2}}\int_{0}^{x+\frac{1}{g}} e^{y}y^{\frac{k}{2}}dy. \tag{4.107}$$

Different choices clearly lead to different normalization of the Wronskians, namely $T$ functions (4.92). This choice has the nice property later on that the exponent of (4.109) is zero at the leading order. In a practical calculation involving subleading terms, one also needs to make a choice for every order in $e^{-\theta}$.

Then for all $n \in \mathbb{Z}$, we have a small solution $\psi_n(x) \equiv \psi_0(x;\theta+i\pi n)$ along the large positive real $x+\theta+i\pi n$ direction.

Next, we want to use the WKB network to evaluate the WKB asymptotics of the Wronskians. In the standard Voros/GMN-style WKB analysis, one studies Wronskians between two of the small solutions joined by a generic WKB line. These Wronskians are controlled by the contour integral along the WKB line of the WKB one form whose leading term is $\sqrt{P(x)}dx$. This collection of Wronskians is incomplete, though, unless all zeroes of $P(x)$ are simple.

As has been developed in [1] and Appendix D.5, WKB analysis can be generalized to study non-simple zeros. Roughly speaking, one also needs the information around the matching regions, which, in the current example, are the order $k$ zero $x_0 = -\frac{1}{g}$, and the large negative $x$. Correspondingly, one can derive WKB asymptotics for Wronskians between two of the small solutions joined by a special WKB line to the same zero, or to negative infinity.

Following from the WKB diagram shown in Fig. 4.2 let us suppose, for convenience, that the numbering of the special WKB lines that are connected to the zero at $x = -\frac{1}{g}$ is $n_0, n_0+1, n_0+2, \ldots, n_0+k+1$. The precise value of $n_0$ depends on the parity of $k$ and $\operatorname{Im}\theta$, which are given in [1] and are not important to us. There are three different scenarios:

- Wronskians between two of the $k+2$ small solutions whose special WKB lines are connected to the zero, namely $i(\psi_n, \psi_{n'})$ for $n_0 \le n < n' \le n_0+k+1$.
- Wronskians between small solutions whose special WKB lines are connected to large negative matching region (to be made precise below), namely $i(\psi_n, \psi_{n'})$ for $n < n' \le n_0$ or $n_0+k+1 \le n < n'$ or $n \le n_0 < n_0+k+1 \le n'$.
- The remaining ones can be related to the first two scenarios using Plücker formula.

In particular, to deal with the first case, it is important to study the local behavior around the zero $x_0 = -\frac{1}{g}$. Locally around $x_0$, a zero of order $k$, the stress tensor should take the form $y^k + \ldots$, with $y$ being the coordinate in the local coordinate system. Indeed, one can always find the coordinate transformation $x \to y(x)$ such that stress tensor takes the form of

$$y^k + a_{k-2}\gamma^k y^{k-2} + \cdots + a_j \gamma^{2+j} y^j + \cdots + a_0 \gamma^2 \tag{4.108}$$

where $\gamma = e^{-\theta \frac{2}{k+2}}$. Importantly there are $k-1$ coefficients $a_j = a_j^{(0)} + \gamma^{k+2} a_j^{(2)} + \gamma^{2(k+2)} a_j^{(4)} + \ldots$ that are uniquely fixed in $\gamma^{k+2}$ asymptotics. One can find a set of nice solutions $A_{k;i}(y)$ to this local problem and evaluate the Wronskian perturbatively. The general procedure to do this is described in Appendix D.5. On the other hand, Wronskians between small solutions $\psi_n(x)$ are equal to the Wronskians between the corresponding local solutions $A_{k;i}(y)$ with a careful treatment on the normalization of the solutions. We will only quote the result here, leaving the details in Appendix D.5,

$$i\left(\psi_n, \psi_{n'}\right) \sim e^{0+O(e^{-\theta})}\left(d^{(k)}_{n'-n} + O(\gamma^2)\right) \tag{4.109}$$

whose leading term is given by the quantum dimension defined as

$$d_n^{(k)} = \frac{e^{\frac{\pi i}{k+2} n} - e^{-\frac{\pi i}{k+2} n}}{e^{\frac{\pi i}{k+2}} - e^{-\frac{\pi i}{k+2}}}. \tag{4.110}$$

Subleading terms are computable order by order in $\gamma$. See Appendix D.5 for the general prescription. There are two exceptions $k = 1, 2$ where we can calculate Wronskians exactly. The important part is that the corrections to the Wronskians come in as integer power of $\gamma$ but start from $\gamma^2$ order.

In the second scenario, the special WKB lines 'meet' at the large negative $x$. It turns out, for some suitably chosen $x_{-\infty}$, a shift of the coordinate $x \to \delta = x - x_{-\infty}$ will transform the quadratic differential into

$$e^{2\delta}\left(1 + g_{\text{eff}}(\theta)\delta\right)^k. \tag{4.111}$$

The details are given in Appendix D.5. Here, what matters to us is that $x_{-\infty}$ has a large negative real part and in the IR limit $\theta \to \infty$ we have

$$x_{-\infty} \sim -\theta - \frac{1}{2} k \log(-g\theta) - \frac{k^2}{4}\frac{\log(-g\theta)}{\theta} + O\Big(\frac{1}{\theta}\Big). \tag{4.112}$$

The coupling $g_{\text{eff}}(\theta)$ is defined by the relation

$$x_{-\infty}(\theta) = \frac{1}{g_{\text{eff}}(\theta)} - \frac{1}{g} \tag{4.113}$$

and goes to 0 in the IR limit $\theta \to \infty$. This is precisely the effective coupling for the infrared free line defect, whose physical meaning will be given below in Section 4.5.3. For now, we only need the fact that $g_{\text{eff}}(\theta) \to 0$ as $\theta \to \infty$. Therefore, we can study the Wronskians of solutions in $g_{\text{eff}}$ expansion.

In the leading order, the local solutions are given by Bessel functions. Therefore by means of Bessel function identities and with normalization factors carefully taken into account, the results are

$$i(\psi_n, \psi_{n'}) \sim \exp\left(\frac{(-1)^n + (-1)^{n'}}{2} e^{i\frac{\pi k}{2}} m_k(g) e^{\theta} + O(e^{-\theta})\right)\left[(n'-n) + O(g_{\text{eff}}^2)\right] \tag{4.114}$$

whenever $n \leq n_0$ and $n' \leq n_0$,

$$i(\psi_n, \psi_{n'}) \sim \exp\left(\frac{(-1)^n + (-1)^{n'}}{2} e^{-i\frac{\pi k}{2}} m_k(g) e^{\theta} + O(e^{-\theta})\right)\left[(n'-n) + O(g_{\text{eff}}^2)\right] \tag{4.115}$$

whenever $n \geq n_0 + k + 1$ and $n' \geq n_0 + k + 1$, and

$$i(\psi_n, \psi_{n'}) \sim \exp\left(\frac{(-1)^n e^{i\frac{\pi k}{2}} + (-1)^{n'} e^{-i\frac{\pi k}{2}}}{2} e^{\theta} m_k(g) + O(e^{-\theta})\right)\left[(n'-n-k) + O(g_{\text{eff}}^2)\right] \tag{4.116}$$

whenever $n \leq n_0$ and $n' \geq n_0 + k + 1$.

In the third scenario, we can just use Plücker formula to reduce to the previous two scenarios. Details can be found in [1].

Recall that the leading order of the second term agrees with the one from the UV expansion and intuitively just counts the number of spacing between different special WKB lines at the left-hand side of the special WKB diagram, see e.g. Fig. 4.2. The exponential factor is the non-perturbative ground state energy shift.

As we discussed in Section 4.1 and at the beginning of this section, the vevs of local integrals of motion for the affine Gaudin model are given by the Wronskians which correspond to generic WKB lines. In the example at hand, there is only one such line depicted by the dotted burgundy line in Fig. 4.2, corresponding to $\mathcal{L}_{\frac{k}{2}}$ in the infrared. Indeed, the

$\mathcal{L}_{\frac{k}{2}}$ line does not support nontrivial chiral WZW primaries. Since the corresponding Wronskian $i(\psi_{-\frac{k+1}{2}}, \psi_{\frac{k+1}{2}})$ is controlled by the contour integral of the WKB momentum along the generic WKB line, it doesn't involve the local analysis around the zero or negative infinity, hence it is simply organized by odd powers of $e^{-\theta}$.

### 4.5.2 $t(x) \neq 0$

When $t(x) = a_+(x)^2 + \partial a_+(x) \neq 0$, the evaluation of the Wronskians via WKB analysis is basically the same as the previous section except for the following modifications.

In the first scenario of the previous section, namely, for the Wronskians of two solutions whose special WKB lines are connected at the zero $x = -\frac{1}{g}$, the local coordinate system in general has an additional piece, compared to (4.108)

$$y^k + a_{k-2}\gamma^k y^{k-2} + \cdots + a_j \gamma^{2+j} y^j + \cdots + a_0 \gamma^2 + \frac{l(l+1)}{y^2} \tag{4.117}$$

where $-l$ is the residue of $a_+(x)$ at the zero. This will change the leading order of (4.109) to be

$$d^{(k)}_{2j+1;l} \equiv \frac{\sin \frac{\pi}{k+2}(2l+1)(2j+1)}{\sin \frac{\pi}{k+2}(2l+1)}. \tag{4.118}$$

The nonzero regular part of $a_+(x)$ has a smaller impact. It will change the coefficients $a_j$, the details of the map $x \mapsto y(x)$, and therefore the higher-order corrections. But importantly, the corrections are still organized by integer powers of $\gamma$.

In the second scenario, where two special WKB lines are connected at the negative infinity, we can again go to the coordinate in $\delta = x - x_{-\infty}$ where the quadratic differential reads

$$e^{2\delta}\left(1 + g_{\text{eff}}(\theta)\delta\right)^k + t\Big(x \mapsto \delta + \frac{1}{g_{\text{eff}}}\Big). \tag{4.119}$$

We are then in a situation very similar to the UV expansion. Therefore, the higher-order corrections of the Wronskians come in powers of $g_{\text{eff}}$.

### 4.5.3 Physical interpretation

According to the ODE/IM correspondence (4.92), which we repeat here, the expectation value of the Kondo line operator in the state $|\ell\rangle$ is given by

$$T_{n;\ell}(\theta) \equiv \langle \ell | \hat{T}_n | \ell \rangle = i \left( \psi_0\Big(x; \theta - \frac{i\pi n}{2}\Big), \psi_0\Big(x, \theta + \frac{i\pi n}{2}\Big) \right) \tag{4.120}$$

where $n = 2j + 1$. We showed in Section 4.4 that the leading term in the UV expansion is given by the dimension $n$ of the representation, $T_{n;\ell} \sim n + \dots$.

We now provide the physical implication of the IR expansion we evaluated using WKB analysis previously in this section. The IR expansion of $T_{n;\ell}(\theta)$ reviews an interesting infrared structure. The leading order has been demonstrated in [1]. We will review briefly now and explain how the structure of higher-order corrections we obtained in this section fits in the paradigm.

Depending on the imaginary part of $\theta$, and whether $0 \le 2j \le k$ or $2j > k$, the RG flow takes the Kondo line operator $L_j[\theta]$ to different IR line operators.

Firstly, if $\theta$ is real, or more precisely, valued in a strip around the real $\theta$ axis of width about[5] $(n - k - 1)\pi$, we have the physical RG flow[6]:

- For $0 \le j \le \frac{k}{2}$, over/exact-screening[7], $T_{n;\ell}(\theta) \sim d^{(k)}_{2j+1;l}$, $L_j$ flows to $\mathcal{L}_j$,
- For $j > \frac{k}{2}$, under-screening, $T_{n;\ell}(\theta) \sim e^{-E(n,\ell,k)e^{\theta}} d^{(k)}_{k+1;l}(n-k)$, $L_j$ flows to $\mathcal{L}_{k/2} \otimes L^{IR}_{j-k/2}$.

Second, if we increase the imaginary part of $\theta$ either positively or negatively, there is an interesting sequence of transitions starting from $|\operatorname{Im}\theta| \sim \frac{(n-k-1)\pi}{2}$, the edge of the strip mentioned above. Every time $|\operatorname{Im}\theta|$ increases by $\pi$, we trade one unit of spin for the topological defect with one unit of spin for the internal degrees of freedom. More precisely, $L_j$ flows to $L^{\mathrm{IR}}_{j-\frac{s}{2}} \otimes \mathcal{L}_{\frac{s}{2}}$, $s = k, k-1, \dots, 0$. After $s$ decreases to zero, i.e. when $|\operatorname{Im}\theta|$ is large enough, we will have the circular RG flows where $L_j$ flows to $L^{\mathrm{IR}}_j$.

Since $e^{\theta}$ labels the RG scale and $\theta \to \infty$ is the deep infrared, we have just demonstrated that the leading term of $T_{n;\ell}(\theta)$ simply tells us which infrared line defects we flow to starting

[5] This is true up to $\pm\pi/2$, depending on the parity of $k$ and $n$.

[6] Recall that $e^{\theta}$ labels the RG scale, so the physical RG flow corresponds to real $\theta$.

[7] This terminology is based on the intuitive physical picture that Kondo defect disappears in the IR because magnetic impurity spin is screened by the bulk fermions. See e.g. [22] for more details.

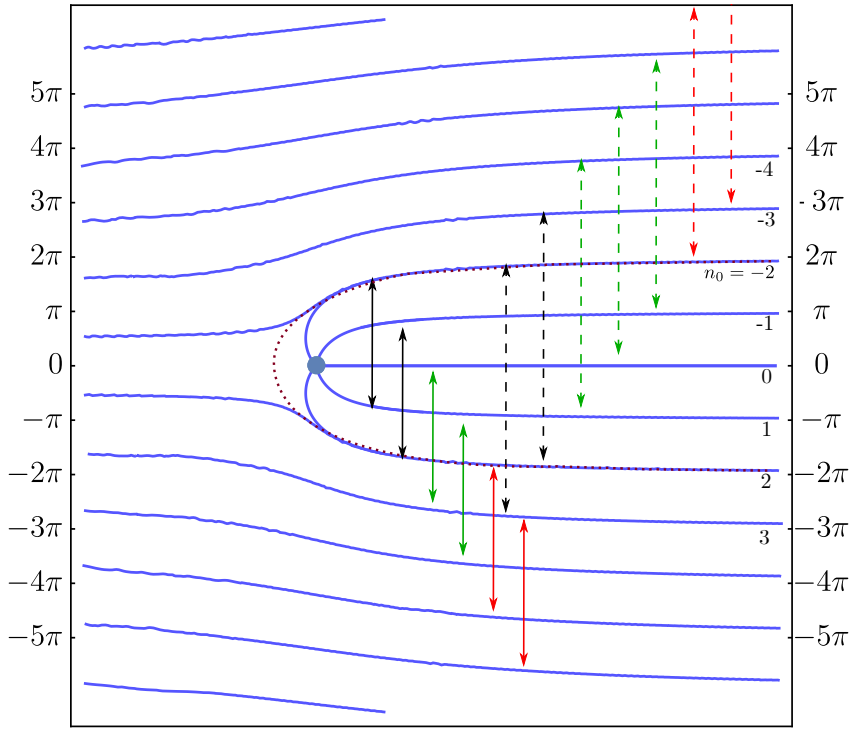


Figure 4.2: Blue curves are the Stokes diagram for $k = 3$ and $\vartheta = 0$. There are five special WKB lines connected to the zero of order $k = 3$. The rest of the special WKB lines connect to the negative infinity. Double headed arrows indicate which two solutions are used in the Wronskian $i(\psi_{n_1}, \psi_{n_2})$ with $n_2 - n_1 = n = 2j + 1$ in different scenarios. The lower (upper) end points to the special WKB lines associated to the small solution $\psi_{n_2}$ ($\psi_{n_1}$). Solid lines ($j = 1$) depict scenarios $0 \leq j \leq \frac{k}{2}$. Colors (black, green and red) of the lines indicate three scenarios as we shift $\mathrm{Im}\,\theta$: physical strip ($L_j$ flows to $\mathcal{L}_j$ ), sequence of transitions ($L_j$ flows to $L^{\mathrm{IR}}_{j-\frac{s}{2}} \otimes \mathcal{L}_{\frac{s}{2}}$, $s = 2j-1, \ldots, 1$) and $L^{\mathrm{IR}}_j$. Dashed lines ($j = 2$) depict scenarios $j > \frac{k}{2}$ respectively. Colors (black, green and red) of the lines indicate three scenarios as we shift $\mathrm{Im}\,\theta$: physical strip ($L_j$ flows to $\mathcal{L}_{k/2} \otimes L^{IR}_{j-k/2}$ ), sequence of transitions ($L_j$ flows to $L^{\mathrm{IR}}_{j-\frac{s}{2}} \otimes \mathcal{L}_{\frac{s}{2}}$, $s = k-1, \ldots, 1$) and $L^{\mathrm{IR}}_j$. The dotted burgundy line denotes the unique generic WKB line that gives rise to the local integrals of motion.

from $L_j$ defined in the UV. Correspondingly, the far IR destiny of UV line defects can be determined from some simple combinatorics from the topology of the WKB network.

Subleading terms are obviously due to the deformation that brings us away from the deep IR. More precisely, we need to look at the RG flow a bit away from the deep IR. In the case of the RG flow that flows to the Kondo line defect $L_j^{\rm IR}$, an infrared free line defect, the effective coupling $g_{\rm eff}(\theta)$ is negative and becomes smaller in the IR. Therefore, the corrections are expected to come in powers of $g_{\rm eff}$, which is small and negative.

On the other hand, topological lines in the infrared are not free and appear in the RG flow as strongly coupled infrared fixed points[8]. Nevertheless, we know a lot about the local operators that are supported on the lines. Among them, it is the least irrelevant operator that contributes the corrections the closest to the deep IR fixed point [21]. On a spin $0 < j < \frac{k}{2}$ Verlinde line in chiral WZW, it is the WZW descendant of the spin 1 operator of dimension $\frac{2}{k+2}$, denoted by $J^a_{-1}\phi^a$. It is a Virasoro primary of scaling dimension $1+\frac{2}{k+2}$ and has zero one-point function. Then a simple dimensional analysis implies that there will be corrections in powers of $\gamma = e^{-\theta\left(\frac{2}{k+2}\right)}$, starting from $\gamma^2$. Another obvious candidate $J^aJ^a$ has dimension 2, thus contributing corrections in integer powers of $\hbar = \gamma^{\frac{k+2}{2}}$, which is more irrelevant. Note that the spin 1 operator $\phi^a$ is not supported on the Verlinde line $\mathcal{L}_{\frac{k}{2}}$, obtained in the exact screening case. This is precisely what we found in the WKB analysis around (4.108) and (4.109).

## 4.6 Some comments about the semiclassical limit

The RG flow of the Kondo defects is often non-perturbative. An important exception occurs when the levels $k_i$ are large: in an appropriate RG scheme, the couplings remain small all the way to the IR. It is useful to illustrate this in the $N = 1$ case.

We can start from the quadratic differential $\lambda^{-2}e^{2x}x^k dx^2$. The RG prescription we used before for the couplings sets

$$\lambda = e^{\frac{1}{g}} g^{-\frac{k}{2}} \tag{4.121}$$

so that the quadratic differential becomes $e^{2x-\frac{2}{g}}(gx)^k dx^2$ which can be mapped by a translation to $e^{2x}(1+gx)^k dx^2$ and treated perturbatively. In these conventions, $g$ is small as $\lambda \gg 1$ in the UV, but flows all the way to infinity in the IR as $\lambda \ll 1$.

[8] Unless the levels $k_i$ are large, in which case the RG flow to a topological line can be perturbative. See the next section.

When $k \gg 1$, these RG conventions are not very good. For example, even if $g \sim k^{-1}$ is small, $(1+gx)^k \sim e^{gkx}$ is not close to 1. Consider, instead, a different definition of $g$ where we employ both a translation and a scale transformation of $x$ to arrive to some $e^{2\alpha(g)x}(1+gx)^k dx^2$. We can map this back to $e^{2x-\frac{2\alpha(g)}{g}} g^k x^k \alpha(g)^{-k-2} dx^2$ and thus to

$$\lambda = e^{\frac{\alpha(g)}{g}} g^{-\frac{k}{2}} \alpha(g)^{1+\frac{k}{2}}. \tag{4.122}$$

If we select $\alpha(g) = 1 - \frac{k}{2}g$, then $e^{2\alpha(g)x}(1+gx)^k dx^2 \sim e^{2x} dx^2$ up to corrections of order $g^2 k$, which are small even if $g \sim k^{-1}$.

This seems a more reliable way to deal with the perturbative RG flow. Now we have

$$\lambda = e^{\frac{1}{g}-\frac{k}{2}} g \Big(g^{-1} - \frac{k}{2}\Big)^{1+\frac{k}{2}}, \tag{4.123}$$

which flows from $g = 0$ to $g = \frac{2}{k}$ from the UV to the IR, so that the coupling is perturbatively small all the way.

This RG scheme also seems appropriate to make contact with the classical affine Gaudin model in a $k \to \infty$ semiclassical limit. In general, define

$$g_i = \frac{1}{\varphi(z)} \frac{1}{z - z_i}. \tag{4.124}$$

This definition is inspired by the classical affine Gaudin Lax matrix (4.9).

Then

$$e^{\frac{2x}{\varphi(z)}} \prod_i (1 + g_i x)^{k_i} dx^2 \tag{4.125}$$

can be mapped to

$$e^{2x} \prod_i \Big(1 + \frac{1}{z - z_i} x\Big)^{k_i} \varphi(z)^2 dx^2 \tag{4.126}$$

and then to

$$\frac{e^{-2z}\varphi(z)^2}{\prod_i (z - z_i)^{k_i}} e^{2x} \prod_i (x - z_i)^{k_i} dx^2 \tag{4.127}$$

so that we have a $z$ RG flow controlled by

$$\lambda = \varphi(z)^{-1} e^z \prod_i (z - z_i)^{\frac{k_i}{2}} \tag{4.128}$$

and fixed points at $z \sim z_i$ where $g_i$ is finite and small, while all other $g_j$ vanish.

## 4.7 Generalizations: $\mathfrak{sl}_3$

The discussion in Section 4.2 of the affine $\mathfrak{sl}_2$ opers, the Bethe equations, and WKB solutions can be easily generalized to higher rank Lie algebras. We demonstrate the case of $\mathfrak{sl}_3$ in this section. We leave a proper discussion of the corresponding Kondo defects and ODE/IM solutions to future work.

### 4.7.1 Basic Definitions

An $\mathfrak{sl}_3$ oper is a complexified third order differential operator

$$\partial_x^3 - t_2(x)\partial_x + t_3(x) \tag{4.129}$$

with a natural transformation law under a change of coordinate

$$\partial_x^3 - t_2(x)\partial_x + t_3(x) = (\partial_x\tilde{x})^2\Big(\partial_{\tilde{x}}^3 - \tilde{t}_2(\tilde{x})\partial_{\tilde{x}} + \tilde{t}_3(\tilde{x})\Big)(\partial_x\tilde{x}). \tag{4.130}$$

We will work with $\mathfrak{sl}_3$ opers for which both $t_2(x)$ and $t_3(x)$ are rational functions.

The data of an $\mathfrak{sl}_3$ oper is equivalent to that of a flat connection

$$\partial_x + \begin{pmatrix} 0 & t_2(x) & t_3(x) \\ 1 & 0 & 0 \\ 0 & 1 & 0 \end{pmatrix}. \tag{4.131}$$

More generally, an $\mathfrak{sl}_3$ oper can be described as a flat connection of the form

$$\partial_x + \begin{pmatrix} a(x) & b(x) & c(x) \\ 1 & \tilde{a}(x) & \tilde{b}(x) \\ 0 & 1 & -a(x) - \tilde{a}(x) \end{pmatrix}. \tag{4.132}$$

modulo gauge transformations by unipotent upper-triangular matrices. Any $\mathfrak{sl}_3$ oper has

a unique *canonical form* (4.131) where

$$t_2(x) = a(x)^2 + a(x)\tilde{a}(x) + \tilde{a}(x)^2 + 2\partial_x a(x) + \partial_x \tilde{a}(x) + b(x) + \tilde{b}(x), \tag{4.133a}$$

$$\begin{aligned} t_3(x) = &-(a(x) + \tilde{a}(x))\big(a(x)\tilde{a}(x) + \partial_x a(x) + 2\partial_x \tilde{a}(x) - b(x)\big) \\ &- \partial_x^2 a(x) - \partial_x^2 \tilde{a}(x) - a(x)\tilde{b}(x) - \partial_x \tilde{b}(x) + c(x). \end{aligned} \tag{4.133b}$$

An $\mathfrak{sl}_3$ $\lambda$-*oper* is a complexified third order differential operator with a particular dependence on the auxiliary complex parameter $\lambda$ of the form

$$\partial_x^3 - t_2(x)\partial_x + t_3(x) + \frac{P(x)}{\lambda^3}, \tag{4.134}$$

where $t_2(x)$ and $t_3(x)$ are rational functions. Equivalently, we can describe this as a flat connection

$$\partial_x + \begin{pmatrix} 0 & t_2(x)\lambda & P(x)\lambda^{-1} + t_3(x)\lambda^2 \\ \lambda^{-1} & 0 & 0 \\ 0 & \lambda^{-1} & 0 \end{pmatrix}. \tag{4.135}$$

More generally, an $\mathfrak{sl}_3$ $\lambda$-oper is defined as a connection of the form

$$\partial_x + \begin{pmatrix} a(x) & b(x)\lambda & P(x)\lambda^{-1} + c(x)\lambda^2 \\ \lambda^{-1} & \tilde{a}(x) & \tilde{b}(x)\lambda \\ 0 & \lambda^{-1} & -a(x) - \tilde{a}(x) \end{pmatrix} \tag{4.136}$$

where $a(x)$, $\tilde{a}(x)$, $b(x)$, $\tilde{b}(x)$ and $c(x)$ are rational functions, modulo gauge transformations by upper-triangular matrices of the form

$$\begin{pmatrix} 1 & v(x)\lambda & w(x)\lambda^2 \\ 0 & 1 & \tilde{v}(x)\lambda \\ 0 & 0 & 1 \end{pmatrix} \tag{4.137}$$

where $v(x)$, $\tilde{v}(x)$ and $w(x)$ are rational functions. Every $\mathfrak{sl}_3$ $\lambda$-oper has a unique *canonical form* as in (4.135).

If we conjugate the connection (4.136) by cyclic permutation matrices then we obtain two alternative formulations of the differential operator (4.134), leading to two alternative (but equivalent) formulations of $\mathfrak{sl}_3$ $\lambda$-opers. Specifically, an $\mathfrak{sl}_3$ $\lambda$-oper can equally be

described as a flat connection of the form

$$\partial_x + \begin{pmatrix} -a(x) - \tilde{a}(x) & 0 & \lambda^{-1} \\ P(x)\lambda^{-1} + c(x)\lambda^2 & a(x) & b(x)\lambda \\ \tilde{b}(x)\lambda & \lambda^{-1} & \tilde{a}(x) \end{pmatrix} \tag{4.138}$$

modulo gauge transformations by matrices

$$\begin{pmatrix} 1 & 0 & 0 \\ w(x)\lambda^2 & 1 & v(x)\lambda \\ \tilde{v}(x)\lambda & 0 & 1 \end{pmatrix}. \tag{4.139}$$

Equivalently, an $\mathfrak{sl}_3$ $\lambda$-oper can also be described as a connection of the form

$$\partial_x + \begin{pmatrix} \tilde{a}(x) & \tilde{b}(x)\lambda & \lambda^{-1} \\ \lambda^{-1} & -a(x) - \tilde{a}(x) & 0 \\ b(x)\lambda & P(x)\lambda^{-1} + c(x)\lambda^2 & a(x) \end{pmatrix} \tag{4.140}$$

modulo gauge transformations by matrices

$$\begin{pmatrix} 1 & \tilde{v}(x)\lambda & 0 \\ 0 & 1 & 0 \\ v(x)\lambda & w(x)\lambda^2 & 1 \end{pmatrix}. \tag{4.141}$$

The unique canonical form of an $\mathfrak{sl}_3$ $\lambda$-oper in the second description (4.138) is given by

$$\partial_x + \begin{pmatrix} 0 & 0 & \lambda^{-1} \\ P(x)\lambda^{-1} + t_3(x)\lambda^2 & 0 & t_2(x)\lambda \\ 0 & \lambda^{-1} & 0 \end{pmatrix}, \tag{4.142}$$

and that of an $\mathfrak{sl}_3$ $\lambda$-oper in the third description (4.140) reads

$$\partial_x + \begin{pmatrix} 0 & 0 & \lambda^{-1} \\ \lambda^{-1} & 0 & 0 \\ t_2(x)\lambda & P(x)\lambda^{-1} + t_3(x)\lambda^2 & 0 \end{pmatrix}. \tag{4.143}$$

### 4.7.2 Miura $\lambda$-opers and singularities of trivial monodromy

A *Miura* $\mathfrak{sl}_3$ *oper* is a connection of the form

$$\partial_x + \begin{pmatrix} a(x) & 0 & 0 \\ 1 & \tilde{a}(x) & 0 \\ 0 & 1 & -a(x) - \tilde{a}(x) \end{pmatrix} \tag{4.144}$$

with $a(x)$ and $\tilde{a}(x)$ rational. Since it is of the general form in (4.132) it defines an $\mathfrak{sl}_3$ oper which corresponds to the differential operator $(\partial_x + a(x))(\partial_x + \tilde{a}(x))(\partial_x - a(x) - \tilde{a}(x))$.

There are two types of apparent singularities, corresponding to the two nodes of the Dynkin diagram of $\mathfrak{sl}_3$. These can be points $w$ where

$$a(x) = \frac{1}{x-w} + d + O(x-w), \qquad \tilde{a}(x) = -\frac{1}{x-w} + d + O(x-w) \tag{4.145}$$

so that, in particular, the constant term of $a(x) - \tilde{a}(x)$ is zero, or points $w'$ where

$$a(x) = \frac{0}{x-w'} - 2d + O(x-w'), \qquad \tilde{a}(x) = \frac{1}{x-w'} + d + O(x-w') \tag{4.146}$$

so that, in particular, the constant term of $a(x) + 2\tilde{a}(x)$ vanishes.

If at a singularity $z$ the Miura $\mathfrak{sl}_3$ oper is of the form

$$a(x) = -\frac{1}{3}\frac{2n_1 + n_2}{x-z} + O(1), \qquad \tilde{a}(x) = \frac{1}{3}\frac{n_1 - n_2}{x-z} + O(1) \tag{4.147}$$

for some non-negative integers $n_1$ and $n_2$, then $z$ is a regular singularity of the $\mathfrak{sl}_3$ oper of trivial monodromy. Indeed, one can bring the Miura $\mathfrak{sl}_3$ oper to the form

$$\partial_x + \begin{pmatrix} r(x) & 0 & 0 \\ (x-z)^{n_1} & \tilde{r}(x) & 0 \\ 0 & (x-z)^{n_2} & -r(x) - \tilde{r}(x) \end{pmatrix} \tag{4.148}$$

where $r(x) = a(x) + \frac{1}{3}\frac{2n_1+n_2}{x-z}$ and $\tilde{r}(x) = \tilde{a}(x) - \frac{1}{3}\frac{n_1-n_2}{x-z}$, which are regular at $z$.

A *Miura* $\mathfrak{sl}_3$ $\lambda$*-oper* is a connection of the form

$$\partial_x + \begin{pmatrix} a_1(x) & 0 & P(x)\lambda^{-1} \\ \lambda^{-1} & \tilde{a}_1(x) & 0 \\ 0 & \lambda^{-1} & -a_1(x) - \tilde{a}_1(x) \end{pmatrix} \tag{4.149}$$

where $a_1(x)$ and $\tilde{a}_1(x)$ are rational functions. This is of the general form (4.136) and so a Miura $\mathfrak{sl}_3$ $\lambda$-oper defines an $\mathfrak{sl}_3$ $\lambda$-oper with

$$t_2(x) = a_1(x)^2 + a_1(x)\tilde{a}_1(x) + \tilde{a}_1(x)^2 + 2\partial_x a_1(x) + \partial_x \tilde{a}_1(x), \tag{4.150a}$$

$$t_3(x) = -(a_1(x) + \tilde{a}_1(x))\big(a_1(x)\tilde{a}_1(x) + \partial_x a_1(x) + 2\partial_x \tilde{a}_1(x)\big) - \partial_x^2 a_1(x) - \partial_x^2 \tilde{a}_1(x). \tag{4.150b}$$

We refer to this as the $\mathfrak{sl}_3$ $\lambda$-oper underlying (4.149). It can be described as a third order differential operator of the form

$$\big(\partial_x + a_1(x)\big)\big(\partial_x + \tilde{a}_1(x)\big)\big(\partial_x - a_1(x) - \tilde{a}_1(x)\big) - \frac{P(x)}{\lambda^3}. \tag{4.151}$$

There are two other gauge equivalent ways of presenting the same Miura $\mathfrak{sl}_3$ $\lambda$-oper as in (4.149), namely

$$\partial_x + \begin{pmatrix} -a_2(x) - \tilde{a}_2(x) & 0 & \lambda^{-1} \\ P(x)\lambda^{-1} & a_2(x) & 0 \\ 0 & \lambda^{-1} & \tilde{a}_2(x) \end{pmatrix} \tag{4.152}$$

with $a_2(x) = \tilde{a}_1(x) - \frac{\partial_x P(x)}{3P(x)}$ and $\tilde{a}_2(x) = -a_1(x) - \tilde{a}_1(x) - \frac{\partial_x P(x)}{3P(x)}$, or

$$\partial_x + \begin{pmatrix} \tilde{a}_3(x) & 0 & \lambda^{-1} \\ \lambda^{-1} & -a_3(x) - \tilde{a}_3(x) & 0 \\ 0 & P(x)\lambda^{-1} & a_3(x) \end{pmatrix} \tag{4.153}$$

with $a_3(x) = -a_1(x) - \tilde{a}_1(x) - \frac{2\partial_x P(x)}{3P(x)}$ and $\tilde{a}_3(x) = a_1(x) + \frac{\partial_x P(x)}{3P(x)}$.

The Miura $\mathfrak{sl}_3$ $\lambda$-oper (4.152) is of the particular form (4.138) so it defines a second $\mathfrak{sl}_3$ $\lambda$-oper. Likewise, the Miura $\mathfrak{sl}_3$ $\lambda$-oper (4.153) is of the form (4.140) and thus it also defines a third $\mathfrak{sl}_3$ $\lambda$-oper. Crucially, all three $\mathfrak{sl}_3$ $\lambda$-opers share the same monodromy data since they are gauge equivalent. This *triality* generalises the duality of $\mathfrak{sl}_2$ $\lambda$-opers associated with a given Miura $\mathfrak{sl}_2$ $\lambda$-oper discussed in Section 4.2.4.

There are three types of apparent singularities, corresponding to the three nodes of the Dynkin diagram of $\widetilde{\mathfrak{sl}}_3$. In particular, we can have the same types of singularities as for a Miura $\mathfrak{sl}_3$ oper in (4.145), namely points $w$ where, cf. (4.145),

$$a_1(x) = \frac{1}{x-w} + d + O(x-w), \qquad \tilde{a}_1(x) = -\frac{1}{x-w} + d + O(x-w) \tag{4.154}$$

so that $a_1(x) - \tilde{a}_1(x)$ has vanishing constant term, or points $w'$ where, cf. (4.146),

$$a_1(x) = \frac{0}{x-w'} - 2d + O(x-w'), \qquad \tilde{a}_1(x) = \frac{1}{x-w'} + d + O(x-w') \tag{4.155}$$

so that $a_1(x) + 2\tilde{a}_1(x)$ has no constant term. Both of these singularities are absent from the $\mathfrak{sl}_3$ $\lambda$-oper underlying (4.149). The third type of apparent singularity is at points $w''$ where

$$a_1(x) = -\frac{1}{x-w''} + d + O(x-w''), \qquad \tilde{a}_1(x) = \frac{0}{x-w''} - 2d + O(x-w'') \tag{4.156}$$

so that $2a_1(x) + \tilde{a}_1(x)$ has no constant term. The singularity (4.156) is not erased in the canonical form of the Miura $\mathfrak{sl}_3$ $\lambda$-oper (4.149). However, since it is of the form (4.147) with $n_1 = n_2 = 1$, by the above arguments for Miura $\mathfrak{sl}_3$ opers it follows that the $\mathfrak{sl}_3$ $\lambda$-oper underlying (4.149) has trivial monodromy at $w''$.

In fact, singularities of both types (4.154) and (4.156) are absent in the canonical form of the second Miura $\mathfrak{sl}_3$ $\lambda$-oper in (4.152). Likewise, both singularities (4.155) and (4.156) are absent in the canonical form of the third Miura $\mathfrak{sl}_3$ $\lambda$-oper (4.152).

If $P(x)$ has a zero of order $k$ at a singularity $z$ of the Miura $\mathfrak{sl}_3$ $\lambda$-oper with

$$a_1(x) = -\frac{1}{3}\frac{2n_1+n_2}{x-z} + O(1), \qquad \tilde{a}_1(x) = \frac{1}{3}\frac{n_1-n_2}{x-z} + O(1) \tag{4.157}$$

then provided $n_1, n_2 \geq 0$ and $n_1 + n_2 \leq k$, the underlying $\mathfrak{sl}_3$ $\lambda$-oper has trivial monodromy. Indeed, one can bring (4.149) to the form

$$\partial_x + \begin{pmatrix} r_1(x) & 0 & (x-z)^{k-n_1-n_2} q(x) \lambda^{-1} \\ (x-z)^{n_1}\lambda^{-1} & \tilde{r}_1(x) & 0 \\ 0 & (x-z)^{n_2}\lambda^{-1} & -r_1(x) - \tilde{r}_1(x) \end{pmatrix} \tag{4.158}$$

where we have written $P(x) = (x-z)^k q(x)$ with $q(z) \neq 0$, $r_1(x) = a_1(x) + \frac{1}{3}\frac{2n_1+n_2}{x-z}$ and $\tilde{r}_1(x) = \tilde{a}_1(x) - \frac{1}{3}\frac{n_1-n_2}{x-z}$, which are clearly regular at $z$.

The behaviour of the second Miura $\mathfrak{sl}_3$ $\lambda$-oper (4.152) at $z$ is given by

$$a_2(x) = \frac{1}{3}\frac{-k+n_1-n_2}{x-z} + O(1), \qquad \tilde{a}_2(x) = \frac{1}{3}\frac{-k+n_1+2n_2}{x-z} + O(1) \tag{4.159}$$

while the third Miura $\mathfrak{sl}_3$ $\lambda$-oper (4.153) behaves as

$$a_3(x) = \frac{1}{3}\frac{-2k + n_1 + 2n_2}{x - z} + O(1), \qquad \tilde{a}_2(x) = \frac{1}{3}\frac{k - 2n_1 - n_2}{x - z} + O(1). \tag{4.160}$$

### 4.7.3 $\lambda$-Opers with singularities of trivial monodromy and affine Bethe equations

A Miura $\mathfrak{sl}_3$ oper on $\mathbb{C}$ with a rank 1 irregular singularity at infinity and whose other singularities are all regular with trivial monodromy is of the form

$$a(x) = -\frac{2\alpha_1 + \alpha_2}{3} - \frac{1}{3}\sum_a \frac{2n_{1,a} + n_{2,a}}{x - z_a} + \sum_i \frac{1}{x - w_i}, \tag{4.161}$$

$$\tilde{a}(x) = \frac{\alpha_1 - \alpha_2}{3} + \frac{1}{3}\sum_a \frac{n_{1,a} - n_{2,a}}{x - z_a} - \sum_i \frac{1}{x - w_i} + \sum_i \frac{1}{x - w_i'} \tag{4.162}$$

where the apparent singularities $w_i$ and $w_i'$ satisfy the Bethe equations

$$-\sum_a \frac{n_{1,a}}{w_i - z_a} + \sum_{j \neq i} \frac{2}{w_i - w_j} - \sum_j \frac{1}{w_i - w_j'} = \alpha_1 \tag{4.163}$$

$$-\sum_a \frac{n_{2,a}}{w_i' - z_a} - \sum_j \frac{1}{w_i' - w_j} + \sum_{j \neq i} \frac{2}{w_i' - w_j'} = \alpha_2. \tag{4.164}$$

We are interested in the case of a Miura $\mathfrak{sl}_3$ $\lambda$-oper with a rank 1 irregular singularity at infinity and whose other singularities are all regular with trivial monodromy. This can be written as

$$a_1(x) = -\frac{2\alpha_1 + \alpha_2}{3} - \frac{1}{3}\sum_a \frac{2n_{1,a} + n_{2,a}}{x - z_a} + \sum_i \frac{1}{x - w_i} - \sum_i \frac{1}{x - w_i''}, \tag{4.165a}$$

$$\tilde{a}_1(x) = \frac{\alpha_1 - \alpha_2}{3} + \frac{1}{3}\sum_a \frac{n_{1,a} - n_{2,a}}{x - z_a} - \sum_i \frac{1}{x - w_i} + \sum_i \frac{1}{x - w_i'}. \tag{4.165b}$$

With $P(x) = e^{(\alpha_1+\alpha_2+\alpha_3)x}\prod_a (x-z_a)^{k_a}$, the second Miura $\mathfrak{sl}_3$ $\lambda$-oper then reads

$$a_2(x) = -\frac{2\alpha_2+\alpha_3}{3} + \frac{1}{3}\sum_a \frac{-k_a+n_{1,a}-n_{2,a}}{x-z_a} - \sum_i \frac{1}{x-w_i} + \sum_i \frac{1}{x-w_i'}, \tag{4.166a}$$

$$\tilde{a}_2(x) = \frac{\alpha_2-\alpha_3}{3} + \frac{1}{3}\sum_a \frac{-k_a+n_{1,a}+2n_{2,a}}{x-z_a} - \sum_i \frac{1}{x-w_i'} + \sum_i \frac{1}{x-w_i''}. \tag{4.166b}$$

The condition that $w_i$ and $w_i'$ are apparent singularities for the first Miura $\mathfrak{sl}_3$ $\lambda$-oper (4.165) and that $w_i''$ are apparent singularities for the second Miura $\mathfrak{sl}_3$ $\lambda$-oper (4.166) leads to the Bethe equations

$$-\sum_a \frac{n_{1,a}}{w_i-z_a} + \sum_{j\neq i}\frac{2}{w_i-w_j} - \sum_j \frac{1}{w_i-w_j'} - \sum_j \frac{1}{w_i-w_j''} = \alpha_1, \tag{4.167}$$

$$-\sum_a \frac{n_{2,a}}{w_i'-z_a} - \sum_j \frac{1}{w_i'-w_j} + \sum_{j\neq i}\frac{2}{w_i'-w_j'} - \sum_j \frac{1}{w_i'-w_j''} = \alpha_2, \tag{4.168}$$

$$-\sum_a \frac{k_a-n_{1,a}-n_{2,a}}{w_i''-z_a} - \sum_j \frac{1}{w_i''-w_j} - \sum_j \frac{1}{w_i''-w_j'} + \sum_{j\neq i}\frac{2}{w_i''-w_j''} = \alpha_3. \tag{4.169}$$

### 4.7.4 WKB expansion and quasi-canonical form

The three Miura $\mathfrak{sl}_3$ $\lambda$-opers (4.149), (4.152) and (4.153) are locally gauge equivalent to a connection of the more symmetric form

$$\partial_x + \begin{pmatrix} a(x) & 0 & P(x)^{\frac{1}{3}}\lambda^{-1} \\ P(x)^{\frac{1}{3}}\lambda^{-1} & \tilde{a}(x) & 0 \\ 0 & P(x)^{\frac{1}{3}}\lambda^{-1} & -a(x)-\tilde{a}(x) \end{pmatrix} \tag{4.170}$$

where $a(x) = a_1(x) + \frac{\partial_x P(x)}{3P(x)}$ and $\tilde{a}(x) = \tilde{a}_1(x)$. We refer to (4.170) as a *Miura* $\widetilde{\mathfrak{sl}}_3$ *oper*. The underlying $\widetilde{\mathfrak{sl}}_3$ *oper*, or *affine* $\mathfrak{sl}_3$ *oper*, is then defined as its equivalence class under gauge transformations by matrices of the form

$$\exp\begin{pmatrix} u(x;\lambda) & v_+(x;\lambda) & w_+(x;\lambda) \\ v_-(x;\lambda) & \tilde{u}(x;\lambda) & \tilde{v}_+(x;\lambda) \\ w_-(x;\lambda) & \tilde{v}_-(x;\lambda) & -u(x;\lambda)-\tilde{u}(x;\lambda) \end{pmatrix} \tag{4.171}$$

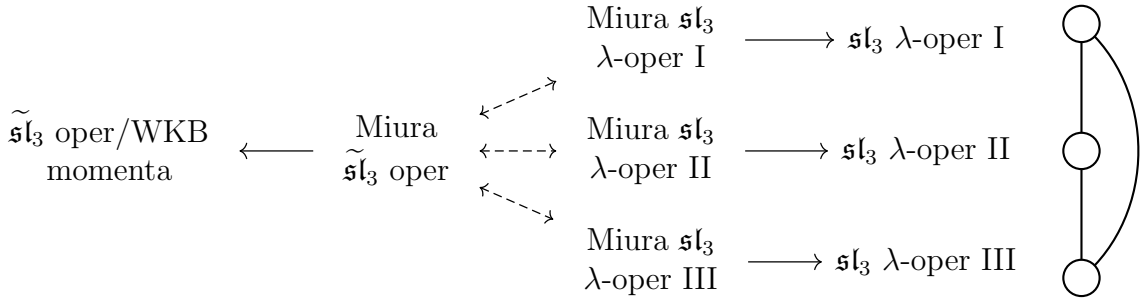


Figure 4.3: The three different types of (Miura) $\mathfrak{sl}_3$ $\lambda$-opers, labelled I, II and III, associated with the three nodes of the Dynkin diagram of $\widetilde{\mathfrak{sl}}_3$. They all share a common $\widetilde{\mathfrak{sl}}_3$ oper which describes the WKB momenta of the third order differential operator (4.134).

where the various functions have the following formal power series expansions

$$
\begin{aligned}
u(x;\lambda) &= \sum_{n=0}^{\infty} P(x)^{-n} u_n(x) \lambda^{3n}, & \tilde{u}(x;\lambda) &= \sum_{n=0}^{\infty} P(x)^{-n} \tilde{u}_n(x) \lambda^{3n}, \\
v_+(x;\lambda) &= \sum_{n=0}^{\infty} P(x)^{-n-\frac{1}{3}} v_n^+(x) \lambda^{3n+1}, & \tilde{v}_+(x;\lambda) &= \sum_{n=0}^{\infty} P(x)^{-n-\frac{1}{3}} \tilde{v}_n^+(x) \lambda^{3n+1}, \\
v_-(x;\lambda) &= \sum_{n=0}^{\infty} P(x)^{-n-\frac{2}{3}} v_n^-(x) \lambda^{3n+2}, & \tilde{v}_-(x;\lambda) &= \sum_{n=0}^{\infty} P(x)^{-n-\frac{2}{3}} \tilde{v}_n^-(x) \lambda^{3n+2}, \\
w_+(x;\lambda) &= \sum_{n=0}^{\infty} P(x)^{-n-\frac{2}{3}} w_n^+(x) \lambda^{3n+2}, & w_-(x;\lambda) &= \sum_{n=0}^{\infty} P(x)^{-n-\frac{1}{3}} w_n^-(x) \lambda^{3n+1}
\end{aligned}
$$

with $u_n(x)$, $\tilde{u}_n(x)$, $v_n^{\pm}(x)$, $\tilde{v}_n^{\pm}(x)$ and $w_n^{\pm}(x)$ rational functions. As we will show below, the $\widetilde{\mathfrak{sl}}_3$ oper controls the WKB asymptotics of the $\lambda$-oper (4.134) underlying the Miura $\mathfrak{sl}_3$ $\lambda$-oper (4.149); see Fig. 4.3.

Recall first that an $\widetilde{\mathfrak{sl}}_3$ oper can be brought to the *quasi-canonical form* [145]

$$
\partial_x + \begin{pmatrix} 0 & q_1(x;\lambda) & q_2(x;\lambda) \\ q_2(x;\lambda) & 0 & q_1(x;\lambda) \\ q_1(x;\lambda) & q_2(x;\lambda) & 0 \end{pmatrix} \tag{4.172}
$$

where the coefficients are given by the formal Laurent series

$$q_1(x;\lambda) = \sum_{n=0}^{\infty} P(x)^{-n-\frac{1}{3}} q_{1,n}(x) \lambda^{3n+1}, \tag{4.173a}$$

$$q_2(x;\lambda) = \frac{P(x)^{\frac{1}{3}}}{\lambda} + \sum_{n=0}^{\infty} P(x)^{-n-\frac{2}{3}} q_{2,n}(x) \lambda^{3n+2}. \tag{4.173b}$$

In the case of the $\widetilde{\mathfrak{sl}}_3$ oper underlying (4.170), the first few orders explicitly read

$$q_{1,0}(x) = \frac{t_2(x)}{3} + \frac{\big(\partial_x P(x)\big)^2}{27 P(x)}, \qquad q_{2,0}(x) = \frac{t_3(x)}{3} + \frac{t_2(x)\partial_x P(x)}{9P(x)} \tag{4.174a}$$

where $t_2(x)$ and $t_3(x)$ are given by (4.150).

Just as in the $\mathfrak{sl}_2$ case considered in Section 4.2.10, the quasi-canonical form (4.172) of an affine $\mathfrak{sl}_3$ oper is not unique. Indeed, it is preserved by residual gauge transformations of the form (4.171) with $u(x;\lambda) = \tilde{u}(x;\lambda) = 0$ and $v_\pm(x;\lambda) = \tilde{v}_\pm(x;\lambda) = w_\mp(x;\lambda)$, the effect of which is to transform the quasi-canonical form as

$$q_1(x;\lambda) \longmapsto q_1(x;\lambda) + \partial_x v_+(x;\lambda), \tag{4.175a}$$

$$q_2(x;\lambda) \longmapsto q_2(x;\lambda) + \partial_x v_-(x;\lambda). \tag{4.175b}$$

We look for flat sections of the $\mathfrak{sl}_3$ $\lambda$-oper (4.134), i.e. solutions of the third order differential equation

$$\left(\partial_x^3 - t_2(x)\partial_x + t_3(x) + \frac{P(x)}{\lambda^3}\right)\psi(x;\lambda) = 0$$

in the form of the WKB ansatz

$$\psi_1(x;\lambda) = \frac{1}{\sqrt[3]{A(x;\lambda)}} e^{\int p_1(x;\lambda)dx}, \qquad \psi_2(x;\lambda) = \frac{1}{\sqrt[3]{A(x;\lambda)}} e^{\int p_2(x;\lambda)dx},$$

$$\psi_3(x;\lambda) = \frac{1}{\sqrt[3]{A(x;\lambda)}} e^{-\int p_1(x;\lambda)dx - \int p_2(x;\lambda)dx}$$

where the normalization factor, fixed by requiring the Wronskian of the three solutions $\psi_1$,

$\psi_2$ and $\psi_3$ to be 1, is given by

$$A(x;\lambda) = 2p_1(x;\lambda)^3 - 2p_2(x;\lambda)^3 + 3(p_1(x;\lambda) - p_2(x;\lambda))p_1(x;\lambda)p_2(x;\lambda) + 3p_2(x;\lambda)\partial_x p_1(x;\lambda) - 3p_1(x;\lambda)\partial_x p_2(x;\lambda). \tag{4.176}$$

Working perturbatively in $\lambda$ we find WKB momenta of the form

$$p_1(x;\lambda) = -\frac{P(x)^{\frac{1}{3}}}{\lambda} - \sum_{n=1}^{\infty} p_{1,n}(x)\lambda^n \tag{4.177a}$$

$$p_2(x;\lambda) = -\frac{P(x)^{\frac{1}{3}}}{e^{-\frac{2\pi i}{3}}\lambda} - \sum_{n=1}^{\infty} p_{2,n}(x)\big(e^{-\frac{2\pi i}{3}}\lambda\big)^n. \tag{4.177b}$$

The first few coefficients of the expansion (4.177a) are given explicitly by

$$p_{1,1}(x) = P(x)^{-\frac{1}{3}}q_{1,0}(x) + \partial_x\left(\frac{2\partial_x P(x)}{9P(x)^{\frac{4}{3}}}\right), \tag{4.178a}$$

$$p_{1,2}(x) = P(x)^{-\frac{2}{3}}q_{2,0}(x) - \partial_x\left(\frac{\partial_x^2 P(x)}{9P(x)^{\frac{5}{3}}} - \frac{7\big(\partial_x P(x)\big)^2}{54P(x)^{\frac{8}{3}}}\right), \tag{4.178b}$$

$$p_{1,3}(x) = \partial_x\left(\frac{2\partial_x t_2(x)}{9P(x)} - \frac{4t_2(x)\partial_x P(x)}{27P(x)^2} + \frac{4\partial_x^3 P(x)}{27P(x)^2} - \frac{16\partial_x P(x)\partial_x^2 P(x)}{27P(x)^3} + \frac{112\big(\partial_x P(x)\big)^3}{243P(x)^4}\right) \tag{4.178c}$$

and those of the expansion (4.177b) read

$$p_{2,1}(x) = P(x)^{-\frac{1}{3}}q_{1,0}(x) + \partial_x\left(\frac{2\partial_x P(x)}{9P(x)^{\frac{4}{3}}}\right), \tag{4.179a}$$

$$p_{2,2}(x) = P(x)^{-\frac{2}{3}}q_{2,0}(x) + \partial_x\left(\frac{t_2(x)}{3P(x)^{\frac{2}{3}}} + \frac{\partial_x^2 P(x)}{9P(x)^{\frac{5}{3}}} - \frac{7\big(\partial_x P(x)\big)^2}{54P(x)^{\frac{8}{3}}}\right), \tag{4.179b}$$

$$p_{2,3}(x) = e^{-\frac{\pi i}{6}}\partial_x\left(\frac{\partial_x t_2(x)}{3\sqrt{3}P(x)} - \frac{2t_2(x)\partial_x P(x)}{9\sqrt{3}P(x)^2} + \frac{2\partial_x^3 P(x)}{9\sqrt{3}P(x)^2} - \frac{8\partial_x P(x)\partial_x^2 P(x)}{9\sqrt{3}P(x)^3} + \frac{56\big(\partial_x P(x)\big)^3}{81\sqrt{3}P(x)^4}\right). \tag{4.179c}$$

From this we find that the pair of WKB momenta $p_1(x;\lambda)$ and $p_2(x;\lambda)$ are related to the coefficients of the quasi-canonical form (4.172) by

$$p_1(x;\lambda) = -q_1(x;\lambda) - q_2(x;\lambda) + \partial_x f_1(x;\lambda), \tag{4.180a}$$

$$p_2(x;\lambda) = -q_1\big(x;e^{-\frac{2\pi i}{3}}\lambda\big) - q_2\big(x;e^{-\frac{2\pi i}{3}}\lambda\big) + \partial_x f_2(x;\lambda) \tag{4.180b}$$

for some functions $f_1(x;\lambda)$ and $f_2(x;\lambda)$.

# Chapter 5

# Conclusions and future directions

In the prior sections, we studied the close relation among integrable Kondo defect lines in conformal field theories, affine opers, affine Gaudin models and the four-dimensional Chern Simons theory.

We start by refining and extending the analysis of Kondo line defects in two-dimensional conformal field theories. Following the quantization recipe given by [24], we explore the properties of Kondo line defect in the perturbation theory. We extend their calculations to the finite level and more generally to the multichannel cases and explicitly verify their RG flows and various integrable properties. On the abstract level, we put Kondo line defect in the larger context of chiral line defects, which are rigid topological and enjoy many similar nice properties as the Kondo defects. We also emphasize many interesting physics phenomena are not accessible from ultraviolet perturbation theory.

We then lift the Kondo defect to the construction of four-dimensional Chern Simons theory, where the Kondo defects are realized by the Wilson lines in the bulk. This makes the integrability of the Kondo defects manifest. As a result, we can readily understand the commutation relation, the Hirota relation, etc. Note the construction of the four-dimensional Chern Simons theory per se is interesting as it provides the first example of the renormalization flow in the 4d CS. Classically, the holomorphic coordinate along the holomorphic plane corresponds to the spectral parameter while we demonstrated that in the quantum theory, it should be the primitive of the meromorphic one form that is interpreted as the spectral parameter, instead of the coordinate.

We show that the most important step in the construction is to figure out the correct choice of the meromorphic one form, which canonically defines a quadratic differential, hence a second-order (holomorphic) differential operator. We conjecture such a map from

a Kondo defect to a second-order differential operator should coincide with the notion of ODE/IM correspondence discussed in the literature. This pathway through 4d Chern Simons opens a new door of understanding the ODE/IM correspondence and provides a recipe for constructing new examples. In the simplest cases like coset and $SU(2)_1$, our proposal reduces to the known correspondence in the literature. Based on this conjecture, we propose new examples of ODE/IM correspondence, which passed many explicit checks.

We then extend the ODE/IM correspondence to excited states. This is made possible by the fact that the second-order differential operators correspond precisely to the notion of affine opers in the mathematical literature. We give a complete recipe for constructing excited states ODE. The explicit one-to-one correspondence between the states and the ODEs are also given based on the close relation with the affine Gaudin model, generalizing the well-known oper-Gaudin correspondence. In particular, these are precisely the states that diagonalize the Kondo line defect. We also point out that Kondo line defects are precisely the transfer matrix of the affine Gaudin model, and the local integral of motion comes from Kondo line defect with a particular property—they need to be IR free.

More directly, we propose the Stokes data of the ODE, with a natural choice of normalization, exactly equals the expectation value of the Kondo line defect. As an application of this idea, we extract the Stokes data in the infrared limit and give a prediction of the corresponding expectation values. Among other things, we map out the phase diagram in the infrared on the complex plane of the spectral parameter which exhibits an interesting wallcrossing phenomenon. To this end, we develop the standard exact WKB analysis to adapt to the more general scenario, which could have interesting applications in other areas.

There are many interesting open questions and future directions:

1. **Higher rank**: It would be natural to extend our work to other Lie algebras [158, 159, 160]. The definition of the Kondo defects is valid for any Lie algebra, with an important caveat: the matrices $t^a$ do not have to be generators of the Lie algebra, they only need to transform in the adjoint representation of the global symmetry group. The RG flow will thus involve extra couplings, controlling the specific choice of $t^a$. 4d Chern-Simons gauge theory predicts integrability for choices of couplings related to representations of the Yangian. It would be nice to understand how these structures manifest themselves in the affine Gaudin description. The definition of affine opers with singularities of trivial monodromy should be possible for general gauge groups and straightforward in type $A$. The precise correspondence between the Stokes data and the UV labels of Kondo defects is less obvious. The IR WKB

analysis is still possible, but will likely require some more refined techniques such as spectral networks [89].

2. **Non-integral levels**: In sections 4.4 and 4.5, we made the assumption that all the level $k_i$ in
$$P(x) = e^{2x} \prod_i (x - x_i)^{k_i} \tag{5.1}$$
are non-negative integers, which corresponds to the WZW model for the product group $\prod_i SU(2)_{k_i}$. We can generalize to Kac-Moody algebras via replacing $k_i$ by $\kappa_i \in \mathbb{C}$. This forces us to study opers on a logarithmic covering space of the complex plane. (It reduces to a finite covering when $\kappa_i$ is rational.) Consequently, we have more Wronskians of small solutions to study, both between the small solutions on the same sheet and across different sheets. It would be interesting to work out some examples and understand their relationship with the expectation values of the local integrals of motions in the affine Gaudin model, which are conjecturally given by the integrals of the WKB momentum [145].

3. **Bulk deformation**: Throughout this article, we considered Kondo line defects in CFTs in the bulk. It is well-known, however, that the bulk theory can be deformed in such a way that the integrable structure remains. Examples of such deformations are given by $J^a \bar{J}^a$ in the WZW model and $\Phi_{1,3}$ in minimal models. The transfer matrices $\hat{T}_j[\theta]$ can be naturally extended as well in such a way that commutativity and the fusion rules are still satisfied. Furthermore, there is evidence [161, 162, 163] that the ODE/IM correspondence can be generalized as well to the so-called 'massive ODE/IM correspondence'. It is natural to expect that the $P$-sinh-Gordon equation with an appropriate generalization of the potential $P(x) = e^{2x} \prod_i (x - x_i)^{k_i}$ should correspond to the integrable Gross-Neveu model.

4. **Coset limits and other models**: We only sketched the limiting procedure $e^{2x} \prod_i (x - x_i)^{k_i} \to \prod_i (x - x_i)^{k_i}$ mapping the Kondo problems to integrable defects in coset models. It would be nice to develop the relation further. Other choices of $P(x)$ should be relevant for integrable line defects in other 2d CFTs. A dictionary may be developed along the lines of [33] from a 4d Chern-Simons gauge theory perspective, or equivalently [35], along the lines of [164] from the point of view of affine Gaudin models.

5. **Excited states oper from 4d CS**: while we found an intriguing relation between the ODE and the meromorphic one form in 4D Chern Simons theory. Such a relation only holds on the level of the ground state. For the excited states, the additional

singularities of trivial monodromy are introduced on top of the vacuum state ODE. It would be very interesting to understand what they correspond to in the construction of 4d Chern Simons.

6. **String theory construction**: one promising way of 'deriving' the ODE/IM correspondence is to look at its string theory embedding. This would be parallel to the construction that leads to the oper-Gaudin correspondence [125]. While the string theory embedding of the simplest version of the 4d Chern Simons theory is known [165, 166], we do not know what is the correct brane construction that gives rise to the setup described in this thesis.

# Chapter 6

# Abelian gauge theory at the boundary

Boundary conformal field theories for a free $d$-dimensional bulk quantum field theory are interesting theoretical objects. On one hand, the correlation functions of bulk local operators are controlled by the free equations of motion. In particular, they are fully determined by the behavior near the boundary, which is encoded in some very simple bulk-to-boundary OPE for the bulk free fields.

The free bulk-to-boundary OPE essentially identifies some special boundary local operators as the boundary values of the bulk free fields and their normal derivatives. The correlation functions of these boundary operators determine all correlation functions of bulk operators. These boundary correlation functions, though, can in principle be as complicated as those of any CFT in $(d-1)$ dimensions.

The case of four-dimensional free Abelian gauge theory (with compact gauge group) is particularly interesting because the bulk theory has an exactly marginal gauge coupling.[1] Furthermore, a BCFT defined for some value of the bulk gauge coupling can typically

[1] If the gauge group is compact, say $U(1)$, the gauge field has an intrinsic normalization and thus the coefficient in front of the bulk Lagrangian is canonically defined even if the bulk theory is free. Local interactions between the gauge fields and any other degrees of freedom localized in non-zero co-dimension obviously cannot renormalize the bulk gauge coupling. Furthermore, the strength of the interactions between the gauge fields and such other degrees of freedom is controlled by the bulk gauge coupling and by quantized gauge charges and thus cannot get renormalized. The only possible beta functions involve gauge-invariant boundary local operators. This fact is often obfuscated in perturbative treatments and then proven with the help of Ward identities, in a manner analogous to the non-renormalization of gauge charges in QED [47, 48, 49, 50, 51, 52, 53].

be deformed to a BCFT defined at a neighboring value of the bulk gauge coupling by conformal perturbation theory in the gauge coupling. The leading order obstruction is the presence of marginal boundary operators in the bulk-to-boundary OPE of the bulk Lagrangian operators $F^2$ and $F \wedge F$, which can lead to a logarithmic divergence as the bulk perturbation approaches the boundary. Generically, no such operators will be present and the BCFT can be deformed.

In this section, we will discuss the properties of some standard BCFT's which can be defined in an arbitrarily weakly-coupled gauge theory, starting with free boundary conditions and then including interacting degrees of freedom at the boundary. On general grounds, we expect that any BCFT which can be defined at arbitrarily weak coupling will take this form.

## 6.1 Boundary Conditions for 4d Abelian Gauge Field

### 6.1.1 Free Boundary Conditions and $SL(2,\mathbb{Z})$ Action

Consider a $U(1)$ gauge field $A_\mu$ on $\mathbb{R}^3 \times \mathbb{R}_+$. We adopt Euclidean signature, and use coordinates $x = (\vec{x}, y)$ where $x^4 \equiv y \geq 0$ is the coordinate on $\mathbb{R}_+$, and $\vec{x}$ are the coordinates on $\mathbb{R}^3$. We denote the components of $x$ as $x^\mu$, $\mu = 1,2,3,4$, and those of $\vec{x}$ as $x^a$, $a = 1,2,3$. The field strength is $F_{\mu\nu} = \partial_\mu A_\nu - \partial_\nu A_\mu$, its Hodge dual is $\tilde{F}_{\mu\nu} = \frac{1}{2}\epsilon_{\mu\nu}{}^{\rho\sigma} F_{\rho\sigma}$ and the self-dual/anti-self-dual components are $F^\pm_{\mu\nu} = \frac{1}{2}(F_{\mu\nu} \pm \tilde{F}_{\mu\nu})$. They satisfy $\frac{1}{2}\epsilon_{\mu\nu}{}^{\rho\sigma} F^\pm_{\rho\sigma} = \pm F^\pm_{\mu\nu}$.

In the absence of interactions with boundary modes, by varying the action

$$S[A,\tau] = \int_{y\geq 0} dy\, d^3\vec{x} \left( \frac{1}{4g^2} F_{\mu\nu}F^{\mu\nu} + \frac{i\theta}{32\pi^2} \epsilon_{\mu\nu\rho\sigma} F^{\mu\nu}F^{\rho\sigma} \right) \tag{6.1}$$

$$= -\frac{i}{8\pi} \int_{y\geq 0} dy\, d^3\vec{x} \left( \tau F^-_{\mu\nu} F^{-\,\mu\nu} - \bar{\tau} F^+_{\mu\nu} F^{+\,\mu\nu} \right) \ , \tag{6.2}$$

we find the bulk equation of motion $\frac{1}{g^2}\partial_\mu F^{\mu\nu} = 0$ and the boundary term

$$\delta S_\partial = -\int_{y=0} d^3\vec{x}\, \delta A^a \left( \frac{1}{g^2} F_{ya} + i \frac{\theta}{4\pi^2} \tilde{F}_{ya} \right) \tag{6.3}$$

$$= \frac{i}{2\pi} \int_{y=0} d^3\vec{x}\, \delta A^a (\tau F^-_{ya} - \bar{\tau} F^+_{ya}) \ . \tag{6.4}$$

Our convention for the orientation is $\epsilon_{abcy} = \epsilon_{abc}$. In equations (6.2)-(6.4) we combined $g$ and $\theta$ in the complex coupling $\tau = \frac{\theta}{2\pi} + \frac{2\pi i}{g^2}$. From eq. (6.4) we see that the possible boundary conditions for the gauge field when no boundary modes are present are

- Dirichlet: $\delta A_a|_{y=0} = 0$, which is equivalent to

$$(F^-_{ya} - F^+_{ya})|_{y=0} = -\tilde{F}_{ya}|_{y=0} = 0 \ ; \tag{6.5}$$

- Neumann:

$$(\tau F^-_{ya} - \bar{\tau} F^+_{ya})|_{y=0} = 0 \ . \tag{6.6}$$

  Equivalently, introducing

$$\gamma = \frac{\mathrm{Re}\tau}{\mathrm{Im}\tau} = \frac{\theta\, g^2}{4\pi^2} \in \mathbb{R} \ , \tag{6.7}$$

  we can write this condition as $(F_{ya} + i\gamma \tilde{F}_{ya})|_{y=0} = 0$, in particular for $\gamma = 0$ it simplifies to the standard Neumann condition $F_{ya}|_{y=0} = 0$.

It is convenient to introduce the boundary currents

$$\begin{aligned} 2\pi i \hat{J}_a &= \tau F^-_{ya}(\vec{x}, y=0) - \bar{\tau} F^+_{ya}(\vec{x}, y=0) \ , \\ 2\pi i \hat{I}_a &= F^-_{ya}(\vec{x}, y=0) - F^+_{ya}(\vec{x}, y=0) \ . \end{aligned} \tag{6.8}$$

in terms of which the Dirichlet condition is $\hat{I} = 0$, and the Neumann condition is $\hat{J} = 0$.

On $\mathbb{R}^4$ this theory enjoys an $SL(2,\mathbb{Z})$ duality group

$$\tau \to \tau' = \frac{a\tau + b}{c\tau + d} \,, \quad a, b, c, d \in \mathbb{Z} \,, \ ad - bc = 1 \ . \tag{6.9}$$

The duality group acts on the fields as

$$\begin{aligned} F^-_{\mu\nu} &\to F'^-_{\mu\nu} = (c\tau + d) F^-_{\mu\nu} \ , \\ F^+_{\mu\nu} &\to F'^+_{\mu\nu} = (c\bar{\tau} + d) F^+_{\mu\nu} \ . \end{aligned} \tag{6.10}$$

When the boundary is introduced, the group $SL(2,\mathbb{Z})$ also acts on the boundary conditions. From (6.10) we see that the action on the boundary currents is

$$\begin{aligned} \hat{J}_a &\to a\hat{J}_a + b\hat{I}_a \ , \\ \hat{I}_a &\to c\hat{J}_a + d\hat{I}_a \ . \end{aligned} \tag{6.11}$$

The Dirichlet and Neumann boundary conditions above are exchanged under the $S$ transformation $\tau \to -\frac{1}{\tau}$, i.e. electric-magnetic duality. Indeed, the $S$ transformation exchanges $\hat{J}$ and $\hat{I}$.

However, comparing eq.s (6.5)-(6.6) and eq.s (6.10)-(6.11) we see that the general $SL(2,\mathbb{Z})$ transformation does not act within the set of boundary conditions that we described above. This is because we assumed that no degrees of freedom are present on the boundary, while the generic $SL(2,\mathbb{Z})$ transformation requires the introduction of topological degrees of freedom on the boundary, namely 3d gauge-fields with Chern-Simons (CS) actions, coupled to the bulk gauge field through a topological $U(1)$ current [5, 167, 168]. Note that even in the presence of these topological degrees of freedom the theory is still free because the action is quadratic. Taking this into account, one finds that the most general free boundary condition for the $U(1)$ gauge field is

$$p\hat{J}_a + q\hat{I}_a = 0 \ , \tag{6.12}$$

where $p, q \in \mathbb{Z}$. This set of boundary conditions is closed under the action (6.11) of $SL(2,\mathbb{Z})$. We will refer to this more general free boundary condition as "$(p,q)$ boundary condition". The $(0,1)$ and $(1,0)$ boundary conditions correspond to the Dirichlet and Neumann boundary conditions above, respectively.

When we impose the $(p,q)$ condition, the unconstrained components of the gauge fields give a current operator on the boundary

$$p'\hat{J}_a + q'\hat{I}_a \tag{6.13}$$

with $pq' - p'q = 1$, whose correlators are just computed by Wick contraction, i.e. the boundary theory is a mean-field theory for this current. We can always shift $(p', q')$ by a multiple of $(p, q)$, and this gives rise to the same current thanks to the boundary condition.

Since the above boundary conditions preserve conformal symmetry, we can regard this system as a free boundary conformal field theory, and rephrase the boundary conditions in terms of a certain bulk-to-boundary OPE of the field strength $F_{\mu\nu}$. Using the equation of motion and the Bianchi identity one finds that the only primary boundary operators that can appear in the bulk-to-boundary OPE of $F_{\mu\nu}$ are conserved currents, see appendix E.2 for a derivation. The free boundary conditions described above correspond to having only one conserved current in this OPE, which can be identified with $p'\hat{J}_a + q'\hat{I}_a$. For instance, for the Dirichlet $(0,1)$ boundary condition

$$F_{\mu\nu}(\vec{x}, y) \underset{y\to 0}{\sim} -g^2 \hat{J}^a(\vec{x}) 2\delta_{a[\mu}\delta_{\nu]y} + \dots \ , \tag{6.14}$$

where the dots denote subleading descendant terms, and the square brackets denote anti-symmetrization. The general $(p, q)$ case can be obtained from the Dirichlet case by acting with an $SL(2, \mathbb{Z})$ transformation (6.10)-(6.11).

### 6.1.2 Two-point Function in the Free Theory

In this section we compute the two-point function $\langle F_{\mu\nu}(x_1)F_{\rho\sigma}(x_2)\rangle$ on $\mathbb{R}^3 \times \mathbb{R}_+$ in the free theory. We use that the two-point function is a Green function, i.e. it satisfies the equations of motion

$$\frac{1}{g^2}\partial_\mu \langle F_{\mu\nu}(x_1)F_{\rho\sigma}(x_2)\rangle = (\delta_{\nu\sigma}\partial_\rho - \delta_{\nu\rho}\partial_\sigma)\delta^4(x_{12}) \ , \tag{6.15}$$

and the Bianchi identity

$$\epsilon_{\tau\lambda\mu\nu}\partial_\lambda \langle F_{\mu\nu}(x_1)F_{\rho\sigma}(x_2)\rangle = 0 \ . \tag{6.16}$$

on $y \geq 0$, and it also satisfies the boundary conditions at $y = 0$. We are denoting $x_{12} \equiv x_1 - x_2$.

To start with, the Green function on $\mathbb{R}^4$ (i.e. without a boundary) is

$$\langle F_{\mu\nu}(x_1)F_{\rho\sigma}(x_2)\rangle_{\mathbb{R}^4} = \frac{g^2}{\pi^2} G_{\mu\nu,\rho\sigma}(x_{12}) \ , \tag{6.17}$$

$$G_{\mu\nu,\rho\sigma}(x) \equiv \frac{I_{\mu\rho}(x)I_{\nu\sigma}(x) - I_{\nu\rho}(x)I_{\mu\sigma}(x)}{(x^2)^2} \ , \tag{6.18}$$

where $I_{\mu\nu}(x) = \delta_{\mu\nu} - \frac{2x_\mu x_\nu}{x^2}$. Starting from (6.17) and using the method of images we can easily write down the two-point function in the presence of the boundary. The calculation is showed in the appendix E.1.

In the case $\gamma = 0$ we find

$$\langle F_{\mu\nu}(x_1)F_{\rho\sigma}(x_2)\rangle_{\mathbb{R}^3\times\mathbb{R}_+} = \frac{g^2}{\pi^2}\left[(1 - s\,v^4)\,G_{\mu\nu,\rho\sigma}(x_{12}) + s\,v^4\,H_{\mu\nu,\rho\sigma}(\vec{x}_{12}, y_1, y_2)\right] \ , \tag{6.19}$$

$$\begin{aligned} H_{\mu\nu,\rho\sigma}(\vec{x}_{12}, y_1, y_2) \equiv 2\frac{1}{(x^2)^2}\,&[X_{1\,\mu}X_{2\,\rho}I_{\nu\sigma}(x_{12}) + X_{1\,\nu}X_{2\,\sigma}I_{\mu\rho}(x_{12}) \\ &- X_{1\,\mu}X_{2\,\sigma}I_{\nu\rho}(x_{12}) - X_{1\,\nu}X_{2\,\rho}I_{\mu\sigma}(x_{12})] \ , \end{aligned} \tag{6.20}$$

for Dirichlet ($s = 1$) and Neumann ($s = -1$) conditions. Here $X_{i\,\mu}$ are the conformally

covariant vectors [169]

$$X_{i\,\mu} \equiv y_i \frac{v}{\xi} \partial_{i\,\mu} \xi = v \left( 2\, \frac{y_i\, s_i\, x_{12\,\mu}}{x_{12}^2} - n_\mu \right) \ , \quad i = 1, 2 \ , \quad s_1 = -s_2 = 1 \ , \tag{6.21}$$

and $\xi$ is the conformally invariant cross-ratio

$$\xi \equiv \frac{x_{12}^2}{4 y_1 y_2} \equiv \frac{v^2}{1 - v^2} \ . \tag{6.22}$$

For the more general Neumann boundary condition with $\gamma \neq 0$ we find

$$\begin{aligned} \langle F_{\mu\nu}(x_1) F_{\rho\sigma}(x_2) \rangle_{\mathbb{R}^3 \times \mathbb{R}_+} = \frac{g^2}{\pi^2} \Bigg[ & \left( \delta^{\rho'}_{[\rho} \delta^{\sigma'}_{\sigma]} + v^4 \left( \frac{1 - \gamma^2}{1 + \gamma^2} \delta^{\rho'}_{[\rho} \delta^{\sigma'}_{\sigma]} - i \frac{\gamma}{1 + \gamma^2} \epsilon_{\rho\sigma}{}^{\rho'\sigma'} \right) \right) G_{\mu\nu,\rho'\sigma'}(x_{12}) \\ & - v^4 \left( \frac{1 - \gamma^2}{1 + \gamma^2} \delta^{\rho'}_{[\rho} \delta^{\sigma'}_{\sigma]} - i \frac{\gamma}{1 + \gamma^2} \epsilon_{\rho\sigma}{}^{\rho'\sigma'} \right) H_{\mu\nu,\rho'\sigma'}(\vec{x}_{12}, y_1, y_2) \Bigg] \ . \end{aligned} \tag{6.23}$$

Even though not manifest, it can be verified that Bose symmetry is satisfied in this expression. From now on we will drop the subscript $\mathbb{R}^3 \times \mathbb{R}_+$.

It is also useful to rewrite this two-point function in terms of the self-dual/anti self-dual components. The selfdual/antiselfdual projectors are

$$P^{\pm}_{\mu\nu}{}^{\rho\sigma} = \tfrac{1}{2} (\delta^{\rho}_{[\mu} \delta^{\sigma}_{\nu]} \pm \tfrac{1}{2} \epsilon_{\mu\nu}{}^{\rho\sigma}) \ . \tag{6.24}$$

We introduce the following notation

$$G^{\pm,\pm}_{\mu\nu,\rho\sigma} \equiv P^{\pm}_{\mu\nu}{}^{\mu'\nu'} P^{\pm}_{\rho\sigma}{}^{\rho'\sigma'} G_{\mu'\nu',\rho'\sigma'} \ , \tag{6.25}$$

$$G^{\pm,\mp}_{\mu\nu,\rho\sigma} \equiv P^{\pm}_{\mu\nu}{}^{\mu'\nu'} P^{\mp}_{\rho\sigma}{}^{\rho'\sigma'} G_{\mu'\nu',\rho'\sigma'} \ , \tag{6.26}$$

and similarly for the structure $H$. The following identities hold

$$G^{\pm,\pm} = 0 \ , \tag{6.27}$$

$$G^{\pm,\mp} - H^{\pm,\mp} = 0 \ . \tag{6.28}$$

Recalling the definition (6.7) of $\gamma$, we obtain

$$\langle F^+_{\mu\nu}(x_1)F^+_{\rho\sigma}(x_2)\rangle = \frac{2}{\pi\,\mathrm{Im}\tau}\frac{\tau}{\bar\tau}\,v^4 H^{++}_{\mu\nu,\rho\sigma}(\vec{x}_{12},y_1,y_2)\ , \tag{6.29}$$

$$\langle F^-_{\mu\nu}(x_1)F^-_{\rho\sigma}(x_2)\rangle = \frac{2}{\pi\,\mathrm{Im}\tau}\frac{\bar\tau}{\tau}\,v^4 H^{--}_{\mu\nu,\rho\sigma}(\vec{x}_{12},y_1,y_2)\ , \tag{6.30}$$

$$\langle F^+_{\mu\nu}(x_1)F^-_{\rho\sigma}(x_2)\rangle = \frac{2}{\pi\,\mathrm{Im}\tau}G^{+-}_{\mu\nu,\rho\sigma}(x_{12})\ , \tag{6.31}$$

$$\langle F^-_{\mu\nu}(x_1)F^+_{\rho\sigma}(x_2)\rangle = \frac{2}{\pi\,\mathrm{Im}\tau}G^{-+}_{\mu\nu,\rho\sigma}(x_{12})\ . \tag{6.32}$$

The result above is the field-strength two-point function in the free theory with Neumann boundary conditions. As we argued in section 6.1.1, the result for the $(p,q)$ boundary conditions (6.12) simply follows from an $SL(2,\mathbb{Z})$ transformation (6.10)-(6.11). As an example, for Dirichlet boundary conditions one finds

$$\langle F^+_{\mu\nu}(x_1)F^+_{\rho\sigma}(x_2)\rangle = \frac{2|\tau|^2}{\pi\,\mathrm{Im}\tau}\,v^4 H^{++}_{\mu\nu,\rho\sigma}(\vec{x}_{12},y_1,y_2)\ , \tag{6.33}$$

$$\langle F^-_{\mu\nu}(x_1)F^-_{\rho\sigma}(x_2)\rangle = \frac{2|\tau|^2}{\pi\,\mathrm{Im}\tau}\,v^4 H^{--}_{\mu\nu,\rho\sigma}(\vec{x}_{12},y_1,y_2)\ , \tag{6.34}$$

$$\langle F^+_{\mu\nu}(x_1)F^-_{\rho\sigma}(x_2)\rangle = \frac{2|\tau|^2}{\pi\,\mathrm{Im}\tau}G^{+-}_{\mu\nu,\rho\sigma}(x_{12})\ , \tag{6.35}$$

$$\langle F^-_{\mu\nu}(x_1)F^+_{\rho\sigma}(x_2)\rangle = \frac{2|\tau|^2}{\pi\,\mathrm{Im}\tau}G^{-+}_{\mu\nu,\rho\sigma}(x_{12})\ . \tag{6.36}$$

### 6.1.3 Coupling to a CFT on the Boundary

Consider now a 3d CFT living on the boundary at $y=0$. We assume that the CFT has a $U(1)$ global symmetry, with associated current $\hat{J}_{\mathrm{CFT}\,a}$. We take the Neumann boundary condition for the gauge field, which corresponds to a mean-field current operator $\hat{I}_a$ on the boundary. The two sectors can be coupled in a natural way, simply by gauging the $U(1)$ symmetry via the $y\to 0$ limit of the bulk gauge field. This amounts to adding the boundary coupling

$$\int_{y=0} d^3\vec{x}\,\hat{J}^a_{\mathrm{CFT}}A_a + \text{seagulls}\ , \tag{6.37}$$

and restricting the spectrum of local boundary operators to the $U(1)$ invariant ones. Charged boundary operators can be made gauge-invariant by attaching to them bulk Wilson lines. Therefore, it still makes sense to consider them after the gauging, but as

endpoints of line operators rather than as local boundary operators.

The boundary coupling modifies the boundary condition of the gauge field to the "modified Neumann" condition

$$\hat{J}_a \equiv \hat{J}_{\text{CFT}\,a} \ . \tag{6.38}$$

Hence as a consequence of the interactions both $\hat{I}_a$ and $\hat{J}_a$ are nontrivial operators.

As we explained above $\tau$ is an exactly marginal coupling, but we should worry about quantum effects breaking the boundary conformal symmetry by generating beta functions for boundary interactions. If the original 3d CFT has no marginal operators, these boundary beta functions start at linear order in the coupling and can be canceled order-by-order in perturbation theory by turning on extra boundary interactions of order $\tau^{-1}$.[2] Barring other non-perturbative phenomena such as the emergence of a condensate, we expect a BCFT to exist for sufficiently large $\tau$, with conformal data perturbatively close to that of the original CFT. We denote this BCFT with $B(\tau, \bar{\tau})$.

If the original 3d CFT has marginal operators the situation is more subtle: turning on boundary couplings $\hat{\lambda}$ will produce a beta function of order $\hat{\lambda}^2$ for the marginal operators. This may or not have the correct sign to cancel the $\tau^{-1}$ contributions. If it does not, we do not expect any unitary BCFT to exist, though one may be able to produce some non-unitary "complex" BCFT with complex couplings.

Conversely, suppose that we are given a BCFT $B(\tau, \bar{\tau})$ defined continuously for arbitrarily weak gauge coupling. If $B(\tau, \bar{\tau})$ is an interacting boundary condition, we expect that if we take the gauge coupling to 0 the properties of $B(\tau, \bar{\tau})$ will approach those of a 3d CFT with a $U(1)$ global symmetry.

As we will discuss later in this section, the bulk correlation functions are determined by the boundary correlation functions of the two conserved boundary current $\hat{I}_a$ and $\hat{J}_a$ defined in eq. (6.8). Due to the boundary condition (6.38), at weak coupling, $\hat{J}_a$ is inherited from the boundary degrees of freedom, and the corresponding charge is carried by the endpoints of bulk Wilson lines ending at the boundary. On the other hand, $\hat{I}_a$ is analogous to the "topological" charge in three-dimensional $U(1)$ gauge theories and the corresponding charge is carried by the endpoints of bulk 't Hooft lines ending at the boundary.

When the coupling is turned off, the conformal dimension of endpoints of 't Hooft lines blows up and the $\langle \hat{I}_a \hat{I}_a \rangle$ correlation functions go to zero. The $\hat{I}_a$ current decouples from the

[2] E.g. if the theory on the boundary is a free scalar field, loop corrections can generate the operator $\phi^2$ on the boundary with coefficient $\sim \tau^{-1} \Lambda_{UV}^2$, where $\Lambda_{UV}$ is the cutoff, but the only implication of this term is that the tuning of $m^2$ needs to be adjusted at order $\tau^{-1}$.

BCFT correlation functions as they collapse to the correlation functions of the underlying 3d CFT $T_{0,1}[B]$ (this is the CFT that we denoted with $T_\infty[B]$ in the introduction).

### 6.1.4 Boundary Propagator of the Photon

In order to compute corrections to boundary correlators and beta functions of boundary couplings in perturbation theory at large $\tau$, we need the propagator of the gauge field between two points on the boundary. Since we are perturbing around the decoupling limit, this can be readily obtained from the knowledge of the two-point function in the free theory (6.23). Recall from the discussion around eq. (6.14) that in the free theory $F_{\mu\nu}$ has a non-singular bulk-to-boundary OPE. So the boundary two-point function of the operator $F_{ab}$ is obtained by specifying the indices to be parallel in eq. (6.23), and then taking the limit in which both insertion points approach the boundary. When taking this limit, we need to pay attention to possible contact terms that can arise due to the following nascent delta-functions

$$\frac{y}{(y^2+\vec{x}^2)^2} \underset{y\to 0}{\longrightarrow} \pi^2\delta^3(\vec{x}) \ , \tag{6.39}$$

and its derivatives. Even though usually we only compute correlators up to contact terms, these kinds of contact terms in the two-point functions of 3d currents do actually contain physical information [170]. In this context, they encode the $\theta$-dependence of the boundary two-point function of $F_{ab}$. Relatedly, they are also needed to obtain the correct boundary propagator of the photon.

To obtain the $(ab,cd)$ components of the two-point function (6.23) we need the components $(ab,cd)$ and $(ya',cd)$ of the structures $G$ and $H$. The structure $G$ gives

$$\left(1+v^4\left(\frac{1-\gamma^2}{1+\gamma^2}\right)\right) G_{ab,cd}(x_{12}) \underset{y_{1,2}\to 0}{\longrightarrow} \frac{2}{1+\gamma^2}\, G^{\text{3d}}_{ab,cd}(\vec{x}_{12}) \ , \tag{6.40}$$

$$-2v^4\frac{\gamma}{1+\gamma^2} i\epsilon_{ab}{}^{ya'}\, G_{ya',cd}(x_{12}) \underset{y_{1,2}\to 0}{\longrightarrow} -\frac{2\gamma}{1+\gamma^2} i\,\pi^2\epsilon_{ab[c}(\partial_{\vec{x}_{12}})_{d]}\delta^3(\vec{x}_{12}) \ . \tag{6.41}$$

Here $G^{\text{3d}}_{ab,cd}$ denotes the same structure as in eq. (6.17) with the replacement of $I_{\mu\nu}$ by the 3d analogue

$$I^{\text{3d}}_{ab}(\vec{x}) \equiv \delta_{ab} - \frac{2x^a x^b}{\vec{x}^2} \ . \tag{6.42}$$

On the other hand the only non-zero component of the structure $H$ in the limit $y_{1,2}\to 0$ is $H_{ya,yb}$, hence the $H$ structure completely drops in the calculation of the propagator. The

result is

$$\langle F_{ab}(\vec{x}_1,0)F_{cd}(\vec{x}_2,0)\rangle = \frac{g^2}{\pi^2}\left[\frac{2}{1+\gamma^2}\,G^{\rm 3d}_{ab,cd}(\vec{x}_{12}) - \frac{2\gamma}{1+\gamma^2} i\,\pi^2 \epsilon_{ab[c}(\partial_{\vec{x}_{12}})_{d]}\delta^3(\vec{x}_{12})\right] . \quad (6.43)$$

It is convenient to go to momentum space, by applying a Fourier transform with respect to the boundary coordinates

$$\langle F_{ab}(\vec{x}_1,0)F_{cd}(\vec{x}_2,0)\rangle \equiv \int \frac{d^3\vec{p}}{(2\pi)^3}\langle F_{ab}(\vec{p},0)F_{cd}(-\vec{p},0)\rangle e^{i\vec{p}\cdot\vec{x}_{12}} . \quad (6.44)$$

We obtain

$$\langle F_{ab}(\vec{p},0)F_{cd}(-\vec{p},0)\rangle = \frac{2g^2}{1+\gamma^2}\left[|\vec{p}|\left(\frac{\delta_{a[c}p_{d]}p_b}{\vec{p}^2} - \frac{\delta_{b[c}p_{d]}p_a}{\vec{p}^2}\right) + \gamma\epsilon_{ab[c}p_{d]}\right] . \quad (6.45)$$

We can finally determine the propagator of the gauge field between two-points in the boundary by imposing that the exterior derivative reproduces the two-point function (6.45). The result is

$$\langle A_a(\vec{p},0)A_b(-\vec{p},0)\rangle \equiv \Pi_{ab}(\vec{p}) = \frac{g^2}{1+\gamma^2}\left[\frac{\delta_{ab} - (1-\xi)\frac{p_a p_b}{\vec{p}^2}}{|\vec{p}|} + \gamma\epsilon_{abc}\frac{p^c}{\vec{p}^2}\right] . \quad (6.46)$$

The parameter $\xi$ is not fixed by requiring consistency with eq. (6.45), and parametrizes a choice of gauge. From the structure of the propagator, we see that the natural perturbative limit is $g^2 \to 0$ with $\gamma$ fixed, which means $\tau \to \infty$ with a fixed ratio $\gamma$ between the real and the imaginary part. Observables are expressed as a power series in $\frac{g^2}{1+\gamma^2}$ with coefficients that are themselves polynomials in $\gamma$, more precisely the coefficient of the order $\mathcal{O}\left(\left(\frac{g^2}{1+\gamma^2}\right)^n\right)$ is a polynomial in $\gamma$ of degree $n$.

### Relations to Large-$k$ and Large-$N_f$ Perturbation Theories

Recall that a 3d Abelian gauge field $a$ with CS action $i\frac{k}{4\pi}\int a\wedge da$ has propagator (up to gauge redundancy)

$$\langle a_a(\vec{p})a_b(-\vec{p})\rangle = \frac{2\pi}{k}\epsilon_{abc}\frac{p^c}{\vec{p}^2} . \quad (6.47)$$

We see that the contact term in eq. (6.45) produced a term in the boundary propagator (6.46) that is identical to the CS one. In particular, from the perturbation theory that

we will consider one can immediately recover results for large-$k$ perturbation theory in Abelian 3d gauge theories, simply by setting (recall that $\gamma = \frac{g^2\theta}{4\pi^2}$)

$$\left(\frac{g^2}{1+\gamma^2}\right)^n \gamma^m \longrightarrow 0 \ , \quad \text{if } m < n \tag{6.48}$$

$$\left(\frac{g^2}{1+\gamma^2}\right)^n \gamma^n \longrightarrow \left(\frac{2\pi}{k}\right)^n \ . \tag{6.49}$$

Indeed, in the limit $g^2 \to \infty$ only the $\theta$-term is left in the bulk action, and the model that we are considering is equivalent to a CS theory on the boundary, with $k = \frac{\theta}{2\pi}$. The only role played by the bulk, in this case, is to allow generic real values of the CS coupling.

We can also compare to the limit of large number of matter flavors $N_f$, in which observables at the IR fixed point of 3d Abelian gauge theories can be computed perturbatively in $1/N_f$. In this regime, after resumming bubble diagrams, one finds the following "effective" propagator (again, up to gauge redundancy)

$$\langle a_a(\vec{p}) a_b(-\vec{p})\rangle \sim \frac{1}{N_f}\frac{\delta_{ab}}{|\vec{p}|} \ . \tag{6.50}$$

The proportionality constant depends on the details of the theory. The resulting "non-local" propagator has precisely the same form of the boundary propagator (6.46) in the case $\gamma = 0$.[3] Hence, once again, the two types of perturbation theories inform each other, and results for one case can be applied in the other case as well. Compared to the large-$k$ perturbation theory, here additional care is needed, because the order at which we are computing a certain observable in the $1/N_f$-expansion does not coincide with the number of internal photon lines in the corresponding diagram, owing to the fact that diagrams with a larger number of internal photon lines can get an enhancement by a positive power of $N_f$ from loops of matter fields. Nevertheless, single diagrams computed in one context can be used in the other context, and we will see an application of this observation later. A generalization of the large-$N_f$ limit is obtained by taking both $N_f$ and $k$ large, with a fixed ratio, and was studied recently in [63]. In this case, one finds a propagator that contains both terms in eq. (6.46), and the same comments about the relation of the two types of perturbation theory apply.

[3]The two types of non-locality have different physical origins, in our setup, the non-locality on the boundary is due to the existence of the bulk, while in the large-$N_f$ limit it emerges due to the resummation of infinitely-many Feynman diagrams. The fact that the resulting two-point functions of the field strength have the same power of momentum is of course no surprise because that is just fixed by the scaling dimension of conserved currents in 3d.

### 6.1.5 Exploring Strong Coupling

As the coupling is increased, the two currents $\hat{I}_a$ and $\hat{J}_a$ should be treated on an even footing. Indeed, they are rotated into each other by the $SL(2,\mathbb{Z})$ group of electric-magnetic dualities of the bulk theory. Assuming no phase transitions, as we approach cusps $\tau \to -\frac{q}{p}$ where the dual gauge coupling becomes weak in some alternative duality frame, we expect dual statements to be true: the $p\hat{J}+q\hat{I}$ current should decouple from the BCFT correlation functions as they collapse to the correlation functions of a new 3d CFT $T_{p,q}[B]$, which gives the dual weakly coupled description of the original BFCT.

Using the notion of duality walls [167, 168], one can argue that $T_{p,q}$ should be obtained from $T_{0,1}$ by Witten's $SL(2,\mathbb{Z})$ action on 3d CFTs equipped with a $U(1)$ global symmetry [5]. This involves coupling $T_{0,1}$ to a certain collection of 3d Abelian gauge fields with appropriate Chern-Simons couplings. This statement requires some care and several caveats about the absence of phase transitions as we vary $\tau$.

In an optimal situation where these phase transitions are absent, this picture implies that the data of $B(\tau,\bar{\tau})$ will approach the data of an infinite collection of 3d CFTs $T_{p,q}$ as $\tau \to -\frac{q}{p}$, sitting in the same universality classes as certain 3d Abelian gauge theories coupled to $T_{0,1}$. This is depicted in fig. 6.1. If we "integrate out" the bulk and restrict our attention to the 3d boundary, what we just described can be stated as the existence of a family of non-local 3d conformal theories (i.e. with no stress-tensor in the spectrum) that continuously interpolate between different local 3d CFTs. More precisely, in the decoupling limit, the 3d theory is a direct product of a 3d CFT and a non-local sector associated with the boundary condition of the free bulk field. This is reminiscent of the construction of [171, 172, 173] in the context of the long-range Ising model.

Let us mention a possible mechanism for a phase transition. As we change continuously $\tau$ from the neighbourhood of the "ungauged cusp" $T_{0,1}$ towards the "gauged cusps" $T_{p,q}$, the dimension of boundary operators are nontrivial functions of $\tau$. A scalar boundary operator $\hat{O}$ might become marginal at a certain codimension 1 wall in the $\tau$-plane. This possibility is depicted in fig. 6.2. In perturbation theory in the vicinity of the wall, we can repeat the logic that we used in the subsection 6.1.3 when discussing perturbation theory around $T_{0,1}$ in presence of boundary marginal operators. Namely, the boundary marginal coupling $\hat{\lambda}$ will generically have a non-trivial beta function, which depends both on $\hat{\lambda}$ and

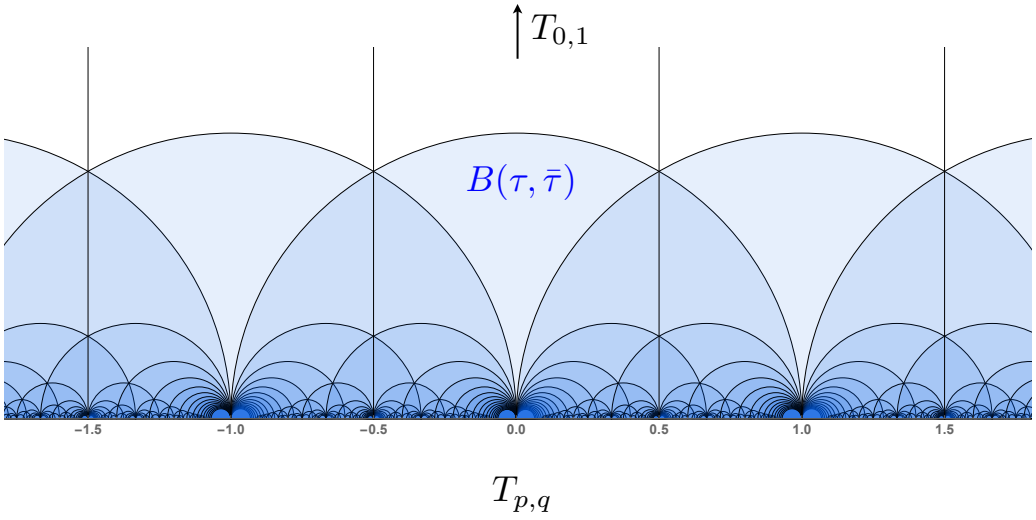


Figure 6.1: The family of conformal boundary conditions $B(\tau, \bar{\tau})$ labeled by the variable $\tau$ in the upper-half plane and by a 3d CFT $T_{0,1}$ with $U(1)$ global symmetry. At the cusp at infinity the current $\hat{I}^a$ decouples and we are left with the local 3d theory $T_{0,1}$ on the boundary, with $U(1)$ current $\hat{J}^a$. Approaching this cusp from $T$-translations of the fundamental domain amounts to adding a CS contact term to the 3d theory, or equivalently to redefine the current $\hat{J}^a$ by multiples of the current $\hat{I}^a$ that is decoupling. This is the $T$ operation on $T_{0,1}$ in the sense of [5]. In the favorable situation in which no phase transitions occur, the BCFT continuously interpolate to the cusps at the rational points of the real axis $\tau = -q/p$, where again the bulk and the boundary decouple and we find new 3d CFTs $T_{p,q}$. These theories are obtained from $T_{0,1}$ with a more general $SL(2,\mathbb{Z})$ transformation, that involves coupling the original $U(1)$ global symmetry to a 3d dynamical gauge field.

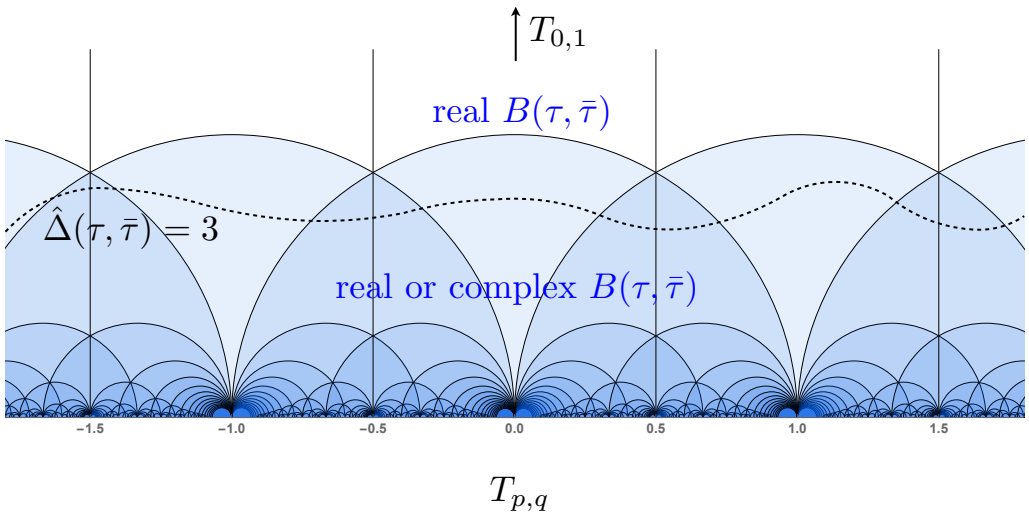


Figure 6.2: A cartoon of a possible phase transition at strong coupling. A scalar boundary operator becomes marginal at a certain curve in the $\tau$ plane, i.e. setting $\hat{\Delta}(\tau,\bar{\tau}) = 3$ we find solutions in the upper-half plane. In conformal perturbation theory from a point on the curve, the beta function takes the form (6.51). We might be unable to find real fixed points for the marginal coupling. In such a situation, $B(\tau,\bar{\tau})$ can only be defined as a complex BCFT. Assuming that we were able to define $B(\tau,\bar{\tau})$ as a real BCFT in perturbation theory around $\tau \to \infty$ by continuity such a real BCFT is ensured to exist in the full region above the wall, but we might be unable to continue it beyond the wall without introducing complex couplings (or breaking conformality).

$\tau$, and whose leading contributions are [4]

$$\beta_{\hat{\lambda}}(\tau,\bar{\tau},\hat{\lambda}) = b_{(F^-)^2,\hat{O}}\,\delta\tau + b_{(F^+)^2,\hat{O}}\,\delta\bar{\tau} + C_{\hat{O}\hat{O}\hat{O}}\hat{\lambda}^2 + \dots \ . \tag{6.51}$$

Here we are perturbing around a point $\tau_0$ on the wall, the coefficient $b$'s and $C$ are (up to numerical factors) the bulk-to-boundary OPE coefficients [174], and the OPE coefficient of the boundary conformal theory, respectively. These OPE coefficients are functions of $\tau_0$. Depending on $\tau_0$ and on the various OPE coefficients, setting $\beta_{\hat{\lambda}} = 0$ one might or might not be able to find a real solution for $\hat{\lambda}$. If a real solution can be found perturbing away from the wall in a certain direction, by continuity $B(\tau,\bar{\tau})$ defines a real BCFT in a region of the $\tau$ plane on that side of the wall. Otherwise, on a side of the wall $B(\tau,\bar{\tau})$ exists only as a non-unitary "complex" BCFT.

### 6.1.6 Two-point Function from the Boundary OPE

In section 6.1.2 we computed the two-point function of the field strength in free theory using the method of images. We will now compute it in the more general case with interactions on the boundary. We will see that it can be fixed completely in terms of the coefficient of the two-point function of the boundary currents. The method that we will use is an explicit resummation of the bulk-to-boundary OPE.

As a consequence of the interaction, the bulk-to-boundary OPE of the field strength contains two independent primary boundary operators, both of them conserved currents, rather than just one like in the free case. The leading terms in this OPE are

$$F_{\mu\nu}(\vec{x},y) \underset{y\to 0}{\sim} \hat{V}_1^a(\vec{x}) 2\delta_{a[\mu}\delta_{\nu]y} - i\epsilon^{abc}\hat{V}_{2\,c}(\vec{x})\delta_{a[\mu}\delta_{\nu]b} + \dots \ . \tag{6.52}$$

The complete form of the above (including all descendants) can be found in (E.15). The boundary currents $\hat{V}_1$ and $\hat{V}_2$ can be expressed in terms of $\hat{J}^a$ and $\hat{I}^a$ as follows

$$\hat{V}_1^a = -g^2\left(\hat{J}^a - \frac{\theta}{2\pi}\hat{I}^a\right) \ , \tag{6.53}$$

$$\hat{V}_2^a = -2\pi\hat{I}^a \ . \tag{6.54}$$

[4] Note that this expression for the beta function is valid also in the decoupling limit $\tau \to \infty$. Indeed in that limit $b_{(F^-)^2,\hat{O}} \propto \tau^{-2}$ and $b_{(F^+)^2,\hat{O}} \propto \bar{\tau}^{-2}$, from which we recover that the leading contributions from the bulk gauge fields are of order $\tau^{-1}$ and $\bar{\tau}^{-1}$.

If the 3d CFT that the gauge field couples to has parity symmetry (i.e. symmetry under reflection of one of the coordinates) then the full boundary CFT $B(\tau, \bar{\tau})$ admits such a symmetry when restricted to $\theta = 0$. Under this symmetry $V_1$ transforms like an ordinary vector, while $V_2$ transforms like an axial vector. We can extend this symmetry to the more general case $\theta \neq 0$ by viewing it as a spurionic symmetry that flips the sign of $\theta$.

Plugging the bulk-to-boundary OPE in the two-point function, one obtains the *boundary channel* decomposition. In this case, since only two boundary primaries appear in the OPE, we can explicitly resum the contributions from all the descendants. The result can be written in terms of the structures defined in (6.23)

$$\begin{aligned}\langle F_{\mu\nu}(x_1) F_{\rho\sigma}(x_2)\rangle = &\left(\alpha_1 \delta^{\mu'}_{[\mu}\delta^{\nu'}_{\nu]} - v^4 \left(\alpha_2\, \delta^{\mu'}_{[\mu}\delta^{\nu'}_{\nu]} + i\frac{\alpha_3}{2}\,\epsilon_{\mu\nu}{}^{\mu'\nu'}\right)\right) G_{\mu'\nu',\rho\sigma}(x_{12}) \\ &+ v^4 \left(\alpha_2\, \delta^{\mu'}_{[\mu}\delta^{\nu'}_{\nu]} + i\frac{\alpha_3}{2}\epsilon_{\mu\nu}{}^{\mu'\nu'}\right) H_{\mu'\nu',\rho\sigma}(\vec{x}_{12}, y_1, y_2)\ . \end{aligned} \tag{6.55}$$

with coefficients

$$\alpha_1 = \tfrac{1}{2}(c_{11}(\tau,\bar{\tau}) + c_{22}(\tau,\bar{\tau})), \quad \alpha_2 = \tfrac{1}{2}\left(c_{11}(\tau,\bar{\tau}) - c_{22}(\tau,\bar{\tau})\right), \quad \alpha_3 = -c_{12}(\tau,\bar{\tau})\ . \tag{6.56}$$

where

$$\langle \hat{V}^a_i(\vec{x}) \hat{V}^b_j(0)\rangle = c_{ij}(\tau,\bar{\tau}) \frac{I^{3\mathrm{d}\,\mathrm{ab}}(\vec{x})}{|\vec{x}|^4} + \text{contact term}\ . \tag{6.57}$$

We see that eq. (6.55) is written explicitly in terms of data of the boundary conformal theory. For the time being, we can ignore the contact term in the current two-point function because it cannot contribute to the two-point function of $F_{\mu\nu}$ at separated points.

To make the action of $SL(2,\mathbb{Z})$ more transparent we will also rewrite the above results in the self-dual/anti self-dual components. The bulk-to-boundary OPE takes the following form

$$F^{\pm}_{\mu\nu}(\vec{x}, y) \underset{y\to 0}{\sim} \hat{V}_{\pm\, a}(\vec{x}) 4P^{\pm\ ay}_{\mu\nu} + \dots\ , \tag{6.58}$$

where

$$\hat{V}_+ = \frac{1}{2}(\hat{V}_1 - i\hat{V}_2) = -\frac{2\pi}{\mathrm{Im}\tau}(\hat{J} - \tau \hat{I})\ , \tag{6.59}$$

$$\hat{V}_- = \frac{1}{2}(\hat{V}_1 + i\hat{V}_2) = -\frac{2\pi}{\mathrm{Im}\tau}(\hat{J} - \bar{\tau} \hat{I})\ . \tag{6.60}$$

An $SL(2,\mathbb{Z})$ transformation acts on $\hat{V}_\pm$ in the same way as it acts on $F^\pm$. In particular under an $S$ transformation $\hat{V}_+ \to \bar{\tau}\,\hat{V}_+$ and $\hat{V}_- \to \tau\,\hat{V}_-$. Using the structures introduced in

section 6.1.2, the result (6.55) can be rewritten in more compact form

$$\langle F^+_{\mu\nu}(x_1)F^+_{\rho\sigma}(x_2)\rangle = (\alpha_2 + i\alpha_3)\, v^4 H^{++}_{\mu\nu,\rho\sigma}(\vec{x}_{12}, y_1, y_2) \ , \tag{6.61}$$

$$\langle F^-_{\mu\nu}(x_1)F^-_{\rho\sigma}(x_2)\rangle = (\alpha_2 - i\alpha_3)\, v^4 H^{--}_{\mu\nu,\rho\sigma}(\vec{x}_{12}, y_1, y_2) \ , \tag{6.62}$$

$$\langle F^+_{\mu\nu}(x_1)F^-_{\rho\sigma}(x_2)\rangle = \alpha_1 G^{+-}_{\mu\nu,\rho\sigma}(x_{12}) \ , \tag{6.63}$$

$$\langle F^-_{\mu\nu}(x_1)F^+_{\rho\sigma}(x_2)\rangle = \alpha_1 G^{-+}_{\mu\nu,\rho\sigma}(x_{12}) \ . \tag{6.64}$$

Note that $\alpha_2 \pm i\alpha_3 = 2c_{\pm\pm}$ while $\alpha_1 = 2c_{+-} = 2c_{-+}$. In this basis the $SL(2,\mathbb{Z})$ action on the above two-point functions can be immediately read from (6.10).

While in this subsection we discussed the two-point function of $F_{\mu\nu}$, clearly a similar computational strategy could be used for an arbitrary $n$-point function, therefore reducing any such bulk correlation functions to correlators of the boundary currents $\hat{J}$, $\hat{I}$. Of course generically for $n > 2$ these correlation functions are not just captured by the coefficients $c_{ij}$, because they are sensitive to the full spectrum of boundary operators entering in the OPE of the currents.

### 6.1.7 One-point Functions from the Bulk OPE

When $x_{12}^2 \ll y^2$ we can expand the two-point function (6.55) in the bulk OPE limit, which is controlled by the OPE of free Maxwell theory

$$F_{\mu\nu}(x)F_{\rho\sigma}(0) \underset{x\to 0}{\sim} \frac{g^2}{\pi^2} G_{\mu\nu,\rho\sigma}(x) + \frac{1}{12}(\delta_{\mu\rho}\delta_{\nu\sigma} - \delta_{\nu\rho}\delta_{\mu\sigma})F^2(0) + \frac{1}{12}\epsilon_{\mu\nu\rho\sigma}F\tilde{F}\,(0) + \dots , \tag{6.65}$$

where we neglected spinning bulk primaries (since they do not acquire vev) and descendants, and we used the shorthand notation $F^2 \equiv F_{\mu\nu}F^{\mu\nu}$ and $F\tilde{F} \equiv F_{\mu\nu}\tilde{F}^{\mu\nu}$.

Plugging the bulk OPE into the l.h.s. of (6.55) one obtains the following *bulk channel decomposition* of the two-point function

$$\begin{aligned}\langle F^{\mu\nu}(x_1)F^{\rho\sigma}(x_2)\rangle \underset{x_1\to x_2}{\sim}\ & \frac{g^2}{\pi^2} G_{\mu\nu,\rho\sigma}(x_{12}) \\ & + \frac{1}{12}(\delta^{\mu\rho}\delta^{\nu\sigma} - \delta^{\nu\rho}\delta^{\mu\sigma})\frac{a_{F^2}(\tau,\bar{\tau})}{y_2^4} + \frac{1}{12}\epsilon^{\mu\nu\rho\sigma}\frac{a_{F\tilde{F}}(\tau,\bar{\tau})}{y_2^4} \\ & + \dots \ ,\end{aligned} \tag{6.66}$$

where $\dots$ denote subleading descendant terms, and we parametrized bulk one-point func-

tions as

$$\langle \mathcal{O}(\vec{x}, y) \rangle = a_{\mathcal{O}} y^{-\Delta_{\mathcal{O}}} \ . \tag{6.67}$$

Comparing (6.66) and (6.55) (see appendix E.3 for details) we obtain a constraint from the contribution of the identity

$$c_{11}(\tau, \bar{\tau}) + c_{22}(\tau, \bar{\tau}) = \frac{4}{\pi \, \mathrm{Im}\tau} \ , \tag{6.68}$$

and the following expressions for the one-point functions[5]

$$a_{F^2}(\tau, \bar{\tau}) = \frac{3}{8} \left( c_{22}(\tau, \bar{\tau}) - c_{11}(\tau, \bar{\tau}) \right) = \frac{3}{4} \left( c_{22}(\tau, \bar{\tau}) - \frac{2}{\pi \, \mathrm{Im}\tau} \right) \ , \tag{6.69}$$

$$a_{F\tilde{F}}(\tau, \bar{\tau}) = i \frac{3}{4} \, c_{12}(\tau, \bar{\tau}) \ . \tag{6.70}$$

This shows that the bulk one-point functions of $F^2$ and $F\tilde{F}$ are determined by the constants $c_{ij}$. Note that these relations are compatible with the (spurionic) parity symmetry, because $a_{F\tilde{F}}$ and $c_{12}$ are odd, while all the other coefficients are even. What we discussed here is a very simple example of the use of the crossing symmetry constraint on bulk two-point functions to determine data of BCFTs [175]. The constraint can be solved exactly in this case because the bulk theory is gaussian.

Equivalently, in selfdual/antiselfdual components

$$a_{F^2_\pm}(\tau, \bar{\tau}) = \frac{3}{16} \left( c_{22}(\tau, \bar{\tau}) \pm 2i \, c_{12}(\tau, \bar{\tau}) - c_{11}(\tau, \bar{\tau}) \right) = -\frac{3}{4} c_{\pm\pm}(\tau, \bar{\tau}) \ . \tag{6.71}$$

Note that due to the constraint in eq. (6.68), the three entries of the matrix $c_{ij}$ actually only contain two independent functions of the coupling. In the appendix E.4 we show how to express $c_{ij}$ (and also the possible contact terms in (6.57)) in terms of two real functions $c_J$ and $\kappa_J$ of $(\tau, \bar{\tau})$, which are the coefficients in the two-point function of $\hat{J}$.

[5]Note that $a_{F^2} \in \mathbb{R}$ while $a_{F\tilde{F}} \in i\mathbb{R}$. To see this, it is useful to think about these coefficients in radial quantization, as the overlap between the state defined by the local operator $F^2/F\tilde{F}$ and the state defined by the conformal boundary condition. Applying an inversion, the overlap gets conjugated. Hence the reality conditions stated above simply follow from the fact that the operator $F^2/F\tilde{F}$ is even/odd under inversion.

### 6.1.8 $c_{ij}(\tau,\bar\tau)$ in Perturbation Theory

Having derived the bulk one-point and two-point functions in terms of the coefficients $c_{ij}(\tau,\bar\tau)$ in the two-point function of the boundary currents, we will now give the leading order results for these coefficients in perturbation theory in $\tau^{-1}$.

Note that thanks to the modified Neumann condition, at leading order $\hat J$ is identified with the U(1) current $\hat J_{\text{CFT}}$, whose two-point function can be parametrized as

$$\langle \hat J^a_{\text{CFT}}(\vec x_1)\hat J^b_{\text{CFT}}(\vec x_2)\rangle = c_J^{(0)}\frac{I^{3\text{d}}_{ab}(\vec x_{12})}{|\vec x_{12}|^4} - i\frac{\kappa_J^{(0)}}{2\pi}\epsilon_{abc}\partial_1^c\delta^3(\vec x_{12})\ . \tag{6.72}$$

Using the expression for $c_{ij}(\tau,\bar\tau)$ in appendix E.4, and plugging $c_J = c_J^{(0)} + \mathcal{O}(\tau^{-1})$ and $\kappa_J = \kappa_J^{(0)} + \mathcal{O}(\tau^{-1})$, we obtain

$$c_{22}(\tau,\bar\tau) = \frac{4}{\pi}\frac{\text{Im}\tau}{|\tau|^2} - 4\frac{(\text{Im}\tau^2 - \text{Re}\tau^2)\,\pi^2 c_J^{(0)} + 4\,\text{Im}\tau\,\text{Re}\tau\,\frac{\kappa_J^{(0)}}{2\pi}}{|\tau|^4} + \mathcal{O}(|\tau|^{-3})\ , \tag{6.73}$$

$$c_{12}(\tau,\bar\tau) = -\frac{4}{\pi}\frac{\text{Re}\tau}{|\tau|^2} + \frac{\text{Im}\tau\,\text{Re}\tau\,\pi^2 c_J^{(0)} - (\text{Im}\tau^2 - \text{Re}\tau^2)\,\frac{\kappa_J^{(0)}}{2\pi}}{|\tau|^4} + \mathcal{O}(|\tau|^{-3})\ . \tag{6.74}$$

$c_{11}(\tau,\bar\tau)$ is obtained by $c_{22}(\tau,\bar\tau)$ using (6.68). Note the compatibility with the (spurionic) parity symmetry, under which both $\text{Re}\tau$ and $\kappa_J^{(0)}$ flip sign, and $c_{22}$ ($c_{12}$) is even (odd, respectively).

We observe that, to this order,

$$\frac{\partial c_{22}}{\partial \text{Re}\tau} + \frac{\partial c_{12}}{\partial \text{Im}\tau} = 0\ . \tag{6.75}$$

An explanation of this relation, and also a reason why it must hold to all orders in perturbation theory, will be provided in section 6.2.

Going to higher orders in $\tau^{-1}$, the correlators of $\hat J$, and in particular the coefficients $c_J$ and $\kappa_J$, will start deviating from those of the CFT. When the CFT is free, these corrections can be computed by ordinary Feynman diagrams on the boundary. We will see examples of this in the following. In the more general case of an interacting CFT, these corrections can be computed in conformal perturbation theory, by lowering an insertion of the bulk Lagrangian (6.2) integrated over the region $y \geq 0$. It would be interesting to characterize the CFT observables that enter the subleading orders of this perturbation theory. We leave

this problem for the future.

### 6.1.9 Displacement Operator

In every BCFT with $d$-dimensional bulk, there exists a boundary scalar operator of protected scaling dimension $d$, the so-called displacement operator. It can be defined as the only scalar primary boundary operator that appears in the bulk-to-boundary OPE of the bulk stress tensor

$$T_{\mu\nu}(\vec{x},y) \underset{y\to 0}{\sim} \frac{d}{d-1}\left(\delta_{\mu y}\delta_{\nu y}-\frac{1}{d}\delta_{\mu\nu}\right)\hat{D}(\vec{x})+\dots \ . \tag{6.76}$$

There is a Ward Identity associated to this operator, namely

$$\int d^d\vec{x}\langle\hat{D}(\vec{x})O_1(\vec{x}_1,y_1)\dots O_n(\vec{x}_n,y_n)\rangle = (\partial_{y_1}+\dots+\partial_{y_n})\langle O_1(\vec{x}_1,y_1)\dots O_n(\vec{x}_n,y_n)\rangle \ , \tag{6.77}$$

that fixes the normalization of the operator. In this normalization its two-point function is

$$\langle\hat{D}(\vec{x}_1)\hat{D}(\vec{x}_2)\rangle = \frac{C_{\hat{D}}}{|\vec{x}_{12}|^{2d}} \ , \tag{6.78}$$

and the quantity $C_{\hat{D}}$ is an observable of the BCFT.

It follows from (6.76) that the displacement operator is the restriction of the component $T_{yy}$ of the stress-tensor to the boundary. In the theory that we are considering the bulk stress-tensor is the usual Maxwell stress-tensor

$$T_{\mu\nu} = \frac{\mathrm{Im}\tau}{2\pi}\left(F_{\mu\rho}F_{\nu}{}^{\rho}-\frac{1}{4}\delta_{\mu\nu}F_{\rho\sigma}F^{\rho\sigma}\right) \ . \tag{6.79}$$

Writing $T_{yy}(y=0)$ in terms of the currents $\hat{I}$ and $\hat{J}$ leads to the following expression for the displacement operator

$$\hat{D} = \frac{\pi}{\mathrm{Im}\,\tau}(|\tau|^2\hat{I}^2+\hat{J}^2-2\mathrm{Re}\tau\,\hat{I}\hat{J}) = \frac{\mathrm{Im}\tau}{4\pi}(\hat{V}_1^2+\hat{V}_2^2) \ . \tag{6.80}$$

The right-hand side of (6.80) contains products of two boundary operators at the same point, that are defined through a point-splitting procedure, similarly to the products on the right-hand side of (6.79). Such a point splitting makes sense for arbitrary $\tau$ even though generically the boundary currents are not generalized free fields. This is because

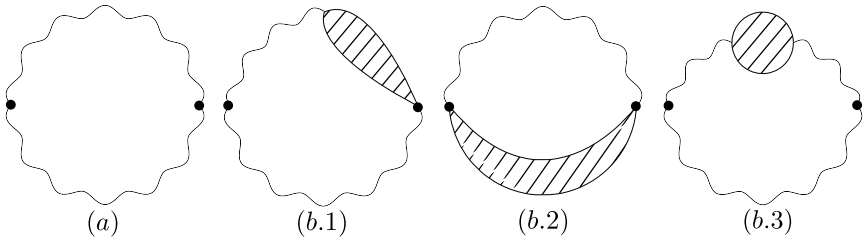


Figure 6.3: Diagrams for the two-point function of the displacement operator. The leading order contribution $(a)$ is the square of the two-point function of the topological current $\hat{I}$. At next-to-leading order we have the diagrams $(b.1)$-$(b.2)$-$(b.3)$ that are also sensitive to the electric current $\hat{J}$. The shaded blobs denote insertions/correlators of $\hat{J}$ in the undeformed CFT.

their dimension and the dimension of $\hat{D}$ are protected, and the contribution of $\hat{D}$ in their OPE is non-singular, so after subtracting the contribution of the identity and possibly of additional operators of scaling dimension $< 4$ we can always take the coincident-point limit.

We can use the expression (6.80) to obtain the first two orders in the perturbative expansion of $C_{\hat{D}}$ universally in terms of the two-point function of the CFT current (6.72). The leading order contribution to $C_{\hat{D}}$ at large $\tau$ comes from the contraction of the $\hat{I}$ currents in the $\hat{I}^2$ term, and is therefore proportional to the square of $c_{22}$ at leading order. At next-to-leading order there is a contribution from the correction to $c_{22}$, and a contribution from the $\hat{I}\hat{J}$ term. See fig. 6.3. The result is

$$C_{\hat{D}} = \frac{6}{\pi^4} - \frac{12}{\pi}\frac{\mathrm{Im}\tau}{|\tau|^2} c_J^{(0)} + \mathcal{O}(|\tau|^{-2}) \ . \tag{6.81}$$

Even though the 3d CFT sector decouples from the bulk in the limit $\tau \to \infty$, and in particular it has a conserved 3d stress tensor, the displacement operator still exists within the sector of boundary operators coming from the free boundary condition of the bulk Maxwell field, and in particular $C_D$ is finite in this limit. Plugging $\mathrm{Re}\,\tau = 0$ and the value of $c_J^{(0)}$ for a theory of two Dirac fermions, namely $c_J^{(0)} = \frac{1}{4\pi^2}$, we find perfect agreement with [52].

### 6.1.10 Three-Point Function $\langle \hat{V}_i \hat{V}_j \hat{D} \rangle$

Some of the distinctive features of the conformal theory living on the boundary of $B(\tau, \bar{\tau})$ are

- the presence of a scalar operator of dimension 4, the displacement operator $\hat{D}$ ; this feature is common to all conformal boundary conditions ;
- the presence of the two $U(1)$ currents $\hat{V}_1$ and $\hat{V}_2$ .

We will now show that the displacement operator $\hat{D}$ appears in the OPE of the currents, with a matrix of OPE coefficients that can be fixed in terms of the coefficients of the bulk one-point functions $a_{F^2}$ and $a_{F\tilde{F}}$, and the coefficient $C_{\hat{D}}$.

To show this, we consider the three-point correlator between the field strength and the displacement operator

$$\langle F_{\mu\nu}(x_1) F_{\rho\sigma}(x_2) \hat{D}(\vec{x}_3) \rangle \ . \tag{6.82}$$

We compute this three-point function in two OPE channels for $F_{\mu\nu}(x_1)F_{\rho\sigma}(x_2)$. In the boundary channel $y_{1,2} \to 0$, using the OPE (6.52) this three-point function can be fixed in terms of the OPE coefficients $\langle \hat{V}_i \hat{V}_j \hat{D} \rangle$ that we want to determine. On the other hand, in the bulk OPE channel $x_{12} \to 0$ this three-point function can be computed in terms of the bulk-boundary two-point functions $\langle O(x_1) \hat{D}(\vec{x}_3) \rangle$ between the displacement and the operators $O$ in the bulk OPE of two $F$'s. The last step of the argument amounts to relating the latter two-point function to the one-point function of $O$ if $O$ is a scalar operator, or to $C_{\hat{D}}$ if $O$ is the stress-tensor.

The coefficients appearing in the three-point function are [176, 177]

$$\langle \hat{V}_i^a(\vec{x}_1) \hat{V}_j^b(\vec{x}_2) \hat{D}(\infty) \rangle = \lambda^{(1)}_{ij\hat{D}+} \ \delta^{ab} + \lambda^{(1)}_{ij\hat{D}-} \ \hat{x}^c_{12} \epsilon^{abc} \ . \tag{6.83}$$

For simplicity we placed the displacement at infinity. $\lambda^{(1)}_{ij\hat{D}+}$ and $\lambda^{(1)}_{ij\hat{D}-}$ are respectively the parity-even/odd OPE coefficients in the conventions of [177], and $\hat{x}^a = x^a/|\vec{x}|$. Recall that under parity $\hat{V}_1$ is a vector while $\hat{V}_2$ is an axial vector, hence the coefficients $\lambda^{(1)}_{11\hat{D}-}, \lambda^{(1)}_{22\hat{D}-}, \lambda^{(1)}_{12\hat{D}+}$ are odd under a spurionic parity transformation, while the others are even.

The details of the calculation are showed in the appendix E.5, and here we will just

give the final result

$$\lambda^{(1)}_{11\hat{D}+} = -\frac{8}{3\pi^2} a_{F^2} + \frac{g^2}{3} C_{\hat{D}} \ , \tag{6.84}$$

$$\lambda^{(1)}_{22\hat{D}+} = \frac{8}{3\pi^2} a_{F^2} + \frac{g^2}{3} C_{\hat{D}} \ , \tag{6.85}$$

$$\lambda^{(1)}_{12\hat{D}+} = -\frac{8}{3\pi^2} \, i a_{F\tilde{F}} \ , \tag{6.86}$$

$$\lambda^{(1)}_{ij\hat{D}-} = 0 \ . \tag{6.87}$$

The parity-odd three-point structures are all set to zero. The spurionic parity symmetry is again satisfied because $\lambda^{(1)}_{12\hat{D}+}$ is proportional to the odd coefficient $a_{F\tilde{F}}$, while the formulas for $\lambda^{(1)}_{11\hat{D}+}$ and $\lambda^{(1)}_{22\hat{D}+}$ are even.

Going to the basis in which the matrix of current-current 2-pt functions is the identity

$$U^l_i U^k_j c_{lk} = \delta_{ij} \ , \tag{6.88}$$

the matrix of OPE coefficients becomes

$$U \lambda^{(1)}_{\hat{D}+} U^T = \frac{2}{\pi^2} \begin{pmatrix} \frac{\mathcal{A} - \frac{\pi^2 C_{\hat{D}}}{8}}{\mathcal{A} - \frac{3}{4\pi^2}} & 0 \\ 0 & \frac{\mathcal{A} + \frac{\pi^2 C_{\hat{D}}}{8}}{\mathcal{A} + \frac{3}{4\pi^2}} \end{pmatrix} \ , \tag{6.89}$$

where

$$\mathcal{A} \equiv \frac{1}{g^2} \sqrt{a^2_{F^2} - a^2_{F\tilde{F}}} \ . \tag{6.90}$$

Recall that $a_{F^2} \in \mathbb{R}$ and $a_{F\tilde{F}} \in i\mathbb{R}$, so $\mathcal{A}$ is real and $\geq 0$. Seemingly the upper entry has a pole at $\mathcal{A} = \frac{3}{4\pi^2}$, which corresponds to the value at the decoupling limit. However recall from (6.81) that $C_{\hat{D}} \to \frac{6}{\pi^4}$ in the decoupling limit, so that actually the entry is finite in the limit.

The upshot of this analysis is that the OPE coefficients between two currents and the displacement can be completely characterized in terms of the two positive quantities $\mathcal{A}$ and $C_{\hat{D}}$, that can be taken to effectively parametrize the position on the conformal manifold. It would be interesting to derive these relations from more standard analytic bootstrap techniques, along the lines of [178, 179, 180].

## 6.2 Free Energy on a Hemisphere

In this section, we study the hemisphere free energy for the conformal boundary conditions of the $U(1)$ gauge field.

Following [181], to any given conformal boundary condition for a $\mathrm{CFT}_4$ we can assign a boundary free energy $F_\partial$, defined as

$$F_\partial = -\frac{1}{2}\log\frac{|Z_{HS^4}|^2}{Z_{S^4}} = -\operatorname{Re}\log Z_{HS^4} + \frac{1}{2}\log Z_{S^4}\ . \tag{6.91}$$

$Z_{S^4}$ denotes the sphere partition function of the CFT, while $Z_{HS^4}$ denotes the partition function of the theory placed on a hemisphere, with the chosen boundary condition on the boundary $S^3$. In writing (6.91) we discarded power-law UV divergences and focused on the universal finite term. Conformal symmetry ensures that the coupling to the curved background can be defined via Weyl rescaling.

In our setup the bulk theory is a $U(1)$ gauge-field with action (6.2), so we have

$$\begin{aligned}
-8\pi\frac{\partial F_\partial}{\partial \operatorname{Im}\tau} &= -\operatorname{Re}\int_{HS^4} d^4x\sqrt{g(x)}\langle F^2(x)\rangle_{HS^4} + \frac{1}{2}\int_{S^4} d^4x\sqrt{g(x)}\langle F^2(x)\rangle_{S^4},\\
-8\pi\frac{\partial F_\partial}{\partial \operatorname{Re}\tau} &= -\operatorname{Re}\int_{HS^4} d^4x\sqrt{g(x)}\langle iF\tilde{F}(x)\rangle_{HS^4} + \frac{1}{2}\int_{S^4} d^4x\sqrt{g(x)}\langle iF\tilde{F}(x)\rangle_{S^4}.
\end{aligned} \tag{6.92}$$

Using a Weyl transformation the one-point functions can be obtained from those on $\mathbb{R}^3\times\mathbb{R}_+$ as

$$\langle F^2(x)\rangle_{HS^4} = \Omega(x)^{-4}\frac{a_{F^2}}{u(x)^4} + \frac{1}{2}\mathcal{A}, \quad \langle F\tilde{F}(x)\rangle_{HS^4} = \Omega(x)^{-4}\frac{a_{F\tilde{F}}}{u(x)^4} + \frac{1}{2}\widetilde{\mathcal{A}}\ . \tag{6.93}$$

Here $x$ is a point on the hemisphere, $\Omega(x)$ is the Weyl factor induced by the stereographic projection, and $u(x)$ denotes the chordal distance between the point $x$ and the boundary $S^3$. The shifts $\mathcal{A}$ and $\tilde{\mathcal{A}}$ stand for a scheme-dependent contribution to the one-point function, due to the ambiguity in the definition of the theory on the curved background: we can always add local counterterms given by a scalar density of dimension four built out of the background curvature, multiplied by the real or imaginary part of the marginal coupling $\tau$, and integrated in the interior of the hemisphere. On the other hand, if we compute the partition function on $S^4$ in the same scheme, the one-point functions on $S^4$ receive contribution only from those counterterms because on $\mathbb{R}^4$ one-point functions must vanish, and there is a relative factor of two because in this case the counterterm is integrated over

the whole sphere. Hence

$$\langle F^2 \rangle_{S^4} = \mathcal{A} \ , \quad \langle F\tilde{F} \rangle_{S^4} = \widetilde{\mathcal{A}} \ , \tag{6.94}$$

such that the ambiguity precisely cancels in (6.92). Here we see the virtue of the choice of normalization in (6.91).

The remaining integral on $HS^4$ has a UV divergence when the point $x$ approaches the boundary $S^3$. We introduce a UV regulator $\epsilon \ll 1$ and restrict the integral to the region $u(x) > \epsilon$. The result is

$$\int_{u(x)>\epsilon} \sqrt{g(x)}\ \Omega(x)^{-4} \frac{1}{u(x)^4} = \frac{2\pi^2}{3\epsilon^3} - \frac{5\pi^2}{3\epsilon} + \frac{4\pi^2}{3} + \mathcal{O}(\epsilon) \ . \tag{6.95}$$

As implicit in the definition of $F_\partial$, we will neglect the power-law UV divergent term and focus on the universal finite piece. Hence we finally obtain

$$\frac{\partial F_\partial}{\partial \operatorname{Im}\tau} = \frac{\pi}{6}\, a_{F^2} = \frac{\pi}{8} c_{22}(\tau,\bar\tau) - \frac{1}{4\operatorname{Im}\tau} \ , \tag{6.96}$$

$$\frac{\partial F_\partial}{\partial \operatorname{Re}\tau} = \frac{\pi}{6}\, i\, a_{F\tilde{F}} = -\frac{\pi}{8} c_{12}(\tau,\bar\tau) \ . \tag{6.97}$$

We used the relations (6.68) to rewrite the result in terms of the two-point functions of the conserved currents. A consequence of this equation is that the relation (6.75) must be valid to all orders in perturbation theory, or more generally whenever $F_\partial$ is well-defined.

Plugging (6.73)-(6.74) in (6.96)-(6.97) and solving the equations we find the following leading behavior of $F_\partial$ at large $\tau$

$$F_\partial \underset{\tau\to\infty}{\sim} -\frac{1}{4}\log\left[\frac{2\operatorname{Im}\tau}{|\tau|^2}\right] + C + \pi \frac{\frac{\pi^2}{2} c_J^{(0)} \operatorname{Im}\tau + \frac{\kappa_J^{(0)}}{2\pi} \operatorname{Re}\tau}{|\tau|^2} + \mathcal{O}(|\tau|^{-2}) \ . \tag{6.98}$$

The first term, which diverges for $\tau \to \infty$, is the value of $F_\partial$ for a free Maxwell field with Neumann boundary conditions [181]. Matching eq. (6.98) with the value of $F_\partial$ for a decoupled system of a Maxwell field with Neumann conditions and a 3d CFT on the boundary, we find that the constant $C$, that remained undetermined by the differential constraint, is in fact the $S^3$ free energy $F_{0,1}$ of the theory $T_{0,1}$.

Using an $SL(2,\mathbb{Z})$ transformation, the same asymptotic behavior holds in the vicinity of any cusp point, upon replacing $\tau$ with the transformed variable $\tau'$ that goes to $\infty$ at the selected cusp and identifying $C$ with the $S^3$ free energy of the decoupled 3d CFT living at

the cusp. Near the cusp where the current $p\hat{J}+q\hat{I}$ decouples from the 3d theory $T_{p,q}$, we have

$$F_\partial \underset{\tau'\to\infty}{\sim} -\frac{1}{4}\log\left[\frac{2\,\mathrm{Im}\tau'}{|\tau'|^2}\right]+F_{p,q}+\mathcal{O}(|\tau'|^{-1})\ . \tag{6.99}$$

where $\tau'=\frac{a\tau+b}{p\tau+q}$, with $aq-bp=1$, and $F_{p,q}$ is the $S^3$ free energy of $T_{p,q}$. Note that

$$-\frac{1}{4}\log\left[\frac{2\,\mathrm{Im}\tau}{|\tau|^2}\right]\underset{\tau'\to\infty}{\sim}-\frac{1}{4}\log\left[\frac{2\,\mathrm{Im}\tau'}{|\tau'|^2}\right]+\frac{1}{2}\log|q|\ , \tag{6.100}$$

$$-\frac{1}{4}\log\left[2\,\mathrm{Im}\tau\right]\underset{\tau'\to\infty}{\sim}-\frac{1}{4}\log\left[\frac{2\,\mathrm{Im}\tau'}{|\tau'|^2}\right]+\frac{1}{2}\log|p|\ . \tag{6.101}$$

Eq. (6.100) implies that the function

$$F_\partial+\frac{1}{4}\log\left[\frac{2\,\mathrm{Im}\tau}{|\tau|^2}\right]\ , \tag{6.102}$$

attains the finite value

$$\frac{1}{2}\log|q|+F_{p,q}\ , \tag{6.103}$$

at all the cusps with $|q|\neq 0$. For the cusp with $q=0$ we can simply use (6.101) to derive that

$$F_\partial+\frac{1}{4}\log\left[2\,\mathrm{Im}\tau\right]\ , \tag{6.104}$$

approaches

$$\frac{1}{2}\log|p|+F_{p,q}\ . \tag{6.105}$$

Hence the function $F_\partial(\tau,\bar{\tau})$ contains information about the $S^3$ free energies of an infinite family of 3d Abelian gauge theories, namely all the theories obtained by applying $SL(2,\mathbb{Z})$ transformations to $T_{0,1}$.

We note in passing that the shift by $\frac{1}{2}\log|q|$ in eq. (6.100) has a nice interpretation in terms of the $S^3$ free energy for a pure CS theory. Indeed, starting with a 4d gauge field with Neumann condition, applying the transformation $ST^k$, i.e. $\tau'=-\frac{1}{\tau+k}$, and taking the decoupling limit $\tau'\to\infty$, we are left with a pure CS theory at level $k$ on the boundary. Hence, the free energy $F_\partial$ in this limit should be the sum of the contribution of the decoupled 4d gauge field with Neumann boundary condition, and the contribution from the CS theory at level $k$, which is $\frac{1}{2}\log|k|$. This is precisely what eq. (6.100) gives. Similarly eq. (6.101) can be interpreted by starting with a 4d gauge field with Dirichlet boundary condition, whose partition function is the left-hand side of (6.101), applying

$ST^kS$, i.e. $\tau' = \frac{\tau}{-k\tau+1}$, and going to the decoupling limit. Again, we find a decoupled 4d gauge field with Neumann boundary condition, and a CS theory at level $k$ on the boundary. The shift by $\frac{1}{2}\log|p|$ in eq. (6.101) precisely reproduces the $\frac{1}{2}\log|k|$ contribution of the CS theory.

## 6.3 A Minimal Phase Transition

In this section we will study a non-trivial BCFT which conjecturally describes a second-order (boundary) phase transition between two free boundary conditions $(p, q)$ and $(p', q')$ of the 4d gauge field, with $pq' - p'q = 1$. In particular, the conjectural BCFT should have a single relevant boundary operator, which can be turned on to flow to either of these free boundary conditions in the IR, depending on the sign of the coupling. We will assume that this BCFT exists for all values of the gauge coupling $\tau$, with no further phase transitions as a function of $\tau$.

Without loss of generality, we can pick two canonical duality frames where the phase transition interpolates between Dirichlet and Neumann boundary conditions or vice versa. We can also pick two duality frames where the phase transition interpolates between Neumann and $(1, 1)$ boundary conditions or vice versa.

- If we go to weak coupling in the former duality frames, the boundary degrees of freedom should describe a phase transition between phases with spontaneously broken or unbroken $U(1)$ global symmetry. We expect that to be described by a critical $O(2)$ model.

- If we go to weak coupling in the latter duality frames, the boundary degrees of freedom should describe a phase transition between two gapped phases with unbroken $U(1)$ global symmetry, but background Chern-Simons coupling which differs by one unit. We expect that to be described by a massless Dirac fermion.

Keeping track of the duality transformations between the different frames, we can assemble an overall picture.

- Denote as $\tau_{DN}$ the gauge coupling associated to the description as a phase transition between Dirichlet and Neumann boundary conditions, so that one "$O(2)$ cusp" is at $\tau_{DN} \to \infty$.

- Then $\tau_{ND} = -1/\tau_{DN}$ is the coupling which is weak at the other $O(2)$ cusp, at $\tau_{DN} \to 0$.
- Shifting the $\theta$ angle by $2\pi$ gives an alternative description as a transition between Dirichlet and $(1,-1)$ boundary conditions, with coupling $\tau_{DN''} = \tau_{DN} - 1$. Dually, we get a transition between Neumann and $(1,1)$ boundary conditions, with coupling $\tau_{NN'} = -\tau_{DN''}^{-1} = \frac{1}{1-\tau_{DN}}$ which is weak at the "Dirac fermion" cusp, $\tau_{DN} \to 1$.
- If we had shifted the $\theta$ angle in the opposite way, we would arrive to a transition between Neumann and $(1,-1)$ boundary conditions, with coupling $\tau_{NN''} = -\tau_{DN'}^{-1} = -\frac{1}{1+\tau_{DN}}$ which is weak at the second "Dirac fermion" cusp, $\tau_{DN} \to -1$.

In the following, we will do most of our calculations in a perturbative expansion around a "Dirac fermion" cusp. The correct boundary theory is actually a Dirac fermion dressed by half a unit of background Chern-Simons coupling [182, 183]. It is convenient to absorb that background Chern-Simons coupling into an improperly-quantized shift of the $\theta$ angle, so that the gauge coupling is denoted as $\tau = \tau_{NN'} - \frac{1}{2} = \frac{1}{2}\frac{1+\tau_{DN}}{1-\tau_{DN}}$. Therefore, denoting with $\psi$ the Dirac fermion, the action that we consider is

$$S[A, \tau + \tfrac{1}{2}] + \int_{y=0} d^3\vec{x}\, i\bar{\psi} \not{D}_A \psi \ . \tag{6.106}$$

The second Dirac fermion cusp is at $\tau \to 0$ and the $O(2)$ cusps are at $\tau = \pm\frac{1}{2}$. See fig.s 6.4-6.5.

Essentially by construction, the picture is compatible with a well-known duality web of particle-vortex, fermion-boson and fermion-fermion dualities [70], which inspired this investigation. In particular, thanks to the particle-vortex duality between the $O(2)$ model and the gauged $O(2)$ model [184, 185], or equivalently thanks to its fermionic version [186], in this case we have a $\mathbb{Z}_2$ subgroup of $SL(2,\mathbb{Z})$ that is a duality of $B(\tau,\bar{\tau})$, i.e. it leaves invariant both the bulk and the boundary condition. This subgroup acts on $\tau = \tau_{NN'} - \frac{1}{2}$ as

$$\tau \to -\frac{1}{4\tau} \ . \tag{6.107}$$

It is interesting to note that the self-dual point $\tau = \frac{i}{2}$, i.e. $\tau_{DN} = i$, is an extreme of $F_\partial$. In our formalism, this is a straightforward consequence of the differential equations (6.96)-(6.97), once we set $c_{11} = c_{22} = \frac{2}{\pi\,\mathrm{Im}\tau}$ and $c_{12} = 0$ – as dictated by self-duality and equation (6.68).[6]

[6] Alternatively, we can implement the reasoning of [187] to show that this property follows from the emergent $\mathbb{Z}_2$ symmetry of the system at the self-dual point.

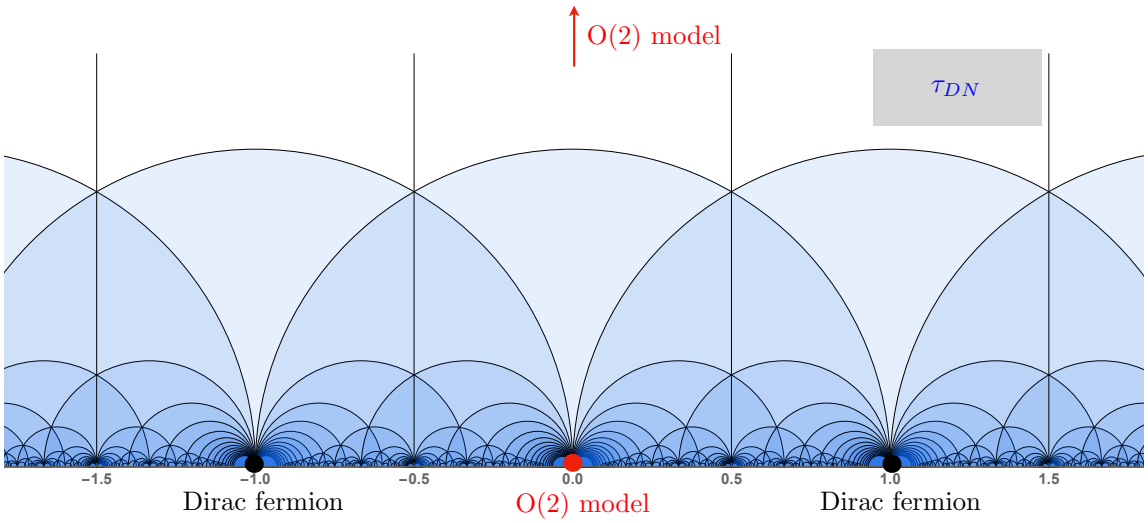


Figure 6.4: The upper-half plane of the gauge coupling $\tau_{DN}$, i.e. in the duality frame in which at $\tau_{DN} \to \infty$ we find the $O(2)$ model on the boundary. Thanks to particle-vortex duality, the cusp in the origin $\tau_{DN} = 0$ also gives a decoupled $O(2)$ model on the boundary. Thanks to the boson-fermion duality between $U(1)_1$ coupled to a critical scalar and a free Dirac fermion, the cusps at $\tau_{DN} = \pm 1$ give a free Dirac fermion.

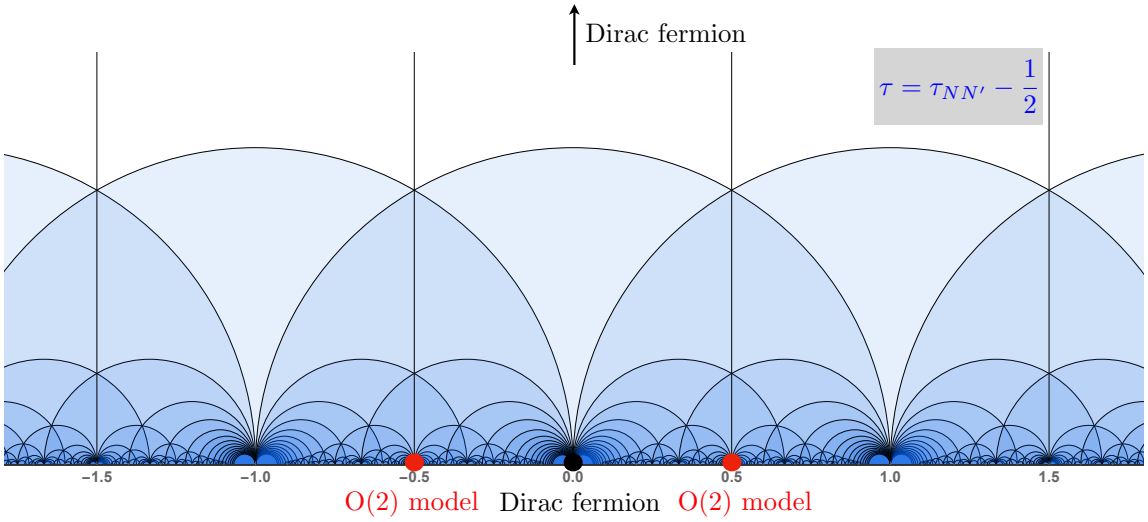


Figure 6.5: The upper-half plane of the gauge coupling $\tau = \tau_{NN'} - \frac{1}{2}$, i.e. in the duality frame in which at $\tau \to \infty$ we find a free Dirac fermion on the boundary. Thanks to fermionic particle-vortex duality, the cusp in the origin $\tau = 0$ also gives a free Dirac fermion on the boundary. Thanks to the boson-fermion duality between $U(1)_{\frac{1}{2}}$ coupled to a Dirac fermion and the $O(2)$ model, the cusps at $\tau = \pm\frac{1}{2}$ give the $O(2)$ model.

Before proceeding, let us mention some of the previous literature on this theory, and comment on the relation to the results that we will present in the rest of this section. The interplay between the 3d dualities and the 4d electric-magnetic duality in the setup with a 3d Dirac fermion coupled to a bulk gauge field was investigated in [70, 71, 72, 73, 74]. In particular [73, 74] studied the transport properties of the boundary theory at the self-dual point. For the theory with an even number of Dirac fermions on the boundary, the two-loop two-point function of the boundary current $\hat{J}$ was obtained in [47] (see also [48, 49, 50, 51]) while the Weyl anomalies (or equivalently the two- and three-point functions of the displacement operator) were computed to next-to-leading order in [52, 188] (for the supersymmetric version of the theory see [189]). The point of view of boundary conformal field theory was first adopted in this theory in [52, 188], but these papers do not consider the action of electric-magnetic duality and the existence of multiple decoupling limits. Besides the transport coefficients and the Weyl anomalies, other boundary observables such as scaling dimensions of operators, or the hemisphere free-energy, were not studied before. Since the duality explained above only exists for the theory with one Dirac fermion, we will first concentrate on this case. Later we will also consider the theory with an even number $2N_f$ of fermions, both at large $N_f$ and in the special case $2N_f = 2$.

### 6.3.1 Perturbative Calculation of Scaling Dimensions

We will compute the anomalous dimensions of the first two fermion bilinear operators $O_s$ of spin $s$, namely

$$O_0 = \bar{\psi}\psi \ , \tag{6.108}$$

$$(O_2)_{ab} = i\big(\bar{\psi}\gamma_{(a}\overset{\leftrightarrow}{D}_{b)}\psi - \text{trace}\big) \ , \tag{6.109}$$

up to two-loop level. Note that in the limit $\tau \to \infty$ of decoupling between bulk and boundary $(O_2)_{ab}$ becomes a conserved current, namely the stress-tensor of the 3d free-fermion CFT.

The anomalous dimension can be obtained from the renormalization of the 1PI correlator of the composite operator with two elementary fields

$$\langle O_s(q=0)\psi(-p)\bar{\psi}(p)\rangle_{\text{1PI}} \ . \tag{6.110}$$

We employ dimensional regularization and minimal subtraction, i.e. we set $d = 3 - 2\epsilon$ and keep the codimension fixed $= 1$, expand the dimensionally-continued loop integrals around

$\epsilon = 0$, and reabsorb the poles in the renormalization constants

$$O_B = Z_O O \ , \tag{6.111}$$
$$\psi_B = Z_\psi \psi \ , \tag{6.112}$$

where the subscript $B$ denotes the bare operators.

Even though the correlator in (6.110) involves the operator $\psi$ that is not gauge-invariant, it is still sensible to renormalize it. The resulting renormalized correlator, as well as the renormalization constant $Z_\psi$, both depend on the choice of gauge-fixing, but the renormalization constant $Z_O$ of the gauge-invariant operator does not, hence we can extract physical information from it.

The renormalization constants admit the loopwise expansion (at small $g^2$ with fixed $\gamma$)

$$Z = 1 + \delta Z = 1 + \sum_n \left( \frac{g^2}{1+\gamma^2} \right)^n \delta Z^{(n)} \ , \tag{6.113}$$

where $\delta Z^{(n)}$ is a polynomial in $\gamma$ of degree $\leq n$, and furthermore by invariance under space reflections only even powers of $\gamma$ are present. The n-loop term $\delta Z^{(n)}$ contains divergences up to $\epsilon^{-n}$, but the familiar RG argument constrains all the coefficients in terms of the ones at lower loop order, except that of the $\epsilon^{-1}$ divergence.

The anomalous dimension is then given by

$$\gamma_O = \frac{d \log Z_O}{d \log \mu} \ . \tag{6.114}$$

The dependence on the renormalization scale $\mu$ is through the $d$-dimensional coupling

$$g_B = \mu^\epsilon g \ . \tag{6.115}$$

In the latter equation we do not need to include a renormalization of the coupling because, as we explained in section 6.1.3, $g$ does not run. Therefore we can rewrite

$$\gamma_O = -\epsilon \frac{\partial \log Z_O}{\partial \log g} \ . \tag{6.116}$$

To compute (6.110) we use the Feynman diagrams in fig.6.8, computed in momentum space, and for simplicity we take the composite operator to carry zero momentum. The Feynman rules given in fig.6.6.

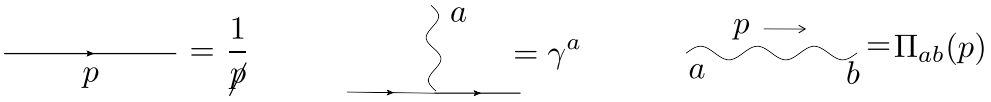


Figure 6.6: Feynman rules. $\Pi_{ab}$ is defined in (6.46).

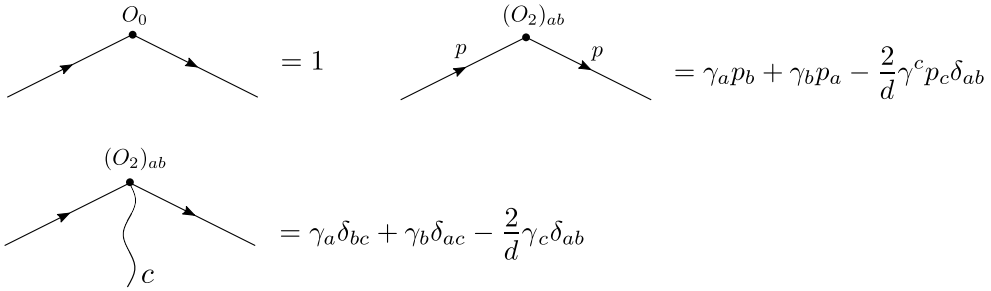


Figure 6.7: Feynman rules for the zero-momentum insertions of the composite operators. Note that there are two vertices associated to $O_2$.

We performed the calculation up to two loops. See appendix E.7 for more details about the computation of the two-loop Feynman diagrams. The resulting renormalization constants are

$$\delta Z_\psi = \frac{g^2}{1+\gamma^2}\frac{2-3\xi}{24\pi^2\epsilon} + \left(\frac{g^2}{1+\gamma^2}\right)^2 \left[\frac{(2-3\xi)^2}{1152\pi^4\epsilon^2} - \frac{9(1-2\gamma^2)\pi^2+16}{3456\pi^4\epsilon}\right] + \mathcal{O}(g^6)\ . \quad (6.117)$$

$$\delta Z_0 = -\frac{g^2}{1+\gamma^2}\frac{2}{3\pi^2\epsilon} + \left(\frac{g^2}{1+\gamma^2}\right)^2 \left[\frac{2}{9\pi^4\epsilon^2} + \frac{9\pi^2(1-2\gamma^2)-8}{108\pi^4\epsilon}\right] + \mathcal{O}(g^6)\ . \quad (6.118)$$

$$\delta Z_2 = \frac{g^2}{1+\gamma^2}\frac{2}{5\pi^2\epsilon} + \left(\frac{g^2}{1+\gamma^2}\right)^2 \left[\frac{2}{25\pi^4\epsilon^2} - \frac{75\pi^2+16}{3000\pi^4\epsilon}\right] + \mathcal{O}(g^6)\ , \quad (6.119)$$

where we denoted $\delta Z_s \equiv \delta Z_{O_s}$. Note that indeed $\delta Z_0$ and $\delta Z_2$ do not depend on the gauge-fixing parameter. As a check, we also verified that the operator $O_1 = \bar{\psi}\gamma^a\psi$ does not get renormalized, i.e. we explicitly computed the renormalization up to two-loop order and found $\delta Z_1 = 0$, as expected for a conserved current. On the other hand, note that $\delta Z_2 \neq 0$. This is a manifestation of the fact that the boundary degrees of freedom do not define a local 3d theory once we couple them to the bulk: the conservation of the boundary would-be stress-tensor is violated at $g \neq 0$, and the system only admits a stress-tensor in the bulk. This means that the short operator of spin 2 must recombine into a long conformal multiplet. In the appendix E.6, we show that this mechanism can be used to compute the one-loop anomalous dimension, and we use this to check the Feynman diagram calculation.

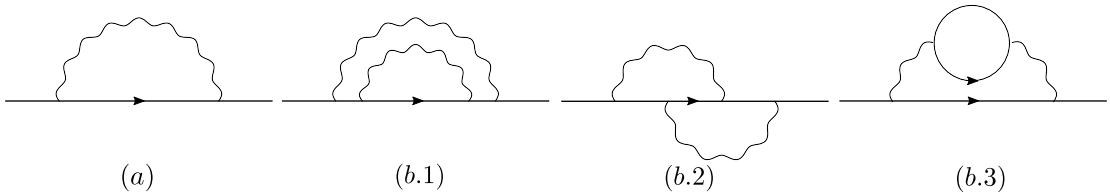


Figure 6.8: One loop and two loops diagrams. We sum over all possible insertions of the composite operators on the internal fermion lines, and also on vertices in the case of $O_2$.

The resulting anomalous dimensions, expressed as a function of $\tau$ are

$$\gamma_0 = -\frac{8}{3\pi}\frac{\text{Im}\tau}{|\tau|^2} + \frac{36\pi^2-32}{27\pi^2}\frac{(\text{Im}\tau)^2}{|\tau|^4} - \frac{8}{3}\frac{(\text{Re}\tau)^2}{|\tau|^4} + \mathcal{O}(|\tau|^{-3}) \ , \tag{6.120}$$

$$\gamma_2 = \frac{8}{5\pi}\frac{\text{Im}\tau}{|\tau|^2} - \frac{150\pi^2+32}{375\pi^2}\frac{(\text{Im}\tau)^2}{|\tau|^4} + \mathcal{O}(|\tau|^{-3}) \ . \tag{6.121}$$

From these results, we can immediately recover the anomalous dimensions for the 3d gauge theory $U(1)_k$ coupled to a Dirac fermion at large $k$ as explained in section 6.1.4. Since this is a local 3d theory, we expect $\gamma_2 = 0$ and indeed this is what we obtain from (6.121). For the anomalous dimension of the scalar bilinear, that starts at two-loop order in this theory, we find

$$\gamma_0 = -\frac{8}{3k^2} + \mathcal{O}(k^{-4}) \ , \tag{6.122}$$

in agreement with [190].[7]

### 6.3.2 Perturbative $F_\partial$

Thanks to the differential equation (6.96)-(6.97), and to the relations derived in appendix E.4, the computation of the hemisphere free energy is reduced to the computation of the two-point functions of the boundary current $\hat{J}$. Up to next-to-leading order, we already wrote the universal formula (6.98) for the hemisphere free energy in terms of the two-point function of the current $\hat{J}_{\text{CFT}}$ of the unperturbed CFT. In this particular setup where the boundary theory at $\tau \to \infty$ is a free Dirac fermion, we can do better without much effort, because the correction to the current two-point function, given by the two diagrams in fig.

[7] In [191] there appears to be a sign mistake in the two-loop diagram that we denoted with (b.2) in fig. 6.8. This mistake leads to a different result for this anomalous dimension given in [192]. Upon correcting that sign, we find perfect agreement with our result. We thank E. Stamou for helping us with this check.

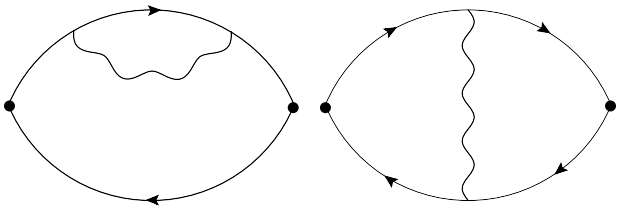

Figure 6.9: Leading corrections to the boundary current two-point function for the Dirac fermion.

6.9, already exists in the literature. For the parity even part of the two-point function, we can either extract the value of these diagrams from the large-$N_f$ calculation of [62], using the similarities between the two perturbative expansions that we explained in 6.1.4, or alternatively use the computation performed directly in the mixed-dimensional setup in [47, 50].[8] The parity-odd part can be obtained from the large-$k$ calculation in [193]. The sum of the diagrams in fig. 6.9 is the next-to-leading order correction for the one-photon irreducible two-point function, which we denote by $\Sigma$, see appendix E.4 for more details. Due to the shift in the real part of $\tau$, i.e. $\tau = \tau_{NN'} - \frac{1}{2}$, we have that $\kappa_\Sigma$ vanishes at leading order in perturbation theory, or equivalently $\kappa_J^{(0)} = 0$. The results mentioned above give

$$c_\Sigma = \frac{1}{8\pi^2} + \frac{92 - 9\pi^2}{144\pi^3}\frac{\mathrm{Im}\tau}{|\tau|^2} + \mathcal{O}(|\tau|^{-2}) \ , \tag{6.123}$$

$$\kappa_\Sigma = \frac{4 + \pi^2}{16}\frac{\mathrm{Re}\tau}{|\tau|^2} + \mathcal{O}(|\tau|^{-2}) \ . \tag{6.124}$$

Using (E.28)-(E.29) to obtain the total two-point function of $\hat{J}$, we find

$$c_J = \frac{1}{8\pi^2} + \frac{368 - 45\pi^2}{576\pi^3}\frac{\mathrm{Im}\tau}{|\tau|^2} + \mathcal{O}(|\tau|^{-2}) \ , \tag{6.125}$$

$$\kappa_J = \frac{16 + 5\pi^2}{64}\frac{\mathrm{Re}\tau}{|\tau|^2} + \mathcal{O}(|\tau|^{-2}) \ . \tag{6.126}$$

[8] In comparing with [47, 50] one needs to take into account that they consider a 3d interface with the gauge field propagating on both sides, rather than a boundary. The propagator of the photon restricted to an interface has a factor of $\frac{1}{2}$ compared to the case of the boundary.

Plugging these values in the formulas (E.31)-(E.37) for $c_{22}$ and $c_{12}$, and solving the differential equations (6.96)-(6.97) we obtain

$$F_\partial = -\frac{1}{4}\log\left[\frac{2\,\mathrm{Im}\tau}{|\tau|^2}\right] + F_{\mathrm{Dirac}} + \frac{\pi}{16}\frac{\mathrm{Im}\tau}{|\tau|^2} + \frac{(368-45\pi^2)(\mathrm{Im}\tau)^2 + (144+45\pi^2)(\mathrm{Re}\tau)^2}{2304|\tau|^4} + \mathcal{O}(|\tau|^{-3})\ . \tag{6.127}$$

We fixed the integration constant by comparing with the decoupling limit, so that $F_{\mathrm{Dirac}}$ is the $S^3$ free energy for a free Dirac fermion (two complex components) [194]

$$F_{\mathrm{Dirac}} = \frac{\log 2}{4} + \frac{3\zeta(3)}{8\pi^2}\ . \tag{6.128}$$

### 6.3.3 Extrapolations to the $O(2)$ Model

We can now attempt to extrapolate the perturbative results obtained above around the Dirac fermion cusp to the $O(2)$ cusp (see fig. 6.5), to obtain the data of the $O(2)$ model. The $O(2)$ model, while being strongly coupled, is a well-studied theory via a variety of techniques, so that we can compare our extrapolations to the known data. Even though so far we only obtained the first two orders in perturbation theory, and one might be wary to already attempt an extrapolation, we will see that the results we obtain are compatible with the known data. We view this as an encouraging indication that the perturbative technique that we are presenting here can indeed be a useful tool to obtain data of 3d Abelian gauge theories, and as a motivation to try to obtain more precise predictions by going to higher orders.

In order to extrapolate, we need to apply a resummation technique. The nice property of our setup is the duality $\tau \leftrightarrow \tau' = -\frac{1}{4\tau}$, which means that the perturbative expansions obtained above also tell us about the behavior of the observables around $\tau' \to \infty$, i.e. the second Dirac fermion cusp. To leverage on this, the idea is to use a "duality-improved" Padé approximant, i.e. a function with a number of free parameters that we can fix by matching to the perturbative result at $\tau \to \infty$, and that is invariant under a duality transformation.

Similar resummations were studied in the context of perturbative string theory [195] and $\mathcal{N} = 4$ super Yang-Mills (SYM) in [196]. In particular [196] introduced Padé-like approximants with the property of being invariant under a subgroup of $SL(2,\mathbb{Z})$, and we will borrow their method. Note that the perturbative results of the previous subsections,

expressed in terms of $g_s = g^2$ and $\theta$, and expanded for small $g_s$ with $\theta$ fixed take the form

$$\gamma_0 = -\frac{4}{3\pi^2} g_s - \frac{8-9\pi^2}{27\pi^4} g_s^2 + \mathcal{O}\left(g_s^3, g_s^3\theta^2\right) \ , \tag{6.129}$$

$$\gamma_2 = \frac{4}{5\pi^2} g_s - \frac{16+75\pi^2}{750\pi^4} g_s^2 + \mathcal{O}\left(g_s^3, g_s^3\theta^2\right) \ , \tag{6.130}$$

$$f_\partial = \frac{1}{32} g_s + \frac{368-45\pi^2}{9216\pi^2} g_s^2 + \mathcal{O}\left(g_s^3, g_s^3\theta^2\right) \ , \tag{6.131}$$

and $f_\partial$ is the boundary free energy where the contributions from free gauge field as well as the constant term have been subtracted. The expressions above all have the pattern

$$a\ g_s(1 + b\ g_s + \mathcal{O}(g_s^2, g_s^2\theta^2)) \ , \tag{6.132}$$

which can be approximated by the manifestly duality-invariant interpolation functions written in [196]. At this order, there are two of their functions that we can use, the integral-power Padé $F_1(g_s, \theta)$ and half-integral-power Padé $F_2(g_s, \theta)$, defined by

$$F_1(g_s, \theta) = \frac{h_1}{g_s^{-1} + (\mathrm{S} \cdot g_s)^{-1} - h_2} \ , \tag{6.133}$$

$$F_2(g_s, \theta) = \frac{h_3 \left(g_s^{-1/2} + (\mathrm{S} \cdot g_s)^{-1/2}\right)}{g_s^{-3/2} + (\mathrm{S} \cdot g_s)^{-3/2} + h_4 \left(g_s^{-1/2} + (\mathrm{S} \cdot g_s)^{-1/2}\right)} \ . \tag{6.134}$$

where $\mathrm{S} \cdot g_s$ is the new gauge coupling under the transformation $\tau \to -\frac{1}{4\tau}$, which reads explicitly

$$\mathrm{S} \cdot g_s = \frac{g_s^2\theta^2 + 16\pi^4}{\pi^2 g_s} \ . \tag{6.135}$$

The unconventional negative power in the above two Padé approximant was devised in [196] to remove the $\theta$ dependence in the Taylor expansion. This is appropriate to match our perturbative expansion up to the order we are considering, because the $\theta$-dependence starts at the subleading order $g_s^3$. On the other hand, while the perturbative expansion of $\mathcal{N} = 4$ SYM is independent of $\theta$ to all orders in perturbation theory, and therefore in that context it is desirable to have an ansatz whose Taylor expansion does not contain $\theta$, in our setup observables do depend on $\theta$ even in perturbation theory. Indeed, by taking a different scaling such as $g_s$ small with $\gamma = \frac{\theta g_s}{4\pi^2}$ fixed, rather than $\theta$ fixed, we would have a non-trivial dependence on $\gamma$ already at the order we are considering, and with this scaling we could not match the observables with the Taylor expansion of the approximants

| | $2+\gamma_1$ | $3+\gamma_2$ | $f_\partial$ |
|---|---|---|---|
| $\epsilon$ expansion | 1.494 | — | 0.124 |
| Bootstrap | 1.5117(25) | — | — |
| $F_1(g_s=\infty,\theta=\pi)$ | 1.406 | 3.635 | 1.039 |
| $F_2(g_s=\infty,\theta=\pi)$ | 1.560 | 3.391 | 0.166 |

Table 6.1: Comparison of the extrapolations with the known data: for the energy operator we are quoting the value from the conformal bootstrap [6], and from the $\epsilon$-expansion [7]. For the sphere free energy we are comparing to the value from the $\epsilon$-expansion in [8].

(6.133)-(6.134). The upshot is that in order to use the duality-improved approximants from [196] we are forced to consider the expansion at small $g_s$ with $\theta$ fixed, and doing so we throw away some of the information contained in the perturbative calculation, namely the $\frac{g_s^2\gamma^2}{(1+\gamma^2)^2} = (2\pi)^2\frac{(\mathrm{Re}\tau)^2}{|\tau|^4}$ terms. It would be desirable to find an ansatz that is: (i) duality invariant; (ii) has a final limit to the real $\tau$ axis (or at least to the $O(2)$ cusp); and (iii) can be matched with the perturbative expansion at small $g_s$ and $\gamma$ fixed (at least up to the order $g_s^2$ at which the observables are currently known).

By matching the coefficients in the expansion up to the order $g_s^2$, we find the unknown coefficients $h_i$ to be

$$h_1 = a, \quad h_2 = b, \quad h_3 = a, \quad h_4 = \frac{1}{4\pi} - b \tag{6.136}$$

In the table 6.1 we show the resulting values of the approximant extrapolated at the $O(2)$ point. The fermion-mass operator is mapped to the energy operator of the $O(2)$ model, whose dimension can be obtained for instance from the conformal bootstrap [6], or from the $\epsilon$-expansion [7]. The spin 2 operator is expected to approach the conserved stress-energy tensor on the boundary in the decoupling limit, hence the dimension should approach the protected value $\Delta_2|_{\text{cusp}} = 3$. As for the hemisphere free energy, one needs to subtract a finite contribution coming from the decoupled gauge field at the $O(2)$ cusp, and the remaining constant gives the sphere free energy of the $O(2)$ model. To our knowledge, this has only been computed using $\epsilon$-expansion [8].

We see that both ansatzes give good approximations for the dimension of the energy operator, and in particular $F_2$ is quite close to the values obtained with the other methods. For the other two observables, we see that the ansatz $F_2$ also gives compatible results, while $F_1$ is not as good. In fig.6.10 we show the plots of the approximants at $\theta = \pi$, i.e. the value of the $O(2)$ cusp, as a function of $g_s$ from 0 to $\infty$.

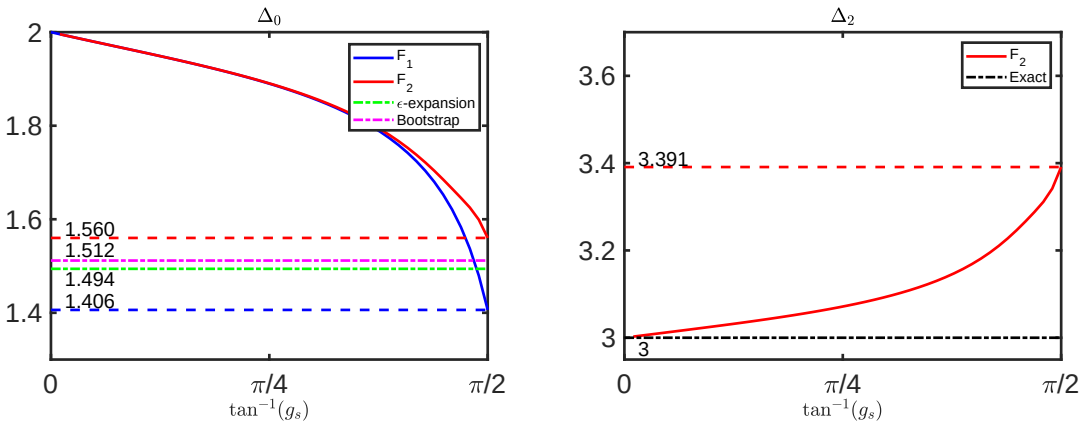


Figure 6.10: Extrapolations of the scaling dimensions from the Dirac fermion point ($\tan^{-1}(g_s) = 0$) to the $O(2)$ point ($\tan^{-1}(g_s) = \pi/2$).

## 6.4 Other Examples

### 6.4.1 $2N_f$ Dirac fermions at large $N_f$

In this section we consider the coupling of $2N_f$ Dirac fermions to the bulk gauge fields, all with the same charge $q = 1$, and we take the limit of large $N_f$ with $\lambda = g^2 N_f$ fixed. For simplicity we take $\theta = 0$. We will see that computing observables in $1/N_f$ expansion, and later taking the limit $\lambda \to \infty$, one can recover the $1/N_f$ expansion in QED$_3$. This would be the expected result if we would take $g^2 \to \infty$ first, obtaining the decoupling limit in which on the boundary we have QED$_3$ with $2N_f$ flavors, and later take $N_f$ large. Hence, the observation here is that these two limits commute. This is interesting because order by order in $1/N_f$ we can explicitly follow observables as exact functions of $\lambda$, and see how they interpolate from the "ungauged cusp" at $\lambda = 0$ to the "gauged cusp" at $\lambda = \infty$.

To derive that the limits commute, it is sufficient to observe that in the limit of large $N_f$ with $\lambda = g^2 N_f$ fixed we can obtain an effective propagator for the photon by resumming the fermionic bubbles, see Fig. 6.12, obtaining (up to gauge redundancy)

$$\Pi_{ab}^{(1/N_f)}(\vec{p}) = \frac{1}{N_f |\vec{p}|} \lambda \sum_{k=0}^{\infty} \left(-\frac{\lambda}{8}\right)^k \left(\delta_{ab} - \frac{p_a p_b}{\vec{p}^{\,2}}\right) \tag{6.137}$$

$$= \frac{8}{N_f |\vec{p}|} \frac{\lambda}{\lambda + 8} \left(\delta_{ab} - \frac{p_a p_b}{\vec{p}^{\,2}}\right) . \tag{6.138}$$

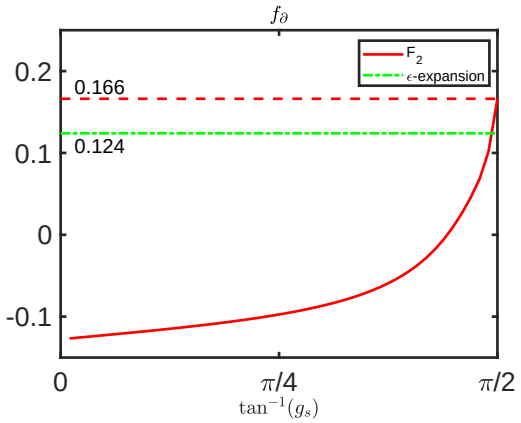


Figure 6.11: Extrapolations of the free energy from the Dirac fermion point ($\tan^{-1}(g_s) = 0$) to the $O(2)$ point ($\tan^{-1}(g_s) = \pi/2$).

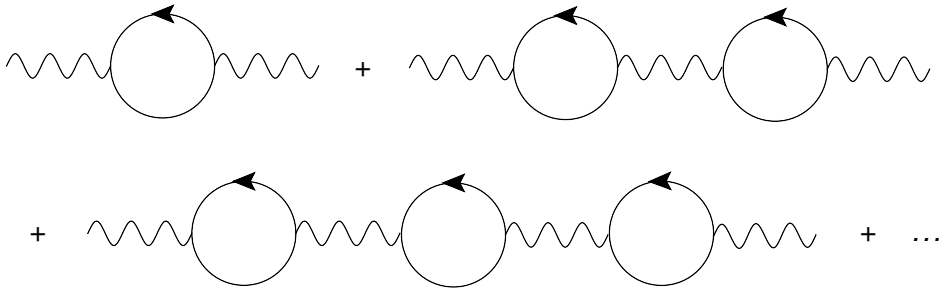

Figure 6.12: The diagrams that contribute to the boundary propagator of the photon in the limit $N_f \to \infty$ with $\lambda = g^2 N_f$ fixed.

In the limit $\lambda \to \infty$ the propagator becomes

$$\Pi_{ab}^{(1/N_f)}(\vec{p}) \underset{\lambda\to\infty}{\longrightarrow} \frac{8}{N_f|\vec{p}|}\left(\delta_{ab} - \frac{p_a p_b}{\vec{p}^{\,2}}\right) \ , \tag{6.139}$$

which coincides with the effective propagator in $\text{QED}_3$ at large $N_f$. It follows that compared to the large-$N_f$ expansion of $\text{QED}_3$, in this setup the diagrams that compute $1/N_f$ corrections are simply dressed by a factor $\lambda/(\lambda+8)$ for each photon propagator. In particular the $1/N_f$-expansion of observables, e.g. boundary scaling dimensions, will approach the corresponding value in large-$N_f$ $\text{QED}_3$ upon taking the limit $\lambda \to \infty$. However, recall that in the $1/N_f$-expansion diagrams that contribute at the same order might have different number of internal photon lines, so we cannot just replace $1/N_f$ with $1/N_f \times \lambda/(\lambda+8)$

everywhere to obtain the exact dependence on $\lambda$ of a certain observable.

Let us now consider the two-point function of the boundary current $\hat{J}$, and obtain from it the hemisphere free energy at large $N_f$. We can obtain the $1/N_f$ correction to the one-photon irreducible two-point function of $\hat{J}$ —computed by the diagrams in Fig. 6.9 with the effective photon propagator (6.138)— by taking the result of the large-$N_f$ calculation in [62] and dressing it by the factor due to the single photon propagator, with the result

$$c_\Sigma = \frac{N_f}{4\pi^2}\left(1 + \frac{1}{N_f}\frac{\lambda}{\lambda+8}\frac{184-18\pi^2}{9\pi^2} + \mathcal{O}\left(N_f^{-2}\right)\right) . \tag{6.140}$$

Correspondingly, from equation (E.31) and (E.35) we have $c_{12} = 0$ and

$$c_{22} = \frac{16}{\pi^2 N_f}\frac{\lambda}{\lambda+8} - \frac{32\,(92-9\pi^2)}{9\pi^4 N_f^2}\frac{\lambda^3}{(\lambda+8)^3} + \mathcal{O}\left(N_f^{-3}\right) . \tag{6.141}$$

We can now plug $c_{22}$ in the differential equation (6.96), appropriately rewritten in terms of the variable $\lambda$. Solving for $F_\partial(\lambda)$ up to the order $1/N_f$ we find

$$F_\partial(\lambda) = \frac{1}{4}\log\left[\frac{\pi N_f(\lambda+8)^2}{64\lambda}\right] + 2N_f F_{\text{Dirac}} + \frac{(92-9\pi^2)}{18\pi^2 N_f}\frac{\lambda^2}{(\lambda+8)^2} + \mathcal{O}\left(N_f^{-2}\right) . \tag{6.142}$$

Recall that the arbitrary integration constant is fixed by matching with the decoupling limit. In the decoupling limit $F_\partial$ is the sum of a contribution from the free fermions on the boundary, namely $2N_f F_{\text{Dirac}}$, and a contribution from the boundary value of the gauge field with Neumann condition, that we discussed in section 6.2. The latter contribution is only a function of $g^2$, and when rewritten in terms of $\lambda$ it gives a $\log(N_f)$ constant term. Hence we need to include such a dependence on $N_f$ in the integration constant, and this is how we obtain the $\log(N_f)$ term in (6.142). Similarly, we find that a $\lambda$-independent term of order $1/N_f$ needs to be included in the integration constant, to ensure that the $1/N_f$ correction vanishes when $\lambda = 0$. The general lesson here is that when we integrate the equation in the $\lambda$ variable, the integration constant required to reproduce the decoupling limit will be a non-trivial function of the parameter $N_f$.

From the $\lambda \to \infty$ limit of (6.142) we can extract the sphere free-energy $\text{QED}_3$ at large $N_f$. More specifically, the latter is obtained by subtracting to the $\lambda \to \infty$ limit of the free energy the contribution of the Neumann boundary condition of the bulk gauge field

computed at $(g')^2 = \frac{4\pi^2}{g^2}$, namely

$$F_{\text{QED}_3} = \lim_{\lambda\to\infty}\left(F_\partial(\lambda) + \frac{1}{4}\log\left[\frac{(g')^2}{\pi}\right]\Big|_{(g')^2=\frac{4\pi^2 N_f}{\lambda}}\right) \tag{6.143}$$

$$= 2N_f F_{\text{Dirac}} + \frac{1}{2}\log\left(\frac{\pi N_f}{4}\right) + \frac{92-9\pi^2}{18\pi^2}\frac{1}{N_f} + \mathcal{O}\left(N_f^{-2}\right) \ . \tag{6.144}$$

Both the logarithmic and the constant terms reproduce perfectly the result of [197]. To our knowledge, the $\mathcal{O}\left(N_f^{-1}\right)$ correction was not computed before.

As we will now briefly review, the free-energy as a function of $N_f$ can be used to diagnose the IR fate of $\text{QED}_3$. For $N_f$ smaller than a critical value $N_f^c$ the theory is conjectured to flow to a flavor-symmetry breaking phase rather than to the conformal phase that exists at large $N_f$. A possible scenario for the transition is that the IR scaling dimension of singlet four-fermion operators would cross marginality [198, 54, 58], implying that the IR fixed point that exists at large $N_f$ merges at $N_f = N_f^c$ with a second fixed point in which the quartic operators are turned on, and they both disappear [55, 199]. After the transition they can still be interpreted as complex fixed points [200, 201]. This scenario was recently investigated in [65, 66] using large $N_f$ techniques and in [202] using the conformal bootstrap. This merger/annihilation scenario, together with the monotonicity of the sphere free-energy along RG, was used in [55] to constrain $N_f^c$: assuming that $F_{\text{QED}_3}$ can still be interpreted as the free-energy of the nearby complex fixed point when $N_f < N_f^c$, the existence of the RG flow from the vicinity of the complex fixed point towards the symmetry breaking phase requires that $F_{\text{QED}_3} > F_{\text{G.B.}}$ for $N_f < N_f^c$. Here $F_{\text{G.B.}} = (2N_f^2+1)F_{\text{scalar}}$ is the free energy of the Goldstone bosons in the symmetry-breaking phase. As an application of the calculation above, we can now run this argument using the large-$N_f$ approximation for $F_{\text{QED}_3}$ in eq. (6.144). It turns out that the coefficient of the $1/N_f$ term is numerically very small, i.e. $\sim 0.02$, so for the interesting values of $N_f$ of order 1 it does not affect significantly this test, and the resulting estimate is $N_f^c \sim 4.4$. For this value of $N_f$, the $1/N_f^2$ corrections that we are neglecting in (6.144) are quite small, and assuming that the smallness of the coefficients persists at higher orders this suggests that the estimate might be reliable.

### 6.4.2 Complex Scalar

In section 6.3 we studied the case of a free fermion on the boundary, and we saw that one of the gauged cusps corresponds to the $O(2)$ Wilson-Fisher model. This is a consequence of the boson/fermion dualities that relate a gauged fermion to a critical scalar, or a gauged critical

scalar to a free fermion [70]. These dualities can be seen as the low-rank analog of the large-$N$ regular fermion/critical scalar dualities in CS-matter theories [203, 204, 205, 75]. Besides the Wilson-Fisher fixed point, the scalars also admit the Gaussian fixed point consisting of $N$ free complex scalars. Likewise, the theory of $N$ Dirac fermions is conjectured to have a second fixed point with quartic interactions turned on, i.e. the UV fixed point of the Gross-Neveu model. The corresponding CS-matter theories are also conjectured to be dual in a level-rank duality fashion, giving the so-called regular boson/critical fermion duality. There is a large amount of evidence for this duality at large $N$, and its extension to finite $N$ was recently studied in [206, 207]. It is not clear whether the duality still holds when $N = 1$. Assuming it does, it would have a nice manifestation in our setup: by starting with a free complex scalar on the boundary, one would find that the cusp at $\tau = 1$ corresponds to the Gross-Neveu CFT with 1 Dirac fermion.[9] One crucial new ingredient of the regular boson/critical fermion dualities is the existence of additional sextic couplings that are classically marginal and potentially lead to multiple fixed points that can be mapped across the duality.

With this motivation in mind, we will now consider the setup with a free complex scalar on the boundary, coupled to the bulk gauge field. The action is

$$S[A,\tau] + \int_{y=0} d^3\vec{x}\, \left(|D_A\phi|^2 + \rho(|\phi|^2)^3\right) . \tag{6.145}$$

The couplings $|\phi|^2$ and $|\phi|^4$ are fine-tuned to zero. This fine-tuning might need to be adjusted as a function of the bulk gauge coupling. At least for $\tau$ large enough, these operators are relevant and correspondingly the beta function is linear in the couplings, so this adjustment is possible. On the other hand, the beta function for the classically marginal operator $|\phi|^6$ will start quadratically in $\rho$ and we need to check the existence of (real) fixed points.

We list the Feynman rules in the Fig. 6.13.

To compute the $\beta$ function of $\rho$ we need to renormalize the six-point vertex. We use the same approach as in the fermion case, i.e. we dimensionally regularize by continuing the dimension of the boundary to $d = 3 - 2\epsilon$, keeping the codimension fixed $= 1$. The boundary action in renormalized variables is

$$\int_{y=0} d^d\vec{x}\, |D\phi_B|^2 + \rho_B|\phi_B|^6 = \int_{y=0} d^d\vec{x}\, Z_\phi^2|D\phi|^2 + Z_\rho\rho\mu^{4\epsilon}|\phi|^6 , \tag{6.146}$$

[9]The Gross-Neveu CFT is expected to exist also for a small number $N$ of Dirac fermion, the UV completion being provided by a Yukawa theory. See [208] for a recent study in $\epsilon$-expansion.

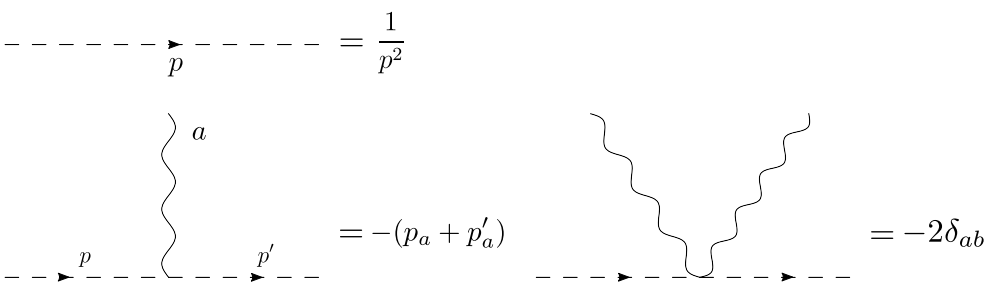


Figure 6.13: Feynman rules with the complex scalar on the boundary

where the subscript $B$ denotes the bare variables. Fig. 6.14 shows the diagrams that contribute to the wavefunction renormalization of the field $\phi$, from which we obtain

$$\delta Z_\phi = -\frac{(3\xi - 8)}{24\pi^2\epsilon}\frac{g^2}{1+\gamma^2} + \mathcal{O}(g^4) \ . \tag{6.147}$$

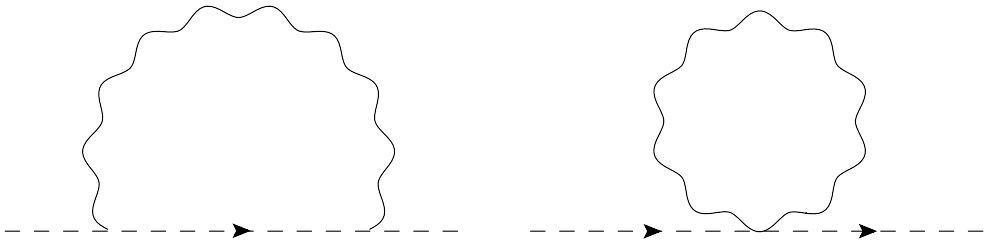

Figure 6.14: One loop diagrams that contribute to the wave-function renormalization.

There are three types of diagram contributing to the six-point vertex counterterm, showed in Fig. 6.15 and 6.16, from which we can compute

$$\rho\delta Z_\rho = \frac{21}{8\pi^2\epsilon}\rho^2 - \frac{3}{4\pi^2\epsilon}\frac{g^2}{1+\gamma^2}\xi\,\rho - \frac{24(1-3\gamma^2)}{\pi^2\epsilon}\left(\frac{g^2}{1+\gamma^2}\right)^3 + \mathcal{O}(\rho^3, \rho^2 g^2, \rho g^4, g^8) \ . \tag{6.148}$$

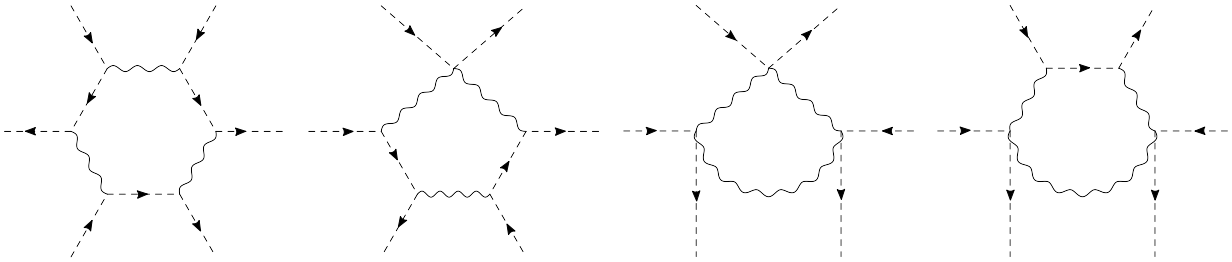

Figure 6.15: Diagrams contributing to $\mathcal{O}(g^6)$ in $\beta_\rho$.

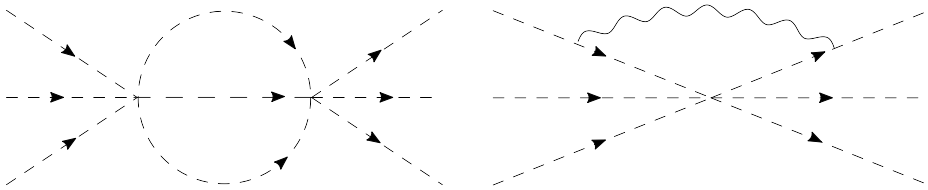

Figure 6.16: Diagrams contributing to $\mathcal{O}(\rho^2)$ and $\mathcal{O}(\rho g^2)$ in $\beta_\rho$.

The $\beta$ function is

$$\beta_\rho(\rho, g) = \left(-4\epsilon\rho - \rho\frac{\partial \log Z_\rho/Z_\phi^6}{\partial \log \mu}\right)\Big|_{\epsilon=0} \tag{6.149}$$

$$= \frac{21}{2\pi^2}\rho^2 - \frac{4}{\pi^2}\rho\frac{g^2}{1+\gamma^2} - \frac{48(1-3\gamma^2)}{\pi^2}\left(\frac{g^2}{1+\gamma^2}\right)^3 + \mathcal{O}(\rho^3, \rho^2 g^2, \rho g^4, g^8)\ . \tag{6.150}$$

Up to this order we find: a zero at $\rho = \rho_*^+ > 0$ from the first two terms, and since $\rho_*^+ = \mathcal{O}(g^2)$ the third term is negligible; and a zero at $\rho = \rho_*^-$ from the second and the third therm, and since $\rho_*^- = \mathcal{O}(g^4)$ the first term is negligible. The positions of the zeroes are

$$\rho_*^+ = \frac{8}{21}\frac{g^2}{1+\gamma^2} + \mathcal{O}(g^4)\ , \qquad \rho_*^- = -12(1-3\gamma^2)\left(\frac{g^2}{1+\gamma^2}\right)^2 + \mathcal{O}(g^6)\ . \tag{6.151}$$

The derivative of $\beta_\rho$ is positive at $\rho_*^+$ and negative at $\rho_*^-$. Hence we have found that perturbatively around large $\tau$ there exists a fixed point $\rho = \rho_*^+$ which is IR stable and gives a scalar potential bounded from below. The fixed point $\rho_*^-$ on the other hand is only physical for $1 - 3\gamma^2 < 0$, because otherwise it gives the wrong sign of the scalar potential, and it is unstable in the RG sense.

Having checked the existence of the fixed point in perturbation theory, we proceed to consider the anomalous dimension of boundary operators in this theory, similarly to what we did in section (6.3.1) for the fermion case. We consider the mass-squared operator $O = |\phi|^2$. Its anomalous dimension can be obtained from the renormalization of the 1PI correlator of the composite operator with two elementary fields

$$\langle O(q=0)\phi(-p)\bar{\phi}(p)\rangle_{1\text{PI}} \ . \tag{6.152}$$

The one-loop (two-loop) diagrams contributing to the three-point function (6.152) are showed in Fig.6.14 (Fig.6.17, respectively).

At one loop, using (6.147), the renormalization constant of the operator is found to be

$$\delta Z_O = -\frac{2}{3\pi^2\epsilon}\frac{g^2}{1+\gamma^2} + \mathcal{O}(g^4) \ , \tag{6.153}$$

and correspondingly the anomalous dimension is

$$\gamma_O = -\frac{4}{3\pi^2}\frac{g^2}{1+\gamma^2} + \mathcal{O}(g^4) \ . \tag{6.154}$$

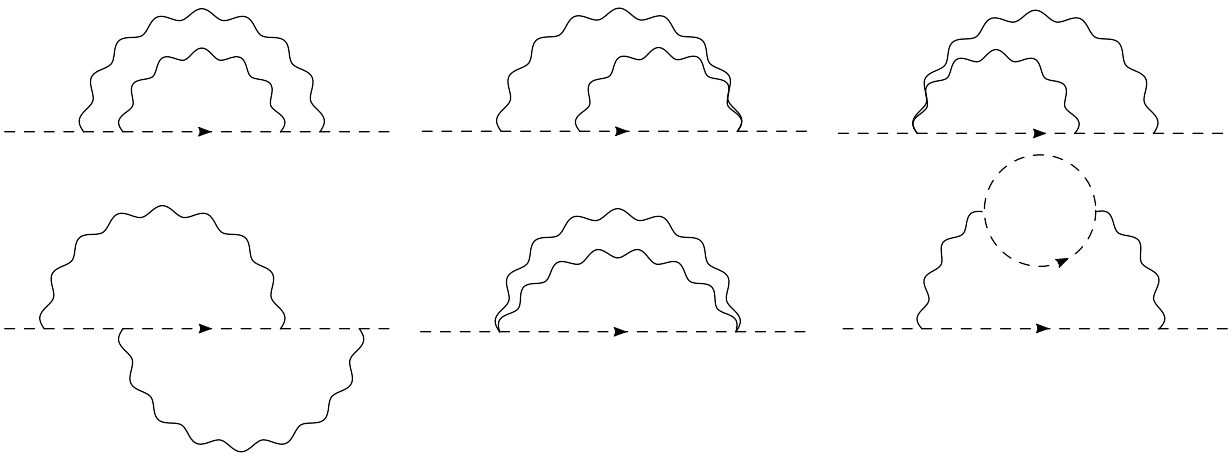

Figure 6.17: One loop and two loops diagrams

Differently from the fermion case, we were not able to evaluate all of the dimensionally regularized integrals coming from the two-loop diagrams of Fig. 6.17. See the appendix E.7 for the details. Knowing the two-loop anomalous dimension would enable extrapolation

to $\tau = 1$ that could be compared with the known estimates of the mass operator in the Gross-Neveu CFT. This is therefore an interesting direction left for the future.

### 6.4.3 $QED_3$ with Two Flavors

In this section, we will discuss a realization in our setup of $QED_3$ coupled to two Dirac (complex two-component) fermions of charge 1. There are several reasons why this is an interesting theory: it is conjectured to describe the easy-plane version of the "deconfined" Néel-VBS quantum phase transition in antiferromagnets [209], and enjoy an emergent $O(4)$ symmetry [210, 211]; while initially believed to be a second-order transition, recent evidence from simulations of the spin system on the lattice [212] and from the conformal bootstrap [213] suggest that this is actually a weakly first-order transition, which can still be compatible with the QED description if the latter has a complex fixed point with $O(4)$ symmetry (see section 5 of [201] and [65]); it is conjectured to enjoy a self-duality [210, 211, 214, 76] and a fermion-boson duality [215].

A simple way to realize QED with two flavors in our setup would be to put the CFT of two Dirac fermions on the boundary, and couple a bulk gauge field to the $U(1)$ symmetry that gives charge 1 to both of them. However in this case we only expect a weakly coupled cusp at $\tau \to \infty$. For the purpose of attempting an extrapolation from weak coupling, it would be desirable to have additional weakly coupled cusps, as in the example of section 6.3. With this idea in mind, a more promising approach is to consider a generalization of the former set-up in which we have two Maxwell gauge fields in the bulk and two Dirac fermions on the boundary, namely two decoupled copies of the theory of section 6.3. By performing an $S$-duality for either of the two gauge fields separately we find again two free Dirac fermions on the boundary. On the other hand, using the larger electric-magnetic duality group that exists for a theory of two gauge fields, we can also go to a duality frame where in the decoupling limit we have precisely QED with two flavors on the boundary.

In the rest of this section we will first review electric-magnetic duality for multiple Maxwell fields, and then show how to get QED with two flavors starting with two copies of a bulk gauge field coupled to a boundary Dirac fermion. The task of performing perturbative calculations of observables in this theory is left for the future.

#### Multiple Maxwell Fields

The action of free bulk $U(1)^n$ gauge theory is determined in terms of $n$ Abelian gauge fields $A^I$, such that $F^I = dA^I$ and an $n \times n$ symmetric matrix of complexified gauge couplings

$\tau_{IJ}$

$$S[A^I, \tau_{IJ}] = \int_{y\geq 0} d^4x \left( \frac{1}{4g_{IJ}^2} F^I_{\mu\nu} F^{J,\mu\nu} + \frac{i\theta_{IJ}}{32\pi^2} \epsilon_{\mu\nu\rho\sigma} F^{I,\mu\nu} F^{J,\rho\sigma} \right) \tag{6.155}$$

$$= -\frac{i}{8\pi} \int_{y\geq 0} d^4x (\tau_{IJ} F^{-I}_{\mu\nu} F^{-J,\mu\nu} - \bar{\tau}_{IJ} F^{+}_{I\mu\nu} F^{+J\mu\nu}), \tag{6.156}$$

where $\tau_{IJ} = \frac{\theta IJ}{2\pi} + \frac{2\pi i}{g_{IJ}^2}$ and we introduced $F^{\pm,I}_{\mu\nu} = \frac{1}{2}(F^I_{\mu\nu} \pm \frac{1}{2}\epsilon_{\mu\nu\rho\sigma} F^{I,\rho\sigma})$. This theory enjoys an $Sp(2n, \mathbb{Z})$ duality group

$$\tau'_{IJ} = (A^K_I \tau_{LM} + B_{IM})(C^{JN} \tau_{NM} + D^J_M)^{-1}, \tag{6.157}$$

where

$$M = \begin{pmatrix} A & B \\ C & D \end{pmatrix} \in Sp(2n, \mathbb{Z}) \ . \tag{6.158}$$

This duality group is generated by the three types of transformations obtained in [216, 217], which we reproduce here [10]

$$\text{T-type: } \begin{pmatrix} I & B \\ 0 & I \end{pmatrix}, \qquad \begin{array}{l} \text{where } I \text{ the } n \times n \text{ identity and } B \text{ is a symmetric} \\ \text{matrix that generates } \tau' = \tau + B, \end{array} \tag{6.159}$$

$$\text{S-type: } \begin{pmatrix} I - J & -J \\ J & I - J \end{pmatrix}, \qquad \begin{array}{l} \text{where } J = \text{diag}(j_1, j_2, \ldots, j_n) \text{ and } j_i \in \{0, 1\}. \\ \text{This gauges those } A_i\text{'s that have } j_i = 1. \end{array} \tag{6.160}$$

$$\text{GL-type: } \begin{pmatrix} U & 0 \\ 0 & U^{-1T} \end{pmatrix}, \qquad \text{where } U \in SL(n, \mathbb{Z}) \text{ generate the rotations } A' = U^{-1T} A. \tag{6.161}$$

In the rest of this section we will be focusing on the case of $n = 2$. Following [216] we

[10] More precisely, these elements generate $Sp(2n, \mathbb{Z})/\sim$, where we identify $S \sim -S$.

define the generators of $Sp(4,\mathbb{Z})$ as

$$T = \left(\begin{array}{cc|cc} 1 & & 1 & \\ & 1 & & 0 \\ \hline & & 1 & \\ \mathbf{0} & & & 1 \end{array}\right) , \qquad S = \left(\begin{array}{cc|cc} 0 & & -1 & \\ & 1 & & 0 \\ \hline 1 & & 0 & \\ & 0 & & 1 \end{array}\right) , \tag{6.162}$$

$$R_1 = \left(\begin{array}{cc|cc} & 1 & & \\ 1 & & & \\ \hline & & & 1 \\ \mathbf{0} & & 1 & \end{array}\right) , \qquad R_2 = \left(\begin{array}{cc|cc} 1 & 1 & & \\ 0 & 1 & & \\ \hline & & 1 & 0 \\ \mathbf{0} & & -1 & 1 \end{array}\right) . \tag{6.163}$$

Furthermore we use the succinct notation $S[1,0]$, $S[0,1]$ to denote the gauging of $A^1$, $A^2$ (respectively) and $T[m,n]$ for the introduction of the Chern-Simons terms $mA^1dA^1 + nA^2dA^2$.

### Targeting two-flavor QED

We now have all the tools to obtain two-flavor $\text{QED}_3$ via an $Sp(4,\mathbb{Z})$ action from a theory of two free fermions. The action of two-flavour $\text{QED}_3$ is [211][11]

$$S[A'^I, \tau'_{IJ}] + \int_{y=0} \left( i\bar{\psi}_1 \not{D}_a \psi_1 + i\bar{\psi}_2 \not{D}_{a+A'^1} \psi_2 + \frac{1}{4\pi} ada + \frac{1}{2\pi} adA'^2 - \frac{1}{4\pi} A'^2 dA'^2 \right) + 2\text{CS}_g \ , \tag{6.164}$$

where $A'^{I=1,2}$ are bulk U(1) gauge fields while $a$ is a 3d spin$_c$ connection. The gravitational term $\text{CS}_g$ is needed because

$$\int_{\partial M} \frac{1}{4\pi} ada + 2\text{CS}_g = 2\pi \int_M \left( -\frac{1}{48} \frac{\text{Tr}\, R \wedge R}{(2\pi)^2} + \frac{1}{8\pi^2} f \wedge f \right) \ , \tag{6.165}$$

[11] Here we are using a different charge normalization compared to [211]. For example, the lowest charged gauge invariant operator is the meson $\bar{\psi}_i \psi_j$, which has charge 1 under gauge field $A'_1$ in our case but charge 2 under the gauge field $X$ in [211]. Our choice is necessary if we want to start from (6.166), because $Sp(4,\mathbb{Z})$ respects the charge normalization. The difference between the charge-two theory and charge-one theory is that the former has fewer monopole operators. Starting with the charge-one theory, we can gauge $\mathbb{Z}_2 \subset U(1)_J$, where $U(1)_J$ is the magnetic $U(1)$ global symmetry. This has the effect of changing the gauge group $G = U(1)$ to $\tilde{G}$ such that $\tilde{G}/\mathbb{Z}_2 = G$. For example, in this case $G = U(1)$, and we gauge $\mathbb{Z}_2 \subset U(1)_J$, then the new gauge group is $\tilde{G} = U(1)$ but with the replacement of the gauge field $A_\mu \to 2A_\mu$, namely all the particle charges are multiplied by 2 [218, 9]. In this way, we obtain the charge-two theory.

which is well-defined for a spin$_c$ connection $a$.[12]

We want to target this action via an $Sp(4,\mathbb{Z})$ transformation from

$$S[A^I,\tau_{IJ}]+\int_{\partial M}(i\bar{\psi}_1\not{D}_{A^1}\psi_1+i\bar{\psi}_2\not{D}_{A^2}\psi_2)\ , \tag{6.166}$$

where $A^{I=1,2}$ are spin$_c$ connections. To this end, we can start from a rotation of the gauge fields by performing a GL-type transformation with

$$U=\begin{pmatrix}1&-1\\0&1\end{pmatrix}\ , \tag{6.167}$$

and then act with $T[1,0](-1)S[1,0]T[-1,0]$.[13] The resulting relation between $\tau$ and $\tau'$ is

$$\begin{pmatrix}\tau_{11}&\tau_{12}\\\tau_{21}&\tau_{22}\end{pmatrix}=\begin{pmatrix}-\tau'_{12}+\tau'_{22}-\frac{(\tau'_{12}+1)(-\tau'_{11}+\tau'_{21}+2)}{\tau'_{11}-1}&\frac{-\tau'_{12}(\tau'_{21}+1)+(\tau'_{11}-1)\tau'_{22}}{\tau'_{11}-1}\\\frac{-(\tau'_{12}+1)\tau'_{21}+(\tau'_{11}-1)\tau'_{22}}{\tau'_{11}-1}&\frac{(\tau'_{11}-1)\tau'_{22}-\tau'_{12}\tau'_{21}}{\tau'_{11}-1}\end{pmatrix}\ . \tag{6.168}$$

The decoupling limit of (6.164) is

$$\begin{pmatrix}\tau'_{11}&\tau'_{12}\\\tau'_{21}&\tau'_{22}\end{pmatrix}=\begin{pmatrix}\infty&0\\0&\infty\end{pmatrix}\ , \tag{6.169}$$

which according to (6.168) corresponds to

$$\begin{pmatrix}\tau_{11}&\tau_{12}\\\tau_{21}&\tau_{22}\end{pmatrix}=\begin{pmatrix}1+\infty&\infty\\\infty&\infty\end{pmatrix}\ , \tag{6.170}$$

by which we mean $\tau_{12}-\tau_{22}=\tau_{21}-\tau_{22}=\tau_{11}-1-\tau_{22}=0$ is satisfied while taking the limit $\tau_{22}\to\infty$.

Let us also write down explicitly the self-dualities of the theory (6.166).[14] Recall from section 6.3 that

$$S[A,\tau]+\int_{y=0}i\bar{\psi}\not{D}_A\psi\ , \tag{6.171}$$

[12] In the sense that this combination of boundary CS term is independent of the choices of different extensions of the boundary into bulk mod $2\pi\mathbb{Z}$

[13] We follow the notation in [70] that the minus sign in $S^2=-1$ denotes charge conjugation.

[14] Note that here we are not shifting the definition of the bulk coupling $\tau$ by $1/2$ as we did in (6.106). So the transformation is the same as the one presented in [70] instead of the transformation $\tau'=-1/4\tau$ that we had in the previous section.

and

$$S[A',\tau'] + \int_{y=0} i\bar{\chi}\not{D}_{A'}\chi \ , \tag{6.172}$$

are equivalent when $\tau' = ST^{-2}ST^{-1} \circ \tau = (\tau-1)/(2\tau-1)$. Applying this to either $A^1$ or $A^2$ in (6.166), we obtain that the decoupling limits in the two following duality frames also correspond to two free Dirac fermions

$$\tau''_{IJ} = S[1,0]T[-2,0]S[1,0]T[-1,0] \circ \tau_{IJ} \ , \tag{6.173}$$

$$\tau'''_{IJ} = S[0,1]T[0,-2]S[0,1]T[0,-1] \circ \tau_{IJ} \ . \tag{6.174}$$

Hence, in the variable $\tau_{IJ}$ the theory (6.166) has weakly coupled cusps at

$$\begin{pmatrix} \tau_{11} & \tau_{12} \\ \tau_{21} & \tau_{22} \end{pmatrix} = \begin{pmatrix} \infty & 0 \\ 0 & \infty \end{pmatrix} \ , \quad \begin{pmatrix} \pm\frac{1}{2} & 0 \\ 0 & \infty \end{pmatrix} \ , \quad \begin{pmatrix} \infty & 0 \\ 0 & \pm\frac{1}{2} \end{pmatrix} \ . \tag{6.175}$$

To summarize, we showed that the theory (6.166) of two bulk gauge fields coupled to two Dirac fermions has two additional duality frames (6.175) in which the boundary theory is still the free theory of two Dirac fermions, and a duality frame (6.170) in which the boundary theory is $\text{QED}_3$ with two flavors. Clearly, additional duality frames corresponding to $\text{QED}_3$ with two flavors can be obtained by applying the transformation (6.168) to either of the additional free-fermions points. This is a promising setup to study $\text{QED}_3$ with two flavors via extrapolation from the weakly-coupled points.

## 6.5 Conclusions and future directions

We conclude by discussing some directions for future investigation.

- A universal feature of the setup considered in this work is the existence of bulk line operators, whose endpoints may be attached to boundary charged operators. It is possible to assign conformal dimensions to the local operators at the location where the line defect ends on the boundary, and these dimensions can be computed perturbatively. Similarly to cusp anomalous dimensions, they are functions of the angle between the defect and the boundary. Starting with the dimensions of the endpoints of 't Hooft lines (and 't Hooft-Wilson lines) around $\tau \to \infty$ with a certain CFT on the boundary, it would be interesting to attempt an extrapolation to the cusps on the real axis, where they approach the dimensions of local monopole operators in the

gauged version of the initial CFT. Concretely, in the example of section 4, from the dimension of the endpoint of a 't Hooft line around the Dirac fermion point one can attempt to recover the scaling dimension of the spin operator of the $O(2)$ model.

- It would be interesting to perform perturbative calculations of anomalous dimensions and of the free energy in the theory with two bulk gauge fields presented in section 6.4.3, and attempt an extrapolation to $\text{QED}_3$ with two flavors. In particular, it is possible to use our setup to test whether this theory exists as a real CFT, by studying the dimension of four-fermion operators and checking whether they cross marginality before we reach the QED cusp, leading to the "phase-transition" described in section 6.1.5.

- In the model considered in section 6.3 we have only used the two-sided extrapolations to give estimates for the $O(2)$ model. However there are infinitely many other cusps on the real axis where strongly-coupled CFTs live, and they are of course amenable to the same extrapolation technique. These theories typically take the form of QED-CS theories, and they also describe interesting phase transitions [219]. A direction for the future would be to use our method to give estimates for the observables of these theories.

- Finally, dualities analogous to the one considered in this work exist for $\mathcal{N} = 2$ gauge theory. One of the simplest examples is the so-called triality [220, 221, 222, 223] generated by $ST$ transformation [217, 224], with $(ST)^3 = 1$. It would be interesting to see how the triality can improve the extrapolation. Thanks to supersymmetric localization the boundary free energy and dimensions of chiral endpoints of line operators are exactly computable [181]. For many other interesting observables, such as the conformal dimensions of operators analogous to $O_0$, which are non-protected, one has to resort to Feynman diagrams.

# References


[1] D. Gaiotto, J. H. Lee, and J. Wu, *Integrable Kondo problems*, arXiv:2003.06694.

[2] D. Gaiotto, J. H. Lee, B. Vicedo, and J. Wu, *Kondo line defects and affine Gaudin models*, arXiv:2010.07325.

[3] L. Di Pietro, D. Gaiotto, E. Lauria, and J. Wu, *3d Abelian Gauge Theories at the Boundary*, *JHEP* **05** (2019) 091, [arXiv:1902.09567].

[4] M. Nakagawa, N. Kawakami, and M. Ueda, *Non-hermitian kondo effect in ultracold alkaline-earth atoms*, *Physical Review Letters* **121** (Nov, 2018).

[5] E. Witten, *SL(2,Z) action on three-dimensional conformal field theories with Abelian symmetry*, hep-th/0307041.

[6] F. Kos, D. Poland, D. Simmons-Duffin, and A. Vichi, *Bootstrapping the O(N) Archipelago*, *JHEP* **11** (2015) 106, [arXiv:1504.07997].

[7] H. Kleinert, J. Neu, V. Schulte-Frohlinde, K. G. Chetyrkin, and S. A. Larin, *Five loop renormalization group functions of O(n) symmetric phi**4 theory and epsilon expansions of critical exponents up to epsilon**5*, *Phys. Lett.* **B272** (1991) 39–44, [hep-th/9503230]. [Erratum: Phys. Lett.B319,545(1993)].

[8] L. Fei, S. Giombi, I. R. Klebanov, and G. Tarnopolsky, *Generalized $F$-Theorem and the $\epsilon$ Expansion*, *JHEP* **12** (2015) 155, [arXiv:1507.01960].

[9] D. Gaiotto, A. Kapustin, N. Seiberg, and B. Willett, *Generalized Global Symmetries*, *JHEP* **02** (2015) 172, [arXiv:1412.5148].

[10] J. Kondo, *Resistance Minimum in Dilute Magnetic Alloys*, *Prog. Theor. Phys.* **32** (1964), no. 1 37–49.

[11] K. G. Wilson, *The Renormalization Group: Critical Phenomena and the Kondo Problem*, *Rev. Mod. Phys.* **47** (1975) 773.

[12] V. M. Filyov and P. B. Wiegmann, *A method for solving the Kondo problem*, *Physics Letters A* **76** (Mar., 1980) 283–286.

[13] N. Andrei, *Diagonalization of the Kondo Hamiltonian*, *Phys. Rev. Lett.* **45** (1980) 379.

[14] A. Tsvelick and P. Wiegmann, *Exact solution of the multichannel kondo problem, scaling, and integrability*, *Journal of Statistical Physics* **38** (1985), no. 1-2 125–147.

[15] N. Andrei and C. Destri, *Solution of the multichannel kondo problem*, *Phys. Rev. Lett.* **52** (Jan, 1984) 364–367.

[16] N. Andrei, K. Furuya, and J. Lowenstein, *Solution of the Kondo Problem*, *Rev. Mod. Phys.* **55** (1983) 331.

[17] A. M. Tsvelick and P. B. Wiegmann, *Exact results in the theory of magnetic alloys*, *Advances in Physics* **32** (Jan., 1983) 453–713.

[18] D. L. Cox and A. Zawadowski, *Exotic Kondo Effects in Metals: Magnetic Ions in a Crystalline Electric Field and Tunneling Centers*, *arXiv:cond-mat/9704103* (Aug., 1997) [cond-mat/9704103].

[19] J. L. Cardy, *Boundary Conditions, Fusion Rules and the Verlinde Formula*, *Nucl. Phys.* **B324** (1989) 581–596.

[20] I. Affleck and A. W. W. Ludwig, *The Kondo effect, conformal field theory and fusion rules*, *Nucl. Phys.* **B352** (1991) 849–862.

[21] I. Affleck and A. W. W. Ludwig, *Critical theory of overscreened Kondo fixed points*, *Nucl. Phys.* **B360** (1991) 641–696.

[22] I. Affleck, *Conformal field theory approach to the Kondo effect*, *Acta Phys. Polon.* **B26** (1995) 1869–1932, [cond-mat/9512099].

[23] P. Fendley, F. Lesage, and H. Saleur, *A Unified framework for the Kondo problem and for an impurity in a Luttinger liquid*, *J. Statist. Phys.* **85** (1996) 211, [cond-mat/9510055].

[24] C. Bachas and M. Gaberdiel, *Loop Operators and the Kondo Problem*, *Journal of High Energy Physics* **2004** (Nov., 2004) 065–065, [hep-th/0411067].

[25] R. Konik and A. LeClair, *Purely transmitting defect field theories*, *Nucl. Phys.* **B538** (1999) 587–611, [hep-th/9703085].

[26] V. V. Bazhanov, S. L. Lukyanov, and A. B. Zamolodchikov, *Integrable structure of conformal field theory, quantum KdV theory and thermodynamic Bethe ansatz*, *Commun. Math. Phys.* **177** (1996) 381–398, [hep-th/9412229].

[27] V. V. Bazhanov, S. L. Lukyanov, and A. B. Zamolodchikov, *Integrable structure of conformal field theory. 2. Q operator and DDV equation*, *Commun. Math. Phys.* **190** (1997) 247–278, [hep-th/9604044].

[28] I. Runkel, *Perturbed Defects and T-Systems in Conformal Field Theory*, *J. Phys.* **A41** (2008) 105401, [arXiv:0711.0102].

[29] K. Costello, *Supersymmetric gauge theory and the Yangian*, arXiv:1303.2632.

[30] K. Costello, *Integrable lattice models from four-dimensional field theories*, *Proc. Symp. Pure Math.* **88** (2014) 3–24, [arXiv:1308.0370].

[31] K. Costello, E. Witten, and M. Yamazaki, *Gauge Theory and Integrability, I*, arXiv:1709.09993.

[32] K. Costello, E. Witten, and M. Yamazaki, *Gauge Theory and Integrability, II*, arXiv:1802.01579.

[33] K. Costello and M. Yamazaki, *Gauge Theory And Integrability, III*, arXiv:1908.02289.

[34] K. Costello and J. Yagi, *Unification of integrability in supersymmetric gauge theories*, arXiv:1810.01970.

[35] B. Vicedo, *Holomorphic Chern-Simons theory and affine Gaudin models*, arXiv:1908.07511.

[36] F. Delduc, S. Lacroix, M. Magro, and B. Vicedo, *A unifying 2d action for integrable $\sigma$-models from 4d Chern-Simons theory*, arXiv:1909.13824.

[37] P. Dorey and R. Tateo, *Anharmonic oscillators, the thermodynamic Bethe ansatz, and nonlinear integral equations*, *Journal of Physics A: Mathematical and General* **32** (Sept., 1999) L419–L425, [hep-th/9812211].

[38] P. Dorey and R. Tateo, *On the relation between Stokes multipliers and the T-Q systems of conformal field theory*, *Nuclear Physics B* **563** (Dec., 1999) 573–602, [hep-th/9906219].

[39] V. V. Bazhanov, S. L. Lukyanov, and A. B. Zamolodchikov, *Higher-level eigenvalues of Q-operators and Schroedinger equation*, *arXiv:hep-th/0307108* (July, 2003) [hep-th/0307108].

[40] V. Bazhanov, S. Lukyanov, and A. Zamolodchikov, *Spectral determinants for Schroedinger equation and Q-operators of Conformal Field Theory*, *Journal of Statistical Physics* **102** (2001), no. 3/4 567–576, [hep-th/9812247].

[41] V. Bazhanov, S. Lukyanov, and A. Zamolodchikov, *Integrable Structure of Conformal Field Theory, Quantum KdV Theory and Thermodynamic Bethe Ansatz*, *Communications in Mathematical Physics* **177** (Apr., 1996) 381–398, [hep-th/9412229].

[42] V. Bazhanov, S. Lukyanov, and A. Zamolodchikov, *Integrable Structure of Conformal Field Theory II. Q-operator and DDV equation*, *Communications in Mathematical Physics* **190** (Dec., 1997) 247–278, [hep-th/9604044].

[43] V. V. Bazhanov, S. L. Lukyanov, and A. B. Zamolodchikov, *Integrable Structure of Conformal Field Theory III. The Yang-Baxter Relation*, *Communications in Mathematical Physics* **200** (Feb., 1999) 297–324, [hep-th/9805008].

[44] P. Dorey, C. Dunning, and R. Tateo, *The ODE/IM Correspondence*, *Journal of Physics A: Mathematical and Theoretical* **40** (Aug., 2007) R205–R283, [hep-th/0703066].

[45] S. L. Lukyanov, *Notes on parafermionic QFT's with boundary interaction*, *Nuclear Physics B* **784** (Nov., 2007) 151–201, [hep-th/0606155].

[46] D. Gaiotto and E. Witten, *Supersymmetric Boundary Conditions in N=4 Super Yang-Mills Theory*, *J. Statist. Phys.* **135** (2009) 789–855, [arXiv:0804.2902].

[47] S. Teber, *Electromagnetic current correlations in reduced quantum electrodynamics*, *Phys. Rev.* **D86** (2012) 025005, [arXiv:1204.5664].

[48] A. V. Kotikov and S. Teber, *Note on an application of the method of uniqueness to reduced quantum electrodynamics*, *Phys. Rev.* **D87** (2013), no. 8 087701, [arXiv:1302.3939].

[49] S. Teber and A. V. Kotikov, *Interaction corrections to the minimal conductivity of graphene via dimensional regularization*, *EPL* **107** (2014), no. 5 57001, [arXiv:1407.7501].

[50] S. Teber and A. V. Kotikov, *The method of uniqueness and the optical conductivity of graphene: New application of a powerful technique for multiloop calculations*, *Theor. Math. Phys.* **190** (2017), no. 3 446–457, [arXiv:1602.01962]. [Teor. Mat. Fiz.190,no.3,519(2017)].

[51] A. V. Kotikov and S. Teber, *Critical behaviour of reduced $QED_{4,3}$ and dynamical fermion gap generation in graphene*, *Phys. Rev.* **D94** (2016), no. 11 114010, [arXiv:1610.00934].

[52] C. P. Herzog and K.-W. Huang, *Boundary Conformal Field Theory and a Boundary Central Charge*, *JHEP* **10** (2017) 189, [arXiv:1707.06224].

[53] D. Dudal, A. J. Mizher, and P. Pais, *On the exact quantum scale invariance of three-dimensional reduced QED theories*, arXiv:1808.04709.

[54] L. Di Pietro, Z. Komargodski, I. Shamir, and E. Stamou, *Quantum Electrodynamics in $d = 3$ from the $\epsilon$ Expansion*, *Phys. Rev. Lett.* **116** (2016), no. 13 131601, [arXiv:1508.06278].

[55] S. Giombi, I. R. Klebanov, and G. Tarnopolsky, *Conformal $QED_d$, $F$-Theorem and the $\epsilon$ Expansion*, *J. Phys.* **A49** (2016), no. 13 135403, [arXiv:1508.06354].

[56] S. M. Chester, M. Mezei, S. S. Pufu, and I. Yaakov, *Monopole operators from the $4 - \epsilon$ expansion*, *JHEP* **12** (2016) 015, [arXiv:1511.07108].

[57] L. Janssen and Y.-C. He, *Critical behavior of the $QED_3$-Gross-Neveu model: Duality and deconfined criticality*, *Phys. Rev.* **B96** (2017), no. 20 205113, [arXiv:1708.02256].

[58] L. Di Pietro and E. Stamou, *Scaling dimensions in $QED_3$ from the $\epsilon$-expansion*, *JHEP* **12** (2017) 054, [arXiv:1708.03740].

[59] L. Di Pietro and E. Stamou, *Operator mixing in the $\boldsymbol{\epsilon}$-expansion: Scheme and evanescent-operator independence*, *Phys. Rev.* **D97** (2018), no. 6 065007, [arXiv:1708.03739].

[60] Y. Ji and A. N. Manashov, *Operator mixing in fermionic CFTs in noninteger dimensions*, *Phys. Rev.* **D98** (2018), no. 10 105001, [arXiv:1809.00021].

[61] N. Zerf, P. Marquard, R. Boyack, and J. Maciejko, *Critical behavior of the $QED_3$-Gross-Neveu-Yukawa model at four loops*, *Phys. Rev.* **B98** (2018), no. 16 165125, [arXiv:1808.00549].

[62] S. Giombi, G. Tarnopolsky, and I. R. Klebanov, *On $C_J$ and $C_T$ in Conformal QED*, *JHEP* **08** (2016) 156, [arXiv:1602.01076].

[63] S. M. Chester, L. V. Iliesiu, M. Mezei, and S. S. Pufu, *Monopole Operators in $U(1)$ Chern-Simons-Matter Theories*, *JHEP* **05** (2018) 157, [arXiv:1710.00654].

[64] J. A. Gracey, *Fermion bilinear operator critical exponents at $O(1/N^2)$ in the QED-Gross-Neveu universality class*, *Phys. Rev.* **D98** (2018), no. 8 085012, [arXiv:1808.07697].

[65] S. Benvenuti and H. Khachatryan, *QED's in 2+1 dimensions: complex fixed points and dualities*, arXiv:1812.01544.

[66] S. Benvenuti and H. Khachatryan, *Easy-plane $QED_3$'s in the large $N_f$ limit*, arXiv:1902.05767.

[67] R. Boyack, A. Rayyan, and J. Maciejko, *Deconfined criticality in the $QED_{3}$-Gross-Neveu-Yukawa model: the $1/N$ expansion revisited*, *arXiv e-prints* (Dec, 2018) arXiv:1812.02720, [arXiv:1812.02720].

[68] R. Boyack, C.-H. Lin, N. Zerf, A. Rayyan, and J. Maciejko, *Transition between algebraic and $\mathbb{Z}_2$ quantum spin liquids at large $n$*, *Phys. Rev. B* **98** (Jul, 2018) 035137.

[69] J. A. Gracey, *Large $N_f$ quantum field theory*, *Int. J. Mod. Phys.* **A33** (2019), no. 35 1830032, [arXiv:1812.05368].

[70] N. Seiberg, T. Senthil, C. Wang, and E. Witten, *A Duality Web in 2+1 Dimensions and Condensed Matter Physics*, *Annals Phys.* **374** (2016) 395–433, [arXiv:1606.01989].

[71] M. A. Metlitski and A. Vishwanath, *Particle-vortex duality of two-dimensional Dirac fermion from electric-magnetic duality of three-dimensional topological insulators*, *Phys. Rev.* **B93** (2016), no. 24 245151, [arXiv:1505.05142].

[72] C. Wang and T. Senthil, *Dual Dirac Liquid on the Surface of the Electron Topological Insulator*, *Phys. Rev.* **X5** (2015), no. 4 041031, [arXiv:1505.05141].

[73] W.-H. Hsiao and D. T. Son, *Duality and universal transport in mixed-dimension electrodynamics*, *Phys. Rev.* **B96** (2017), no. 7 075127, [arXiv:1705.01102].

[74] W.-H. Hsiao and D. T. Son, *Self-Dual $\nu = 1$ Bosonic Quantum Hall State in Mixed Dimensional QED*, arXiv:1809.06886.

[75] O. Aharony, *Baryons, monopoles and dualities in Chern-Simons-matter theories*, *JHEP* **02** (2016) 093, [arXiv:1512.00161].

[76] A. Karch and D. Tong, *Particle-Vortex Duality from 3d Bosonization*, *Phys. Rev.* **X6** (2016), no. 3 031043, [arXiv:1606.01893].

[77] B. Rosenstein, B. Warr, and S. H. Park, *Dynamical symmetry breaking in four Fermi interaction models*, *Phys. Rept.* **205** (1991) 59–108.

[78] J. Zinn-Justin, *Four fermion interaction near four-dimensions*, *Nucl. Phys.* **B367** (1991) 105–122.

[79] T. Aoki, T. Kawai, S. Sasaki, A. Shudo, and Y. Takei, *Virtual turning points and bifurcation of stokes curves for higher order ordinary differential equations*, *Journal of Physics A: Mathematical and General* **38** (2005), no. 15 3317.

[80] H. Dillinger, E. Delabaere, and F. Pham, *Résurgence de voros et périodes des courbes hyperelliptiques*, *Annales de l'Institut Fourier* **43** (1993), no. 1 163–199.

[81] A. Voros, *The return of the quartic oscillator. the complex wkb method*, *Annales de l'I.H.P. Physique théorique* **39** (1983), no. 3 211–338.

[82] H. J. Silverstone, *Jwkb connection-formula problem revisited via borel summation*, *Physical review letters* **55** (1985), no. 23 2523.

[83] T. Kawai and Y. Takei, *Algebraic analysis of singular perturbation theory*, vol. 227. American Mathematical Soc., 2005.

[84] Y. Takei, *Wkb analysis and stokes geometry of differential equations*, in *Analytic, algebraic and geometric aspects of differential equations*, pp. 263–304. Springer, 2017.

[85] K. Iwaki and T. Nakanishi, *Exact wkb analysis and cluster algebras*, *Journal of Physics A: Mathematical and Theoretical* **47** (2014), no. 47 474009.

[86] R. Balian, G. Parisi, and A. Voros, *Quartic oscillator*, in *Feynman Path Integrals* (S. Albeverio, P. Combe, R. Høegh-Krohn, G. Rideau, M. Sirugue-Collin, M. Sirugue, and R. Stora, eds.), (Berlin, Heidelberg), pp. 337–360, Springer Berlin Heidelberg, 1979.

[87] A. Voros, *Spectre de l'équation de Schrödinger et méthode BKW*. Université de Paris-Sud. Département de Mathématique, 1982.

[88] D. Gaiotto, G. W. Moore, and A. Neitzke, *Wall-crossing, Hitchin Systems, and the WKB Approximation*, arXiv:0907.3987.

[89] D. Gaiotto, G. W. Moore, and A. Neitzke, *Spectral networks*, *Annales Henri Poincare* **14** (2013) 1643–1731, [arXiv:1204.4824].

[90] C. Bachas and M. Gaberdiel, *Loop operators and the Kondo problem*, *JHEP* **11** (2004) 065, [hep-th/0411067].

[91] A. Klümper and P. A. Pearce, *Conformal weights of rsos lattice models and their fusion hierarchies*, *Physica A: Statistical Mechanics and its Applications* **183** (1992), no. 3 304 – 350.

[92] R. J. Baxter, *Exactly solved models in statistical mechanics*. Elsevier, 2016.

[93] A. Kuniba, T. Nakanishi, and J. Suzuki, *T-systems and Y-systems in integrable systems*, *J. Phys.* **A44** (2011) 103001, [arXiv:1010.1344].

[94] S. J. van Tongeren, *Introduction to the thermodynamic Bethe ansatz*, arXiv:1606.02951. [J. Phys.A49,no.32,323005(2016)].

[95] V. V. Bazhanov, S. L. Lukyanov, and A. M. Tsvelik, *Analytical results for the coqblin-schrieffer model with generalized magnetic fields*, *Physical Review B* **68** (Sep, 2003).

[96] S. Lukyanov, E. Vitchev, and A. Zamolodchikov, *Integrable model of boundary interaction: the paperclip*, *Nuclear Physics B* **683** (Apr, 2004) 423–454.

[97] S. L. Lukyanov and A. B. Zamolodchikov, *Integrable circular brane model and coulomb charging at large conduction*, *Journal of Statistical Mechanics: Theory and Experiment* **2004** (May, 2004) P05003.

[98] S. L. Lukyanov and P. Werner, *Universal scaling behaviour of the single electron box in the strong tunnelling limit*, *Journal of Statistical Mechanics: Theory and Experiment* **2006** (Nov, 2006) P11002–P11002.

[99] S. L. Lukyanov, *Notes on parafermionic qfts with boundary interaction*, *Nuclear Physics B* **784** (Nov, 2007) 151–201.

[100] S. L. Lukyanov and P. Werner, *Resistively shunted josephson junctions: quantum field theory predictions versus monte carlo results*, *Journal of Statistical Mechanics: Theory and Experiment* **2007** (Jun, 2007) P06002–P06002.

[101] S. L. Lukyanov and A. B. Zamolodchikov, *Integrable boundary interaction in 3d target space: The "pillow-brane" model*, *Nuclear Physics B* **873** (Aug, 2013) 585–613.

[102] P. Dorey, C. Dunning, F. Gliozzi, and R. Tateo, *On the ODE/IM correspondence for minimal models*, *J. Phys. A* **41** (2008) 132001, [arXiv:0712.2010].

[103] K. Ito, M. Mariño, and H. Shu, *Tba equations and resurgent quantum mechanics*, *Journal of High Energy Physics* **2019** (2019), no. 1 228.

[104] I. Affleck and A. W. W. Ludwig, *Universal noninteger "ground-state degeneracy" in critical quantum systems*, *Phys. Rev. Lett.* **67** (Jul, 1991) 161–164.

[105] D. Friedan and A. Konechny, *On the boundary entropy of one-dimensional quantum systems at low temperature*, *Phys. Rev. Lett.* **93** (2004) 030402, [hep-th/0312197].

[106] C.-M. Chang, Y.-H. Lin, S.-H. Shao, Y. Wang, and X. Yin, *Topological Defect Lines and Renormalization Group Flows in Two Dimensions*, *JHEP* **01** (2019) 026, [arXiv:1802.04445].

[107] M. Kormos, I. Runkel, and G. M. T. Watts, *Defect flows in minimal models*, *JHEP* **11** (2009) 057, [arXiv:0907.1497].

[108] H. Casini, I. S. Landea, and G. Torroba, *The g-theorem and quantum information theory*, *JHEP* **10** (2016) 140, [arXiv:1607.00390].

[109] J. Frohlich, J. Fuchs, I. Runkel, and C. Schweigert, *Kramers-Wannier duality from conformal defects*, *Phys. Rev. Lett.* **93** (2004) 070601, [cond-mat/0404051].

[110] J. Frohlich, J. Fuchs, I. Runkel, and C. Schweigert, *Duality and defects in rational conformal field theory*, *Nucl. Phys.* **B763** (2007) 354–430, [hep-th/0607247].

[111] V. B. Petkova and J. B. Zuber, *Generalized twisted partition functions*, *Phys. Lett.* **B504** (2001) 157–164, [hep-th/0011021].

[112] P. Fendley, M. P. Fisher, and C. Nayak, *Boundary conformal field theory and tunneling of edge quasiparticles in non-abelian topological states*, *Annals of Physics* **324** (2009), no. 7 1547–1572.

[113] A. Karch, D. Tong, and C. Turner, *A Web of 2d Dualities:* $\mathbf{Z}_2$ *Gauge Fields and Arf Invariants*, *SciPost Phys.* **7** (2019) 007, [arXiv:1902.05550].

[114] K. Graham and G. M. T. Watts, *Defect lines and boundary flows*, *JHEP* **04** (2004) 019, [hep-th/0306167].

[115] P. Dorey and R. Tateo, *Anharmonic oscillators, the thermodynamic Bethe ansatz, and nonlinear integral equations*, *J. Phys.* **A32** (1999) L419–L425, [hep-th/9812211].

[116] V. V. Bazhanov, S. L. Lukyanov, and A. B. Zamolodchikov, *Spectral determinants for Schrodinger equation and Q operators of conformal field theory*, *J. Statist. Phys.* **102** (2001) 567–576, [hep-th/9812247].

[117] P. Dorey and R. Tateo, *On the relation between stokes multipliers and the tq systems of conformal field theory*, *Nuclear physics B* **563** (1999), no. 3 573–602.

[118] D. Gaiotto, *Opers and TBA*, arXiv:1403.6137.

[119] E. Witten, *Integrable Lattice Models From Gauge Theory*, *arXiv:1611.00592 [cond-mat, physics:hep-th, physics:math-ph]* (Nov., 2016) [arXiv:1611.00592].

[120] K. Costello and M. Yamazaki, *Gauge theory and integrability IV*, *to appear*.

[121] A. Beilinson and V. Drinfeld, *Quantization of Hitchin's Integrable System and Hecke Eigensheaves*. 1991.

[122] D. Ben-Zvi and E. Frenkel, *Spectral Curves, Opers and Integrable Systems*, *arXiv:math/9902068* (Nov., 2002) [math/9902068].

[123] B. Feigin and E. Frenkel, *Quantization of soliton systems and Langlands duality*, *arXiv:0705.2486 [hep-th]* (Oct., 2009) [arXiv:0705.2486].

[124] E. Frenkel, *Gaudin model and opers*, *arXiv:math/0407524* (Mar., 2005) [math/0407524].

[125] D. Gaiotto and E. Witten, *Knot Invariants from Four-Dimensional Gauge Theory*, *Advances in Theoretical and Mathematical Physics* **16** (2012), no. 3 935–1086, [arXiv:1106.4789].

[126] G. A. Kotousov and S. L. Lukyanov, *ODE/IQFT correspondence for the generalized affine $\mathfrak{ Sl}(2)$ Gaudin model*, *arXiv:2106.01238 [cond-mat, physics:hep-th, physics:math-ph]* (June, 2021) [arXiv:2106.01238].

[127] J. Wu, *Anisotropic Kondo line defect and ODE/IM correspondence*, *arXiv:2106.07792 [hep-th, physics:math-ph]* (June, 2021) [arXiv:2106.07792].

[128] H. Saleur, *Lectures on nonperturbative field theory and quantum impurity problems*, cond-mat/9812110.

[129] H. Saleur, *Lectures on nonperturbative field theory and quantum impurity problems: Part 2*, cond-mat/0007309.

[130] I. Affleck and A. W. W. Ludwig, *Exact critical theory of the two impurity Kondo model*, *Phys. Rev. Lett.* **68** (1992) 1046–1049.

[131] A. Tsvelick and P. Wiegmann, *Exact results in the theory of magnetic alloys*, *Advances in Physics* **32** (1983), no. 4 453–713, [https://doi.org/10.1080/00018738300101581].

[132] V. J. Emery and S. Kivelson, *Mapping of the two-channel kondo problem to a resonant-level model*, *Phys. Rev. B* **46** (Nov, 1992) 10812–10817.

[133] E. Frenkel, *Opers on the projective line, flag manifolds and Bethe Ansatz*, *Mosc. Math. J.* **4** (8, 2004) 655–705, [math/0308269].

[134] B. Feigin and E. Frenkel, *Quantization of soliton systems and Langlands duality*, in *Exploring new structures and natural constructions in mathematical physics*, vol. 61, pp. 185–274, 2011. arXiv:0705.2486.

[135] B. Feigin, M. Jimbo, and E. Mukhin, *Integrals of motion from quantum toroidal algebras*, *J. Phys. A* **50** (2017), no. 46 464001, [arXiv:1705.07984].

[136] V. V. Bazhanov and S. L. Lukyanov, *Integrable structure of Quantum Field Theory: Classical flat connections versus quantum stationary states*, *JHEP* **09** (2014) 147, [arXiv:1310.4390].

[137] E. Frenkel and D. Hernandez, *Spectra of quantum KdV Hamiltonians, Langlands duality, and affine opers*, *Commun. Math. Phys.* **362** (2018), no. 2 361–414, [arXiv:1606.05301].

[138] D. Masoero and A. Raimondo, *Opers for higher states of quantum KdV models*, arXiv:1812.00228.

[139] B. Feigin and E. Frenkel, *Free field resolutions in affine Toda field theories*, *Phys. Lett. B* **276** (1992) 79–86.

[140] B. Feigin and E. Frenkel, *Integrals of motion and quantum groups*, *Lect. Notes Math.* **1620** (1996) 349–418, [hep-th/9310022].

[141] J. Evans, M. Hassan, N. MacKay, and A. Mountain, *Local conserved charges in principal chiral models*, *Nucl. Phys. B* **561** (1999) 385–412, [hep-th/9902008].

[142] J. Evans and A. Mountain, *Commuting charges and symmetric spaces*, *Phys. Lett. B* **483** (2000) 290–298, [hep-th/0003264].

[143] J. M. Evans, *Integrable sigma models and Drinfeld-Sokolov hierarchies*, *Nucl. Phys. B* **608** (2001) 591–609, [hep-th/0101231].

[144] S. Lacroix, M. Magro, and B. Vicedo, *Local charges in involution and hierarchies in integrable sigma-models*, *JHEP* **09** (2017) 117, [arXiv:1703.01951].

[145] S. Lacroix, B. Vicedo, and C. Young, *Affine Gaudin models and hypergeometric functions on affine opers*, *Adv. Math.* **350** (2019) 486–546, [arXiv:1804.01480].

[146] H. M. Babujian and R. Flume, *Off-shell Bethe Ansatz equation for Gaudin magnets and solutions of Knizhnik-Zamolodchikov equations*, *Mod. Phys. Lett. A* **9** (1994) 2029–2040, [hep-th/9310110].

[147] B. Feigin, E. Frenkel, and N. Reshetikhin, *Gaudin model, Bethe ansatz and correlation functions at the critical level*, *Commun. Math. Phys.* **166** (1994) 27–62, [hep-th/9402022].

[148] E. Frenkel, *Gaudin model and opers*, in *Workshop on Infinite Dimensional Algebras and Quantum Integrable Systems*, 7, 2004. math/0407524.

[149] A. Kapustin and E. Witten, *Electric-Magnetic Duality And The Geometric Langlands Program*, *Commun. Num. Theor. Phys.* **1** (2007) 1–236, [hep-th/0604151].

[150] D. Gaiotto and E. Witten, *Knot Invariants from Four-Dimensional Gauge Theory*, *Adv. Theor. Math. Phys.* **16** (2012), no. 3 935–1086, [arXiv:1106.4789].

[151] E. Frenkel, *Langlands correspondence for loop groups*, vol. 103. Cambridge Studies in Advanced Mathematics, Cambridge University Press, 2007.

[152] S. Lacroix, B. Vicedo, and C. A. Young, *Cubic hypergeometric integrals of motion in affine Gaudin models*, *Adv. Theor. Math. Phys.* **24** (2020), no. 1 155–187, [arXiv:1804.06751].

[153] B. L. Feigin, A. M. Semikhatov, V. A. Sirota, and I. Yu. Tipunin, *Resolutions and characters of irreducible representations of the N=2 superconformal algebra*, *Nucl. Phys.* **B536** (1998) 617–656, [hep-th/9805179].

[154] V. G. Kac, *Infinite-dimensional Lie algebras*. Cambridge University Press, 1990.

[155] B. Feigin, E. Frenkel, and V. Toledano Laredo, *Gaudin models with irregular singularities*, *Adv. Math.* **223** (2010) 873–948, [math/0612798].

[156] V. Schechtman and A. Varchenko, *Arrangements of hyperplanes and Lie algebra homology*, *Invent. Math.* **106** (1991), no. 1 139–194.

[157] P. Dorey and R. Tateo, *On the relation between Stokes multipliers and the T-Q systems of conformal field theory*, *Nucl. Phys. B* **563** (1999) 573–602, [hep-th/9906219]. [Erratum: Nucl.Phys.B 603, 581–581 (2001)].

[158] J. Suzuki, *Functional relations in stokes multipliers and solvable models related touq(a(1)n)*, *Journal of Physics A: Mathematical and General* **33** (May, 2000) 3507–3521.

[159] P. Dorey, C. Dunning, and R. Tateo, *Differential equations for generalsu(n) bethe ansatz systems*, *Journal of Physics A: Mathematical and General* **33** (Nov, 2000) 8427–8441.

[160] P. Dorey, C. Dunning, D. Masoero, J. Suzuki, and R. Tateo, *Abcd and odes*, 2007.

[161] S. Lukyanov and A. Zamolodchikov, *Quantum Sine(h)-Gordon Model and Classical Integrable Equations*, *JHEP* **07** (2010) 008, [arXiv:1003.5333].

[162] P. Dorey, S. Faldella, S. Negro, and R. Tateo, *The Bethe Ansatz and the Tzitzeica-Bullough-Dodd equation*, *Phil. Trans. Roy. Soc. Lond. A* **371** (2013) 20120052, [arXiv:1209.5517].

[163] S. Negro, *Integrable structures in quantum field theory*, *Journal of Physics A Mathematical General* **49** (Aug., 2016) 323006, [arXiv:1606.02952].

[164] B. Vicedo, *On integrable field theories as dihedral affine Gaudin models*, *Int. Math. Res. Not.* **2020** (2020), no. 15 4513–4601, [arXiv:1701.04856].

[165] K. Costello and J. Yagi, *Unification of integrability in supersymmetric gauge theories*, *arXiv:1810.01970 [hep-th, physics:math-ph]* (Nov., 2018) [arXiv:1810.01970].

[166] M. Ashwinkumar, M.-C. Tan, and Q. Zhao, *Branes and Categorifying Integrable Lattice Models*, *Advances in Theoretical and Mathematical Physics* **24** (2020), no. 1 1–24, [arXiv:1806.02821].

[167] D. Gaiotto and E. Witten, *S-Duality of Boundary Conditions In N=4 Super Yang-Mills Theory*, *Adv. Theor. Math. Phys.* **13** (2009), no. 3 721–896, [arXiv:0807.3720].

[168] A. Kapustin and M. Tikhonov, *Abelian duality, walls and boundary conditions in diverse dimensions*, *JHEP* **11** (2009) 006, [arXiv:0904.0840].

[169] D. M. McAvity and H. Osborn, *Conformal field theories near a boundary in general dimensions*, *Nucl. Phys.* **B455** (1995) 522–576, [cond-mat/9505127].

[170] C. Closset, T. T. Dumitrescu, G. Festuccia, Z. Komargodski, and N. Seiberg, *Comments on Chern-Simons Contact Terms in Three Dimensions*, *JHEP* **09** (2012) 091, [arXiv:1206.5218].

[171] M. F. Paulos, S. Rychkov, B. C. van Rees, and B. Zan, *Conformal Invariance in the Long-Range Ising Model*, *Nucl. Phys.* **B902** (2016) 246–291, [arXiv:1509.00008].

[172] C. Behan, L. Rastelli, S. Rychkov, and B. Zan, *A scaling theory for the long-range to short-range crossover and an infrared duality*, arXiv:1703.05325.

[173] C. Behan, L. Rastelli, S. Rychkov, and B. Zan, *Long-range critical exponents near the short-range crossover*, *Phys. Rev. Lett.* **118** (2017), no. 24 241601, [arXiv:1703.03430].

[174] A. Karch and Y. Sato, *Conformal Manifolds with Boundaries or Defects*, *JHEP* **07** (2018) 156, [arXiv:1805.10427].

[175] P. Liendo, L. Rastelli, and B. C. van Rees, *The Bootstrap Program for Boundary $CFT_d$*, *JHEP* **07** (2013) 113, [arXiv:1210.4258].

[176] M. S. Costa, J. Penedones, D. Poland, and S. Rychkov, *Spinning Conformal Correlators*, *JHEP* **11** (2011) 071, [arXiv:1107.3554].

[177] A. Dymarsky, J. Penedones, E. Trevisani, and A. Vichi, *Charting the space of 3D CFTs with a continuous global symmetry*, arXiv:1705.04278.

[178] A. Bissi, T. Hansen, and A. Söderberg, *Analytic Bootstrap for Boundary CFT*, *JHEP* **01** (2019) 010, [arXiv:1808.08155].

[179] D. Mazáč, L. Rastelli, and X. Zhou, *An Analytic Approach to $BCFT_d$*, arXiv:1812.09314.

[180] A. Kaviraj and M. F. Paulos, *The Functional Bootstrap for Boundary CFT*, arXiv:1812.04034.

[181] D. Gaiotto, *Boundary F-maximization*, arXiv:1403.8052.

[182] L. Alvarez-Gaume, S. Della Pietra, and G. W. Moore, *Anomalies and Odd Dimensions*, *Annals Phys.* **163** (1985) 288.

[183] E. Witten, *Fermion Path Integrals And Topological Phases*, *Rev. Mod. Phys.* **88** (2016), no. 3 035001, [arXiv:1508.04715].

[184] M. E. Peskin, *Mandelstam 't Hooft Duality in Abelian Lattice Models*, *Annals Phys.* **113** (1978) 122.

[185] C. Dasgupta and B. I. Halperin, *Phase Transition in a Lattice Model of Superconductivity*, *Phys. Rev. Lett.* **47** (1981) 1556–1560.

[186] D. T. Son, *Is the Composite Fermion a Dirac Particle?*, *Phys. Rev.* **X5** (2015), no. 3 031027, [arXiv:1502.03446].

[187] M. Baggio, N. Bobev, S. M. Chester, E. Lauria, and S. S. Pufu, *Decoding a Three-Dimensional Conformal Manifold*, *JHEP* **02** (2018) 062, [arXiv:1712.02698].

[188] C. Herzog, K.-W. Huang, and K. Jensen, *Displacement Operators and Constraints on Boundary Central Charges*, *Phys. Rev. Lett.* **120** (2018), no. 2 021601, [arXiv:1709.07431].

[189] C. P. Herzog, K.-W. Huang, I. Shamir, and J. Virrueta, *Superconformal Models for Graphene and Boundary Central Charges*, *JHEP* **09** (2018) 161, [arXiv:1807.01700].

[190] V. S. Alves, M. Gomes, S. V. L. Pinheiro, and A. J. da Silva, *The Perturbative Gross Neveu model coupled to a Chern-Simons field: A Renormalization group study*, *Phys. Rev.* **D59** (1999) 045002, [hep-th/9810106].

[191] W. Chen, G. W. Semenoff, and Y.-S. Wu, *Two loop analysis of nonAbelian Chern-Simons theory*, *Phys. Rev.* **D46** (1992) 5521–5539, [hep-th/9209005].

[192] W. Chen, M. P. A. Fisher, and Y.-S. Wu, *Mott transition in an anyon gas*, *Phys. Rev.* **B48** (1993) 13749–13761, [cond-mat/9301037].

[193] V. P. Spiridonov and F. V. Tkachov, *Two loop contribution of massive and massless fields to the Abelian Chern-Simons term*, *Phys. Lett.* **B260** (1991) 109–112.

[194] I. R. Klebanov, S. S. Pufu, and B. R. Safdi, *F-Theorem without Supersymmetry*, *JHEP* **10** (2011) 038, [arXiv:1105.4598].

[195] A. Sen, *S-duality Improved Superstring Perturbation Theory*, *JHEP* **11** (2013) 029, [arXiv:1304.0458].

[196] C. Beem, L. Rastelli, A. Sen, and B. C. van Rees, *Resummation and S-duality in N=4 SYM*, *JHEP* **04** (2014) 122, [arXiv:1306.3228].

[197] I. R. Klebanov, S. S. Pufu, S. Sachdev, and B. R. Safdi, *Entanglement Entropy of 3-d Conformal Gauge Theories with Many Flavors*, *JHEP* **05** (2012) 036, [arXiv:1112.5342].

[198] J. Braun, H. Gies, L. Janssen, and D. Roscher, *Phase structure of many-flavor $QED_3$*, *Phys. Rev.* **D90** (2014), no. 3 036002, [arXiv:1404.1362].

[199] S. Gukov, *RG Flows and Bifurcations*, arXiv:1608.06638.

[200] D. B. Kaplan, J.-W. Lee, D. T. Son, and M. A. Stephanov, *Conformality Lost*, *Phys. Rev.* **D80** (2009) 125005, [arXiv:0905.4752].

[201] V. Gorbenko, S. Rychkov, and B. Zan, *Walking, Weak first-order transitions, and Complex CFTs*, *JHEP* **10** (2018) 108, [arXiv:1807.11512].

[202] Z. Li, *Solving $QED_3$ with Conformal Bootstrap*, arXiv:1812.09281.

[203] S. Giombi, S. Minwalla, S. Prakash, S. P. Trivedi, S. R. Wadia, and X. Yin, *Chern-Simons Theory with Vector Fermion Matter*, *Eur. Phys. J.* **C72** (2012) 2112, [arXiv:1110.4386].

[204] O. Aharony, G. Gur-Ari, and R. Yacoby, *Correlation Functions of Large N Chern-Simons-Matter Theories and Bosonization in Three Dimensions*, *JHEP* **12** (2012) 028, [arXiv:1207.4593].

[205] G. Gur-Ari and R. Yacoby, *Correlators of Large N Fermionic Chern-Simons Vector Models*, *JHEP* **02** (2013) 150, [arXiv:1211.1866].

[206] O. Aharony, S. Jain, and S. Minwalla, *Flows, Fixed Points and Duality in Chern-Simons-matter theories*, *JHEP* **12** (2018) 058, [arXiv:1808.03317].

[207] A. Dey, I. Halder, S. Jain, L. Janagal, S. Minwalla, and N. Prabhakar, *Duality and an exact Landau-Ginzburg potential for quasi-bosonic Chern-Simons-Matter theories*, *JHEP* **11** (2018) 020, [arXiv:1808.04415]. [JHEP18,020(2020)].

[208] L. Fei, S. Giombi, I. R. Klebanov, and G. Tarnopolsky, *Yukawa CFTs and Emergent Supersymmetry*, *PTEP* **2016** (2016), no. 12 12C105, [arXiv:1607.05316].

[209] T. Senthil, L. Balents, S. Sachdev, A. Vishwanath, and M. P. A. Fisher, *Quantum criticality beyond the landau-ginzburg-wilson paradigm*, *Phys. Rev. B* **70** (Oct, 2004) 144407.

[210] P.-S. Hsin and N. Seiberg, *Level/rank Duality and Chern-Simons-Matter Theories*, *JHEP* **09** (2016) 095, [arXiv:1607.07457].

[211] C. Córdova, P.-S. Hsin, and N. Seiberg, *Time-Reversal Symmetry, Anomalies, and Dualities in (2+1)d*, *SciPost Phys.* **5** (2018), no. 1 006, [arXiv:1712.08639].

[212] Y. Q. Qin, Y.-Y. He, Y.-Z. You, Z.-Y. Lu, A. Sen, A. W. Sandvik, C. Xu, and Z. Y. Meng, *Duality between the deconfined quantum-critical point and the bosonic topological transition*, *Phys. Rev.* **X7** (2017), no. 3 031052, [arXiv:1705.10670].

[213] L. Iliesiu, "The Nèel-VBA quantum phase transition and the conformal bootstrap." Talk at the Workshop: "Developments in Quantum Field Theory and Condensed Matter Physics" at the Simons Center for Geometry and Physics, http://scgp.stonybrook.edu/video_portal/video.php?id=3809.

[214] C. Xu and Y.-Z. You, *Self-dual Quantum Electrodynamics as Boundary State of the three dimensional Bosonic Topological Insulator*, *Phys. Rev.* **B92** (2015), no. 22 220416, [arXiv:1510.06032].

[215] C. Wang, A. Nahum, M. A. Metlitski, C. Xu, and T. Senthil, *Deconfined quantum critical points: symmetries and dualities*, *Phys. Rev.* **X7** (2017), no. 3 031051, [arXiv:1703.02426].

[216] L. K. Hua and I. Reiner, *On the generators of the symplectic modular group*, *Transactions of the American Mathematical Society* **65** (1949), no. 3 415–426.

[217] T. Dimofte, D. Gaiotto, and S. Gukov, *Gauge Theories Labelled by Three-Manifolds*, *Commun. Math. Phys.* **325** (2014) 367–419, [arXiv:1108.4389].

[218] Z. Komargodski and N. Seiberg, *A symmetry breaking scenario for $QCD_3$*, *JHEP* **01** (2018) 109, [arXiv:1706.08755].

[219] J. Y. Lee, C. Wang, M. P. Zaletel, A. Vishwanath, and Y.-C. He, *Emergent Multi-flavor QED3 at the Plateau Transition between Fractional Chern Insulators: Applications to graphene heterostructures*, *Phys. Rev.* **X8** (2018), no. 3 031015, [arXiv:1802.09538].

[220] K. A. Intriligator and N. Seiberg, *Mirror symmetry in three-dimensional gauge theories*, *Phys. Lett.* **B387** (1996) 513–519, [hep-th/9607207].

[221] J. de Boer, K. Hori, H. Ooguri, Y. Oz, and Z. Yin, *Mirror symmetry in three-dimensional theories, SL(2,Z) and D-brane moduli spaces*, *Nucl. Phys.* **B493** (1997) 148–176, [hep-th/9612131].

[222] J. de Boer, K. Hori, and Y. Oz, *Dynamics of N=2 supersymmetric gauge theories in three-dimensions*, *Nucl. Phys.* **B500** (1997) 163–191, [hep-th/9703100].

[223] O. Aharony, A. Hanany, K. A. Intriligator, N. Seiberg, and M. J. Strassler, *Aspects of N=2 supersymmetric gauge theories in three-dimensions*, *Nucl. Phys.* **B499** (1997) 67–99, [hep-th/9703110].

[224] T. Dimofte, D. Gaiotto, and S. Gukov, *3-Manifolds and 3d Indices*, *Adv. Theor. Math. Phys.* **17** (2013), no. 5 975–1076, [arXiv:1112.5179].

[225] P. Di Francesco, P. Mathieu, and D. Senechal, *Conformal Field Theory*. Graduate Texts in Contemporary Physics. Springer-Verlag, New York, 1997.

[226] L. Hollands and A. Neitzke, *Exact WKB and abelianization for the $T_3$ equation*, arXiv:1906.04271.

[227] R. Adhikari, R. Dutt, A. Khare, and U. P. Sukhatme, *Higher-order wkb approximations in supersymmetric quantum mechanics*, *Phys. Rev. A* **38** (Aug, 1988) 1679–1686.

[228] C. M. Bender, K. Olaussen, and P. S. Wang, *Numerological analysis of the wkb approximation in large order*, *Phys. Rev. D* **16** (Sep, 1977) 1740–1748.

[229] D. Dumas and A. Neitzke, *Opers and nonabelian Hodge: numerical studies*, arXiv:2007.00503.

[230] E. Lauria, M. Meineri, and E. Trevisani, *Spinning operators and defects in conformal field theory*, arXiv:1807.02522.

[231] M. Beccaria and A. A. Tseytlin, *Vectorial $AdS_5/CFT_4$ duality for spin-one boundary theory*, *J. Phys.* **A47** (2014), no. 49 492001, [arXiv:1410.4457].

[232] F. Gliozzi, P. Liendo, M. Meineri, and A. Rago, *Boundary and Interface CFTs from the Conformal Bootstrap*, *JHEP* **05** (2015) 036, [arXiv:1502.07217].

[233] M. Billò, V. Gonçalves, E. Lauria, and M. Meineri, *Defects in conformal field theory*, *JHEP* **04** (2016) 091, [arXiv:1601.02883].

[234] H. Osborn and A. C. Petkou, *Implications of conformal invariance in field theories for general dimensions*, *Annals Phys.* **231** (1994) 311–362, [hep-th/9307010].

[235] D. T. Barfoot and D. J. Broadhurst, *Z(2) X S(6) Symmetry of the Two Loop Diagram*, *Z. Phys.* **C41** (1988) 81.

[236] K. G. Chetyrkin and F. V. Tkachov, *Integration by Parts: The Algorithm to Calculate beta Functions in 4 Loops*, *Nucl. Phys.* **B192** (1981) 159–204.

[237] F. V. Tkachov, *A Theorem on Analytical Calculability of Four Loop Renormalization Group Functions*, *Phys. Lett.* **100B** (1981) 65–68.

[238] D. J. Broadhurst, J. A. Gracey, and D. Kreimer, *Beyond the triangle and uniqueness relations: Nonzeta counterterms at large N from positive knots*, *Z. Phys.* **C75** (1997) 559–574, [hep-th/9607174].

[239] Z.-W. Huang and J. Liu, *NumExp: Numerical epsilon expansion of hypergeometric functions*, *Comput. Phys. Commun.* **184** (2013) 1973–1980, [arXiv:1209.3971].

# APPENDICES

# Appendix A

# Conventions

We will follow the convention from [225, 90]. We choose orthonormal basis $\{t^a\}$, namely Killing form $K(t^a, t^b) = \delta^{a,b}$, so adjoint indices can be raised and lowered freely. Note that we define the Killing form with a normalization constant,

$$K(X, Y) \equiv \frac{1}{h^\vee \psi^2} \operatorname{Tr}(\mathrm{ad}X \mathrm{ad}Y) \tag{A.1}$$

so that,

$$\sum_{a,b} f^{abc} f^{abd} = h^\vee \psi^2 \delta^{ab} \tag{A.2}$$

where $\psi^2$ is the length squared of the longest root, which account for the arbitrary normalization of the generators. We will choose $\psi^2 = 2$, unless otherwise stated, and structure constant $f^{abc}$ is defined in

$$[t^a, t^b] = i f^{abc} t^c \tag{A.3}$$

Using the definitions above, we are ready to list some useful identities for $\mathfrak{su}(2)$. Representations of $\mathfrak{su}(2)$ are labelled by nonnegative half integer $j$, denoted as $R_j$, we have the following

$$\operatorname{Tr}_{R_j}(t^a t^b) = I_{R_j} \delta^{ab}, \tag{A.4}$$

$$\operatorname{Tr}_{R_j}\left(t^a t^b t^c\right) = \frac{i}{2} f^{abc} I_{R_j} \tag{A.5}$$

$$\operatorname{Tr}_{R_j}\left(t_a t_b t_c t_d\right) = \frac{1}{2}\alpha_j I_{R_j}\left(\delta_{ab}\delta_{cd} + \delta_{ad}\delta_{bc}\right) + \frac{1}{2}\beta_j I_{R_j}\left(\delta_{ac}\delta_{bd}\right), \tag{A.6}$$

with

$$C_2(R_j) = j(j+1)\psi^2, \quad \dim(R_j) = 2j+1 \tag{A.7}$$

$$I_{R_j} = \frac{1}{3} j(j+1)(2j+1)\psi^2, \quad f_{abc} = \sqrt{2}\epsilon_{abc} \tag{A.8}$$

$$\alpha_j = \frac{4}{5}\left(j(j+1) + \frac{1}{2}\right), \quad \beta_j = \frac{4}{5}(j(j+1) - 2). \tag{A.9}$$

# Appendix B

# Perturbative analysis of Ising line defect

Consider the defect Lagrangian given in [108], where a Majorana fermion $\gamma$ is introduced as an auxiliary defect degree of freedom within a massless free fermion bulk. As we are interested in chiral line defects, we differ from the reference in that $\gamma$ is perturbed only chirally as

$$g \int_x \psi(x,0)\gamma(x) \tag{B.1}$$

in addition to the kinetic term of $\gamma$. We take the mode expansion on the cylinder in the NS sector

$$\psi(x,t) = \sum_{n\in\mathbb{Z}+\frac{1}{2}} b_n e^{i\frac{n}{R}(x-t)} \tag{B.2}$$

$$\gamma(x) = \sum_{n\in\mathbb{Z}+\frac{1}{2}} \gamma_n e^{i\frac{n}{R}x}, \tag{B.3}$$

where the modes obey $\{b_n, b_m\} = \{\gamma_n, \gamma_m\} = \frac{1}{2\pi R}\delta_{n+m}$. The coupling then becomes

$$g \int_x \psi(x,0)\gamma(x) = 2\pi R g \sum_{n>0} (b_{-n}\gamma_n - \gamma_{-n}b_n) \tag{B.4}$$

where $n$ are positive half-integers. Taking the vacuum expectation value of its exponential, the surviving contribution is $\exp(2\pi R g^2 \sum_{n>0} \gamma_{-n}\gamma_n)$. Combining with the kinetic term contribution $\exp(\sum_{n>0} n\gamma_{-n}\gamma_n)$ (with an appropriate relative normalization constant) and

integrating over the $\gamma$ modes, we get the product

$$\sqrt{2}e^{2\pi Rg^2 \log e^{-1}\epsilon g^2} \prod_{m=0}^{\frac{R}{\epsilon}} \frac{m+1/2+2\pi Rg^2}{m+1/2} = \frac{\sqrt{2\pi}e^{2\pi Rg^2 \log e^{-1} Rg^2}}{\Gamma\left(\frac{1}{2}+2\pi Rg^2\right)} + O(\epsilon). \tag{B.5}$$

where we normalized the answer correctly in the UV and included a constant counterterm.

Reintroducing $\theta$ and setting $2\pi Rg^2 = 1$ we get

$$T_S(\theta) = \frac{\sqrt{2\pi}e^{\theta e^\theta - e^\theta}}{\Gamma(\frac{1}{2}+e^\theta)}. \tag{B.6}$$

If we evaluate vevs on states other than the vacuum, the exponential is modified as $\exp(2\pi Rg^2 \sum_{n>0} \epsilon_n \gamma_{-n}\gamma_n)$ where $\epsilon_n = -1$ for occupied states. A finite collection of factors in the answer is modified to $m+1/2-2\pi Rg^2$. Similarly, in the Ramond sector one replaces $m+\frac{1}{2}$ with $m+1$ and includes a zeromode contribution.

# Appendix C

# Perturbative analysis of WZW line defects

## C.1 Perturbative analysis of WZW line defects

We study chiral line defects in $\mathfrak{su}(2)$ WZW models, which are defined as

$$\hat{T}_{\mathcal{R}} := \mathrm{Tr}_{\mathcal{R}} \mathcal{P} \exp\left( ig \int_0^{2\pi R} d\sigma \; t_a J^a(\sigma, 0) \right) \tag{C.1}$$

where $g$ is the dimensionless coupling, $t_a$ are generators of $\mathfrak{su}(2)$ in representation $\mathcal{R}$, and $J^a$ are chiral WZW currents [1]. On the cylinder of radius $R$, the currents admit the mode expansion

$$J^a(s) = \frac{1}{R} \sum_{n \in \mathbb{Z}} J^a_n e^{-ns/R} \tag{C.2}$$

with coordinates $s = \tau + i\sigma$ on the cylinder. The modes obey the typical commutation relations of the affine Kac-Moody algebra, $[J^a_n, J^b_m] = i f_{abc} J^c_{n+m} + kn\delta_{ab}\delta_{n+m,0}$. We will follow the Lie algebra conventions from [225, 90]. For completeness, we also review them in Appendix A.

[1] The roman letters $a, b, c, d$ will be reserved for group theory indices.

### C.1.1 Definition of the quantum operator $\hat{T}_{\mathcal{R}}$

For small $g$, the line operator $\hat{T}_{\mathcal{R}}$ wrapping the cylinder admits the expansion

$$\hat{T}_{\mathcal{R}} = \sum_{N=0}^{\infty} (ig)^N \hat{T}_{\mathcal{R}}^{(N)}$$

where

$$\hat{T}_{\mathcal{R}}^{(N)} = \mathrm{Tr}_{\mathcal{R}}(t^{a_1} \cdots t^{a_N}) \Big( \prod_{i=1}^{N} \int_0^{2\pi R} d\sigma_i \Big) \theta_{\sigma_1 > \cdots > \sigma_N} J^{a_1}(\sigma_1) \cdots J^{a_N}(\sigma_N).$$

In the above classical expression for the line operator, the currents are not ordered. However, a quantum line operator requires an regularization scheme which prescribes an appropriate ordering for the currents which is consistent with the desired properties of $\hat{T}_{\mathcal{R}}$. Furthermore, the currents themselves must be regularized, which can be done by assigning a cutoff on the mode expansion of $J(\sigma)$. In doing so, we follow the regularization prescription given in [90].

However, our treatment differs from [90] in the computation of the operator, where we need to compute the full expression of the normal-ordered operator to $O(g^4)$ rather than just the leading contributions in the classical limit $\kappa \to \infty$. We also keep track of the length scale $R$ of the cylinder, which allows us, as we will describe below, to make connections, to thermodynamic Bethe ansatz, Hirota relations and computations from ODE/IM correspondence.

We now review the regularization prescription used in [90]. As part of the regularization scheme, a current ordering is chosen to respects the desired symmetries of the quantum line defect. It is reasonable to assume $\hat{T}_{\mathcal{R}}$ to be invariant under the following transformations: (1) cyclic permutations of the inserted currents and (2) reversing the orientation of the defect combined with taking $\mathcal{R}$ to its conjugate representation $\bar{\mathcal{R}}$. A current ordering which respects cyclic invariance and orientation reversal (combined with $\mathcal{R} \to \bar{\mathcal{R}}$) is

$$\hat{T}_{\mathcal{R}}^{(N)} = \mathrm{Tr}_{\mathcal{R}}(t^{a_1} \cdots t^{a_N}) \Big( \prod_{i=1}^{N} \int_0^{2\pi R} d\sigma_i \Big) \theta_{\sigma_1 > \cdots > \sigma_N} \frac{1}{2N} \Big[ J^{a_1}(\sigma_1) \cdots J^{a_N}(\sigma_N) + \text{cyclic} + \text{reversal} \Big].$$

We also need the regularized chiral WZW currents by imposing a short distance cutoff [90]:

$$J^a(\sigma) = \frac{1}{R} \sum_{n \in \mathbb{Z}} J_n^a e^{-in\sigma/R - |n|\epsilon/2R}.$$

By expanding the currents into modes, each contribution to $\hat{T}_{\mathcal{R}}$ becomes the product of four terms which can be independently evaluated: the group theory factor, appropriately-ordered modes, products of regulators $e^{|n_i|\epsilon/2R}$, and integrals over $\sigma_i$. The integrals over $\sigma_i$ yield delta functions on which only certain terms for which the sums of the mode numbers are equal to zero are supported. Note that this implies translation invariance of the operator along $\sigma$ direction.

This will be our new definition of $\hat{T}_{\mathcal{R}}$ hereon. The expressions of the first few orders are given below

$$\begin{aligned}
&\hat{T}^{(0)}_{\mathcal{R}} = \dim \mathcal{R}, \quad \hat{T}^{(1)}_{\mathcal{R}} = 0, \quad \hat{T}^{(2)}_{\mathcal{R}} = 2\pi^2 \mathrm{Tr}_{\mathcal{R}}(t^a t^b) J^a_0 J^b_0 \\
&\hat{T}^{(3)}_{\mathcal{R}} = \frac{2\pi^2}{3}\mathrm{Tr}_{\mathcal{R}}(t^a t^b t^c)\left[\frac{\pi}{3} J^a_0 J^b_0 J^c_0 + \sum_{n\neq 0} \frac{i}{n} J^a_{-n} J^b_n J^c_0 e^{-|n|\epsilon/R} + \text{cyclic} + \text{reversal}\right] \\
&\hat{T}^{(4)}_{\mathcal{R}} = \frac{\pi^2}{2}\mathrm{Tr}_{\mathcal{R}}(t^a t^b t^c t^d)\left[\frac{\pi^2}{6} J^a_0 J^b_0 J^c_0 J^d_0 + \sum_{n\neq 0} \frac{i\pi}{n} J^a_{-n} J^b_n J^c_0 J^d_0 e^{-|n|\epsilon/R}\right. \\
&+ \sum_{n\neq 0} \frac{1}{n^2}(J^a_{-n} J^b_n J^c_0 J^d_0 - J^a_{-n} J^b_0 J^c_n J^d_0) e^{-|n|\epsilon/R} + \sum_{m,l,m+l\neq 0} \frac{1}{ml} J^a_m J^b_{-m-l} J^c_l J^d_0 e^{-(|m|+|l|+|m+l|)\epsilon/2R} \\
&\left. - \frac{1}{2}\sum_{m,n\neq 0} \frac{1}{mn} J^a_{-n} J^b_n J^c_{-m} J^d_m e^{-(|m|+|n|)\epsilon/R} + \text{cyclic} + \text{reversal}\right]
\end{aligned} \tag{C.3}$$

This is the same expression in [90]. Note that up until now, no knowledge of the representation $\mathcal{R}$, namely $\mathrm{Tr}_{\mathcal{R}}(t^a t^b t^c \dots)$ have been used, except for the cyclic properties of the trace.

The last ingredient we need is the renormalization scheme, i.e. the prescription of removing the short distance cutoff $\epsilon$ and replacing bare couplings with renormalized couplings. As in [90], there are two types of local counterterms involved, the identity operator 1 and the marginal operator $t \cdot J$. The effects of 1 and $t \cdot J$ are, respectively, to multiply the result by an overall factor $e^{RG(g,\epsilon)}$ and redefine the coupling $g$ to $F(g,\epsilon)$, where $G(g,\epsilon)$ and $F(g,\epsilon)$ are power series in $g$. For the reason that will be clear soon, it is very helpful to make the renormalization scheme explicit and generic, as we will do in the next section.

### C.1.2 Computation of normal-ordered line operator

To facilitate our calculations later, we will first normal order the expressions (C.3). It is done by moving all positive modes to the right of the negative modes. Specifically, we need

to use the commutation relation repeatedly such that the subcripts of $J_n$ are in ascending order.[2] In the case of equal subscripts equal $n$, we define normal ordered expression to be totally symmetric. For example,

$$J_n^a J_n^b \to J_n^{(a} J_n^{b)} + \frac{i}{2} f^{abc} J_{2n}^c \tag{C.4}$$

Similarly for longer products $J_n^{a_1} J_n^{a_2} J_n^{a_3} \dots J_n^{a_m}$. We include $1/m!$ in the symmetrization.

We then proceed with the renormalization by removing counterterms proportional to $R$ and performing the following redefinition in the coupling:

$$g \to g\lambda + g^2\lambda^2\Big[ -2\log\epsilon + C_0\Big] + g^3\lambda^3\Big[ +4(\log\epsilon)^2 - (2k+4C_0)\log\epsilon + D\Big] + \cdots ,$$

where $g$ on the right hand side is the renormalized coupling. $C_0$ and $D$ are arbitrary renormalization scheme constant that depend possibly on the representation but not on $\epsilon$. We also include $\lambda$ to possibly rescale the coupling. The renormalized and normal-ordered $SU(2)$ line operator $\hat{T}_j$ to $O(g^4)$ is

$$\begin{aligned}
\hat{T}_j^{(0)} &= 2j+1, \\
\hat{T}_j^{(2)} &= 4\pi^2\lambda^2 x_j J_0^a J_0^a, \\
\hat{T}_j^{(3)} &= -16i\pi^2\lambda^3 x_j \left\{ \sum_{n>0} \frac{i}{2n} f_{abc} J_{-n}^a J_0^b J_n^c + \sum_{n>0} \frac{2}{n} J_{-n}^a J_n^a - \log R\ J_0^a J_0^a - \frac{k}{2} \right\} \\
\hat{T}_j^{(4)} &= 8\pi^2\lambda^4 x_j \left\{ \sum_{n,m,n+m\neq 0} \Big[ \frac{2}{3m(m+n)} : J_{-m-n}^a J_0^b J_m^a J_n^b : - \frac{1}{3nm} : J_{-m-n}^a J_0^a J_m^b J_n^b : \Big] \right. \\
&\quad \left. + \sum_{n,m>0} \frac{1}{nm} \Big[ : J_{-n}^a J_{-m}^a J_m^b J_n^b : - : J_{-n}^a J_{-m}^b J_m^a J_n^b : \Big] \right.
\end{aligned}$$

[2]The normal-ordering procedure is relatively straightforward and yet very tedious. The strategy is reorganizing and relabeling the summations so that the sums run over positive indices and subsequently applying the affine Kac-Moody commutation relations. In particular, for the terms with sums over two indices which appear at $O(g^4)$, after organizing the summations such that all indices run over positive indices $n, m > 0$, the sums require additional division into the cases $\sum_{n,m>0} = \sum_{n>m>0} + \sum_{m>n>0} + \sum_{m=n>0}$ for proper normal ordering. Furthermore, at some point of the normal-ordering procedure, modes such as $J_{m-n}$ or $J_{n-m}$ as well as $J_n$,$J_{-n}$, $J_m$, or $J_{-m}$ will be present in the same term. This suggests that a further subdivision of the summation into $\sum_{n>m>0} = \sum_{n>0,n>m>n/2} + \sum_{n>0,n/2>m>0} + \sum_{m=n/2>0,n \text{ even}}$ and similarly for $\sum_{m>n>0}$ is necessary.

$$
\begin{aligned}
&+\sum_{n>0}\frac{1}{n^2}\Big[2J^a_{-n}J^b_0J^b_0J^a_n-J^a_{-n}J^a_0J^b_0J^b_n-J^a_{-n}J^b_0J^a_0J^b_n\Big]\\
&+\sum_{n,m>0}\frac{3i}{nm}f_{abc}:J^a_{-n}J^b_{-m+n}J^c_m:+\sum_{n>m>0}\frac{i}{nm}f_{abc}[J^a_{-n}J^b_{-m}J^c_{m+n}+J^a_{-m-n}J^b_mJ^c_n]\\
&+\sum_{n>0}\frac{6i}{n}\Big[\log R-\frac{1}{3}(H_{\lfloor\frac{n}{2}\rfloor}+H_{\lfloor\frac{n-1}{2}\rfloor})\Big]f_{abc}J^a_{-n}J^b_0J^c_n+\sum_{n>0}\frac{2i}{n^2}f_{abc}J^a_{-n}J^b_0J^c_n\\
&+\sum_{n,m>0}\frac{3}{nm}J^a_{-m-n}J^a_{m+n}-\sum_{n>m>0}\frac{6}{nm}J^a_{m-n}J^a_{-m+n}-\sum_{n>0}\frac{2}{n^2}J^a_{-2n}J^a_{2n}\\
&+\sum_{n>0}\frac{6}{n^2}J^a_{-n}J^a_n+\sum_{n>0}\frac{24}{n}\Big[\log R-\frac{1}{2}(H_{\lfloor\frac{n}{2}\rfloor}+H_{\lfloor\frac{n-1}{2}\rfloor})-\frac{k}{12}\Big]J^a_{-n}J^a_n\\
&+\frac{\pi^2}{12}(2\alpha_j+\beta_j)(J^a_0J^a_0)^2+\Big[2k\log R-6(\log R)^2-\frac{\pi^2}{6}\big(\beta_j-8j(j+1)\big)\Big]J^a_0J^a_0\\
&+\Big[\frac{3}{4}k^2-6k(1+\log R)\Big]\Bigg\},
\end{aligned}
\tag{C.5}
$$

where the representation of $\mathfrak{su}(2)$ are labelled by the half-integer $j$ and $x_j$ is half of the Dynkin index defined in Appendix A. : : denotes the normal ordering operation, where an equal fraction of each ambiguous combination is taken in a symmetric manner when there are ambiguities (i.e. when there exist modes with same mode numbers). One can consider the leading terms in $k$ to verify that its large $k$ limit matches with the result given in [90].

### C.1.3 Verification of the commutativity and Hirota relation

As explained above (2.23) and the footnote in Section 2.4.1, we identify $2\pi R = e^\theta$ and verify directly that $\hat{T}^{(N)}_j$ all commute. Therefore we have

$$
[\hat{T}_j[\theta],\hat{T}_{j'}[\theta']]=0, \tag{C.6}
$$

We also want to verify Hirota relations [91, 92, 93]

$$
\hat{T}_j[\theta+\tfrac{i\pi}{2}]\hat{T}_j[\theta-\tfrac{i\pi}{2}]=1+\hat{T}_{j+\frac{1}{2}}[\theta]\hat{T}_{j-\frac{1}{2}}[\theta], \tag{C.7}
$$

which can be written perturbatively in $g$ as

$$
2\hat{T}^{(0)}_j\hat{T}^{(2)}_j=\hat{T}^{(0)}_{j+\frac{1}{2}}\hat{T}^{(2)}_{j-\frac{1}{2}}+\hat{T}^{(0)}_{j-\frac{1}{2}}\hat{T}^{(2)}_{j+\frac{1}{2}}, \tag{C.8}
$$

$$\hat{T}_j^{(0)}(\hat{T}_j^{(3)+} + \hat{T}_j^{(3)-}) = \hat{T}_{j+\frac{1}{2}}^{(0)}\hat{T}_{j-\frac{1}{2}}^{(3)} + \hat{T}_{j-\frac{1}{2}}^{(0)}\hat{T}_{j+\frac{1}{2}}^{(3)}, \tag{C.9}$$

$$\hat{T}_j^{(0)}(\hat{T}_j^{(4)+} + \hat{T}_j^{(4)-}) + \hat{T}_j^{(2)}\hat{T}_j^{(2)} = \hat{T}_{j+\frac{1}{2}}^{(0)}\hat{T}_{j-\frac{1}{2}}^{(4)} + \hat{T}_{j-\frac{1}{2}}^{(0)}\hat{T}_{j+\frac{1}{2}}^{(4)} + \hat{T}_{j-\frac{1}{2}}^{(2)}\hat{T}_{j+\frac{1}{2}}^{(2)} \tag{C.10}$$

where the superscripts $\pm$ indicate shifts in the argument by $\pm\frac{i\pi}{2}$.

It turns out (C.7) is satisfied if

$$D = D_0 - \frac{4\pi^2}{3}j(j+1) \tag{C.11}$$

where $D_0$ and $C_0$ are arbitrary constants that are independent of the representation $j$ and $\epsilon$, which we choose the arbitrary constant $D_0 = -\frac{5\pi^2}{6}$ and $C_0 = 0$.

Note that due to commutativity (C.6), in the common eigenspace, we can just deal with eigenvalues of $\hat{T}_j(\theta)$ and their functional relations. Nevertheless, we chose to verify the operator version of the Hirota relation, which is a stronger equation.

### C.1.4 Expectation values

Let us compute the expectation value between primary states in representation $l$. We follow again the normalization in [225], where $J_0^a J_0^a = 2l(l+1)$ when acting on a primary state $|l\rangle$. The renormalized expectation value, which follows directly from the normal-ordered operator, is

$$\begin{aligned}
\langle T_n(g,R)\rangle_l = n
&- g^2\lambda^2 x_j[8\pi^2 l(l+1)] \\
&+ g^3\lambda^3 x_j[32\pi^2 l(l+1)\log R + 8\pi^2 k - 16\pi^2 C_0 l(l+1)] \\
&- g^4\lambda^4 x_j\Big[96\pi^2 l(l+1)(\log R)^2 - 16\pi^2\big(k(2l(l+1)-3) + 6C_0 l(l+1)\big)\log R \\
&\frac{1}{15}(-2)\pi^2\left(4l(l+1)\left(2\pi^2\left(3n^2\left(l^2+l+3\right) - 5\left(l^2+l+1\right)\right) - 15C_0^2\right)\right. \\
&\qquad \left. +180(C_0-2)k + 45k^2\right)\Big],
\end{aligned}$$

We can also calculate the expectation value over excited states. This will be done in a future paper.[2]

### C.1.5 Beta function and effective coupling

Beta function can be found to be

$$\beta(g) \equiv \frac{\partial g}{\partial \log \Lambda} = 2\lambda g^2 + 2k\lambda^2 g^3 + \cdots . \tag{C.12}$$

The ratio $\frac{c_1}{c_0^2}$ from $\beta(g) = c_0 g^2 + c_1 g^3 + \cdots$ is independent of the renormalization scheme and equals $\frac{k}{2}$. In accordance with the discussion in Section 2.4.1, we will choose $\lambda = -\frac{1}{2}$.

It is not hard to see that any constants or higher order terms in the beta function can be arbitrarily adjusted by redefining $g$. In particular, we fix it to be

$$\beta(g) = -\frac{g^2}{1 + \frac{k}{2} g} \tag{C.13}$$

which give rise to a scale via dimensional transmutation.

$$\mu = e^{-1/g} g^{k/2}$$

through dimensional transmutation. Since $\mu$ enters into any observable computed using $\hat{T}_j$ only through the combination $R\mu$, the result is only dependent on $e^{\theta} e^{1/g} g^{-k/2}$. This combination can be used to define the effective coupling $g_{\text{eff}}(\theta)$ by

$$e^{-1/g_{\text{eff}}(\theta)} g_{\text{eff}}^{k/2}(\theta) = e^{\theta} e^{-1/g} g^{k/2}.$$

### C.1.6 generalisation to multiple $su(2)$

The computations above can be easily generalized to $\prod_i su(2)_i$ defined by

$$\hat{T}_{\mathcal{R}}(\{g_i\}) := \text{Tr}_{\mathcal{R}}\, \mathcal{P} \exp\left( i \int_0^{2\pi} d\sigma \; g_i t^a J_i^a(\sigma) \right) \tag{C.14}$$

which admits the expansion

$$\hat{T}_{\mathcal{R}}\left(\{g_i\}\right) = \sum_{N=0}^{\infty} i^N \hat{T}_{\mathcal{R}}^{(N)} \tag{C.15}$$

Generators in the mode expansion of the current satisfy Kac Moody algebra and commute if they belong to different $su(2)$ ,

$$\left[J^a_{i,n}, J^b_{j,m}\right] = \delta_{ij}(\sqrt{-1} f^{abc} J^c_{i,n+m} + \kappa_i n \delta^{ab} \delta_{n+m,0}) \tag{C.16}$$

After performing the integrals over $\sigma$, we get the operator $\boldsymbol{T}^{(N)}_{\mathcal{R}}$, which is to simply modify (C.3) by summing over generators in different $su(2)$ factors, for example,

$$\hat{T}^{(2)}_{\mathcal{R}} = 2\pi^2 \mathrm{Tr}_{\mathcal{R}}(t^a t^b) \sum_{i,j} g_i g_j J^a_{i,0} J^b_{j,0} \tag{C.17}$$

$$\hat{T}^{(3)}_{\mathcal{R}} = \frac{2\pi^2}{3} \mathrm{Tr}_{\mathcal{R}}(t^a t^b t^c) \sum_{i,j,k} g_i g_j g_k \left[ \frac{\pi}{3} J^a_{i,0} J^b_{j,0} J^c_{k,0} + \sum_{n\neq 0} \frac{i}{n} J^a_{i,-n} J^b_{j,n} J^c_{k,0} e^{-|n|\epsilon/R} + \text{cyclic} + \text{reversal} \right] \tag{C.18}$$

To demonstrate the computation, it is enough to take an example of $su(2) \times su(2)$. We renormalize $\hat{T}^{(N)}_{\mathcal{R}}$ up to $N = 4$ in the same manner as in the last section[3], where renormalization is done by performing the following redefinition of the coupling

$$\begin{aligned} g_1 \to & g_1 + g_1^2(-2\log\epsilon + C_1) + g_1 g_2 C_3 + g_2^2 \mathrm{C}_5 + g_1^3 \left(4\log^2\epsilon - 2(k_1 + 2C_1)\log\epsilon + D_1\right) \\ & + g_1^2 g_2(-4C_3 \log\epsilon + D_3) + g_1 g_2^2 \big[ -2(2C_5 + k_2)\log\epsilon + D_5 \big] + g_2^3 D_7 + \dots \\ g_2 \to & g_2 + g_2^2(-2\log\epsilon + C_2) + g_1 g_2 C_4 + g_1^2 \mathrm{C}_6 + g_2^3 \left(4\log^2\epsilon - 2(k_2 + 2C_2)\log\epsilon + D_2\right) \\ & + g_2^2 g_1(-4C_4 \log\epsilon + D_4) + g_2 g_1^2 \big[ -2(2C_6 + k_1)\log\epsilon + D_6 \big] + g_1^3 D_8 + \dots \end{aligned} \tag{C.19}$$

where $C_i$ and $D_i$ are arbitrary constants independent of the cutoff $\epsilon$. Beta function is then

$$\beta_{g_1}(g_1, g_2) = 2\lambda g_1^2 + 2\lambda^2 \big[ k_1 g_1^3 + C_3 g_1^2 g_2 - (C_3 - 2C_5 - k_2) g_1 g_2^2 - 2C_5 g_2^3 \big] + \dots \tag{C.20}$$

$$\beta_{g_2}(g_1, g_2) = 2\lambda g_2^2 + 2\lambda^2 \big[ k_2 g_2^3 + C_4 g_1 g_2^2 - (C_4 - 2C_6 - k_1) g_1^2 g_2 - 2C_6 g_1^3 \big] + \dots \tag{C.21}$$

As we discussed in Section 3.5.1, DE/IM predicts that there exists a renormalization scheme such that beta functions are of the form

$$\beta_{g_1} = \frac{g_1^2}{1 + \frac{1}{2}\sum_j k_j g_j} = g_1^2 - \frac{1}{2}\big[ k_1 g_1^3 + k_2 g_1^2 g_2 \big] + \mathcal{O}(g_1^4, g_1^3 g_2, g_1^2 g_2^2, g_1 g_2^3, g_2^4) \tag{C.22}$$

[3]The results are too cumbersome to be presented here. Contact the author if you would like to grab a beer and drink over it.

and a similar expression for $\beta_{g_2}$. This fixes the renormalization constants

$$\lambda = -\frac{1}{2}, \quad C_5 = C_6 = 0, \quad C_3 = k_2, \quad C_4 = k_1 \tag{C.23}$$

The expectation value of $\hat{T}_n$ over WZW primary states can be easily computed

$$\begin{aligned}
&\langle l_1, l_2 | T_n(g_1, g_2, R) | l_1, l_2 \rangle = n - 8\pi^2 x_j \lambda^2 \left( g_1^2 \ell_1 (1 + \ell_1) + 2 g_1 g_2 \ell_1 \ell_2 + g_2^2 \ell_2 (1 + \ell_2) \right) \\
&+8\pi^2 \lambda^3 x_j \Big[ - 2 C_1 g_1^2 l_1 (g_1 l_1 + g_1 + g_2 l_2) + g_1^3 k_1 \\
&\quad - 2 g_2 (C_2 g_2 l_2 (g_1 l_1 + g_2 l_2 + g_2) + g_1 (g_1 l_1 (k_2 + k_2 l_1 + k_1 l_2) + g_2 l_2 (k_1 + k_2 l_1 + k_1 l_2))) \\
&\quad + 4 \log R \left( g_1^3 l_1 (l_1 + 1) + g_1^2 g_2 l_1 l_2 + g_1 g_2^2 l_1 l_2 + g_2^3 l_2 (l_2 + 1) \right) + g_2^3 k_2 \Big] + \cdots
\end{aligned} \tag{C.24}$$

where a WZW primary is labeled by two half integers $|l_1, l_2\rangle$. We do not show the full result here to fourth order in the total couplings $g_1, g_2$ but the full result in terms of slightly different coupling variables will be written in Appendix D.3.3.

# Appendix D

# WKB analysis

## D.1 Exact solutions of the harmonic oscillator ODE

In this section we study Wronskians of exact solutions of the ODE for Ising model discussed in 3.3

$$e^{-2\theta}\partial_x^2\psi(x) = (x^2-2)\psi(x) \tag{D.1}$$

which can be solved easily using, say, parabolic cylinder functions $U(a,z)$, the standard solutions of

$$\frac{\mathrm{d}^2 w}{\mathrm{d}z^2} - \left(\frac{1}{4}z^2 + a\right) w = 0 \tag{D.2}$$

It is related to the Whittaker and Watson's parabolic cylinder functions, commonly used in, say, Mathematica, by $D_\nu(z) = U\left(-\frac{1}{2}-\nu, z\right)$. It has the property that if $U(a,z)$ is a solution to (D.2), $U(a,\pm z)$ and $U(-a,\pm iz)$ are also solutions and all of them are entire functions of $a$ and $z$. Given the large $z$ asymptotics

$$U(a,z) \sim \mathrm{e}^{-\frac{1}{4}z^2} z^{-a-\frac{1}{2}} + \ldots, \qquad |\mathrm{phase}(z)| < \frac{3}{4}\pi \tag{D.3}$$

we identify $\psi_0$, the small solution along the ray of $e^{-\theta/2}$ defined in (3.37), to be

$$\psi_0 = 2^{-1/4} e^{\frac{e^\theta}{2}} e^{-\theta(2e^\theta+1)/4} U\left[-e^\theta, \sqrt{2}e^{\theta/2} z\right] \tag{D.4}$$

and infinite other solutions

$$\psi_n(x;\theta) \equiv \psi_0(x;\theta + i\pi n) \tag{D.5}$$

With the help of the Wronskians

$$(U(a,z),U(a,-z)) = \frac{\sqrt{2\pi}}{\Gamma\left(\frac{1}{2}+a\right)} \tag{D.6}$$

$$(U(a,z),U(-a,\pm iz)) = \mp i\exp[\pm i\pi\left(\frac{1}{2}a+\frac{1}{4}\right)] \tag{D.7}$$

We obtain the results in 3.3

$$i(\psi_n,\psi_{n+1}) = 1, \qquad i(\psi_{-1},\psi_2) = e^{-2\pi i e^{\theta}} \tag{D.8}$$

$$i(\psi_{-1},\psi_1) = \frac{\sqrt{2\pi}e^{\theta e^{\theta}-e^{\theta}}}{\Gamma(\frac{1}{2}+e^{\theta})} \tag{D.9}$$

## D.2 WKB analysis

### D.2.1 WKB asymptotics

Consider now the linear family

$$T(x) = \frac{U(x)}{\hbar^2} + \mathfrak{t}(x) \tag{D.10}$$

where $\mathfrak{t}(x)$ is a reference stress tensor and $U(x)$ a quadratic differential. When we have singularities, $\mathfrak{t}(x)$ should not be more singular than $U(x)$.

The solutions and transport coefficients for the corresponding Schröedinger equation have a very rich asymptotic behaviour as $\hbar \to 0$. This has been studied by a vast literature on the WKB approximation, culminating in the Voros analysis [81, 80, 79]. Useful insights can also be inherited by the WKB analysis of the Lax connection of Hitchin systems[88, 89], with the help of a certain "conformal limit" [118].

Take $\arg\hbar$ to lie in an interval $[\vartheta-\frac{\pi}{2},\vartheta+\frac{\pi}{2}]$. The "GMN-style" WKB analysis focusses on the complement $\overline{\mathcal{S}}_\vartheta$ of the "spectral network" $\mathcal{S}_\vartheta$ of flow lines

$$e^{-i\vartheta}\sqrt{U(x)}dx \in \mathbb{R} \tag{D.11}$$

originating from the zeroes of $U(x)$.

We will focus on situations where $U(x)$ has at least one regular or irregular singularity,

so that the flow lines generically end at the singularities. Each point $x_p$ away from $\mathcal{S}_\vartheta$ belongs to a flow line which goes from a singularity to a singularity. We can associate to $x_p$ two "small solutions" $\psi_\pm^{x_p}(x)$, defined up to rescaling, which are the parallel transport along the flow line of solutions which decay to zero as they approach the two singularities along the flow line.

For convenience, denote as $\psi_a(x)$ the collection of small solutions which are selected at the singularities by the above procedure. These will include all the $\psi_i^{x_s}(x)$ at all irregular singularities and one of the two monodromy eigenvectors $\psi_\pm^{x_s}(x)$ at the regular singularities. We normalize each of the $\psi_a(x)$ once and for all in some way at each singularity. Then we have

$$\psi_\pm^{x_p}(x) \sim \psi_{a_\pm^{x_p}}(x) \tag{D.12}$$

with some normalization coefficients we will now estimate.

A straightforward WKB analysis indicates that $\psi_\pm^{x_p}(x)$ are "WKB solutions" in the connected component of $\overline{\mathcal{S}}_\vartheta$ to which $x_p$ belongs, in the sense that as $\hbar \to 0$ with $\arg \hbar \in [\vartheta - \frac{\pi}{2}, \vartheta + \frac{\pi}{2}]$ one has

$$\psi_\pm^{x_p}(x) \sim \frac{1}{\sqrt{2p(x;\hbar)}} e^{\pm \int_{x_p}^x p(x;\hbar)} \tag{D.13}$$

where the WKB one form $p(x;\hbar)dx$ is recursive solution of

$$p(x;\hbar)^2 + \frac{3}{4}\frac{(\partial_x p(x;\hbar))^2}{p(x;\hbar)^2} - \frac{1}{2}\frac{\partial_x^2 p(x;\hbar)}{p(x;\hbar)} = \frac{U(x)}{\hbar^2} + \mathfrak{t}(x) \tag{D.14}$$

of the form

$$p(x;\hbar) = \frac{\sqrt{U(x)}}{\hbar} + \hbar p_1(x) + \hbar^3 p_2(x) + \cdots \tag{D.15}$$

We can compare the relative normalization of $\psi_\pm^{x_p}(x)$ and $\psi_{a_\pm^{x_p}}(x)$ and thus compute the asymptotic behaviour of the Wronskians

$$W(\psi_{a_+^{x_p}}(x), \psi_{a_-^{x_p}}(x))_{x_p} \tag{D.16}$$

where the two small solutions are compared along the flow line passing by $x_p$.

The Wronskian is controlled by the integral of $p(x;\hbar)$ along the flow line. In particular, the leading asymptotics are controlled by the periods of $ydx$ on the spectral curve $y^2 = U(x)$.

We can think about $p(x;\hbar)$ as the Jacobian of a local coordinate transformation which

maps the Schröedinger operator to $\partial_s^2 - 1$. It can be thus defined as an actual function as

$$p(x;\hbar) = \frac{W(\psi_{a_+^{x_p}}(x), \psi_{a_-^{x_p}}(x))_{x_p}}{2\psi_{a_+^{x_p}}(x)\psi_{a_-^{x_p}}(x)} \tag{D.17}$$

### D.2.2 Simple zeroes vs higher order zeroes

If $U(x)$ has only simple zeroes, the GMN-style analysis is sufficient to completely characterize the asymptotics of the transport data, as the (cross-ratios of) Wronskians along flow lines are a complete collection of local coordinates on the space of flat connections.

If $U(x)$ has higher-order zeros, then the Wronskians along flow lines are not enough and we need to compare solutions in the neighbourhood of the zeroes by a more refined analysis, which we will develop below. Even for simple zeroes, this analysis is an important sanity check on the GMN-style analysis.

#### Comparison at a simple zero

Near a simple zero $x_1$, we should be able to find a local coordinate $s$ such that the Schrödinger operator has the Airy form $\partial_s^2 - s$. In such a local coordinate, the solution that fast decays along the positive real axis is given by Airy function $\sqrt{2\pi}\mathrm{Ai}(s)$ with the large $s$ asymptotics

$$\frac{1}{\sqrt{2}} s^{-\frac{1}{4}} e^{-\frac{2}{3}s^{\frac{3}{2}}} \tag{D.18}$$

We define the three nice solutions as

$$\mathrm{Ai}_a(s) \equiv \sqrt{2\pi} e^{-\frac{\pi i a}{3}} \mathrm{Ai}(e^{\frac{2\pi i a}{3}} s) \tag{D.19}$$

which have Wronskian $W(\mathrm{Ai}_a(s), \mathrm{Ai}_{a+1}(s)) = -i$.

Back in the original coordinate, the corresponding solutions, defined in (D.13) take the form

$$\psi_a^{x_1}(x) = \frac{1}{\sqrt{\partial_x s(x;\hbar)}} \mathrm{Ai}_a\left(s(x;\hbar)\right) \tag{D.20}$$

The local coordinate must solve the equation

$$s(x;\hbar)\partial_x s(x;\hbar)^2 + \frac{3}{4}\frac{\partial_x^2 s(x;\hbar)^2}{\partial_x s(x;\hbar)^2} - \frac{1}{2}\frac{\partial_x^3 s(x;\hbar)}{\partial_x s(x;\hbar)} = \frac{U(x)}{\hbar^2} + \mathfrak{t}(x) \tag{D.21}$$

Using the asymptotics of the Airy functions we can match the $\psi_a^{x_1}(x)$ with the small solutions in the contiguous regions of $\overline{\mathcal{S}}_\vartheta$, i.e the three $\psi_a(x)$ associated to the three singularities reached by the flow lines originating at $x_1$. The Wronskians evaluated at $x_1$ obviously coincide with the Wronskians evaluated in the contiguous regions of $\overline{\mathcal{S}}_\vartheta$.

**Comparison at a zero of order $n$**

Near a zero $x_n$ of order $n$, we should be able to find a local coordinate $s$ such that the Schrödinger operator has the form $\partial_s^2 - s^n$. In such a local coordinate, a solution which decays along the positive real axis takes the form

$$A_n(s) = \sqrt{\frac{2s}{\pi(n+2)}} K_{\frac{1}{n+2}}\left(\frac{2}{n+2} s^{1+\frac{n}{2}}\right) \tag{D.22}$$

with large $s$ asymptotics

$$A_n(s) \sim \frac{1}{\sqrt{2} s^{n/4}} e^{-\frac{2}{n+2} s^{1+\frac{n}{2}}} \tag{D.23}$$

We can produce $n+2$ solutions by a rotation

$$A_{n;a}(s) = e^{-\frac{\pi i}{n+2} a} A_n(e^{\frac{2\pi i}{n+2} a} s) \tag{D.24}$$

Setting $n = 1$, we have $A_{1;a}(s) = \mathrm{Ai}_a(s)$. Because $A_n(s)$ only involves powers $s^{k(n+2)}$ and $s^{k(n+2)+1}$, we can write

$$A_{n;a}(s) = e^{-\frac{\pi i}{n+2} a} F_n(s) + e^{\frac{\pi i}{n+2} a} G_n(s) \tag{D.25}$$

where $F_n$ and $G_n$ involve respectively the $s^{k(n+2)}$ and $s^{k(n+2)+1}$ powers. It follows that

$$A_{n;a-1}(s) + A_{n;a+1}(s) = \left(e^{\frac{\pi i}{n+2}} + e^{-\frac{\pi i}{n+2}}\right) A_{n;a}(s) \tag{D.26}$$

The Wronskian of consecutive solutions is $-i$. With this, we can compute $(A_{n;a}, A_{n;b})$ for any $a$ and $b$.

We have corresponding solutions

$$\psi_a^{x_n}(x) = \frac{1}{\sqrt{\partial_x s(x;\hbar)}} A_{n;a}\left(s(x;\hbar)\right) \tag{D.27}$$

which satisfy the same linear relations. We can match them to the $n+2$ solutions $\psi_a(x)$ associated to the $n+2$ singularities reached by the flow lines originating at $x_n$.

### D.2.3 Examples:

**Quadratic potential**

$$\hbar^2 \partial_x^2 \psi(x) = (x^2 - E)\psi(x) \tag{D.28}$$

where $E > 0$. There are two first order zeros at $x = \pm\sqrt{E}$ and one irregular singularity at $x = \infty$. There are four anti-Stokes lines connected to the infinity, so three are four small solutions. We will normalize (and regularize) these four solutions, according to the recipe in the general discussion above. Let's start with $\psi_0(x)$, which is defined to be, up to the overall normalization, the unique solution that decays exponentially fast towards infinity along the positive real line. Let $I_0(x)$ be an anti-derivative of $\sqrt{x^2 - E}$, in an angular sector around the infinity that contains the positive real line, then the statement of the WKB approximation is that

$$\psi_0(x) \sim C_0 \frac{\sqrt{\hbar}}{\sqrt{2}(x^2 - E)^{1/4}} e^{-\frac{1}{\hbar} I_0(x)}, \tag{D.29}$$

for any $x$ on the WKB flow lines connected to the positive infinity. One might want to choose be $I_0(x) = \int_\infty^x \sqrt{y^2 - E} dy$. This integral clearly diverges, and we regularize by

$$I_0(x) = \lim_{L \to \infty} \left( \int_L^x dy \sqrt{y^2 - E} + \frac{L^2}{2} - \frac{1}{2} E \log L + D_0 \right) \tag{D.30}$$

It is useful to know its asymptotics towards $x \to \infty$.

$$\psi_0 \sim C_0 \frac{\sqrt{\hbar}}{\sqrt{2}(x^2 - E)^{1/4}} e^{-\frac{1}{\hbar} I_0(x; D_0)} \tag{D.31}$$

$$\overset{x \to \infty}{\sim} C_0 \frac{\sqrt{\hbar}}{\sqrt{2x}} e^{-\frac{1}{\hbar} D_0} x^{\frac{E}{2\hbar}} e^{-\frac{1}{\hbar} \frac{x^2}{2}} \tag{D.32}$$

and similarly we have a small solution $\psi_1$ in the direction $\sqrt{\hbar} e^{-\frac{i\pi}{2}}$.

$$\psi_1 \sim C_1 \frac{-i\sqrt{\hbar}}{\sqrt{2}(x^2 - E)^{1/4}} e^{\frac{1}{\hbar} I_1(x; D_1)} \tag{D.33}$$

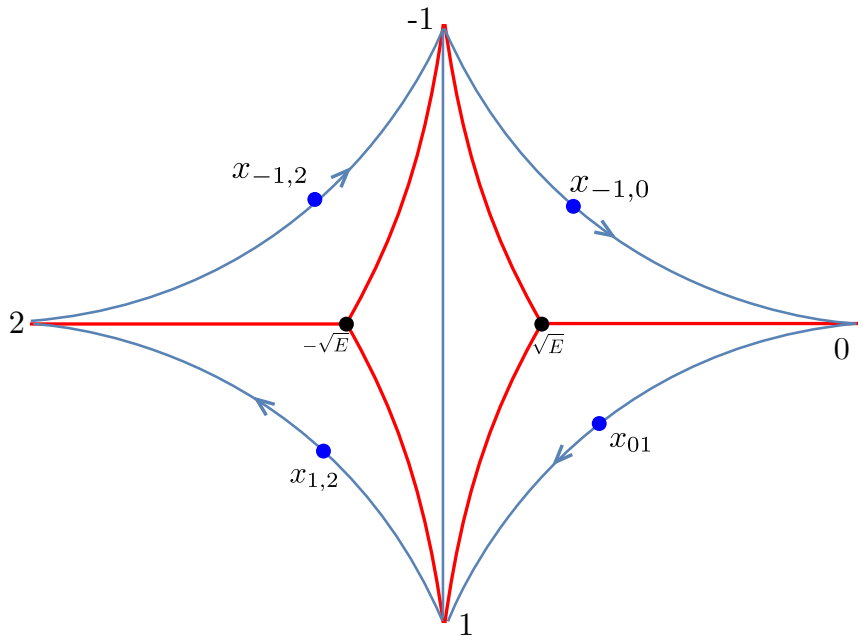


Figure D.1: WKB diagram for the differential equation (D.28). Generic flow lines and WKB lines are colored blue and red respectively.

where $I_1(x)$ is defined in the same way as $I_0(x)$ except $L$ is taken towards infinity in the direction $\sqrt{\hbar}e^{-\frac{i\pi}{2}}$. And we get two more constants $C_1$ and $D_1$ we need to fix. We fix them once and for all by defining $C_0 = 1$, $D_0 = -\frac{1}{4}(E + 2E\log 2 - E\log E)$ and for $n \in \mathbb{Z}$

$$\psi_n(x;\hbar) \equiv \psi_0(x;\hbar e^{-i\pi n}) \tag{D.34}$$

It is easy to check that $\psi_n(x;\hbar)$ satisfy the differential equation (D.28) and decrease exponentially fast along rays of direction $\sqrt{\hbar}e^{-\frac{in\pi}{2}}$. (D.34) fixes $D_n$ such that their dependence will drop out in calculating wronskians. This amounts to fixing the ambiguity of the ground state energy in the $T$ functions. The choice of $C_i$ is determined by matching the Wronkians with the standard normalization of $T$ functions. We can then compute the asymptotics of the Wronskians. For example,

$$(\psi_0, \psi_1) \sim -ie^{\frac{1}{\hbar}(I_1(x)-I_0(x))} = -i \tag{D.35}$$

evaluated at any point in the sector $\mathcal{S}_0$, where the asymptotics of both $\psi_0$ and $\psi_1$ are valid. We therefore just obtained the central result of Wronskians: it is controlled by the

(vanishing) contour integral from one asymptotic infinity to another

$$I_1(x) - I_0(x) = \lim_{L_0\to\infty_0, L_1\to\infty_1} \left( \int_{L_1}^{L_0} dy \sqrt{y^2 - E} + \frac{L_1^2}{2} - \frac{1}{2} E \log L_1 - \frac{L_0^2}{2} + \frac{1}{2} E \log L_0 \right) \tag{D.36}$$

The Wronskian is independent of $x$ and asymptotic in $\hbar$. Similarly, we have

$$(\psi_n, \psi_{n+1}) \sim -ie^{(-1)^n \frac{1}{\hbar}(I_{n+1}(x) - I_n(x))} = -i \tag{D.37}$$

We can now calculate the cross ratio

$$\chi_\gamma \equiv \frac{(\psi_0, \psi_1)\,(\psi_{-1}, \psi_2)}{(\psi_{-1}, \psi_0)\,(\psi_1, \psi_2)} \tag{D.38}$$

$$= \exp\left[ \frac{1}{\hbar} (I_{-1}(x_{-1,2}) - I_{-1}(x_{-1,0}) + I_0(x_{-1,0}) - I_0(x_{01}) + I_1(x_{01}) - I_1(x_{12}) + I_2(x_{12}) - I_2(x_{-1,2})) \right] \tag{D.39}$$

$$= \exp \frac{1}{\hbar} \oint dy\ \sqrt{y^2 - E} = e^{-2\pi i \frac{E}{2\hbar}} \tag{D.40}$$

We can confirm we have the correct Wronskians from a different perspective, discussed in the previous section, namely by comparing the asymptotics with the local solutions around zeros and evaluate the Wronskians using local solutions. Let's illustrate how it works. Around the zero $x = \sqrt{E}$, the Schrodinger equation is linearized as

$$\partial_s^2 \psi(s) = s\psi(s) \tag{D.41}$$

where $s = \alpha(x - \sqrt{E})$ and $\alpha = (2\sqrt{E}/\hbar^2)^{1/3}$. Three nice local solutions are given by $\mathrm{Ai}_a(s)$ defined in (D.19). Compare the normalization between $\mathrm{Ai}_a(s)$ and $\psi_n(x)$ in the region where both asymptotics (D.18) and linearized differential equation (D.41) are valid , we have

$$\psi_n(x) \sim \alpha^{-1/2} \mathrm{Ai}_n(\alpha x), \quad n = -1, 0, +1 \tag{D.42}$$

Since $(\mathrm{Ai}_n, \mathrm{Ai}_{n+1}) = -i$, we therefore arrive at the same expression (D.37). The same is true around the other zero $x = -\sqrt{E}$.

To evaluate (D.38), we need to know the relation between $\psi_3$ and $\psi_{-1}$. Note that the differential equation (D.28) is regular in the whole complex plane, so its solutions are entire functions, as we have found explicitly in Appendix D.1. [1] Therefore when we do the

[1] There is no problem with all the square root in the asymptotic expressions above since they are only

analytic continuation, there is no true monodromy but only *formal monodromy* coming from the asymptotics[2]. For example, $\psi_n$ and $\psi_{n+4}$ are proportional to each other since both are the (unique) fast decreasing solution along the ray of $\sqrt{\hbar}e^{-\frac{in\pi}{2}}$ and the relative coefficient is given by the formal monodromy

$$\psi_{n+4}(x) = e^{-2\pi i\Lambda_0}\psi_n(x),\ n \in \text{odd} \tag{D.43}$$

where $\Lambda_0 = -\frac{1}{2} - \frac{E}{2\hbar}$ is the exponent of the formal monodromy. When $n$ is even, we just replace $\hbar \to -\hbar$.

We are now ready to evaluate the spectral coordinate,

$$\chi_\gamma \equiv \frac{(\psi_0, \psi_1)\,(\psi_{-1}, \psi_2)}{(\psi_{-1}, \psi_0)\,(\psi_1, \psi_2)} \sim -e^{2\pi i\Lambda_0} = e^{-2\pi i\frac{E}{2\hbar}} \tag{D.44}$$

which agree with (D.40).

We can also take $E$ to be zero, namely

$$\hbar^2\partial_x^2\psi(x) = x^2\psi(x) \tag{D.45}$$

Two first order zeros collapse into a single second order zero. Our GMN-style analysis (D.31)-(D.44) still applies, namely the only spectral coordinate $\chi \sim 1$. To carry out the second perspective, we need to compare four small solutions $\psi_n$ to the local solutions $A_{2;a}$ defined in (D.24) around $x = 0$, a second order zero.

$$\partial_s^2\psi(s) = s^2\psi(s) \tag{D.46}$$

where $s = \hbar^{-1/2}x$. We therefore have the identification

$$\psi_n(x) \sim \hbar^{1/4}\mathrm{A}_{2;n}(\hbar^{-1/2}x) \tag{D.47}$$

Since $(\mathrm{A}_{2;n}, \mathrm{A}_{2;n+1}) = -i$ and the connection formula (D.194), it is easy to see $\chi_\gamma = 1$.

### Cubic potential

Let's study

$$\hbar^2\partial_x^2\psi(x) = (\frac{x^2}{2} - gx^3 - E)\psi(x) \tag{D.48}$$

expected to be valid in a particular angular sector. The examples in this article are (D.18) and (D.3)

[2]One can calculate the monodromy explicitly and see it is indeed trivial.

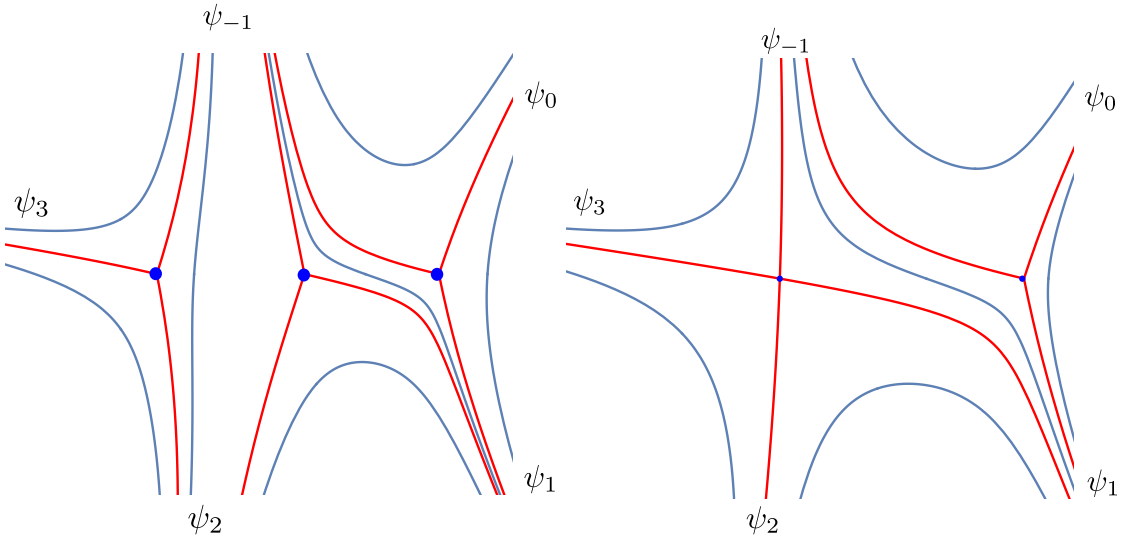


Figure D.2: WKB diagram for the differential equation (D.48). Generic flow lines and WKB lines are colored blue and red respectively.On the left, $E > 0$ and there are three simple zeros. On the right, $E = 0$ and there are one simple zero and one second order zero.

For simplicity, let's assume $g$ and $E$ are real positive. When $g$ is small enough, we have three zeros on the real axis denoted as $x_\pm$, $x_1$, which in small $g$ are

$$x_\pm \sim \pm\sqrt{2E} + \mathcal{O}(g), \quad x_1 \sim \frac{1}{2g} + \mathcal{O}(g) \tag{D.49}$$

We have five small solutions at the infinity

$$\psi_0 \sim \frac{\sqrt{\hbar}}{\sqrt{2}Q(x)^{1/4}} e^{-\frac{1}{\hbar}I_0(x;D_0)}, \qquad \psi_n(x;\hbar) \equiv \psi_0(x;\hbar e^{-i\pi n}) \tag{D.50}$$

where $Q(x) = \frac{x^2}{2} - gx^3 - E$, and the regularized integral is defined as

$$I_0(x) = \lim_{L\to\infty}\left(\int_L^x dy\sqrt{Q(y)} + \frac{2i}{5}\sqrt{g}L^{5/2} - \frac{iL^{3/2}}{6\sqrt{g}} - \frac{iL^{1/2}}{16g^{3/2}} + D_0\right) \tag{D.51}$$

Again, we have $(\psi_n, \psi_m) = -i$, whenever $\psi_n$ and $\psi_m$ are connected to the same zero and $n < m$. We have two spectral coordinates $\chi_A$ and $\chi_B$, which are controlled by the contour integral along cycles $\gamma_1$ and $\gamma_2$ for the exactly same reason in the quadratic case.

Let's see what happens if we take $E = 0$, where two zeros $x_\pm$ collide. We still have a closed contour $\gamma_1$, which can be shrunk to a point. So we have $\chi_A = 1$. On the other hand, we have problems evaluating the other spectral coordinate $\chi_B$ using GMN-style approach, since $\psi_2$ and $\psi_4$ are not connected by flow lines. This is where our second perspective is useful. $(\psi_{-1}, \psi_2)$ can be evaluated from the Wronskians of local solutions around the zeros. Specifically, we choose $D_0$ in $I_0(x)$ such that it matches exactly to the nice solution around the simple zero $x_1$. We therefore have $(\psi_{-1}, \psi_0) = (\psi_0, \psi_1) = (\psi_1, \psi_2) = -i$. $\psi_{-1}$ and $\psi_2$ will be matched with the local solutions around the double zero,

$$(\psi_{-1}, \psi_2) = e^{\frac{2}{\hbar}\int_{x_1}^0 dy\ \sqrt{Q(y)}}(A_{2;-1}, A_{2;1}) = -i\sqrt{2}e^{\frac{2}{\hbar}\int_{x_1}^0 dy\ \sqrt{Q(y)}} \tag{D.52}$$

Therefore we have our second spectral coordinate

$$\chi_B \equiv \frac{(\psi_0, \psi_1)\,(\psi_{-1}, \psi_2)}{(\psi_{-1}, \psi_0)\,(\psi_1, \psi_2)} = \sqrt{2}e^{\frac{2}{\hbar}\int_{x_1}^0 dy\ \sqrt{Q(y)}} \tag{D.53}$$

If all three zeros collide, spectral coordinate can be then evaluated using local solutions $\{A_{3,a}\}$ to be

$$\chi_A = \chi_B = \frac{1+\sqrt{5}}{2} \tag{D.54}$$

The same result can also be found via symmetry consideration discussed in [226, 88].

### D.2.4 WKB analysis for the WZW ODE/IM

**Matching around the zero:**

Because of our choice of normalization of the small solutions, involving the integral of the WKB momentum starting from $x = -\frac{1}{g}$, the small solution connected to the zero will match directly the small solutions of the local equation

$$e^{-2\theta}\partial_y^2\psi_{\rm loc}(y) = g^k e^{-\frac{2}{g}} y^k \psi_{\rm loc}(y) \tag{D.55}$$

and the Wronskians will match asymptotically the local Wronskians. In particular, we will have WKB asymptotics

$$i(\psi_n, \psi_{n'}) \sim \frac{e^{\frac{\pi i}{k+2}(n'-n)} - e^{-\frac{\pi i}{k+2}(n'-n)}}{e^{\frac{\pi i}{k+2}} - e^{-\frac{\pi i}{k+2}}} \equiv d^{(k)}_{n'-n} \tag{D.56}$$

whenever $n_0 \leq n \leq n_0 + k + 1$ and $n_0 \leq n' \leq n_0 + k + 1$.

**Matching around the negative infinity:**

We will use the Lambert W function $W(z)$, which is defined to be the principal solution of $z = W(z)e^{W(z)}$.

We can expand the potential around $x = x_0$, with real part of $x_0$ assumed to be large negative:

$$(1+gx)^k e^{2\theta+2x} = (1 + \frac{1}{\frac{1}{g}+x_0}\delta)^k e^{2\theta+2x_0+k\log(1+gx_0)} e^{2\delta} \tag{D.57}$$

where $\delta \equiv x - x_0$ is small. If $x_0$ is chosen such that $2\theta + 2x_0 + k\log(1+gx_0) = 0$, namely

$$x_0 \sim -\theta - \frac{1}{2}k\log(-g\theta) - \frac{k^2}{4}\frac{\log(-g\theta)}{\theta} + \mathcal{O}(\frac{1}{\theta}) \tag{D.58}$$

the potential behaves like $e^{2\delta}$ around $x_0$. The choice of imaginary part of $x_0$ is not unique. The possible choices lie on the special WKB lines. Let us choose one above the real axis, and label the line on which $x_0$ lies, to be $n_{x_0}$.

Therefore we would like to match the solutions in the large negative region around $x_0$ to solutions of the local equation

$$\partial_\delta^2 \psi(x_0+\delta) = e^{2\delta}\psi(x_0+\delta) \tag{D.59}$$

Because we normalize the small solutions as in (3.49), the WKB parallel transport of small solutions $\{\psi_n(x;\theta)\}_{n\leq n_0}$ from positive infinity to large negative $x$ will accumulate a WKB "phase"

$$-(-1)^n e^\theta \int_{-\frac{1}{g}}^{-\infty} e^x (1+gx)^{\frac{k}{2}} dx \tag{D.60}$$

computed along a contour which passes above the real axis. That evaluates to

$$(-1)^n e^\theta e^{i\frac{\pi k}{2}} e^{-\frac{1}{g}} g^{\frac{k}{2}} \Gamma(1+\frac{k}{2}) \equiv \frac{1}{2}(-1)^n e^\theta e^{i\frac{\pi k}{2}} m_k(g) \tag{D.61}$$

where we define the function

$$m_k(g) \equiv e^{-\frac{1}{g}} g^{\frac{k}{2}} \Gamma\left(1+\frac{k}{2}\right) \tag{D.62}$$

Thus we expect to match the small solutions to Bessel functions as

$$\psi_n \sim e^{\frac{1}{2}(-1)^n e^{\theta} e^{i\frac{\pi k}{2}} m_k(g)} \left( \frac{1}{\sqrt{\pi}} K_0(e^{x-x_0}) - \pi i (n - n_{x_0}) \frac{1}{\sqrt{\pi}} I_0(e^{x-x_0}) \right) \tag{D.63}$$

for a WKB line above the real axis, i.e. $n \leq n_0$, where the relative coefficients are fixed by requiring $\psi_n$ to decrease asymptotically fast along the corresponding special WKB lines. Note the shift $n_{x_0}$ in the coefficient from (3.59). For a WKB line below the real axis, i.e. $n \geq n_0 + k + 1$, we have

$$\psi_n \sim e^{\frac{1}{2}(-1)^n e^{\theta} e^{-i\frac{\pi k}{2}} m_k(g)} \left( \frac{1}{\sqrt{\pi}} K_0(e^{x-x_0}) - \pi i (n - n_{x_0} - k) \frac{1}{\sqrt{\pi}} I_0(e^{x-x_0}) \right) \tag{D.64}$$

Recall that $(K_0(e^x), I_0(e^x)) = 1$, we finally estimate

$$i(\psi_n, \psi_{n'}) \sim e^{\frac{(-1)^n + (-1)^{n'}}{2} e^{\theta} e^{i\frac{\pi k}{2}} m_k(g)} (n' - n) \tag{D.65}$$

whenever $n \leq n_0$ and $n' \leq n_0$.

Similarly, we have

$$i(\psi_n, \psi_{n'}) \sim e^{\frac{(-1)^n + (-1)^{n'}}{2} e^{\theta} e^{-i\frac{\pi k}{2}} m_k(g)} (n' - n) \tag{D.66}$$

whenever $n \geq n_0 + k + 1$ and $n' \geq n_0 + k + 1$. Notice the change in the phase factor in the exponential.

Finally, if $n \leq n_0$ and $n' \geq n_0 + k + 1$ we get

$$i(\psi_n, \psi_{n'}) \sim e^{\frac{(-1)^n e^{i\frac{\pi k}{2}} + (-1)^{n'} e^{-i\frac{\pi k}{2}}}{2} e^{\theta} m_k(g)} (n' - n - k). \tag{D.67}$$

Note that $n_{x_0}$ doesn't appear in any of the Wronskian, as expected.

If $n = n_0$ and $n' = n_0 + k + 1$ we have

$$i(\psi_{n_0}, \psi_{n_0+k+1}) \sim 1 = d^{(k)}_{k+1} \tag{D.68}$$

from both estimates. This is an useful sanity check.

If a Wronskian does not belong to the above ranges we can use Plücker formulae to relate it to the ones that belong to the above ranges and obtain the WKB asymptotics. One can easily get convinced that all Wronskians can be obtained this way. For example,

say that $n_0 \leq n \leq n_0 + k + 1$ and $n' \geq n_0 + k + 1$. Then we can write

$$i(\psi_n, \psi_{n'}) = -(\psi_n, \psi_{n'})(\psi_{n_0}, \psi_{n_0+k+1}) = -(\psi_{n_0}, \psi_n)(\psi_{n_0+k+1}, \psi_{n'}) - (\psi_n, \psi_{n_0+k+1})(\psi_{n_0}, \psi_{n'}) \tag{D.69}$$

which can be written as

$$\begin{aligned} i(\psi_n, \psi_{n'}) \sim & d^{(k)}_{n_0+k+2-n} e^{\frac{(-1)^{n_0+k+1}+(-1)^{n'}}{2} e^{-i\frac{\pi k}{2}} e^{\theta} m_k(g)} (n' - n_0 - k - 1) + \\ & + d^{(k)}_{n_0+k+1-n} e^{\frac{(-1)^{n_0+k}+(-1)^{n'}}{2} e^{-i\frac{\pi k}{2}} e^{\theta} m_k(g)} (n' - n_0 - k) \end{aligned} \tag{D.70}$$

Notice that either of the two exponential factors is trivial, as either $(-1)^{n_0+k+1}+(-1)^{n'} = 0$ or $(-1)^{n_0+k} + (-1)^{n'} = 0$. The two summands will exchange dominance whenever $e^{-i\frac{\pi k}{2}} e^{\theta}$ becomes pure imaginary.

Similarly if $n \leq n_0$ and $n_0 \leq n' \leq n_0 + k + 1$ we can write

$$i(\psi_n, \psi_{n'}) = -(\psi_n, \psi_{n_0})(\psi_{n'}, \psi_{n_0+k+1}) - (\psi_n, \psi_{n_0+k+1})(\psi_{n_0}, \psi_{n'}) \tag{D.71}$$

which can be written as

$$\begin{aligned} i(\psi_n, \psi_{n'}) \sim & d^{(k)}_{n'+1-n_0} e^{\frac{(-1)^{n}+(-1)^{n_0}}{2} e^{\theta} e^{i\frac{\pi k}{2}} m_k(g)} (n_0 - n) + \\ & + d^{(k)}_{n'-n_0} e^{\frac{(-1)^{n}+(-1)^{n_0+1}}{2} e^{i\frac{\pi k}{2}} e^{\theta} m_k(g)} (n_0 + 1 - n) \end{aligned} \tag{D.72}$$

Finally, we should specify the value of $n_0$:

- If $k$ is odd, the WKB analysis jumps whenever $e^{\theta}$ is pure imaginary. Real $\theta$ is not "special" and can be used as a starting point for the WKB analysis. Then $n_0 = -\frac{k+1}{2}$.
- If $k$ is even, then the WKB analysis jumps whenever $e^{\theta}$ is real. If we sit at $\theta$ with imaginary part $i\frac{\pi}{2}$ then $n_0 = -\frac{k}{2} - 1$, while if we sit at $\theta$ with imaginary part $-i\frac{\pi}{2}$ then $n_0 = -\frac{k}{2}$.

## D.3 Perturbative solutions of ODE

### D.3.1 $SU(2)_k$ vacuum expectation value

The Schrodinger equation for the vacuum expectation value of line defects in the $\mathfrak{su}(2)_k$ WZW model is

$$e^{-2\theta}\partial_x^2\psi(x) = (1+gx)^k e^{2x}\psi(x).$$

The T function

$$T_n(\theta) = i\Big(\psi(x;\theta - \frac{i\pi n}{2}), \psi(x;\theta + \frac{i\pi n}{2})\Big)$$

is defined as the Wronskian of the wavefunctions with shifted $\theta$ arguments; by general arguments this quantity is independent of $x$. The label $n$ in this section is equal to the dimension of the representation of $SU(2)$ and is related to the spin label $j$ in the direct perturbative line defect calculation by $n = 2j+1$.

The differential equation can be rearranged such that it only depends on a particular combination of $g$ and $\theta$. Upon shifting $x$ by $-1/g$,

$$g^{-k}e^{2/g}e^{-2\theta}\partial_x^2\psi(x) = x^k e^{2x}\psi(x),$$

so the wavefunction after the shift of x only depends on the combination $g^{k/2}e^{-1/g}e^{\theta}$. It is helpful to collect this quantity into an effecive coupling $g_{\text{eff}}(\theta)$ as

$$g_{\text{eff}}(\theta)^{k/2}e^{-1/g_{\text{eff}}(\theta)} = g^{k/2}e^{-1/g}e^{\theta},$$

admitting the $g$-expansion

$$g_{\text{eff}}(\theta) = g + \theta g^2 + \theta(\theta - \frac{k}{2})g^3 + \theta(\theta^2 - \frac{5}{4}k\theta + \frac{k^2}{4})g^4 + \cdots .$$

Since $T_n(\theta)$ is independent of $x$, the perturbative regime to be compared with the direct two-dimensional line defect computation can be characterized by the asymptotics of the wavefunction at large negative $x$. In this limit, the wavefunction $\psi(x;\theta)$ exhibits simple linear behavior in x and can be parametrized up to exponential corrections as

$$\psi(x;\theta) \sim -Q(\theta)(x + \frac{1}{g}) - \tilde{Q}(\theta)$$

in terms of auxiliary functions $Q$, $\tilde{Q}$. This parametrization realizes the QQ relations for $T_n$:

$$T_n(\theta) = i\Big[Q(\theta + \frac{i\pi n}{2})\tilde{Q}(\theta - \frac{i\pi n}{2}) - Q(\theta - \frac{i\pi n}{2})\tilde{Q}(\theta + \frac{i\pi n}{2})\Big].$$

In the above, we included the shift of $x$ so that both $Q$ and $\tilde{Q}$ are functions of $g_{\text{eff}}(\theta)$ only. Then we can express $Q$ and $\tilde{Q}$ in the general form

$$Q(\theta) = \frac{1}{\sqrt{\pi}}(1 + q_1 g_{\text{eff}}(\theta) + q_2 g_{\text{eff}}(\theta)^2 + \cdots)$$

$$\tilde{Q}(\theta) = \frac{1}{\sqrt{\pi}}(-\frac{1}{g_{\text{eff}}(\theta)} + \tilde{q}_0 + \tilde{q}_1 g_{\text{eff}}(\theta) + \cdots)$$

such that the $\psi$ asymptotics receive $g_{\text{eff}}$-corrections to its slope as well as to its constants. In fact, normalizing the T function as $T_1 = 1$ determines the expansion coefficients of $Q$ in terms of that of $\tilde{Q}$. Doing so, it turns out that $T_n$ only depend on $\tilde{q}_i$ starting at $\mathcal{O}(g^4)$:

$$T_n(\theta) = n - \frac{\pi^2}{12} kn(n^2-1)g^3 + \frac{\pi^2}{24} kn(n^2-1)(3k - 6\theta - 2\tilde{q}_0 + 8\tilde{q}_1)g^4 + \cdots .$$

To determine the coefficients, we proceed with the systematic order-by-order solution of the Schrodinger equation.

Let us express the wavefunction $\psi(x;\theta)$ as a series $\psi = \sum_{i=0}^{\infty} g^i \psi^i$ in $g$ and perform a weak coupling expansion of the Schrodinger equation around UV fixed point $g = 0$:

$$\mathcal{O}(1): \qquad e^{-2\theta}\partial_x^2 \psi^{(0)} = e^{2x}\psi^{(0)}$$

$$\mathcal{O}(g): \qquad e^{-2\theta}\partial_x^2 \psi^{(1)} = e^{2x}(\psi^{(1)} + kx\psi^{(0)})$$

and so on. We only require up to $\mathcal{O}(g)$ to compare with the direct perturbative calculation. The ambiguities in the solutions $\psi^{(i)}$ coming from the integration constants are fixed by imposing that the solution decays exponentially and it does so in a very particular manner as to agree with the WKB asymptotics given in the main body of the text.

As explained in the main body of the text, the unique solution at $\mathcal{O}(1)$ satisfying these constraints is given in terms of a Bessel function

$$\psi^{(0)}(x;\theta) = \frac{1}{\sqrt{\pi}} K_0(e^{x+\theta}).$$

The large negative $x$ behavior of $\psi^{(0)}(x;\theta)$ is

$$\psi^{(0)}(x;\theta) \sim -\frac{1}{\sqrt{\pi}}(x + \theta + \gamma - \log 2)$$

and so $\tilde{q}_0 = -\frac{k}{4} + \gamma - \log 2$.

The solution at $\mathcal{O}(g)$, up to an integration constant $c(\theta)$, is

$$\psi^{(1)}(x;\theta) = -\frac{k}{\sqrt{\pi}}\Bigg[I_0(e^{x+\theta})\int_x^\infty K_0(e^{x'+\theta})^2 x' e^{2(x'+\theta)}dx' \\ + K_0(e^{x+\theta})\int_{c(\theta)}^x K_0(e^{x'+\theta})I_0(e^{x'+\theta})x' e^{2(x'+\theta)}dx'\Bigg]$$

In the equation, $I_0(e^{x+\theta})$ diverges exponentially at large positive $x$, so upper limit of the first integral in the above has been chosen such that the solution decays exponentially in that limit. It is possible to fix the remaining constant $c(\theta)$ as at $\mathcal{O}(1)$ such that the total solution matches with the WKB asymptotics. However, a simpler way (which works at least at this order) is to notice that our asymptotic parametrization of $\psi$ in terms of $Q$, $\tilde{Q}$ picks out a coefficient multiplying $x$ which is constant and is in particular independent of $\theta$. At $\mathcal{O}(g)$, such a constant is equal to $-\frac{k}{4\sqrt{\pi}}$. Note further that only $K_0(e^{x+\theta})$ contributes a term proportional to $x$ (more precisely, $-\frac{x}{\sqrt{\pi}}$) in the limit $x \to -\infty$. It follows that, according to our parametrization of the wavefunction, $c(\theta)$ must be chosen such that the integral multiplying $K_0(e^{x+\theta})$ is equal to $1/4$ at $x \to -\infty$. We can simply take such a condition to be the definition of $c(\theta)$, and this renders the precise form of $c(\theta)$ unnecessary.

The large negative $x$ behavior of $\psi^{(1)}$ is then

$$\psi^{(1)}(x;\theta) \sim -\frac{k}{4\sqrt{\pi}}(x - \theta - 2 - \gamma + \log 2)$$

and $\tilde{q}_1 = \frac{k^2}{32} - \frac{k}{2}(\frac{3}{2} + \gamma - \log 2)$.

Therefore, with our choice of parametrization at $x \to -\infty$, $T_n$ is

$$T_n(\theta) = n - \frac{\pi^2}{12}kn(n^2-1)g^3 + \frac{\pi^2}{4}kn(n^2-1)(\frac{5}{8}k - \theta - 1 - \gamma + \log 2)g^4 + \cdots .$$

It is possible to choose a renormalization scheme in the direct two-dimensional calculation such that the vacuum expecation value of the line defect in the $SU(2)_k$ WZW model matches with the above result from the Schrodinger equation. Namely, a shift of the coupling as

$$g \to \lambda g + \lambda^2 g^2(-2\log\epsilon + k - 2\gamma - 2\log\pi) + \cdots$$

with $2\pi R = e^\theta$ and the choice $\lambda = -1/2$, results in the above formula for $T_n$. Constants in the expectation value which are independent of $\theta$ can always be accounted for by trivial

shifts of the coupling. However, it is still nontrivial that $\tilde{q}_1$ can directly be verified to be independent of $\theta$ and the precise $\theta$ dependence matches as this term is robust to local counterterms. Hirota bilinear relations are satisfied rather trivially at the level of the vev, as there is no nontrivial $n$ dependence apart from that coming from an overall Dynkin index factor. However, Hirota is nontrivial at the level of the expectations between primary states, which we now proceed to show.

### D.3.2 $SU(2)_k$ expectation value between primaries

Based on evidence from existing literature [116, 117], we propose that the Schrodinger equation

$$\partial_x^2\psi_l(x) = \Big[e^{2\theta}e^{2x}(1+gx)^k + \frac{l(l+1)}{(x+1/g)^2}\Big]\psi_l(x)$$

yields the solution whose Wronskian give rise to the T function $T_{n,l}(\theta) := \langle\hat{T}_n(\theta)\rangle_l = \langle l|\hat{T}_n(\theta)|l\rangle$ evaluated between primary states with level $l$. $T_{n,l}(\theta)$ are defined again in terms of the wavefunctions as

$$T_n(\theta) = i\Big(\psi_l(x;\theta - \frac{i\pi n}{2}), \psi_l(x;\theta+\frac{i\pi n}{2})\Big).$$

An asymptotic parametrization of $\psi_l(x;\theta)$ can be determined by analyzing the solutions to the degenerations of the Schrodinger equation at $x \to -\infty$ and at $g \to 0$, and then carefully matching the solutions in the regime of interest $1/g \gg -x \gg 0$. The resulting parametrization is

$$\psi_l(x;\theta) \sim -\frac{x}{2l+1}\Big[\frac{l+1}{g^l}Q_l(\theta) - g^{l+1}l\tilde{Q}_l(\theta)\Big] - \frac{1}{2l+1}\Big[\frac{1}{g^{l+1}}Q_l(\theta) + g^l\tilde{Q}_l(\theta)\Big]$$

where $Q_l$, $\tilde{Q}_l$ now gain an $l$-dependence in their powers of $g_{\text{eff}}(\theta)$ as

$$\begin{aligned}
Q_l(\theta) &= \frac{g_{\text{eff}}(\theta)^l}{\sqrt{\pi}}(1 + q_{l,1}g_{\text{eff}}(\theta) + \cdots)\\
\tilde{Q}_l(\theta) &= \frac{g_{\text{eff}}(\theta)^{-l}}{\sqrt{\pi}}(-\frac{1}{g_{\text{eff}}(\theta)} + \tilde{q}_{l,0} + \tilde{q}_{l,1}g_{\text{eff}}(\theta) + \cdots).
\end{aligned}$$

This parametrization realizes the QQ relations for $T_{n,l}$, with an extra normalization con-

stant:

$$T_n(\theta) = \frac{i}{2l+1}\Big[Q_l(\theta+\frac{i\pi n}{2})\tilde{Q}_l(\theta-\frac{i\pi n}{2}) - Q_l(\theta-\frac{i\pi n}{2})\tilde{Q}_l(\theta+\frac{i\pi n}{2})\Big].$$

Normalizing again as $T_{1,l}=1$, $T_{n,l}(\theta)$ now depends on $\tilde{q}_{l,i}$ starting at $\mathcal{O}(g^3)$:

$$\begin{aligned}T_{n,l}(\theta) = n &- \frac{\pi^2}{6}n(n^2-1)l(l+1)g^2\\ &+\frac{\pi^2}{12}n(n^2-1)\Big[k(2l^2+l-1)-4l\big((l+1)\theta+\tilde{q}_{l,0}\big)\Big]g^3\\ &-\frac{\pi^2}{360}n(n^2-1)\Big[45k^2(l^2-1)-30k[(l+1)(8l-3)\theta+(4l-1)\tilde{q}_{l,0}]\\ &+l(l+1)[7\pi^2l^2+27\pi^2l+26\pi^2-3(l^2+l+3)\pi^2n^2+180\theta^2]\\ &+120l\tilde{q}_{l,0}(\tilde{q}_{l,0}+3\theta)+120\tilde{q}_{l,1}(2l-1)\Big]g^4+\cdots.\end{aligned}$$

Let us expand $\psi_l=\sum_{i=0}^{\infty}g^i\psi_l^{(i)}$ as before and obtain an order-by-order weak coupling expansion of the differential equation. As is easy to see, the $l$-dependent term drops out and we end up with the same equations up to $\mathcal{O}(g)$ as in the vev case:

$$\mathcal{O}(1): \qquad e^{-2\theta}\partial_x^2\psi_l^{(0)} = e^{2x}\psi_l^{(0)}$$

$$\mathcal{O}(g): \qquad e^{-2\theta}\partial_x^2\psi_l^{(1)} = e^{2x}(\psi_l^{(1)}+kx\psi_l^{(0)})$$

and so on. Note that the equations do receive contributions from the $l$-dependent term starting at $\mathcal{O}(g^2)$, though we won't need them for the purposes of comparing to the line defect calculation. That the $\mathcal{O}(1)$, $\mathcal{O}(g)$ equations remain the same as the vev case indicates $\psi_l^{(0)}=\psi^{(0)}$ and $\psi_l^{(1)}=\psi^{(1)}$. The only difference then is the parametrization of the wavefunction at $x\to-\infty$ and thus the definition of the coefficients $\tilde{q}_{l,i}$. The resulting coefficients are

$$\begin{aligned}\tilde{q}_{l,0} &= -\frac{k}{4}+(l+1)(\gamma-\log 2)\\ \tilde{q}_{l,1} &= \frac{1}{96}\Big[3k^2-8l(l+1)[\pi^2+6(\gamma-\log 2)^2]-24k[3+2l+(l+2)(\gamma-\log 2)]\Big]\end{aligned}$$

and the expectation value is

$$\begin{aligned}T_{n,l}(\theta) = n &- \frac{\pi^2}{6} n(n^2-1)l(l+1)g^2 \\ &+ \frac{\pi^2}{12} n(n^2-1)\Big[k(2l(l+1)-1) - 4l(l+1)(\theta+\gamma-\log 2)\Big]g^3 \\ &- \frac{\pi^2}{1440} n(n^2-1)\Big[45k^2(4l(l+1)-5) \\ &+ 4l(l+1)[7\pi^2 l(l+1) + 36\pi^2 - 3(l(l+1)+3)\pi^2 n^2 + 180(\theta+\gamma-\log 2)^2] \\ &+ 120k[3\theta + 3 - \gamma(8l(l+1)-3) - 3\log 2 - 4l(l+1)(2\theta+1-2\log 2)]\Big]g^4 + \cdots .\end{aligned}$$

Now we must verify from the results of the direct line defect calculation that (1) a renormalization scheme can be chosen such that the it matches the above $T_{n,l}(\theta)$ from the Schrodinger analysis and (2) the renormalized result satisfies Hirota bilinear relations. Both are nontrivial statements, respectively as local counterterms cannot depend on $\theta$ or $l$ and as $T_{n,l}(\theta)$ has a nontrivial $n$ dependence.

With some work, both (1) and (2) can be verified to hold, where the Schrodinger solution determines a unique renormalization scheme for the defect. The shift in the coupling

$$\begin{aligned}g \to \lambda g &+ \lambda^2 g^2\Big[-2\log\epsilon + k - 2\gamma - 2\log\pi\Big] \\ &+ \lambda^3 g^3\Big[4(\log\epsilon)^2 - 2(3k - 4\gamma - 4\log\pi)\log\epsilon + k^2 \\ &- 2k(2+3\gamma+3\log\pi) + \frac{\pi^2}{3}(2-n^2) + 4(\gamma+\log\pi)^2\Big] + \cdots\end{aligned}$$

with $\lambda = -1/2$ in the perturbative calculation yields an expectation value matching $T_{n,l}(\theta)$, and the result satisfies Hirota.

### D.3.3 Multichannel expectation values

In the multichannel Kondo problem with $m$ channels, i.e. $\prod_{i=1}^m su(2)_{k_i}$, we are interested in studying the perturbative sector where all couplings $g_i$ with $i = 1, 2, \cdots, n$ become small. Therefore a convenient thing to do is to have an overall small constant $g$ which encodes the scaling behavior of all couplings $g_i$ and parametrize the couplings as $g_i = \frac{g}{1+gz_i}$. The expansion can be done with respect to a single infinitesimal parameter $g$ and other finite parameters $z_i$ can be used to index the positions of the individual couplings.There should

be, however, one constraint as there are now a total of $m+1$ parameters $(g, z_i)$. We take this to be, e.g. $\sum_i z_i = 0$. Note that we can invert the above relation to get $\frac{1}{g_i} = \frac{1}{g} + z_i$ or $\frac{1}{g} = \frac{1}{m}\sum_i \frac{1}{g_i}$ indicating that the (inverse of) $g$ is the mean of (inverses of) $g_i$.

We propose that the Schrodinger equation for the ground states of the $m$-channel Kondo problem is

$$\partial_x^2\psi(x) = \Big[e^{2\theta+2x}\prod_{i=1}^{m}(1+g_i x)^{k_i} + u(x)^2 - \partial_x u(x)\Big]\psi(x)$$

where

$$u(x) = \sum_{i=1}^{m}\frac{l_i}{x+1/g_i}.$$

Another choice of $u$, namely $\tilde{u}(x) = \sum_{i=1}^{m}\frac{-l_i-1}{x+1/g_i}$, works as well but we proceed with $u$ rather than $\tilde{u}$.

Substituting for $g_i$ as described above and shifting $x \to x - 1/g$, one gets

$$\partial_x^2\psi(x) = \left[e^{2\theta}e^{-2/g}g^{\sum_i k_i}\prod_i(1+gz_i)^{-k_i}e^{2x}\prod_i(x+z_i)^{k_i} + \Big(\sum_i\frac{l_i}{x+z_i}\Big)^2 + \sum_i\frac{l_i}{(x+z_i)^2}\right]\psi(x).$$

This indicates that the solutions only depend on $z_i$ and the following combination which can be absorbed into an effective coupling $g_{\rm eff}(\theta)$:

$$e^{-1/g_{\rm eff}(\theta)}g_{\rm eff}(\theta)^{\sum_i k_i/2} \equiv e^{\theta}e^{-1/g}g^{\sum_i k_i/2}\prod_i(1+gz_i)^{-k_i/2}.$$

The effective coupling $g_{\rm eff}(\theta)$ now depends on $m$ as well as $\theta$. Its expansion in $g$ is

$$g_{\rm eff}(\theta) = g + \theta g^2 + \theta(\theta - \frac{1}{2}\sum_i k_i)g^3 + \frac{1}{4}\Big[\theta(4\theta - \sum_i k_i)(\theta - \sum_i k_i) + \sum_i z_i^2\Big]g^4 + \cdots .$$

The $g$-expansion of the Schrodinger equation to $\mathcal{O}(g)$ does not depend on $u$. Hence the asymptotic solutions $\psi^{(0)}$ and $\psi^{(1)}$ of $\psi = \sum_i g^i\psi^{(i)}$ are equal to that for the vevs of the single-channel Kondo problem, with $k$ substituted for $\sum_i k_i$.

For the rest of this subsection, we focus on the case $m = 2$, or $su(2)_{k_1} \times su(2)_{k_2}$, for simplicity. As was done for the single-channel primaries, the asymptotic parametrization of the multichannel solution $\psi$ in terms of $Q$,$\tilde{Q}$ can be determined by analyzing the large negative $x$ limit of the Schrodinger equation, i.e. the limit where only the $u$-dependent

terms survive, and then considering the solution in the regime $1/g \gg -x \gg 0$. This yields the parametrization

$$\psi(x;\theta) \sim -\frac{1}{2(l_1+l_2)+1}\Bigg\{\frac{Q(\theta)}{g^{l_1+l_2+1}}\Big[1+gx\Big(1+2(l_1+l_2)-\frac{l_1}{1+gz_1}-\frac{l_2}{1+gz_2}\Big)\Big] \\ +\tilde{Q}(\theta)g^{l_1+l_2}\Big[1-gx\Big(\frac{l_1}{1+gz_1}+\frac{l_2}{1+gz_2}\Big)\Big]\Bigg\}$$

with Q-functions

$$Q(\theta) = \frac{g_{\text{eff}}(\theta)^{l_1+l_2}}{\sqrt{\pi}}(1+q_1 g_{\text{eff}}(\theta)+\cdots)$$

$$\tilde{Q}(\theta) = \frac{g_{\text{eff}}(\theta)^{-l_1-l_2}}{\sqrt{\pi}}(-\frac{1}{g_{\text{eff}}(\theta)}+\tilde{q}_0+\tilde{q}_1 g_{\text{eff}}(\theta)+\cdots).$$

The multichannel function $T_n(\theta)$ is defined similarly as for the single-channel primaries, with the replacement $l \to l_1+l_2$.

As before, the normalization $T_1 = 1$ expresses $q_i$ in terms of $\tilde{q}_i$ and perturbative solutions $\psi^{(0)}$, $\psi^{(1)}$ can be compared with the asymptotic parametrization to obtain the coefficients

$$\begin{aligned}\tilde{q}_0 =& -\frac{k_1+k_2}{4}+(l_1+l_2+1)(\gamma-\log 2)\\ \tilde{q}_1 =& \frac{1}{96}\Big[3(k_1^2+k_2^2)-24(k_1+k_2)[(\gamma-\log 2+2)(l_1+l_2+2)-1]\\ &+6k_1k_2-8(l_1+l_2)(l_1+l_2+1)[\pi^2+6(\gamma-\log 2)^2]\Big]\end{aligned}$$

These coefficients suffice to determine the multichannel $T_n(\theta)$ function

$$
\begin{aligned}
T_n(\theta) &= n - g^2\Big[\frac{1}{6}n(n^2-1)\pi^2(l_1+l_2)(l_1+l_2+1)\Big] \\
&+ g^3\Big[\frac{1}{12}\pi^2 n(n^2-1)(k_1(2l_1^2+(4l_2+2)l_1+2l_2(l_2+1)-1) \\
&+ k_2(2l_2+2(l_1^2+2l_2l_1+l_1+l_2^2)-1)-4(l_1+l_2)(l_1+l_2+1)(t+\gamma-\log 2))\Big] \\
&- g^4\Big[\frac{\pi^2}{1440}n(n^2-1)[-30k_1(4(l_1+l_2)(-3k_2(l_1+l_2+1)+8(l_1+l_2+1)t \\
&+ 4(l_1+l_2-(l_1+l_2+1)\log(4)))+15k_2+16l_1+16l_2 \\
&+ 4\gamma(8l_2+8(l_1^2+2l_2l_1+l_1+l_2^2)-3)-12t-12+\log(4096)) \\
&- 120k_2(4(l_1+l_2)(2(l_1+l_2+1)t+l_1+l_2-2(l_1+l_2+1)\log(2))+4l_1+4l_2 \\
&+ \gamma(8l_2+8(l_1^2+2l_2l_1+l_1+l_2^2)-3)-3t-3+\log(8)) \\
&+ 45k_1^2(4l_1^2+(8l_2+4)l_1+4l_2(l_2+1)-5)+45k_2^2(4l_1^2+(8l_2+4)l_1+4l_2(l_2+1)-5) \\
&+ 4((l_1+l_2)(l_1+l_2+1)(\pi^2(-3(l_1^2+2l_2l_1+l_1+l_2^2+l_2+3)n^2+7(l_1+l_2)^2 \\
&+ 7l_1+7l_2+36)+180(t+\gamma-\log(2))^2]\Big]. \qquad \text{(D.73)}
\end{aligned}
$$

Comparing with the perturbative defect calculations, the following renormalization scheme with the shifts

$$
\begin{aligned}
g_1 &\to \lambda g_1 + \lambda^2 g_1^2[-2\log\epsilon - 2\gamma + k_1 - 2\log\pi - 2z_1] + \lambda^2 g_1 g_2[k_2] \\
&\quad + \lambda^3 g_1^3[4(\log\epsilon)^2 - 2(-4\gamma + 3k_1 - 4\log\pi - 4z_1)\log\epsilon + D_1] \\
&\quad + \lambda^3 g_1^2 g_2[-4k_2\log\epsilon + D_3] + \lambda^3 g_1 g_2^2[-2k_2\log\epsilon + D_5] + \lambda^3 g_2^3[D_7] \\
g_2 &\to \lambda g_2 + \lambda^2 g_2^2[-2\log\epsilon - 2\gamma + k_2 - 2\log\pi - 2z_2] + \lambda^2 g_2 g_1[k_1] \\
&\quad + \lambda^3 g_2^3[4(\log\epsilon)^2 - 2(-4\gamma + 3k_2 - 4\log\pi - 4z_2)\log\epsilon + D_2] \\
&\quad + \lambda^3 g_2^2 g_1[-4k_1\log\epsilon + D_4] + \lambda^3 g_2 g_1^2[-2k_1\log\epsilon + D_6] + \lambda^3 g_1^3[D_8]
\end{aligned}
$$

with $\lambda = -1/2$ and the conditions

$$\begin{aligned}
D_1 + D_3 + D_5 + D_7 =& -4k_1 z_1 - 2k_2 z_1 - 2k_2 z_2 + \gamma(-6k_1 - 6k_2 + 8(z_1 + \log\pi)) \\
&+ k_1^2 + 2k_2 k_1 - 4k_1 + k_2^2 - 4k_2 - 6k_1 \log\pi - 6k_2 \log\pi \\
&- \frac{1}{3}\pi^2\left(n^2 - 2\right) + 4z_1^2 + 2z_1 + 2z_2 + 8z_1 \log\pi + 4\gamma^2 + 4\log^2\pi \\
D_2 + D_4 + D_6 + D_8 =& -4k_2 z_2 - 2k_1 z_2 - 2k_1 z_1 + \gamma(-6k_2 - 6k_1 + 8(z_2 + \log\pi)) \\
&+ k_2^2 + 2k_1 k_2 - 4k_2 + k_1^2 - 4k_1 - 6k_2 \log\pi - 6k_1 \log\pi \\
&- \frac{1}{3}\pi^2\left(n^2 - 2\right) + 4z_2^2 + 2z_2 + 2z_1 + 8z_2 \log\pi + 4\gamma^2 + 4\log^2\pi
\end{aligned}$$

matches multichannel Schrodinger analysis and the result satisfies Hirota bilinear relations. In the above, the two auxiliary variables $z_1$ and $z_2$ can be identified by the condition $z_1 + z_2 = 0$.

## D.4 Details of UV expansion for excited states

In this appendix, we verify the claim (4.92) for a few examples explicitly by working perturbatively in $g$ to $O(g^4)$. Next, based on these examples, we summarize a general recipe in the case of zero twist $\alpha_+ = 0$. We then end this section with some remarks and checks with nonzero twist.

### D.4.1 Examples of UV perturbative matching

Let us perform a perturbative UV analysis of the proposed excited state Schrödinger equations and compare them to $SU(2)_k$ WZW line defects evaluated between certain excited states. We use the Chevalley basis rather than the orthonormal basis used in [1]. To establish notation, we write the change of basis explicitly:

$$J_n^a J_m^a = J_n^+ J_m^- + J_n^- J_m^+ + 2J_n^0 J_m^0 \tag{D.74}$$

$$f^{abc} J_n^a J_m^b J_l^c = 12i(J_n^{[+} J_m^- J_l^{0]}). \tag{D.75}$$

We will consider the following states as examples:

$$J_{-1}^+|0,k\rangle, \quad J_{-2}^+|0,k\rangle. \tag{D.76}$$

From the discussion in Subsection 4.3.3, for generic values of $k$, they are described by Miura $\lambda$-opers with

$$a_+^{(1)}(x) = -\frac{1}{x-w'}, \tag{D.77}$$

$$a_+^{(2)}(x) = \frac{1}{x-w} - \frac{1}{x-w_1'} - \frac{1}{x-w_2'}, \tag{D.78}$$

respectively. Note, however, that the state $J_{-2}^+|0,-1\rangle$ is a special case of (D.77) since, as we conjectured in 4.3.3, it corresponds to the generalized Miura $\lambda$-oper

$$a_+(x) = -\frac{1}{x}. \tag{D.79}$$

The left hand side of the claim (4.92) is an obvious, alebit tedious, task, namely to compute the $g$ expansion of the expectation value of the operator $\hat{T}_n(\theta)$ in a certain state. This operator was calculated in the Appendix E of [1]. Note that if we normalize the expectation values of the line defect as[3]

$$\langle T_n(\theta)\rangle_r := \frac{1}{r\kappa}\langle 0,k|J_r^-\hat{T}_n(\theta)J_{-r}^+|0,k\rangle \tag{D.80}$$

then the ordinary form of the Hirota bilinear relations

$$\left\langle T_n\left(\theta+\frac{i\pi}{2}\right)\right\rangle_r\left\langle T_n\left(\theta-\frac{i\pi}{2}\right)\right\rangle_r = 1+\langle T_{n+1}(\theta)\rangle_r\langle T_{n-1}(\theta)\rangle_r \tag{D.81}$$

holds.[4]

Finding the $g$ expansion of the Wronskian on the right hand side of (4.92) is not obvious. In [1], we proposed an approach based on a combination of various limits. The basic idea consists of two steps: (1) analyze the solution of the Schrödinger equation in the regime $1/g \gg -x$ and $-x \gg 0$ separately and (2) match the solutions in the intermediate region $1/g \gg -x \gg 0$.

We can recycle many of the result from [1] as modifications of the Schrödinger equation

[3] In this appendix only, we write the excited expectation values with angled brackets to emphasize that $\langle T_n(\theta)\rangle_r$ are quantities which are directly evaluated from the defect operator computed in [1]. The quantities we write as $T_n(\theta)$ in the perturbative analysis below correspond to the Wronskian result we obtain from the Schrödinger equation.

[4] One could choose not to use the normalization $\frac{1}{rk}$ in (D.80), but the Hirota relations would then have $(rk)^2$ in place of 1 and the following perturbative analyses acquire extra normalization factors.

by the potential terms do not contribute to the perturbative expansion of the differential equation at $O(1)$ and $O(g)$. Hence, we may use the direct evaluation result of the wavefunction in [1] given by

$$\psi = \psi^{(0)} + g\psi^{(1)} + \cdots \tag{D.82}$$

with

$$\psi^{(0)}(x;\theta) \sim -\frac{1}{\sqrt{\pi}}(x + \theta + \gamma - \log 2)$$
$$\psi^{(1)}(x;\theta) \sim -\frac{k}{4\sqrt{\pi}}(x - \theta - 2 - \gamma + \log 2)$$

at large negative $x$. Also, we introduce the effective coupling $g_{\text{eff}}(\theta)$ defined by [1]

$$g_{\text{eff}}(\theta)^{k/2} e^{-1/g_{\text{eff}}(\theta)} = g^{k/2} e^{-1/g} e^{\theta} \tag{D.83}$$

with the $g$ expansion

$$g_{\text{eff}}(\theta) = g + \theta g^2 + \theta\Big(\theta - \frac{k}{2}\Big)g^3 + \theta\Big(\theta^2 - \frac{5}{4}k\theta + \frac{k^2}{4}\Big)g^4 + \cdots . \tag{D.84}$$

**$J^+_{-1}|0,k\rangle$, one $w'$, no $w$**

For the case with one $w'$ and no $w$, the excited state equation is

$$\partial_x^2 \psi(x;\theta) = \left[e^{2\theta} g e^{-2/g} x^k e^{2x} + \frac{8}{(k+2x)^2}\right]\psi(x;\theta). \tag{D.85}$$

We propose that this equation encodes the excited line defect expectation value $\langle T_n(\theta)\rangle_1$. The perturbative analysis as an expansion in $g$ is done after shifting $x \to x + 1/g$.

The asymptotics of $\psi$ can be determined by carefully analyzing the solutions of the Schrödinger equation in the regime $1/g \gg -x \gg 0$. Doing so, the wavefunction can be parametrized as

$$\psi(x;\theta) \sim -\frac{1}{3g^2} Q(g_{\text{eff}})[1 + (k+2x)g] - \frac{g}{3}\tilde{Q}(g_{\text{eff}})\Big[1 - \frac{1}{2}(k+2x)g\Big], \tag{D.86}$$

where

$$Q(g_{\rm eff}) = \frac{g_{\rm eff}(\theta)}{\sqrt{\pi}}(1 + q_1 g_{\rm eff}(\theta) + \cdots), \tag{D.87a}$$

$$\tilde{Q}(g_{\rm eff}) = \frac{g_{\rm eff}(\theta)^{-1}}{\sqrt{\pi}}\Big( - \frac{1}{g_{\rm eff}(\theta)} + \tilde{q}_0 + \tilde{q}_1 g_{\rm eff}(\theta) + \cdots \Big). \tag{D.87b}$$

Before the shift $x \to x+1/g$, the dependence of $\psi$ on $g$ and $\theta$ combine into $g_{\rm eff}(\theta)$ such that $\psi$ becomes a function of $x$ and $g_{\rm eff}$ only. The explicit $g$ dependence in the parametrization of $\psi$ above comes purely from the shift $x \to x + 1/g$.

As the general analysis in the next subsection will suggest, the difference $\#w' - \#w$ is responsible for the various factors present above. The overall coefficient $1/3$ in the asymptotics of $\psi$ arises via the combination $(2(\#w' - \#w) + 1)^{-1}$, as does the overall power of $g_{\rm eff}^{\pm(\#w'-\#w)}$ in the expression of $Q$, $\tilde{Q}$.

As usual, the T-function can be expressed as the quantum Wronskian

$$T_n(\theta) = \frac{i}{3}\Big[Q\Big(\theta + \frac{i\pi n}{2}\Big)\tilde{Q}\Big(\theta - \frac{i\pi n}{2}\Big) - Q\Big(\theta - \frac{i\pi n}{2}\Big)\tilde{Q}\Big(\theta + \frac{i\pi n}{2}\Big)\Big]. \tag{D.88}$$

The coefficients $q_i$ can be expressed in terms of $\tilde{q}_i$ by imposing the condition $T_1 = 1$. The explicit expression of $T_n(\theta)$ up to $O(g^4)$ requires the knowledge of $\tilde{q}_0$ and $\tilde{q}_1$. Comparing the parameterization of $\psi$ in terms of $Q, \tilde{Q}$ with the direct perturbative evaluation up to $O(g)$, we obtain

$$\begin{aligned}
\tilde{q}_0 &= \frac{1}{4}(-5k + 8\gamma - 8\log 2) \\
\tilde{q}_1 &= -\frac{15k^2}{32} - \frac{1}{4}k(5 + \log 2) + \gamma\Big(\frac{k}{4} + \log 4\Big) - \frac{\pi^2}{6} - \gamma^2 - (\log 2)^2.
\end{aligned}$$

The full expression for $T_n(\theta)$ to $O(g^4)$ is then

$$\begin{aligned}
T_n(\theta) = n &- g^2\Big[\frac{1}{3}\pi^2 n(n^2-1)\Big] + g^3\Big[\frac{1}{12}\pi^2 n(n^2-1)(7k - 8\theta - 8\gamma + \log 256)\Big] \\
&- g^4\Big[\frac{1}{288}\pi^2 n(n^2-1)[195k^2 - 120k(5\theta + 1 - 5\log 2) - 24\gamma(25k \\
&- 24\theta + \log 16777216) + 8\pi^2(10 - 3n^2) + 288(\theta - \log 2)^2 + 288\gamma^2]\Big] + O(g^5).
\end{aligned}$$

This expression satisfies the Hirota bilinear relations and has been verified to match the

perturbative line defect computation for $\langle T_n(\theta)\rangle_1$ in a suitable renormalization scheme, where $g$ is shifted as

$$\begin{aligned} g \to{}& \lambda g + \lambda^2 g^2 \Big[k - 2\log\epsilon - 2\gamma - 2\log\pi\Big] \\ &+ \lambda^3 g^3 \Big[2\log\epsilon(-3k + 2\log\epsilon + 4\gamma + 4\log\pi) + (k-4)k \\ &- 6k\log\pi + \gamma(8\log\pi - 6k) + \frac{1}{6}\pi^2(n^2+1) + 4\gamma^2 + 4(\log\pi)^2\Big] + O(g^4) \end{aligned}$$

with $\lambda = -1/2$.

### $J^+_{-2}|0,k\rangle$, two $w'$, one $w$

For the case with two $w'$ and one $w$, the excited state equation is

$$\partial_x^2\psi(x;\theta) = \left[e^{2\theta} g e^{-2/g} x^k e^{2x} + \frac{8(k^2 + k(4x+5) + 4(x^2+x+1))}{(k^2+4kx+k+4x(x+1))^2}\right]\psi(x;\theta). \tag{D.89}$$

We propose that this equation encodes the excited line defect expectation value $\langle T_n(\theta)\rangle_2$.

As in the previous case, the wavefunction can be parametrized

$$\psi(x;\theta) \sim -\frac{1}{3g^2}Q(g_{\text{eff}})[1 + (1+k+2x)g] - \frac{g}{3}\tilde{Q}(g_{\text{eff}})[1 - \frac{1}{2}(1+k+2x)g], \tag{D.90}$$

where $Q(g_{\text{eff}})$ and $\tilde{Q}(g_{\text{eff}})$ are as in (D.87). The expression for $T_n(\theta)$ in terms of $Q$, $\tilde{Q}$ remains the same as in (D.88). Comparing the parameterization of $\psi$ in terms of $Q$, $\tilde{Q}$ with the direct perturbative evaluation up to $O(g)$, we obtain

$$\begin{aligned} \tilde{q}_0 &= \frac{1}{4}(-5k + 8\gamma - 4 - 8\log 2), \\ \tilde{q}_1 &= \gamma\Big(\frac{k}{4} + 1 + \log 4\Big) + \frac{1}{96}\Big(-3k(15k + 64 + \log 256) - 8\big(2\pi^2 + 3(1+\log 4)^2\big)\Big) - \gamma^2. \end{aligned}$$

The full expression for $T_n(\theta)$ to $O(g^4)$ is

$$\begin{aligned}T_n(\theta) &= n - \frac{1}{3}\pi^2 g^2 n\left(n^2-1\right) + \frac{1}{12}\pi^2 g^3 n\left(n^2-1\right)\left(-8\gamma - 8\theta + 7k + 4 + \log 256\right)\\ &\quad + \frac{1}{288}\pi^2 g^4 n\left(n^2-1\right)\Big( - 72(-2\gamma - 2\theta + 1 + \log 4)^2 - 195k^2\\ &\qquad + 120k(5\gamma + 5\theta - 1 - 5\log 2) + 8\pi^2\left(3n^2-10\right)\Big)\end{aligned}$$

This expression satisfies the Hirota bilinear relations and has been verified to match the perturbative line defect computation for $\langle T_n(\theta)\rangle_2$ in a suitable renormalization scheme, where $g$ is shifted as

$$\begin{aligned}g &\to \lambda g + \lambda^2 g^2\Big[k - 2\log(\pi\epsilon) - 2\gamma - \Big(1+\frac{i}{2}\Big)\Big]\\ &\quad + \lambda^3 g^3\Big[k^2 + \frac{1}{24}\Big((-198+3i)k + 4\pi^2(n^2+1) + 3\big(32(\log\pi)^2 + (59+52i)\big)\Big)\\ &\quad + \big(-6k + 8\gamma + (4+2i)\big)\log(\pi\epsilon) - 6\gamma k + 4\log(\epsilon)\log(\pi^2\epsilon) + 4\gamma^2 + (4+2i)\gamma\Big] + O(g^4)\end{aligned}$$

with $\lambda = -1/2$.

$J^+_{-2}|0,-1\rangle$

With

$$a_+(x) = -\frac{1}{x} \tag{D.91}$$

we have the ODE

$$\partial_x^2\psi(x;\theta) = \left[e^{2\theta} g e^{-2/g} x^k e^{2x} + \frac{2}{x^2}\right]\psi(x;\theta). \tag{D.92}$$

$$\psi(x;\theta) \sim -\frac{1}{3g^2}Q(g_{\text{eff}})[1+2gx] - \frac{g}{3}\tilde{Q}(g_{\text{eff}})[1-gx], \tag{D.93}$$

where again $Q(g_{\text{eff}})$ and $\tilde{Q}(g_{\text{eff}})$ are as in (D.87). We can similarly find the Wronskian

$$\begin{aligned} T_n(\theta) = n &- \frac{1}{3}\pi^2 g^2 n\left(n^2-1\right) - \frac{1}{12}\pi^2 g^3 n\left(n^2-1\right)\left(8\gamma+8\theta+3-8\log 2\right) \\ &\frac{1}{288}\pi^2 g^4 n\left(n^2-1\right)\Big[+8\pi^2\left(3n^2-10\right)-288\gamma^2-24\gamma(24\theta+13-24\log 2) \\ &+3\left(-104\theta-96(\theta-\log 2)^2-49+104\log 2\right)\Big] \end{aligned}$$

with

$$\begin{aligned} \tilde{q}_0 &= \frac{1}{4}+2(\gamma-\log 2), \\ \tilde{q}_1 &= \frac{1}{96}\left(-16\left(6(\log 2-\gamma)^2+\pi^2\right)+24(3\gamma+5-3\log 2)+3\right). \end{aligned}$$

### D.4.2 A general perturbative prescription

One can easily see the pattern of the steps in the previous example and might wonder if it is possible to perform the perturbative analysis in a uniform way without specifying particular values for $w_i'$ and $w_i$, i.e. without solving the Bethe equations explicitly. Here in this section, we provide such a recipe for zero spin and zero twist.

In considering the Schrödinger equation in the regime $1/g \gg -x \gg 0$, one first solves the equation with just the potential terms and then expands in $g$ until one has $O(x)$ contributions. That is, for $(\#w', \#w) = (p, q)$ we take (after shifting $x \mapsto x + 1/g$) the $g$ expansion of the solution to

$$\partial_x^2\psi(x;\theta) = \left[a(x)^2 + a'(x)\right]\psi(x;\theta) \tag{D.94}$$

where

$$a(x) = -\sum_{a=1}^{p}\frac{1}{x-w_a'} + \sum_{i=1}^{q}\frac{1}{x-w_i}. \tag{D.95}$$

Notice that one exact solution of such an equation is

$$\frac{\prod_{i=1}^{q}(x+1/g-w_i)}{\prod_{a=1}^{p}(x+1/g-w_a')} = g^{p-q}\Big[1-g\Big((p-q)x-\sum_{a=1}^{p}w_a'+\sum_{i=1}^{q}w_i\Big)+\cdots\Big]. \tag{D.96}$$

Expanding up to the order shown is sufficient for $p > q$, but one needs to consider an $O(g^2)$

term for $p = q$. Here, we concern ourselves with just the $p > q$ cases as the $p = q$ case is treated in a similar but more involved way.

The solution above is that proportional to $\tilde{Q}$ of the previous subsection. An exact second solution turns out to be more elusive, but this can be overcome by the fact that we only need the perturbative form of second solution. The second solution can then be determined by imposing that

$$T_n(\theta) = i\left(\psi\Big(x;\theta - \frac{i\pi n}{2}\Big), \psi\Big(x;\theta + \frac{i\pi n}{2}\Big)\right), \tag{D.97}$$

i.e. the shifted Wronskian of the wavefunction, is normalized as

$$T_n(\theta) = \frac{i}{2(p-q)+1}\Big[Q\Big(\theta + \frac{i\pi n}{2}\Big)\tilde{Q}\Big(\theta - \frac{i\pi n}{2}\Big) - Q\Big(\theta - \frac{i\pi n}{2}\Big)\tilde{Q}\Big(\theta + \frac{i\pi n}{2}\Big)\Big]. \tag{D.98}$$

Doing so, one finds that the parametrization of the wavefunction for the cases $p > q$ becomes

$$\begin{aligned}\psi(x;\theta) \sim -\frac{1}{2(p-q)+1}\Bigg\{ &\frac{Q(g_{\text{eff}})}{g^{p-q+1}}\Big[1 + \frac{p-q+1}{p-q} g\Big((p-q)x - \sum_{a=1}^{p} w'_a + \sum_{i=1}^{q} w_i\Big)\Big] \\ &+ g^{p-q}\tilde{Q}(g_{\text{eff}})\Big[1 - g\Big((p-q)x - \sum_{a=1}^{p} w'_a + \sum_{i=1}^{q} w_i\Big)\Big]\Bigg\}\end{aligned}$$

with

$$\begin{aligned}Q(g_{\text{eff}}) &= \frac{g_{\text{eff}}^{p-q}}{\sqrt{\pi}}(1 + q_1 g_{\text{eff}}(\theta) + \cdots) \\ \tilde{Q}(g_{\text{eff}}) &= \frac{g_{\text{eff}}^{-(p-q)}}{\sqrt{\pi}}\Big(-\frac{1}{g_{\text{eff}}(\theta)} + \tilde{q}_0 + \tilde{q}_1 g_{\text{eff}}(\theta) + \cdots\Big).\end{aligned}$$

We see that $\tilde{q}_0$ and $\tilde{q}_1$, determined by comparison to the direct perturbative $g$ expansion of the Schrödinger equation, will only depend on the difference of sums of $w'$'s and $w$'s.

The analysis in this subsection can be generalized to other spin modules and those with twists.

### D.4.3 nonzero twist $\alpha_+ \neq 0$

Mimicking the case of $\alpha_+ = 0$, we proceed with the UV expansion as follows. We are interested in the ODE

$$\partial_x^2 \psi(x) = \left[e^{2x+2\theta}(1+gx)^k + t(x)\right] \psi(x) \tag{D.99}$$

Consider the matching region $\frac{1}{g} \gg -x \gg 0$. The first inequality means we are reduced to

$$\partial_x^2 \psi_{\mathrm{I}}(x) = \left[e^{2x+2\theta} + \alpha_+^2\right] \psi_{\mathrm{I}}(x) \tag{D.100}$$

The solution is given by

$$\psi_{\mathrm{I}}(x) = K_{\alpha_+}(e^{x+\theta}) \sim \Gamma(-\alpha_+)2^{-1-\alpha_+}e^{\alpha_+(x+\theta)} + \Gamma(\alpha_+)2^{\alpha_+-1}e^{-\alpha_+(x+\theta)}, \quad x \to -\infty \tag{D.101}$$

Recall Miura part $t(x) = a_+(x)^2 + \partial_x a_+(x)$, takes the form

$$a_+(x) = -\alpha_+ - \frac{l}{x+1/g} + \dots \tag{D.102}$$

where $\alpha_+$ is generic enough.

The second inequality means

$$\partial_x^2 \psi_{\mathrm{II}}(x) = \left[a_+(x)^2 + \partial_x a_+(x)\right] \psi_{\mathrm{II}}(x) \tag{D.103}$$

whose solutions are given by

$$\psi_{\mathrm{II}}(x) = c_1\Gamma(\alpha_+)2^{\alpha_+-1}e^{\int^x dx' \ a_+(x')} + c_2\Gamma(-\alpha_+)2^{-1-\alpha_+}e^{\int^x dx' \ \tilde{a}_+(x')} \tag{D.104}$$

where $\tilde{a}_+(x)$ is defined to be the Weyl reflection of $a_+(x)$, i.e. $\tilde{a}_+(x) = a_+(x) + f[a_+(x)]$, where for any given function $a(x)$, we define

$$f[a(x)] \equiv \frac{e^{-2\int^x dx' a(x')}}{\int^x dx' e^{-2\int^{x'} dx'' a(x'')}}. \tag{D.105}$$

Since both $\psi_{\mathrm{I}}(x)$ and $\psi_{\mathrm{II}}(x)$ are approximate solutions to (D.99) in the matching region

$\frac{1}{g} \gg -x \gg 0$, we can take the coefficient

$$c_1 \sim e^{\alpha(\theta-\frac{1}{g})} g^l, \tag{D.106}$$

$$c_2 \sim e^{-\alpha(\theta-\frac{1}{g})} g^{-l}. \tag{D.107}$$

Recall that $\frac{1}{g_{\text{eff}}} = \frac{1}{g} - \theta + \dots$. Thus it is very natural to define

$$\begin{aligned} Q[g_{\text{eff}}] &= e^{-\frac{\alpha_+}{g_{\text{eff}}}} g_{\text{eff}}^l \big[1 + q_1 g_{\text{eff}} + q_2 g_{\text{eff}}^2 + \dots\big], \\ \tilde{Q}[g_{\text{eff}}] &= e^{\frac{\alpha_+}{g_{\text{eff}}}} g_{\text{eff}}^{-l} \big[-1 + \tilde{q}_1 g_{\text{eff}} + \tilde{q}_2 g_{\text{eff}}^2 + \dots\big], \\ T_n &= \frac{i}{2\sin\pi\alpha_+} \Big( Q^{(+n)}[g_{\text{eff}}] \tilde{Q}^{(-n)}[g_{\text{eff}}] - Q^{(-n)}[g_{\text{eff}}] \tilde{Q}^{(+n)}[g_{\text{eff}}] \Big). \end{aligned} \tag{D.108}$$

One can calculate $T_{n;l} = \langle l | \hat{T}_n | l \rangle$ to be

$$T_{n;l} = \frac{\sin(n\pi\alpha_+)}{\sin\pi\alpha_+} + g\Big( n\pi(2l - k\alpha_+)\cos(n\pi\alpha_+) + 2(q_1 - \tilde{q}_1)\sin(n\pi\alpha_+) \Big) + \dots \tag{D.109}$$

Note that the leading term is precisely the character

$$\mathrm{Tr}_{\mathcal{R}}\, e^{i2\pi\alpha_+ t^0} = \frac{\sin n\pi\alpha_+}{\sin\pi\alpha_+}. \tag{D.110}$$

## D.5 WKB analysis

### D.5.1 General remarks and organizations

Given a $\mathfrak{sl}_2$ $\lambda$-oper, the goal of this appendix is to develop techniques to evaluate the Stokes data, namely the Wronskians between certain solutions (referred to as *small solutions* defined below) to the corresponding Schrödinger equation. Our formalism is based on the WKB analysis, which culminates in the Voros analysis [79, 80, 81, 82, 83, 84, 85, 86, 87, 88, 89]. We refer readers to the appendix of [1] and references therein for a review of WKB analysis and other related recent progress. Contrary to the common wisdom, we will find that in the general situation including the examples in this article, the standard WKB analysis will not provide a complete collection of Stokes data, which we briefly review below.

The WKB analysis is concerned with the holomorphic differential equation

$$\partial_x^2\psi = \left[\frac{P(x)}{\hbar^2} + t(x)\right]\psi \equiv T(x)\psi(x) \tag{D.111}$$

defined on a Riemann surface by using the oper coordinate transformation between patches

$$\psi(x) = \frac{1}{\sqrt{\partial_x\tilde{x}(x)}}\tilde{\psi}(\tilde{x}(x)). \tag{D.112}$$

Here we start with brief definitions of two main players, Stokes diagrams and small solutions. Other relevant notions will be explained wherever needed.

$T(x)$ and $P(x)dx^2$ are referred to as the stress tensor and the quadratic differential respectively. We will briefly review the analysis. For any angle $\vartheta \in \mathbb{R}/2\pi\mathbb{Z}$, $\vartheta$-*WKB lines* are curves in the complex plane where

$$\mathrm{Im}\left[e^{i\vartheta}\sqrt{P(x)}dx \cdot \partial_t\right] = 0 \tag{D.113}$$

where $\partial_t$ is the tangent vector of the curve. One such line passes through any point in the $x$ plane. a WKB curve is *special* if it ends on a zero of $P$ or on an asymptotic region of exponentially fast decrease for $P$. The union of all special WKB lines is called a WKB diagram/spectral network. See Footnote 4.

For each singularity of $P(x)$, we can define a set of *small solutions*. In particular, for each special WKB line coming into the singularity, we define a small solution to be the unique solution (up to normalization) that decays exponentially fast approaching the singularity along the corresponding special WKB line. We will choose the normalization such that asymptotically near the singularity, it matches with the WKB solutions $\psi_\pm^{\mathrm{WKB}}(x)$. The definition of the WKB solutions and the associated WKB coordinate system will be given in Section D.5.2.

We would like to find the Wronskians between small solutions. The standard GMN/Voros-style WKB analysis is interested in contour integrals along the generic WKB lines connecting every pairs of Stokes sectors, while, importantly, staying away from the zeros of the quadratic differential $P(x)$. They are indeed all we need to provide a complete collection of Wronskians when all zeroes of the quadratic differential $P(x)$ are simple. However, more generally, the collection is not complete and we also need information from the local analysis of the *matching region*.

An example where we need a generalized WKB analysis would be a polynomial oper

with non-simple zeros. And the zeros are the *matching region* we need to understand. More precisely, for each zero of $P(x)$, we can define a *local* coordinate system and nice local solutions therein. Let's consider first $t(x) = 0$. For each zero $x_0$ of order $n$, we want to find a coordinate system $\tilde{y}(x)$ such that the oper of interest

$$\frac{P(x)}{\hbar^2} \tag{D.114}$$

becomes

$$\frac{\tilde{y}^n}{\hbar^2} + O(\hbar^0) \tag{D.115}$$

where $\tilde{y}(x_0) = 0 + O(\hbar^2)$. We also require the (possibly nonzero) subleading $\hbar$ terms in $\tilde{y}(x)$ are regular at $x_0$.

Generically one can't find $\tilde{y}(x)$ such that the stress tensor takes exactly the form $\frac{\tilde{y}^n}{\hbar^2}$. Instead, it turns out the best one can do is

$$\frac{\tilde{y}^n}{\hbar^2} + a_{n-2}\tilde{y}^{n-2} + \cdots + a_1\tilde{y} + a_0. \tag{D.116}$$

The constant coefficients can be determined order by order in $\hbar$,

$$a_m = a_m^{(0)} + \hbar^2 a_m^{(2)} + \hbar^4 a_m^{(4)} + \dots \tag{D.117}$$

In particular when $n = 1$, namely, around a simple zero, there always exists a coordinate system such that the stress tensor takes the form $\frac{\tilde{y}}{\hbar^2}$. We can also write $y = \hbar^{-\frac{2}{n+2}}\tilde{y}$, in which the stress tensor takes the form

$$y^n + a_{n-2}\hbar^{\frac{2n}{n+2}}y^{n-2} + \cdots + a_j\hbar^{\frac{2j+4}{n+2}}y^j + \cdots + a_0\hbar^{\frac{4}{n+2}}. \tag{D.118}$$

We will discuss how to find such a local coordinate system and nice local solutions defined in there, as well as the cases with $t(x) \neq 0$, in Subsection D.5.2.

Another example of the *matching region* is the negative infinity of the oper with exponential potential. The details on how to deal with such matching region is given in Subsection D.5.7.

We will first describe three different coordinate systems in detail and the transformation between them in Section D.5.2. Next in Section D.5.3, we will explain why the WKB analysis away from the zeros is not enough and what information from the local analysis is crucial to give a complete collection of Wronskians/Stokes data. We then give a general recipe for evaluating the Wronskians by incorporating the missing local information while

deferring the local perturbative analysis of extracting the local information to Section D.5.5.

In order to verify our proposed recipe, we carry out numerical computations. The method of numerical implementation is given in Section D.5.4.

Finally, we apply the generalized WKB analysis to the nice examples at hand including polynomial oper with non-simple zeros in Section D.5.6 and the exponential case that describes the chiral WZW model in Section D.5.7.

### D.5.2 Coordinate systems

We would like to define interesting local coordinate systems with good $\hbar \to 0$ asymptotics. There are a few useful coordinate systems we will use frequently in this thesis:

- the original one, denoted as $x$, where $T = \frac{1}{\hbar^2} P(x) + t(x)$,
- the local coordinate around a zero, $y$ or $\tilde{y}$, where $T = y^n + \dots$ or $\frac{\tilde{y}^n}{\hbar^2} + \dots$,
- the WKB coordinate $s_{ab}$ where $T = \frac{1}{4}$.

#### WKB coordinate systems

Near each (Stokes sector of a) singularity $a$ of the quadratic differential $P(x)dx^2$ we can find a solution $\psi_a^{\mathrm{WKB}}$ which decreases exponentially fast approaching the singularity. It is given as a specific asymptotic expansion near the singularity,

$$\psi_a^{\mathrm{WKB}} = \frac{1}{\sqrt{\pm \partial_x s_a^{\mathrm{asy}}(x)}} e^{\mp \frac{1}{2} s_a^{\mathrm{asy}}(x)} \tag{D.119}$$

where $s_a^{\mathrm{asy}}(x)$ is a primitive of twice the *WKB momentum* $p_a^{\mathrm{asy}}(x) = \frac{1}{2}\partial_x s_a^{\mathrm{asy}}(x)$, which satisfies the differential equation

$$p_a^{\mathrm{asy}}(x)^2 + \frac{3}{4}\left(\frac{\partial_x p_a^{\mathrm{asy}}(x)}{p_a^{\mathrm{asy}}(x)}\right)^2 - \frac{1}{2}\frac{\partial_x^2 p_a^{\mathrm{asy}}(x)}{p_a^{\mathrm{asy}}(x)} = T(x). \tag{D.120}$$

The one form $p_a^{\mathrm{asy}}(x)dx$ is also referred to as the WKB one form. If we write $p_a^{\mathrm{asy}}(x)$ in $\hbar$ asymptotics as

$$p_a^{\mathrm{asy}}(x;\hbar) = \frac{p_{-1}^{\mathrm{asy}}(x)}{\hbar} + \hbar p_1^{\mathrm{asy}}(x) + \hbar^3 p_3^{\mathrm{asy}}(x) + \cdots \tag{D.121}$$

the equation (D.120) can then be written as a recursive equation for $p_n(x)$. The leading term is given by $p_{-1}^{\text{asy}}(x) \sim \sqrt{P(x)}$.

For a polynomial singularity at $x = \infty$, the asymptotic expansion $s_a^{\text{asy}}(x)$ involves increasingly negative powers of $x$, with coefficients which are Laurent polynomials in $\hbar$. In order to fix the normalization at $x = \infty$ we only need to worry about powers of $x$ greater than $-1$, so the last two terms are unimportant. For a singularity of odd degree, the expansion involves fractional powers of $x$ and thus $s_a^{\text{asy}}(x)$ can be chosen unambiguously to have no constant term. For a singularity of even degree, there will be a $\log x$ term and we will have to make some choice. Of course, sometimes there are some natural nonzero choices of the constant as well. See, for example, Section D.5.6. For more generic cases, we will fix the constant terms of $s_a^{\text{asy}}(x)$ on a case-by-case basis.

Once we fix the constant term in $s_a^{\text{asy}}(x)$, the normalization of the WKB solutions $\psi_a^{\text{WKB}}$ is then fixed. This then further fixes the normalization of the small solutions, which, as we defined in section D.5.1, are normalized to match the WKB solutions asymptotically near the singularity.

Although we defined $s_a^{\text{asy}}(x)$ only as an asymptotic series, it is easy to produce actual functions which have such an asymptotic expansion: given any other solution[5] $\psi_*$ which is not proportional to $\psi_a$, we could define

$$e^{s_{a,*}(x)} = \frac{1}{(\psi_a, \psi_*)} \frac{\psi_*(x)}{\psi_a(x)} \tag{D.122}$$

Redefinitions of $\psi_*$ by multiples of $\psi_a$ would just shift $e^{s_{a,*}(x)}$ by an $x$-independent constant.

For generic $x$, we sit along a generic WKB line associated to a pair of small solutions $\psi_a(x)$ and $\psi_b(x)$, with some normalization determined at the corresponding directions at infinity or singularities.

These solutions have good $\hbar \to 0$ asymptotics in a certain sector of width $\pi$ in the $\hbar$ plane. So does their ratio, which defines an useful local coordinate

$$z_{ab}(x) \equiv e^{s_{ab}(x)} = \frac{1}{(\psi_a, \psi_b)} \frac{\psi_b(x)}{\psi_a(x)} \tag{D.123}$$

Then

$$\partial_x z_{ab} = \frac{1}{\psi_a^2} \tag{D.124}$$

[5]Unless we state explicitly otherwise, by a *solution*, we mean an actual function, as opposed to a WKB solution, which is an asymptotic expansion.

so that the solutions $\psi_a$ and $\psi_b$ map to 1 and $(\psi_a, \psi_b) z_{ab}$ in the $z_{ab}$ coordinate. Or equivalently, the stress tensor in $z_{ab}$ coordinate is $T(z_{ab}) = 0$.

Also,

$$\partial_x s_{ab} \equiv 2p_{ab}(x) = \frac{(\psi_a, \psi_b)}{\psi_a(x)\psi_b(x)} \tag{D.125}$$

and thus the solutions $\psi_a$ and $\psi_b$ map to $e^{-\frac{1}{2}s_{ab}(x)}$ and $(\psi_a, \psi_b)e^{\frac{1}{2}s_{ab}(x)}$ in the $s_{ab}$ coordinate. Equivalently, the stress tensor in $s_{ab}$ coordinate is $T(s_{ab}) = \frac{1}{4}$

$s_{ab}(x)$ can be determined in the following way. Similar to (D.120), the WKB momentum $p_{ab}(x) \equiv \frac{1}{2}\partial_x s_{ab}$ satisfies the differential equation

$$p_{ab}(x)^2 + \frac{3}{4}\left(\frac{\partial_x p_{ab}(x)}{p_{ab}(x)}\right)^2 - \frac{1}{2}\frac{\partial_x^2 p_{ab}(x)}{p_{ab}(x)} = T(x) \tag{D.126}$$

which can be solved recursively to find the WKB expansion of $p(x)$ away from zeroes of $P(x)$:

$$p(x) = \frac{1}{\hbar}\sqrt{P(x)} + \hbar\frac{16P^2(x)t(x) - 5P'(x)^2 + 4P(x)P''(x)}{32P(x)^{\frac{5}{2}}} + \cdots \tag{D.127}$$

It is easy to see that $p_{n>0}(x)$ will involve increasingly negative powers of $p_{-1}(x) = \sqrt{P(x)}$. Therefore the zeros of $P(x)$ remain the places where the WKB approximation breaks down, regardless of $t(x)$.

In order to compute $s_{ab}$ from $p_{ab}$, we need to fix the integration constants. This is done by expanding $p(x)$ near the singularity and comparing term-by-term with $s_a^{\text{asy}}(x)$.

It is easy to express $s_{ab}$ as a regularized contour integral. We can write

$$s_{ab}(x) = s_{ab}(\bar{x}) + \int_{\bar{x}}^{x} p_{ab}(u)du \tag{D.128}$$

and send $\bar{x}$ towards the singularity $x_a$:

$$s_{ab}(x) = \lim_{\bar{x}\to x_a}\left[s_a^{\text{asy}}(\bar{x}) + \int_{\bar{x}}^{x} p_{ab}(u)du\right]. \tag{D.129}$$

Another useful observation is that

$$e^{s_{ab}(x)+s_{ba}(x)} = \frac{1}{(\psi_a, \psi_b)(\psi_b, \psi_a)} \tag{D.130}$$

and $p_{ab}+p_{ba}=0$, so that

$$\log\left[(\psi_a,\psi_b)(\psi_b,\psi_a)\right]=-\lim_{\bar{x}\to x_a}\lim_{\bar{x}'\to x_b}\left[s_a^{\rm asy}(\bar{x})+s_b^{\rm asy}(\bar{x}')+\int_{\bar{x}}^{\bar{x}'}p_{ab}(u)du\right] \tag{D.131}$$

with the integral taken along a path equivalent to the WKB line between $x_a$ and $x_b$. The overall sign can be determined by computing the Wronskian explicitly:

$$(\psi_a,\psi_b)=e^{-\frac{1}{2}s_{ab}(x)-\frac{1}{2}s_{ba}(x)}\frac{\sqrt{p_{ab}(x)}}{\sqrt{p_{ba}(x)}}. \tag{D.132}$$

**Local coordinate system around zeros**

Here in this section, we explain how one can find explicitly the coordinate system in which $\frac{1}{\hbar^2}P(x)$ around a zero of order $n$ takes the form of

$$\frac{\tilde{y}^n}{\hbar^2}+a_{n-2}\tilde{y}^{n-2}+\cdots+a_1\tilde{y}+a_0 \tag{D.133}$$

where $a_i=a_i^{(0)}+a_i^{(2)}\hbar^2+a_i^{(4)}\hbar^4+\ldots$. Or with $y=\hbar^{-\frac{2}{n+2}}\tilde{y}$,

$$y^n+a_{n-2}\hbar^{\frac{2n}{n+2}}y^{n-2}+\cdots+a_j\hbar^{\frac{2j+4}{n+2}}y^j+\cdots+a_0\hbar^{\frac{4}{n+2}}. \tag{D.134}$$

In this section, we will mostly use $\tilde{y}$ so that only integer power of $\hbar$ will appear.

When we have nontrivial $t(x)=a(x)^2+\partial_x a(x)$, and $a(x)$ has residue $-l$ at $x_0$,

$$\frac{\tilde{y}^n}{\hbar^2}+a_{n-2}\tilde{y}^{n-2}+\cdots+a_1\tilde{y}+a_0+\frac{l(l+1)}{\tilde{y}^2} \tag{D.135}$$

or

$$y^n+a_{n-2}\hbar^{\frac{2n}{n+2}}y^{n-2}+\cdots+a_j\hbar^{\frac{2j+4}{n+2}}y^j+\cdots+a_0\hbar^{\frac{4}{n+2}}+\frac{l(l+1)}{y^2} \tag{D.136}$$

In particular if $t(x)$ is nontrivial but regular at the zero of interest $x_0$, we should find the stress tensor takes the local form (D.116) and (D.118).

Below we will see that $\tilde{y}(x)$ can be uniquely determined with no ambiguity and that it is unavoidable to have the coefficients $a_i$ by providing two different ways of finding such $\tilde{y}(x)$. By doing so we will explain why the coefficients $a_m$ are unavoidable. (1) In comparing the local coordinate and other coordinates, we need to have some parameters to adjust so that

the cross ratios defined from the local solutions coincide with the same cross-ratio built from $\psi_n(x)$. (2) $a_m$ need to be specific values to make the coordinate transformation $\tilde{y}(x)$ non-divergent at the interested zero.

***local* coordinate transformation**

We call this a local map since it is only valid in the neighborhood of the zero

$$\hbar \ll \tilde{y}^2 \ll \tilde{y} \sim (x - x_0) \ll 1. \tag{D.137}$$

Suppose we are interested in the zero of order $n$, then apparently one can always do a shift in the coordinate such that

$$P(x) = t_1 x + t_2 x^2 + t_3 x^3 + \cdots + t_N x^N \tag{D.138}$$

where $t_1 = t_2 = \cdots = t_{n-1} = 0$ and $x = 0$ is the order $n$ zero of interest. By solving the following equation

$$\left(\frac{\partial \tilde{y}}{\partial x}\right)^2 \left(\frac{\tilde{y}^n}{\hbar^2} + a_{n-2}\tilde{y}^{n-2} + \cdots + a_1 \tilde{y} + a_0\right) - \frac{1}{2}\{\tilde{y}, x\} = \frac{P(x)}{\hbar^2} \tag{D.139}$$

order by order in $\hbar$ and $x$, we can determine the coordinate transformation $\tilde{y}(x)$ and more importantly $\{a_m\}$ explicitly as functions of $\{t_n, t_{n+1}, \ldots, t_N\}$.

***non-local* coordinate transformation**

To state again, we want to find a coordinate transformation $\tilde{y}(x)$ with respect to a zero $x_0$ of order $n$ satisfying

$$\left(\frac{\partial \tilde{y}}{\partial x}\right)^2 \left(\frac{\tilde{y}^n}{\hbar^2} + a_{n-2}\tilde{y}^{n-2} + \cdots + a_1 \tilde{y} + a_0\right) - \frac{1}{2}\{\tilde{y}, x\} = \frac{P(x)}{\hbar^2} \tag{D.140}$$

where $\tilde{y}(x) = \tilde{y}_0(x) + \hbar \tilde{y}_1(x) + \hbar^2 \tilde{y}_2(x) + \ldots$. This equation can be solved recursively order by order in $\hbar$, and at each order we have a first order differential equation. The leading order equation $\tilde{y}_0'^2 \tilde{y}_0^n = P(x)$ is solved by

$$\tilde{y}_0(x) = \left(\frac{n+2}{2} \int_{x_0}^{x} \sqrt{P(x')} dx'\right)^{\frac{2}{n+2}}. \tag{D.141}$$

The integration constant is fixed by choosing the integration starting point from the interested zero $x_0$ of order $n$, such that locally around $x_0$, $\tilde{y}_0(x)$ start from linear order in $(x - x_0)$ and vanishes at $x_0$.

At the order of $\hbar^{-1}$, we have a homogeneous differential equation $n\tilde{y}_1 y_0' + 2\tilde{y}_0\tilde{y}_1' = 0$, which is solved by

$$\tilde{y}_1(x) = \frac{c_1}{\tilde{y}_0(x)^{n/2}}. \tag{D.142}$$

Since $\tilde{y}_0(x)$ vanishes at the zero $x_0$ and we require $\tilde{y}(x)$ to be regular there, the only choice is to choose $c_1 = 0$, hence $\tilde{y}_1(x) = 0$. The same is true for ever odd order in $\hbar$.

At the order of $\hbar^0$, we end up with the an inhomogeneous first order differential equation for $\tilde{y}_2(x)$. We fix the homogeneous part $\frac{1}{\tilde{y}_0(x)^{n/2}}$ of the solution by choosing the lower limit of the integral at $x_0$. This renders $\tilde{y}_2(x)$ regular, and in general nonzero, at $x_0$. For example

$$\text{simple zero: } \tilde{y}_2(x) = \frac{1}{\sqrt{\tilde{y}_0(x)}}\int_{x_0}^{x}\sqrt{\tilde{y}_0(x')}\frac{-3(\tilde{y}_0'')^2 + 2\tilde{y}_0'\tilde{y}_0'''}{8\tilde{y}_0(\tilde{y}_0')^3}dx', \tag{D.143}$$

$$\text{double zero: } \tilde{y}_2(x) = \frac{1}{\tilde{y}_0(x)}\int_{x_0}^{x}\tilde{y}_0(x')\frac{-4a_0^{(0)}(\tilde{y}_0')^4 - 3(\tilde{y}_0'')^2 + 2\tilde{y}_0'\tilde{y}_0'''}{8\tilde{y}_0^2(\tilde{y}_0')^3}dx', \tag{D.144}$$

$$\text{cubic zero: } \tilde{y}_2(x) = \frac{1}{\tilde{y}_0(x)^{3/2}}\int_{x_0}^{x}\tilde{y}_0^{3/2}\frac{-4a_0^{(0)}\tilde{y}_0'^4 - 4a_1^{(0)}\tilde{y}_0\tilde{y}_0'^4 - 3\tilde{y}_0''^2 + 2\tilde{y}_0'\tilde{y}_0'''}{8\tilde{y}_0^3\tilde{y}_0'^3}. \tag{D.145}$$

Furthermore, one can also understand the necessity of the coefficients $a_i$ in (D.134) from the fact that we need them in order to have $\tilde{y}_2(x)$ non-divergent at $x_0$.

### Relating two coordinate systems

#### Near a simple zero

There are three special WKB lines emanating from a simple zero. Therefore, near a simple zero, we can access three small solutions $\psi_a$, $\psi_b$, $\psi_c$, decaying exponentially along the three special WKB lines respectively. Apparently there must be a linear relation among them, sometimes referred to as Plücker relations.

$$(\psi_a, \psi_b)\psi_c + (\psi_c, \psi_a)\psi_b + (\psi_b, \psi_c)\psi_a = 0. \tag{D.146}$$

On the other hand, there exists a *local* coordinate system $y$ associated to this simple zero, in which the stress tensor reads $T(y) = y$. The coordinate $y$ satisfies the differential equation

$$\left(\frac{\partial y(x)}{\partial x}\right)^2 y(x) + \frac{3}{4}\left(\frac{\partial_x^2 y(x)}{\partial_x y(x)}\right)^2 - \frac{1}{2}\frac{\partial_x^3 y(x)}{\partial_x y(x)} = T(x) \tag{D.147}$$

and can be expanded as $\hbar \to 0$ to be $y(x) = \hbar^{-\frac{2}{3}}(\tilde{y}_0 + \hbar^2 \tilde{y}_2 + \hbar^4 \tilde{y}_4 + \dots)$. Then the nice local solutions in this local coordinate system are given by (D.196),

$$\mathrm{Ai}_a(y) = \sqrt{2\pi} e^{-\frac{\pi i a}{3}} \mathrm{Ai}(e^{\frac{2\pi i a}{3}} y). \tag{D.148}$$

In particular, we have

$$\mathrm{Ai}_{-1}(y) - \mathrm{Ai}_0(y) + \mathrm{Ai}_1(y) = 0. \tag{D.149}$$

Define $y(x)$ by

$$\frac{\mathrm{Ai}_1(y(x))}{\mathrm{Ai}_{-1}(y(x))} = \frac{(\psi_c, \psi_a)\psi_b}{(\psi_a, \psi_b)\psi_c}. \tag{D.150}$$

This obviously satisfies also

$$-\frac{\mathrm{Ai}_0(y(x))}{\mathrm{Ai}_{-1}(y(x))} = \frac{(\psi_b, \psi_c)\psi_a}{(\psi_a, \psi_b)\psi_c}, \quad -\frac{\mathrm{Ai}_1(y(x))}{\mathrm{Ai}_0(y(x))} = \frac{(\psi_c, \psi_a)\psi_b}{(\psi_b, \psi_c)\psi_a} \tag{D.151}$$

which gives us the relation between small solutions $\psi_\bullet(x)$ and the local solutions $\mathrm{Ai}_\bullet(y(x))$. For example,

$$\partial_x y(x) \psi_a^2(x) = \frac{(\psi_c, \psi_a)(\psi_a, \psi_b)}{i(\psi_b, \psi_c)} \mathrm{Ai}_0(y(x))^2. \tag{D.152}$$

We can now relate $y$ to $s_{ab}$ and to the other WKB coordinates nearby:

$$\frac{\mathrm{Ai}_1(y(x))}{\mathrm{Ai}_0(y(x))} = -\frac{(\psi_a, \psi_b)(\psi_c, \psi_a)}{(\psi_b, \psi_c)} e^{s_{ab}(x)}. \tag{D.153}$$

The coordinate $s_{ab}(x)$ depend on the normalization of the local solutions $\mathrm{Ai}_a(y)$ and small solutions $\psi_a(x)$. One can define an alternative local WKB coordinate, i.e. an alternative primitive of $p_{ab}(x)$, that is independent of the normalization of the solutions, given as follows

$$e^{s_{abc}(x)} \equiv \frac{(\psi_c, \psi_a)\psi_b}{(\psi_b, \psi_c)\psi_a} = \frac{(\psi_a, \psi_b)(\psi_c, \psi_a)}{(\psi_b, \psi_c)} e^{s_{ab}(x)} = -\frac{\mathrm{Ai}_1(y(x))}{\mathrm{Ai}_0(y(x))}. \tag{D.154}$$

If we expand the right hand side $-\frac{\mathrm{Ai}_1(y(x))}{\mathrm{Ai}_0(y(x))}$ in an asymptotic expansion at large $y(x)$ using

$$\mathrm{Ai}_a(y) \sim \frac{1}{\sqrt{\pm 2 \partial_y S(y)}} e^{\mp S(y)} \tag{D.155}$$

where the function $S(y) = \frac{2}{3}y^{3/2} + \frac{5}{48}\frac{1}{y^{3/2}} + \dots$. we get

$$S(y) \sim \frac{2\tilde{y}_0^{3/2}}{3\hbar} + \hbar\left(\frac{5}{48\tilde{y}_0^{3/2}} + \tilde{y}_0^{1/2}\tilde{y}_2\right) + \hbar^3\cdots = \frac{1}{\hbar}\int_{x_0}^{x}\sqrt{P(x')}dx' + \hbar(\dots) \tag{D.156}$$

then we can obtain the $\hbar$ expansion of $s_{abc}(x)$,

$$s_{abc}(x) = \frac{\pi}{2} + 2\left(\frac{2}{3}y(x,\hbar)^{3/2} + \frac{5}{48}\frac{1}{y(x,\hbar)^{3/2}} + \frac{1105}{9216}\frac{1}{y(x,\hbar)^{9/2}} + \dots\right) \tag{D.157}$$

$$= \frac{\pi}{2} + 2\left(\frac{2\tilde{y}_0(x)^{3/2}}{3\hbar} + \left(\frac{5}{48\tilde{y}_0(x)^{3/2}} + \tilde{y}_0(x)^{1/2}\tilde{y}_2(x)\right)\hbar + \dots\right). \tag{D.158}$$

We can think about this as a regularized version of the integral of $2p_{ab}$ from the zero to $x$. More precisely, as all the ingredients of the definition above have good WKB asymptotics, we will show below that the $\hbar$ expansion exactly coincide with the contour integral of $\frac{1}{2}p_{ab}$ from $x$ to $x$ along a path $\gamma_{abc}$ which winds around the zero while keeping away from it: namely, up to some multiple of $i\frac{\pi}{2}$ we have

$$s_{abc}(x) = \int_{\gamma_{abc}(x)} p_{ab}(u)du. \tag{D.159}$$

We should really keep track of factors of $\pm i$ in front of the exponents:

$$e^{s_{abc}(x)} = \frac{\frac{\sqrt{p_{ab}(x)}}{\sqrt{p_{ba}(x)}}\frac{\sqrt{p_{ca}(x')}}{\sqrt{p_{ac}(x')}}}{\frac{\sqrt{p_{bc}(x'')}}{\sqrt{p_{cb}(x'')}}} e^{\frac{1}{2}s_{ab}(x)-\frac{1}{2}s_{ac}(x')}e^{-\frac{1}{2}s_{ca}(x')+\frac{1}{2}s_{cb}(x'')}e^{\frac{1}{2}s_{bc}(x'')-\frac{1}{2}s_{ba}(x)}. \tag{D.160}$$

We now show explicitly why (D.159) is true at the first two orders. Recall that the WKB momentum is

$$p(x,\hbar) = \frac{1}{\hbar}\sqrt{P(x)} + \hbar\Big[\frac{-5P'^2 + 4PP''}{32P^{5/2}}\Big] + \dots \tag{D.161}$$

The leading order is easy since $\sqrt{P(x)}$ is integrable at the zero and we can just pinch the contour to the zero

$$2\frac{2\tilde{y}_0(x)^{3/2}}{3\hbar} = \frac{2}{\hbar}\int_{x_0}^{x}\sqrt{P(x')}dx'. \tag{D.162}$$

The order $\hbar$ is not as obvious

$$\frac{5}{48}\tilde{y}_0(x)^{-3/2}+\tilde{y}_0(x)^{1/2}\tilde{y}_2(x)=\frac{5}{48}\frac{1}{\int_{x_0}^{x}\sqrt{P(x)}}+\int_{x_0}^{x}\tilde{y}_0^{-1/2}(x')Q(x')dx' \tag{D.163}$$

where

$$Q(x)=\frac{-3\tilde{y}_0''^2+2\tilde{y}_0'\tilde{y}_0'''}{8\tilde{y}_0'^3} \tag{D.164}$$

is generically nonzero and regular as $x\to x_0$. Let's now try to understand how this realizes a primitive of the WKB one form at the order of $\hbar$, which is $\frac{4PP''-5P'^2}{32P^{5/2}}$. Apparently, it is not integrable at the zero $x_0$ because it is divergent there. However, we can rewrite it as

$$p_1(x)=\frac{4PP''-5P'^2}{32P^{5/2}}=\left[\frac{4PP''-5P'^2}{32P^{5/2}}+\frac{5}{32}\frac{\sqrt{P(x)}}{\tilde{y}_0^3}\right]-\frac{5}{32}\frac{\sqrt{P(x)}}{\tilde{y}_0^3} \tag{D.165}$$

$$=\frac{Q(x)}{\sqrt{\tilde{y}_0}}-\frac{5}{32}\frac{\sqrt{P(x)}}{\tilde{y}_0^3}. \tag{D.166}$$

Note that generically around the zero $x_0$, the behavior of $\tilde{y}_0(x)$ is

$$\tilde{y}_0(x)=\left(\frac{3}{2}\int_{x_0}^{x}\sqrt{P(x')}dx'\right)^{\frac{2}{3}}\overset{x\to x_0}{\to}\#(x-x_0)+\dots \tag{D.167}$$

So the first term in (D.166) is integrable, and we can shrink the contour $\gamma_{abc}(x)$ to the zero. The second term is badly divergent but a total derivative

$$-\frac{5}{32}\frac{\sqrt{P(x)}}{\tilde{y}_0^3}=\left(\frac{5}{48}\frac{1}{\tilde{y}_0^{3/2}}\right)'=\left(\frac{10}{72}\frac{1}{\int_{x_0}^{x}\sqrt{P(x')dx'}}\right)'. \tag{D.168}$$

Therefore, we have found a good primitive of $p_1(x)$, which is the order $\hbar$ part of $p(x,\hbar)$

$$\int_{x_0}^{x}\frac{Q(x')}{\sqrt{\tilde{y}_0}}dx'+\frac{5}{48}\frac{1}{\tilde{y}_0(x)^{3/2}}. \tag{D.169}$$

This finishes the proof of (D.159) at the order of $\hbar$. This way of separating divergent total derivative from the less divergent part in (D.166) is very reminiscent of a more well-known way [227, 228] to evaluate the contour integral, which goes as follows. Write

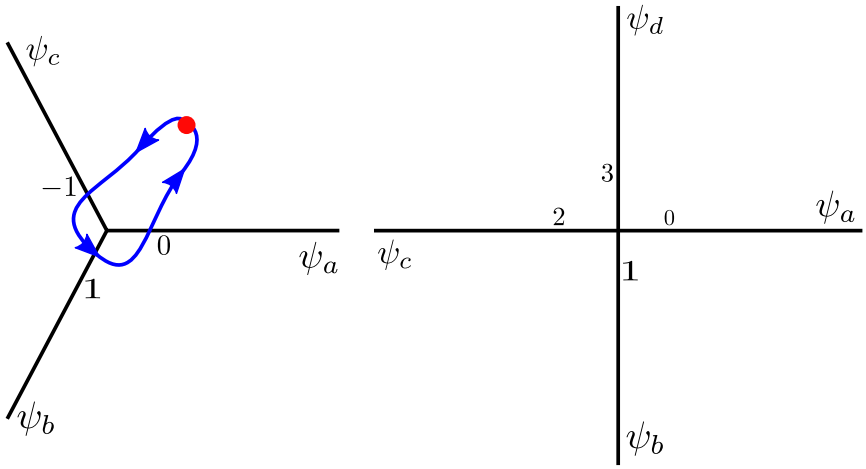


Figure D.3: The Stokes diagrams in the local coordinate system around the simple zero and the double zero. The numbers close to the origin label the numbering for the nice local solutions $A_i(y)$ we use in this section, whereas $\psi_\bullet$ label the corresponding small solutions.

$P(x) = V(x) - E$.

$$p_1(x) = \frac{4PP'' - 5P'^2}{32P^{5/2}} = \frac{4(V-E)V'' - 5V'^2}{32(V-E)^{5/2}} \tag{D.170}$$

$$= \left[\frac{1}{8}\frac{V''}{(V-E)^{3/2}} - \frac{5}{48}\frac{V''}{(V-E)^{3/2}}\right] + \frac{5}{48}\frac{d}{dx}\frac{V'}{(V-E)^{3/2}} \tag{D.171}$$

$$= \frac{1}{24}\frac{d}{dE}\frac{V''}{(V-E)^{1/2}} + \frac{5}{48}\frac{d}{dx}\frac{V'}{(V-E)^{3/2}}. \tag{D.172}$$

Notice that the first term is integrable at the zero and the second term is a total derivative.

**Near a double zero**

If the quadratic differential $P(x)$ has a double zero at $x_0$, then there are four special WKB lines emanating from $x_0$, around which we can access four small solutions, which are denoted as $\psi_a$, $\psi_b$, $\psi_c$, $\psi_d$ in the Fig. D.3. We now have linear relations

$$\begin{aligned}
(\psi_a, \psi_b)\psi_c + (\psi_c, \psi_a)\psi_b + (\psi_b, \psi_c)\psi_a &= 0, \\
(\psi_b, \psi_c)\psi_d + (\psi_d, \psi_b)\psi_c + (\psi_c, \psi_d)\psi_b &= 0, \\
(\psi_c, \psi_d)\psi_a + (\psi_a, \psi_c)\psi_d + (\psi_d, \psi_a)\psi_c &= 0, \\
(\psi_d, \psi_a)\psi_b + (\psi_b, \psi_d)\psi_a + (\psi_a, \psi_b)\psi_d &= 0.
\end{aligned} \tag{D.173}$$

One can define a nontrivial cross-ratio out of the four solutions $\chi = \frac{(\psi_a,\psi_b)(\psi_c,\psi_d)}{(\psi_b,\psi_c)(\psi_d,\psi_a)}$, which is close to 1 as $\hbar \to 0$. Note that the Wronskians between non-adjacent solutions are not accessible to the standard WKB analysis. One of the goals of this section is to provide a way to evaluate such Wronskians by relating to the local coordinate system around this double zero.

Recall that from the general expression (D.134), the Schrödinger equation in this local coordinate system takes the form

$$\partial_y^2 A(y) = \left[y^2 + \hbar a(\hbar)\right] A(y) \tag{D.174}$$

with $a(\hbar) = a_0 + \hbar^2 a_2 + \hbar^4 a_4 + \dots$ being some function of $\hbar$ that can be determined in $\hbar \to 0$ asymptotics from the differential equation

$$(\partial_x y(x))^2 \left[y(x)^2 + \hbar a(\hbar)\right] + \frac{3}{4}\left(\frac{\partial_x^2 y(x)}{\partial_x y(x)}\right)^2 - \frac{1}{2}\frac{\partial_x^3 y(x)}{\partial_x y(x)} = T(x). \tag{D.175}$$

Nice local solutions to (D.174) are given in (D.189), (D.191) and (D.211), which we denote as $A_i$, $i \in \mathbb{Z}$. To relate these local solutions to the small solutions $\psi_a$, $\psi_b$, $\psi_c$, $\psi_d$, we now require

$$\frac{(A_2, A_0)A_1(y(x))}{(A_1, A_2)A_0(y(x))} = \frac{(\psi_c, \psi_a)\psi_b}{(\psi_b, \psi_c)\psi_a} \equiv e^{s_{abc}(x)} \tag{D.176}$$

which also implies easily

$$\frac{(A_2, A_0)A_1(y(x))}{(A_0, A_1)A_2(y(x))} = \frac{(\psi_c, \psi_a)\psi_b}{(\psi_a, \psi_b)\psi_c} \equiv e^{s_{cba}(x)}. \tag{D.177}$$

On the other hand, if the cross-ratio of $A_i$ is adjusted to be $\chi$, that can be written as

$$\frac{(A_2, A_3)A_1(y(x))}{(A_3, A_1)A_2(y(x))} = \frac{(\psi_c, \psi_d)\psi_b}{(\psi_d, \psi_b)\psi_c} \equiv e^{s_{cbd}(x)} \tag{D.178}$$

etcetera.

In short, we have a good coordinate in all four sectors. In particular, that means we could determine this way the asymptotic expansion of the cross-ration $\chi$. On the other hand, that asymptotic expansion is already computable from a contour integral of $p(x)$ on a contour wrapping around the double zero while keeping away from it.

We can now relate $y$ to $s_{ab}$ and to the other WKB coordinates nearby:

$$\frac{(A_2, A_0)A_1(y(x))}{(A_1, A_2)A_0(y(x))} = e^{s_{abc}(x)} = \frac{(\psi_c, \psi_a)\psi_b}{(\psi_b, \psi_c)\psi_a}. \tag{D.179}$$

If we expand the left hand side in an asymptotic expansion at large $y(x)$, we can obtain the $\hbar$ expansion of $e^{s_{abc}(x)}$ as follows. Asymptotically at large $y$, $A_0(y) \sim \frac{1}{\sqrt{2\partial_y S(y)}} e^{-S(y)}$, with

$$S(y) \sim \frac{y^2}{2} + \frac{1}{2}a\hbar \log y + \frac{3 + a^2\hbar^2}{16} y^{-2} + \left(-\frac{19a\hbar}{64} - \frac{a^3\hbar^3}{64}\right) y^{-4} + O(y^{-6}) \tag{D.180}$$

$$\sim \frac{\tilde{y}_0^2}{2\hbar} + \hbar\Big[\frac{3}{16}\frac{1}{\tilde{y}_0^2} + \tilde{y}_0\tilde{y}_2 + \frac{1}{2}a^{(0)} \log \tilde{y}_0 - \frac{1}{4}a^{(0)} \log \hbar\Big] + O(\hbar^3) \tag{D.181}$$

where we have parameterized the $\hbar \to 0$ asymptotics $y(x) = \hbar^{-1/2}(\tilde{y}_0(x) + \hbar^2 \tilde{y}_2(x) + O(\hbar^4))$ and $a(\hbar) = a^{(0)} + \hbar^2 a^{(2)} + O(\hbar^4)$. We then obtain the $\hbar$ expansion of $s_{abc}(x)$

$$\log \frac{(A_2, A_0)}{(A_1, A_2)} - \frac{\pi i}{2} + 2\left(\frac{\tilde{y}_0(x)^2}{2\hbar} + \hbar\Big[\frac{3}{16}\frac{1}{\tilde{y}_0(x)^2} + \tilde{y}_0(x)\tilde{y}_2(x) + \frac{1}{2}a^{(0)} \log \tilde{y}_0(x) - \frac{1}{4}a^{(0)} \log \hbar\Big] + O(\hbar^3)\right).$$

Let's note a crucial point of (D.179). While $(\psi_c, \psi_a)$ cannot be computed by a naive WKB contour integral away from the zeroes, everything else in (D.179) can be in principle evaluated: $(A_1, A_2)$ is normalized to be $-i$; $(A_2, A_0)$ will be computed in (D.214); $(\psi_b, \psi_c)$ is controlled by a WKB contour integral. Therefore (D.179) provides an interesting prediction of $(\psi_c, \psi_a)$. So the relation above should really be written as

$$(\psi_c, \psi_a) = (A_2, A_0)\frac{(\psi_b, \psi_c)}{(A_1, A_2)}\frac{A_1(y(x))}{\psi_b(x)}\frac{\psi_a(x)}{A_0(y(x))} \tag{D.182}$$

Note that $A_1(y(x))$ and $A_0(y(x))$ have to be proportional to $\sqrt{y'(x)}\psi_b(x)$ and $\sqrt{y'(x)}\psi_a(x)$, respectively. Therefore to figure out $(\psi_c, \psi_a)$, which is $x$ independent, we just need to figure out the constants of proportionality. We can do so by comparing the $\hbar$ expansions and read out the $x$ independent terms.

### D.5.3 Recipe for evaluating Wronskians

1. If we have $\psi(x)$ either exact or numerical solution, we can just evaluate $(\psi_n, \psi_m)$. Normalization of the solutions are not important if one is only interested in the cross ratios.

2. If two solutions $\psi_n$ and $\psi_m$ are connected to the same zero of order $k$, we have to choose a branch of $\tilde{y}_0 = \left(\frac{k+2}{2}\int\sqrt{P}dx\right)^{\frac{2}{k+2}}$. This is equivalent to choosings how the local solutions $A_{k;a}(y)$ correspond to the small solutions $\psi_a(x)$. For each pair $\psi_n(x) \propto [\partial_x y(x)]^{-1/2} A_{k;a}(y)$, $\psi_n(x) \propto [\partial_x y(x)]^{-1/2} A_{k;a}(y)$, we can just read out the constant of proportionality from the large $x$ asymptotics in the corresponding directions. If we denote the constants of proportionality as $C_n(\hbar)$ and $C_m(\hbar)$, the Wronskians are just
$$(\psi_n, \psi_m) = C_n(\hbar) C_m(\hbar) (A_{k;a}, A_{k,b}). \tag{D.183}$$

3. If two solutions $\psi_n$ and $\psi_m$ are not connected via special WKB lines to the same zero, we can use Plücker relation to reduce to the previous case.

4. What remains is to figure out the Wronskians between local solutions $(A_{k;a}, A_{k,b})$. This will be done via perturbation theory in Section D.5.5.

### D.5.4 Numerical implementation

Here in this section, we explain how we implement the numerics. In particular, given an ODE
$$\partial_x^2 \psi(x) = \left(\frac{P(x)}{\hbar^2} + t(x)\right)\psi \tag{D.184}$$
we would like to find the corresponding small solutions and evaluate the Wronskians between them.

Let's first consider the case where $P(x)$ is a polynomial of degree $n$ and $t(x) = 0$. In this case the ODE is regular everywhere on the complex plane with $n+2$ asymptotic direction towards the irregular singularity at infinity. Then the task would be to find the decaying solutions along each asymptotic direction. However, initial value problems are more natural in numerics, where one usually specifies the initial condition (the value of $\psi$ and $\partial_x\psi$ at a chosen initial point) and numerically integrate outward along a certain direction. An obvious way to proceed is the so-called shooting method, which reduces the boundary value problems to initial value problems and one adjusts the initial condition

until the desired decaying asymptotics is reached. However, it turns out that, in practice, large $x$ asymptotics is very sensitive to the initial condition at small $x$ thus it is very hard to reach a decent accuracy.

Instead, we employ the inward integration approach where the boundary condition at a certain large value of $x$ is provided by the chosen WKB solutions. Intuitively this works better for us because the unwanted dominant solution is suppressed by the inward integration. We will see more examples of the numerical calculation below.

It's not hard to imagine that dealing with small $\hbar$ is challenging for numerics since it exponentially suppresses the solution. This can be easily resolved by a rescaling of the coordinate. For example, under a change of coordinate $y = \hbar^{-2/5}x$

$$\frac{x^3 - ax^2}{\hbar^2} \Leftrightarrow y^3 - a\hbar^{-\frac{2}{5}}y^2 \tag{D.185}$$

Therefore, the result only depends on the combination $a\hbar^{-\frac{2}{5}}$. In the numerics we will study the latter and vary $a$. Wronskians and cross ratios will be invariant under the rescaling of the coordinate. If one wants to study the wavefunctions, we can easily restore the $\hbar$ dependence by going back to the original coordinate.

There are other numerical implementation methods available[6]. See, e.g. [229] for a recent study.

### D.5.5 Solutions near zeros and their Wronskians

In general, given a local form around a zero of generic integer order $k$ where the stress tensor is regular

$$\frac{\tilde{y}^k}{\hbar^2} + a_{k-2}\tilde{y}^{k-2} + \cdots + a_1\tilde{y} + a_0 \tag{D.186}$$

which becomes under $\tilde{y} = \hbar^{\frac{2}{k+2}}y$,

$$T_k^{\text{local}}(y) = y^k + a_{k-2}\gamma^k y^{k-2} + \cdots + a_j\gamma^{2+j}y^j + \cdots + a_0\gamma^2 \tag{D.187}$$

where $\gamma = \hbar^{\frac{2}{k+2}}$ and

$$a_m = a_m^{(0)} + \gamma^{k+2}a_m^{(2)} + \gamma^{2(k+2)}a_m^{(4)} + \dots \tag{D.188}$$

Let's attempt to solve the ODE perturbatively in $\gamma$. At the leading order, the Schrödinger operator is just $\partial_y^2 - y^k$. A set of nice solutions has been given in [1], which we now review.

[6] We thank Andy Neitzke for the helpful correspondence.

We choose the solution that decays along the positive real axis which takes the form

$$A^{(0)}_{k;0}(y)=\sqrt{\frac{2y}{\pi(k+2)}}K_{\frac{1}{k+2}}\left(\frac{2}{k+2}y^{1+\frac{k}{2}}\right) \tag{D.189}$$

with large $y$ asymptotics

$$A^{(0)}_{k;0}(y)\sim\frac{1}{\sqrt{2}y^{k/4}}e^{-\frac{2}{k+2}y^{1+\frac{k}{2}}}. \tag{D.190}$$

We can produce more solutions by a rotation

$$A^{(0)}_{k;a}(y)=e^{-\frac{\pi i}{k+2}a}A^{(0)}_{k;0}(e^{\frac{2\pi i}{k+2}a}y). \tag{D.191}$$

It deserves some remarks here. The definition for (D.189) is obvious because we want $\frac{1}{\sqrt{2\partial_y S(y)}}e^{-S(y)}$ type of asymptotics. Because of the rotational symmetry $y\to e^{\frac{2\pi i}{k+2}}y$, the definition (D.191) is equivalent to

$$A^{(0)}_{k;a}(y=e^{-\frac{2\pi i}{k+2}a}R)\equiv e^{-\frac{\pi i}{k+2}a}A^{(0)}_{k;0}(R),R\in\mathbb{R}_+ \tag{D.192}$$

The inclusion of the factor $e^{-\frac{\pi i}{k+2}a}$ is such that asymptotically along the ray of $e^{-\frac{2\pi i}{k+2}a}$

$$A^{(0)}_{k;a}(y)\sim\frac{1}{\sqrt{2e^{\pi i a}y^{k/2}}}e^{-e^{\pi i a}\frac{2}{k+2}y^{1+\frac{k}{2}}}. \tag{D.193}$$

As a result, all neighbouring Wronskians $(A^{(0)}_{k;a},A^{(0)}_{k;a+1})=-i$. This brings a side effect that $A^{(0)}_{k;a}=-A^{(0)}_{k;a+k}$. Had we defined $A^{(0)}_{k;a}(y)$ in (D.191) without the factor $e^{-\frac{\pi i}{k+2}a}$, we would have $A^{(0)}_{k;a}=A^{(0)}_{k;a+k}$. Furthermore, thanks to the identity

$$A^{(0)}_{k;a-1}(y)+A^{(0)}_{k;a+1}(y)=\left(e^{\frac{\pi i}{k+2}}+e^{-\frac{\pi i}{k+2}}\right)A^{(0)}_{k;a}(y) \tag{D.194}$$

we can compute for any $a$ and $b$, $i(A^{(0)}_{k;a},A^{(0)}_{k;b})=d^{(k)}_{b-a}$, where

$$d^{(k)}_n=\frac{e^{\frac{\pi i}{k+2}n}-e^{-\frac{\pi i}{k+2}n}}{e^{\frac{\pi i}{k+2}}-e^{-\frac{\pi i}{k+2}}}. \tag{D.195}$$

Setting $k = 1$, we are reduced to the Airy functions

$$A^{(0)}_{1;a}(y) \equiv \mathrm{Ai}^{(0)}_a(y) \equiv \sqrt{2\pi} e^{-\frac{\pi i a}{3}} \mathrm{Ai}(e^{\frac{2\pi i a}{3}} y). \tag{D.196}$$

To obtain higher order corrections, we parameterize the solution as

$$A(y) = \sum_{n \geq 0} \gamma^n A^{(n)}(y) \tag{D.197}$$

where for now we suppressed the subscript. The differential equation $\partial_y^2 A(y) = T_k^{\mathrm{local}}(y) A(y)$ is expanded order by order in $\gamma$ as

$$\begin{aligned}
\gamma^0 :& \partial^2 A^{(0)} - y^k A^{(0)} = 0, \\
\gamma^1 :& \partial^2 A^{(1)} - y^k A^{(1)} = 0, \\
\gamma^2 :& \partial^2 A^{(2)} - y^k A^{(2)} = a_0^{(0)} A^{(0)}, \\
\gamma^3 :& \partial^2 A^{(3)} - y^k A^{(3)} = a_1^{(0)} y A^{(0)} + a_0^{(0)} A^{(1)}, \\
\gamma^4 :& \partial^2 A^{(4)} - y^k A^{(4)} = a_2^{(0)} y^2 A^{(0)} + a_1^{(0)} y A^{(1)} + a_0^{(0)} A^{(2)}.
\end{aligned} \tag{D.198}$$

We fix the normalization of the solutions by matching with the WKB asymptotics, which is uniquely defined as

$$\frac{1}{\sqrt{\pm 2 \partial_y S}} e^{\mp S} \tag{D.199}$$

where $S = \frac{2}{k+2} y^{\frac{k+2}{2}} + \dots$ is a (fractional) power series of $y$, with no constant term. When the zero of even order, there is also $\log y$, which we choose to be the principal branch. For example,

$$\begin{aligned}
T_k^{\mathrm{local}}(y) &= y, & S &= \tfrac{2}{3} y^{3/2} + \tfrac{5}{48} \tfrac{1}{y^{3/2}} + \tfrac{1105}{9216} \tfrac{1}{y^{9/2}} + \dots \\
T_k^{\mathrm{local}}(y) &= y^2 + a\gamma^2, & S &= \tfrac{1}{2} y^2 + \tfrac{a\gamma^2}{2} \log y + \tfrac{3 + a^2 \gamma^4}{16} \tfrac{1}{y^2} + \dots \\
T_k^{\mathrm{local}}(y) &= y^3 + b\gamma^3 y + a\gamma^2, & S &= \tfrac{2}{5} y^{5/2} + b\gamma^3 y^{1/2} - a\gamma^2 \tfrac{1}{y^{1/2}} + \dots \\
T_k^{\mathrm{local}}(y) &= y^4 + c\gamma^4 y^2 + b\gamma^3 y + a\gamma^2, & S &= \tfrac{1}{3} y^3 + \tfrac{c\gamma^4}{2} y + \tfrac{b\gamma^3}{2} \log y + \tfrac{c^2 \gamma^8 - 4a\gamma^2}{8} \tfrac{1}{y} + \dots
\end{aligned} \tag{D.200}$$

We can now give the prescription for determining the solutions order by order in $\gamma$. The small $A_{k;a}(y)$, which decays along the ray of $\exp(-\frac{2\pi i}{k+2} a)$, is given by

$$A_{k;a}(y; \gamma, \{a_i\}) = A^{(0)}_{k;a}(y) + \gamma A^{(1)}_{k;a}(y) + \gamma^2 A^{(2)}_{k;a}(y) + \dots \tag{D.201}$$

$A_{k;a}$ can be obtained recursively in the following way. We already defined the leading order $A^{(0)}_{k;a}$ above. Obviously WKB solutions (D.199) expand in power of $\gamma$ starting from $\gamma^2$, so we need to choose $A^{(1)}_{k;a} = 0$. And for each $A^{(n)}_{k;a}$ with $n \geq 2$, we need to solve an inhomogeneous ODE with two integration constants to fix, one of which is fixed by requiring the solution to decay along the chosen direction and the other one is fixed to match the normalization of the WKB solution (D.199). In practice, as seen in the examples below, this is achieved by choosing the lower limit of the integration to be at infinity.

Given two small solutions $A_{k;a} = A^{(0)}_{k;a} + \gamma^2 A^{(2)}_{k;a} + \gamma^3 A^{(3)}_{k;a} + \dots$ and $A_{k;b} = A^{(0)}_{k;b} + \gamma^2 A^{(2)}_{k;b} + \gamma^3 A^{(3)}_{k;b} + \dots$, their Wronskian reads

$$\begin{aligned}(A_{k;a}, A_{k;b}) = (A^{(0)}_{k;a}, A^{(0)}_{k;b}) + \gamma^2\Big[(A^{(2)}_{k;a}, A^{(0)}_{k;b}) + (A^{(0)}_{k;a}, A^{(2)}_{k;b})\Big] + \gamma^3\Big[(A^{(3)}_{k;a}, A^{(0)}_{k;b}) + (A^{(0)}_{k;a}, A^{(3)}_{k;b})\Big] \\ + \gamma^4\Big[(A^{(4)}_{k;a}, A^{(0)}_{k;b}) + (A^{(0)}_{k;a}, A^{(4)}_{k;b}) + (A^{(2)}_{k;a}, A^{(2)}_{k;b})\Big] + \dots \end{aligned} \tag{D.202}$$

In particular, we can verify that $(A_{k;a}, A_{k;a+1}) = (A^{(0)}_{k;a}, A^{(0)}_{k;a+1}) = -i$ with no higher order corrections. More interesting ones are the Wronskians between non-consecutive small solutions. We will give concrete examples below for the double zero and cubic zero, since it is trivial for simple zero.

If, on the other hand, we are interested in the local coordinate system around a zero that is a singularity of trivial monodromy, we would have

$$\frac{\tilde{y}^k}{\hbar^2} + a_{k-2}\tilde{y}^{k-2} + \dots + a_1\tilde{y} + a_0 + \frac{l(l+1)}{\tilde{y}^2} \tag{D.203}$$

or

$$y^k + a_{k-2}\hbar^{\frac{2k}{k+2}} y^{k-2} + \dots + a_j\hbar^{\frac{2j+4}{k+2}} y^j + \dots + a_0\hbar^{\frac{4}{k+2}} + \frac{l(l+1)}{y^2} \tag{D.204}$$

where $t(x) = a(x)^2 + \partial_x a(x)$, and $a(x)$ has residue $-l$ at $x_0$. The perturbative solutions can be found in a similar procedure as above except that we need to start with different solutions at the leading order. Since the Schrödinger operator at the leading order is $\partial^2 - y^k - \frac{l(l+1)}{y^2}$, the solutions that agree with the asymptotics (D.190) and (D.193) are given by

$$A^{(0)}_{k,l;0}(y) = \sqrt{\frac{2y}{\pi(k+2)}} K_{\frac{1+2l}{k+2}}\left(\frac{2}{k+2} y^{1+\frac{k}{2}}\right) \tag{D.205}$$

$$A^{(0)}_{k,l;a}(y) = e^{-\frac{\pi i}{k+2}a} A^{(0)}_{k,l;0}(e^{\frac{2\pi i}{k+2}a} y) \tag{D.206}$$

whose Wronskians are given by

$$i(A^{(0)}_{k,l;a}, A^{(0)}_{k,l;b}) = \frac{\sin\frac{\pi}{k+2}(2l+1)(b-a)}{\sin\frac{\pi}{k+2}(2l+1)}. \tag{D.207}$$

One sanity check is to look at $i(A^{(0)}_{k;a}, A^{(0)}_{k;a+k+2})$. One would like this to be zero since there is a unique decaying solution along a certain ray and therefore two must be proportional to each other. This is indeed mostly true since $2l+1 \in \mathbb{Z}$. It fails when $2l+1$ is an integer multiple of $k+2$, where we have

$$i(A^{(0)}_{k;a}, A^{(0)}_{k;a+k+2}) = (-1)^{(k+1)\frac{2l+1}{k+2}}(k+2). \tag{D.208}$$

This is another manifestation of the requirement that $2l \leq k$.

**Example: double zero**

Consider the ODE

$$\partial^2_{\tilde{y}}\tilde{A}(\tilde{y}) = (\frac{\tilde{y}^2}{\hbar^2} + a)\tilde{A}(\tilde{y}) \tag{D.209}$$

where $a = a^{(0)} + \hbar^2 a^{(2)} + \hbar^4 a^{(4)} + \dots$. To find perturbative solution, we rewrite using $\gamma = \hbar^{1/2}$ and $\tilde{y} = \gamma y$, and we have

$$\partial^2_y A(y) = \left(y^2 + \gamma^2 a\right) A(y). \tag{D.210}$$

It is not hard to see that all the equations at the odd power of $\gamma$ are homogeneous and WKB solutions only involve even powers of $\gamma$, so solutions $A = \sum \gamma^j A^{(j)}$ only involve even powers of $\gamma$, namely $A = \sum \gamma^{2j} A^{(j)} = \sum \hbar^j A^{(j)}$, where the leading order is given by

$$A^{(0)}_{2;n} = \sqrt{\frac{y}{2\pi}} K_{\frac{1}{4}}\left(\frac{1}{2}y^2 e^{\pi i n}\right), \tag{D.211}$$

One of the immediate consequences is that the Wronskians $(A_n, A_m) = (A^{(0)}_n, A^{(0)}_m) + \dots$ are corrected by integer powers of $\hbar$.

On the other hand, the ODE[7] (D.209) can be solved exactly by using

$$\tilde{A}_0(\tilde{y},\hbar) = \left(\frac{\hbar}{2}\right)^{\frac{1-a\hbar}{4}} D_{-\frac{1+a\hbar}{2}}\left(\frac{\sqrt{2}\tilde{y}}{\sqrt{\hbar}}\right) \tag{D.212}$$

$$\tilde{A}_n(\tilde{y},\hbar) = \tilde{\psi}_0(\tilde{y}, \hbar e^{-i\pi n}). \tag{D.213}$$

Their Wronskians can be evaluated easily. For example, $i(\tilde{A}_n, \tilde{A}_{n+1}) = 1$,

$$i(\tilde{A}_{-1},\tilde{A}_1) = \frac{\sqrt{2\pi}}{\Gamma(\frac{1}{2}-\frac{a\hbar}{2})}\left(\frac{\hbar}{2}\right)^{\frac{a\hbar}{2}}, \quad i(\tilde{A}_{-1},\tilde{A}_2) = e^{ia\pi\hbar}. \tag{D.214}$$

The cross ratio

$$\chi \equiv \frac{(\tilde{A}_0,\tilde{A}_1)(\tilde{A}_{-1},\tilde{A}_2)}{(\tilde{A}_{-1},\tilde{A}_0)(\tilde{A}_1,\tilde{A}_2)} = e^{i\pi a\hbar} \tag{D.215}$$

which exactly coincides with the contour integral $\exp \oint p(x,\hbar)dx$ around this double zero of the WKB momentum which has a pole

$$p(x,\hbar) = \frac{x}{\hbar} + \frac{a\hbar}{2x} - \frac{3\hbar + a^2\hbar^3}{8x^3} + \frac{19a\hbar^3 + a^3\hbar^5}{16x^5} + \dots \tag{D.216}$$

**Example: cubic zero**

In the local coordinate system around a cubic zero, $T(\tilde{y}) = \frac{\tilde{y}^3}{\hbar^2} + b\tilde{y} + a$, where

$$b = b^{(0)} + \hbar^2 b^{(2)} + \hbar^4 b^{(4)} + \dots \tag{D.217}$$

$$a = a^{(0)} + \hbar^2 a^{(2)} + \hbar^4 a^{(4)} + \dots \tag{D.218}$$

or equivalently the stress tensor is $y^3 + b\gamma^3 y + a\gamma^2$ with $\gamma = \hbar^{2/5}$. The leading order solutions are defined in (D.189) and (D.191). Since here in this section we only flesh out details for three solutions, for convenience we write $\phi_0 = A^{(0)}_{3;0}$, $\phi_1 = A^{(0)}_{3;1}$, $\phi_{-1} = A^{(0)}_{3;-1}$.

Let's now solve the ODE perturbatively using the prescription described in D.5.5. Let's

[7] The reason we solve (D.209) instead of the one in $y$ coordinate is because we have $\hbar^2$ in the former, so that we can apply the trick $\hbar \to \hbar e^{-i\pi n}$ to find other solutions. Due to the same reason, we don't shift $\hbar \to \hbar e^{-i\pi n}$ in the Jacobian part $\hbar^{-1/4}$ if one wants to go back to $y$ coordinate.

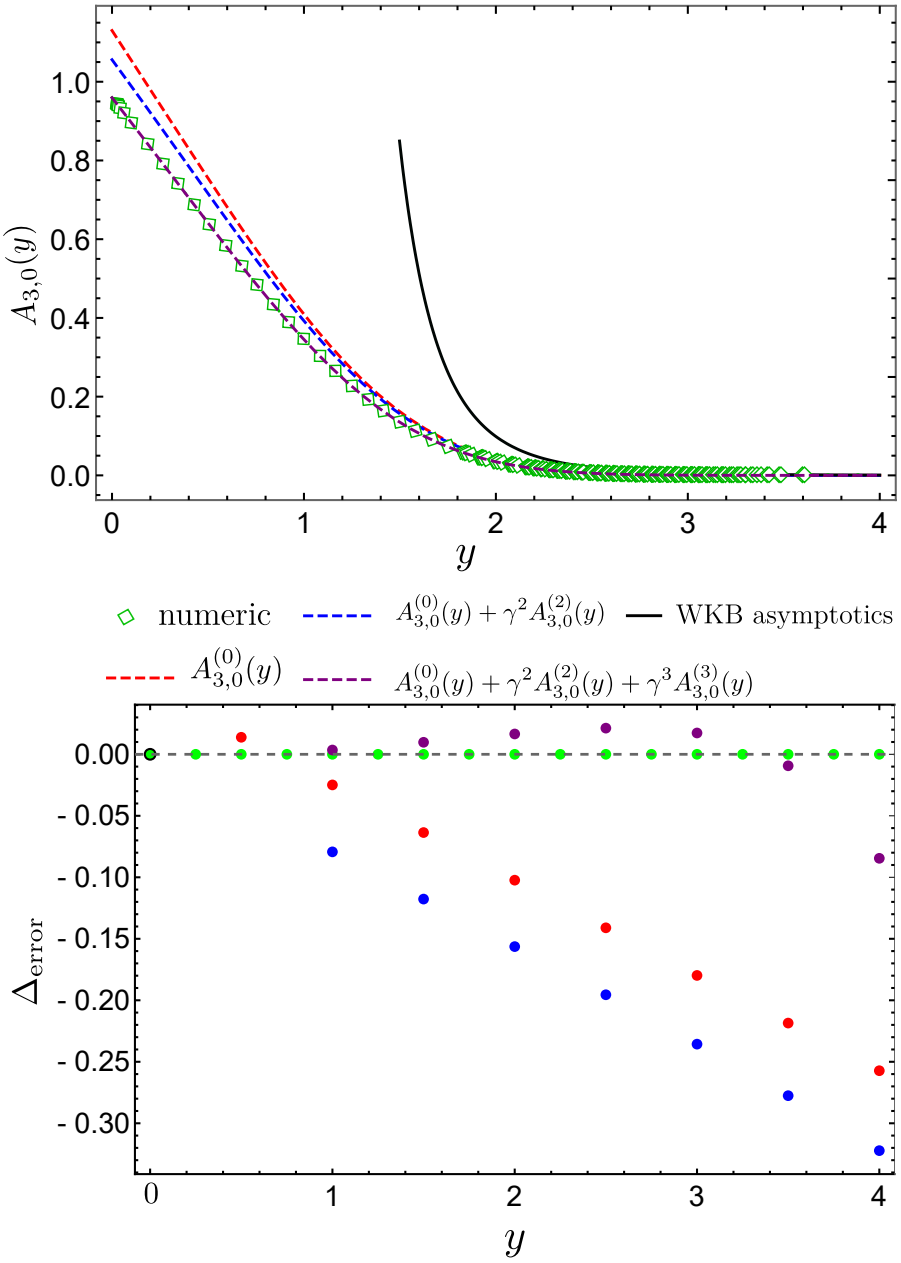


Figure D.4: Numerical and analytic evaluation in the local coordinate system around a cubic zero defined at the beginning of Subsection D.5.5. Parameters used are chosen in a rather generic way: $\hbar = \frac{1}{5}$, $a = -\frac{4}{21}$, $b = \frac{1}{2}$. (Top) Various approximate evaluations of $A_{3,0}(y)$. Approximation gets better with higher corrections included. (Bottom) $\Delta_{\text{error}} \equiv \frac{\partial_x^2 \psi(x)}{\psi(x)} - \frac{1}{\hbar^2} P(x)$. We don't show the $\Delta_{\text{error}}$ for the WKB asymptotic solution since the error is too big. The legend of coloring is shared in both diagrams.

denote the small solution along the ray $e^{-i2\pi n/5}$ as

$$A_{k;n}(y) = \sum_{n\geq 0} \gamma^j A^{(j)}_{k;n}(y). \tag{D.219}$$

Wronskians between these functions are easily evaluated

$$(A_{3,0}, A_{3,1}) = 1 \tag{D.220}$$

$$(A_{3,-1}, A_{3,1}) = (A^{(0)}_{3,-1}, A^{(0)}_{3,1}) + \gamma^2 a^{(0)} \left[(A^{(0)}_{3,-1}, A^{(2)}_{3,1}) + (A^{(2)}_{3,-1}, A^{(0)}_{3,1})\right] + O(\gamma^3)\dots \tag{D.221}$$

### D.5.6 Examples: polynomial oper

**Ex:** $P(x) = x^2 - 2a$

The stress tensor is $T(x) = \frac{x^2-2a}{\hbar^2}$. There are four small solutions, given by the parabolic functions

$$\psi_0(x) = \left(\frac{\hbar}{2}\right)^{\frac{1}{4}+\frac{a}{2\hbar}} D_{-\frac{1}{2}+\frac{a}{\hbar}}\left(\frac{\sqrt{2}x}{\sqrt{\hbar}}\right), \quad \psi_n(x,\theta) = \psi_0(x, \theta + i\pi n) \tag{D.222}$$

with Wronskians $i(\psi_n, \psi_{n+1}) = 1$ and

$$i(\psi_{-1}, \psi_1) = \frac{\left(\frac{\hbar}{2}\right)^{-a/\hbar}\sqrt{2\pi}}{\Gamma\left(\frac{1}{2}+\frac{a}{\hbar}\right)}, \quad i(\psi_{-1}, \psi_2) = e^{-2i\pi\frac{a}{\hbar}}. \tag{D.223}$$

The normalization in (D.222) is such that in its large $x$ asymptotic expansion $\frac{1}{\sqrt{\pm 2\partial_x S(x)}} e^{\mp S(x)}$, there is no constant term in the primitive $S(x)$.

In $\hbar$ asymptotics, $i(\psi_{-1}, \psi_1) = (2e)^{1/\hbar}\left(1 + \frac{1}{24}\hbar + \frac{1}{1152}\hbar^2 - \frac{1003}{414720}\hbar^3 + O(\hbar^4)\right)$. Let us try to reproduce this in two other ways: contour integral of WKB momentum and using local coordinate systems.

The WKB momentum is $p(x,\hbar) = \frac{\sqrt{x^2-2}}{\hbar} + p_1(x)\hbar + p_3(x)\hbar^3 + \dots$. Since

$$\int^L \sqrt{x'^2 - 2}dx' \overset{L\to\infty}{\longrightarrow} \frac{L^2}{2} + const - \log L + O\Big(\frac{1}{L^2}\Big) \tag{D.224}$$

we can regularize the integral at infinity by defining

$$\int_{\infty}^{x} \equiv \lim_{L\to\infty} \int_{L}^{x} + \left(\frac{L^2}{2} + A - \log L\right). \tag{D.225}$$

We will choose the constant $A = 0$ in this article to normalize the WKB solutions. With this normalization, the large $x$ asymptotics will take the form of only power of $x$ without any constant[8]

$$\int_{\infty}^{x} \sqrt{x'^2 - 2}dx' \sim \frac{x^2}{2} - \log x + \frac{1}{4}x^2 + \dots \tag{D.226}$$

Therefore, the leading term of the integral of the WKB momentum is

$$\int_{-i\infty}^{i\infty} \sqrt{x'^2 - 2}dx' = \log 2e, \quad \int_{-i\infty}^{i\infty} p_1(x)dx = -\frac{1}{24}, \quad \int_{-i\infty}^{i\infty} p_3(x)dx = \frac{7}{2880}. \tag{D.227}$$

Therefore we get

$$i(\psi_{-1}, \psi_1) = e^{-\int_{-i\infty}^{i\infty} p(x,\hbar)} = (2e)^{1/\hbar}\left(1 + \frac{1}{24}\hbar + \frac{1}{1152}\hbar^2 - \frac{1003}{414720}\hbar^3 + O(\hbar^4)\right). \tag{D.228}$$

We can also find this result via going to the local coordinate system. Essentially one needs to figure out the constant of proportionality in $(\partial_x y(x,\hbar))^{-1/2} A(y(x)) \propto \psi(x)$. To this end, we look at the large $x$ asymptotics of both sides. By definition, the large $x$ asymptotics of $\psi(x)$ is given by $\frac{1}{\sqrt{\pm 2\partial_x S(x)}} e^{\mp S(x)}$, where

$$\begin{aligned} S(x) = \frac{x^2}{2\hbar} - \frac{a}{\hbar}\log x + \left(\frac{a^2}{4\hbar} + \frac{3\hbar}{16}\right)\frac{1}{x^2} + \left(\frac{a^3}{8\hbar} + \frac{19a\hbar}{32}\right)\frac{1}{x^4} \\ + \left(\frac{5a^4}{48\hbar} + \frac{145a^2\hbar}{96} + \frac{99\hbar^3}{256}\right)\frac{1}{x^6} + \dots \end{aligned} \tag{D.229}$$

which has no constant term according to our definition. On the other hand, the large $x$ asymptotics of $(\partial_x y(x,\hbar))^{-1/2} A(y(x))$ exactly matches with (D.229), modulo a possible

[8] There are some other natural choices as well. For example, we chose $A = -\log\sqrt{2e}$ in [1] such that the regularized integral $\int_{\infty}^{x} \sqrt{x'^2 - 2}dx'$ coincides with $\int_{\sqrt{2}}^{x} \sqrt{x'^2 - 2}dx'$. With this, $\int_{-i\infty}^{i\infty} \sqrt{x'^2 - 2}dx' = 0$, and consequently we don't have the prefactor $(2e)^{1/\hbar}$ in $i(\psi_{-1}, \psi_1)$

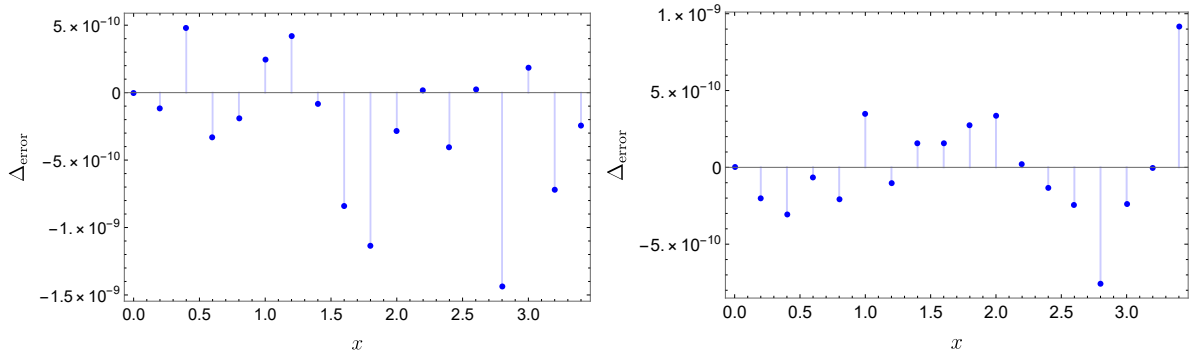


Figure D.5: Numerical error $\Delta_{\text{error}} \equiv \frac{\partial_x^2 \psi(x)}{\psi(x)} - \frac{1}{\hbar^2} P(x)$. (Left) $P(x) = x^2 - 2$ and $\hbar = 1$ (Right) $P(x) = x^3 - x^2$ and $\hbar = 1$. This is just to illustrate numerical error is indeed very small.

constant term in $S(x)$. With $y(x) = \hbar^{-2/3}(y_0 + \hbar^2 y_2 + \hbar^4 y_4 + \dots)$ and (D.156), we have

$$\tilde{S}(y) = \frac{2y_0(x)^{3/2}}{3\hbar} + \left( \frac{5}{48 y_0(x)^{3/2}} + y_0(x)^{1/2} y_2(x) \right) \hbar + \dots \tag{D.230}$$

$$= \left( \frac{x^2}{2} - \log \sqrt{2e} - \log x + \frac{1}{4} \frac{1}{x^2} + \dots \right) \frac{1}{\hbar} + \left( -\frac{1}{48} + \frac{3}{16 x^2} + \dots \right) \hbar. \tag{D.231}$$

Therefore $S(x) = \tilde{S}(y(x)) + \frac{1}{2} \left( \frac{1}{\hbar} \log 2e + \frac{1}{24} \hbar + \dots \right)$, and

$$\psi_1(x) = e^{\frac{1}{2}\left( \frac{1}{\hbar} \log 2e + \frac{1}{24} \hbar + \dots \right)} \left( \partial_x y(x, \hbar) \right)^{-1/2} A_1(y(x)) \tag{D.232}$$

hence

$$i(\psi_{-1}, \psi_1) = e^{\frac{1}{\hbar} \log 2e + \frac{1}{24} \hbar + \dots} (A_{-1}(y), A_1(y)) = e^{\frac{1}{\hbar} \log 2e + \frac{1}{24} \hbar + \dots}. \tag{D.233}$$

There is one cross ratio defined by

$$\chi = \frac{(\psi_0, \psi_1)(\psi_{-1}, \psi_2)}{(\psi_{-1}, \psi_0)(\psi_1, \psi_2)} = e^{-2\pi i \frac{a}{\hbar}}. \tag{D.234}$$

Furthermore, the exact solutions are solved by parabolic cylinder functions, which we can use to test our numerical calculation.

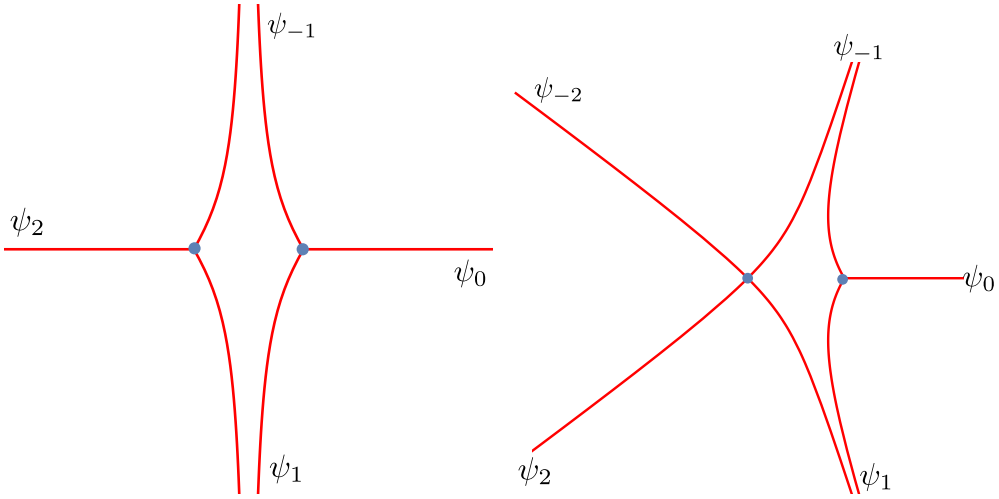


Figure D.6: Stokes diagram for (Left) $P(x) = x^2 - 2a$, (Right) $P(x) = x^3 - x^2$.

**Ex:** $P(x) = x^3 - x^2$

There is one simple zero, one double zero and five asymptotic directions. The Stokes diagram is shown in Fig. D.6.

In the local coordinate system around the double zero,

$$\tilde{T}(y,\hbar) = y^2 - 2a(\hbar), \quad a(\hbar) = \frac{7i}{64}\hbar - \frac{119119i\hbar^3}{131072} + \frac{10775385621i\hbar^5}{268435456} + \dots \tag{D.235}$$

Recall that

$$y_2(x) = \frac{1}{y_0(x)} \int_{x_0}^{x} y_0(x') \frac{8a_0^{(0)}(y_0')^4 - 3(y_0'')^2 + 2y_0'y_0'''}{8y_0^2(y_0')^3} dx' \tag{D.236}$$

the integrand around $x = 0$ is

$$\frac{a^{(0)} - \frac{7i}{64}}{x} + \frac{-1687i - 960a^{(0)}}{5760} + \dots \tag{D.237}$$

therefore we have to choose $a^{(0)} = \frac{7i}{64}$. And since typically $y_0(x) \sim \alpha x + \dots$, $y_2(x)$ will be nonzero at the zero $x = 0$.

With a suitably chosen branch cut, namely from 1 to positive infinity along the real

axis, the large $x$ asymptotics is given by

$$\int_1^x ix'\sqrt{1-x'}dx' \sim c_1 x^{5/2} + c_2 x^{3/2} + c_3 x^{1/2} + 0 + c_4 x^{-1/2} + \dots \tag{D.238}$$

and $\int_1^0 ix'\sqrt{1-x'}dx' = -\frac{4i}{15}$. Recall that we choose to regularize the integral at infinity by removing the powers of divergence without adding any constant term. As a result, the regularized contour integral of the WKB momentum

$$\int_{e^{-\frac{2\pi i}{5}}\infty}^{e^{\frac{2\pi i}{5}}\infty} ix'\sqrt{1-x'}dx' = 0. \tag{D.239}$$

So the leading order of $i(\psi_{-1}, \psi_1)$ is 1.

Let's try to reproduce $i(\psi_{-1}, \psi_1)$ using two local coordinate systems separately. We use $y_\pm(x)$ to denote the local coordinate system around the simple/double zero, respectively. At the leading order

$$S_+(y_+(x)) = \frac{2y_{+,0}(x)^{3/2}}{3\hbar} + \dots = \frac{1}{\hbar}\int_1^x ix'\sqrt{1-x'}dx' + \dots \tag{D.240}$$

$$S_-(y_-(x)) = \frac{y_{-,0}(x)^2}{2\hbar} + \dots = \frac{1}{\hbar}\int_0^x ix'\sqrt{1-x'}dx' + \dots \tag{D.241}$$

One might find this puzzling: since the constant term in the large $x$ asymptotics of $S_+$ is zero but is nonzero in $S_-$. This means that

$$(\partial_x y_+(x))^{-1/2} A_+(y(x)) = \psi(x) = e^{\pm\frac{4i}{15\hbar}+\dots} (\partial_x y_-(x))^{-1/2} A_-(y(x)). \tag{D.242}$$

But this is not problematic because the nontrivial factor actually cancels in the Wronskian. Therefore, they give the same $i(\psi_{-1}, \psi_1) = 1 + \dots$, as expected. This Wronskian actually has nontrivial $\hbar$ corrections, which we will present below.

First, of course, we can integrate the WKB momentum along the generic WKB line

$$i(\psi_{-1}, \psi_1) = \exp \int_{e^{-\frac{2\pi i}{5}}\infty}^{e^{\frac{2\pi i}{5}}\infty} p(x,\hbar)dx = \exp\left(0 + \frac{7\pi}{32}\hbar - \frac{119119\pi}{65536}\hbar^3 \dots\right) \tag{D.243}$$

$$\tilde{S}(y) = \frac{2y_0(x)^{3/2}}{3\hbar} + \left(\frac{5}{48y_0(x)^{3/2}} + y_0(x)^{1/2}y_2(x)\right)\hbar + \dots \tag{D.244}$$

One can obtain the same result in local coordinate system around the simple zero and the double zero.

As an example of Wronskians that cannot be evaluated by the contour integral of the WKB momentum, let's try to calculate $i(\psi_{-1}, \psi_2)$. Again we go to the local coordiante system around the double zero $x_- = 0$ and we have

$$\left(\frac{\partial y_-(x)}{\partial x}\right)^{-1/2} A_{-;a}(y_-(x)) \propto \psi_{-1}(x), \tag{D.245}$$

$$\left(\frac{\partial y_-(x)}{\partial x}\right)^{-1/2} A_{-;a+3}(y_-(x)) \propto \psi_2(x). \tag{D.246}$$

To find the proportionality constant, we can just look at the large $x$ asymptotics along the corresponding direction and compare both side term by term. The leading term is $\exp\left(-\frac{4i}{15\hbar}\right)$. The subleading terms can be found numerically.

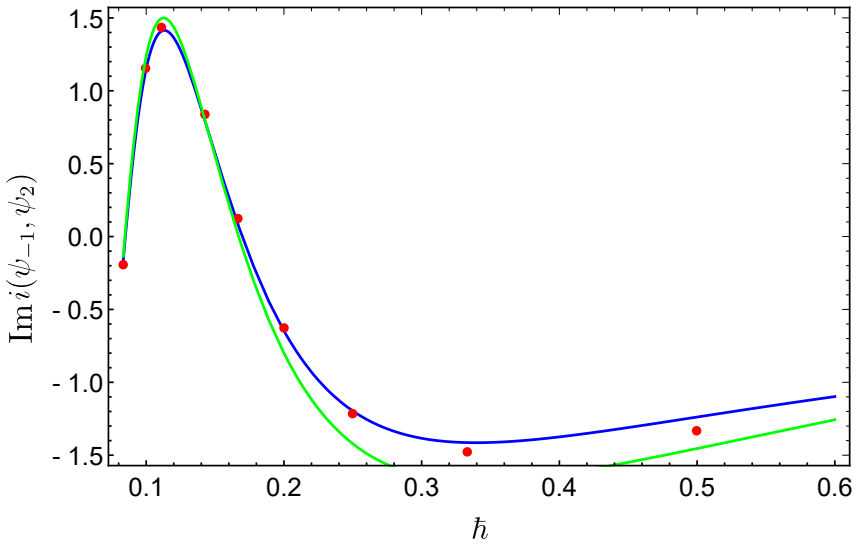


Figure D.7: Evaluations of the Wronskian $i(\psi_{-1}, \psi_2)$. The red dots are the numerical result. The blue line and the red line are the analytic prediction from the local coordinate system around the double zero up to $\hbar^{-1}$ and $\hbar$ order respectively given in (D.249).

We are now ready to calculate the cross ratios. There are two independent cross ratios

defined as follows

$$\chi_1 \equiv \frac{(\psi_{-1},\psi_{-2})\,(\psi_1,\psi_2)}{(\psi_{-1},\psi_1)\,(\psi_2,\psi_{-2})}, \quad \chi_2 \equiv \frac{(\psi_0,\psi_1)\,(\psi_{-1},\psi_2)}{(\psi_0,\psi_{-1})\,(\psi_1,\psi_2)}. \tag{D.247}$$

$\chi_1$ is easily evaluated in the local coordinate system around the double zero. It coincides with the contour integral of the WKB momentum along a small circle around the double zero. From the end of the Subsection D.5.5, this evaluates to be

$$\chi_1 = e^{2\pi i a(\hbar)}. \tag{D.248}$$

The second cross ratio boils down to $-i(\psi_{-1},\psi_2)$, namely

$$-\chi_2 = i(\psi_{-1},\psi_2) = \sqrt{2}\exp\Big[-\frac{8i}{15\hbar} - \hbar(\lim_{R\to+\infty} S_\hbar(e^{\frac{2\pi i}{5}}R) + S_\hbar(e^{-\frac{4\pi i}{5}}R))\Big] \tag{D.249}$$

where

$$S_\hbar(x) = \frac{3}{16}\frac{1}{y_0^2} + y_0 y_2 - a^{(0)}\log y_0 \tag{D.250}$$

and we also parametrize the coordinate transformation as usual

$$y(x) = y_0(x) + \hbar^2 y_2(x) + \dots \tag{D.251}$$

This agrees quite well with the numerical evaluation shown in Fig. D.7.

### D.5.7 Example: chiral WZW

#### trivial theory

When the level $k = 0$, we have a trivial theory with central charge $c = 0$ and the only primary operator being the vacuum

$$\partial_x^2\psi(x) = e^{2\theta}e^{2x}\psi(x). \tag{D.252}$$

The WKB diagram takes the form of Fig. D.8. By use of the asymptotics of the Bessel function for large real positive argument

$$\frac{1}{\sqrt{\pi}}K_\nu(z) \sim \frac{1}{\sqrt{2z}}e^{-z}. \tag{D.253}$$

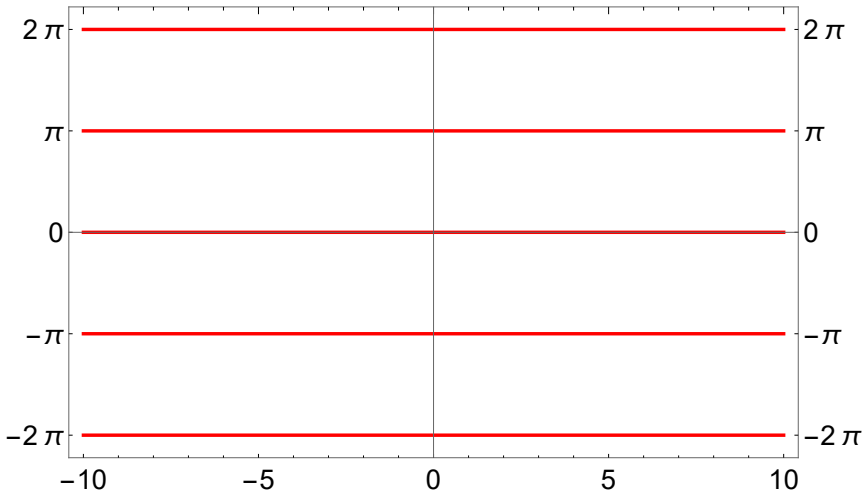


Figure D.8: Stokes diagram for $P(x) = e^{2x}$, which corresponds to $SU(2)_0$ trivial theory. There are infinite number of special WKB lines depicted as red paralell lines.

Small solutions are given by

$$\begin{aligned} \psi_0 &= \frac{1}{\sqrt{\pi}} K_0(e^{\theta+x}), \\ \psi_n &= \psi_0(x; \theta + ni\pi) = \frac{1}{\sqrt{\pi}} \Big( K_0(e^{\theta+x}) - i\pi n I_0(e^{\theta+x}) \Big) \end{aligned} \tag{D.254}$$

with the Wronskians given by $i(\psi_n, \psi_{n'}) = n' - n$ from $(K_0(e^{\theta+x}), I_0(e^{\theta+x})) = 1$.

### Matching around the zero

When $t(x) = 0$, after shifting the coordinate, the stress tensor looks like

$$\frac{1}{\hbar^2} e^{2x} x^k. \tag{D.255}$$

In the local coordinate around the zero,

$$y^k + a_{k-2}\gamma^k y^{k-2} + \cdots + a_j \gamma^{2+j} y^j + \cdots + a_0 \gamma^2 \tag{D.256}$$

where $\gamma = \hbar^{\frac{2}{k+2}}$. When $k = 1$, it just equals $y$ without corrections in $\gamma$. When $k \geq 2$, the stress tensor in the local coordinate system generically have nonzero coefficients $a_i$. For

example, when $k = 2$, we found that

$$a = -\frac{1}{8} + \frac{40911}{1024}\hbar^2 + O(\hbar^4). \tag{D.257}$$

**Matching around the negative infinity**

Suppose $\delta = x - x_{-\infty}$ is a local coordinate around $x_{-\infty}$, which has a large negative real part. Then

$$P(x) = e^{2\theta+2x}(1+gx)^k \tag{D.258}$$

$$= e^{2\delta}e^{2\theta+2x_{-\infty}+k\log(1+gx_{-\infty})}\left(1+\frac{\delta}{x_{-\infty}+\frac{1}{g}}\right)^k. \tag{D.259}$$

We would like to find $x_{-\infty}$ such that the exponent $2\theta + 2x_0 + k\log(1+gx_{-\infty}) = 0$. And hopefully in the IR limit $\theta \to \infty$, the denominator in the parenthesis $x_{-\infty} + \frac{1}{g}$ is large so we can perform perturbation theory. This indeed can be done.

We can solve the equation $2\theta + 2x_{-\infty} + k\log(1+gx_{-\infty}) = 0$ by[9]

$$x_{-\infty} \sim -\theta - \frac{1}{2}k\log(-g\theta) - \frac{k^2}{4}\frac{\log(-g\theta)}{\theta} + O\Big(\frac{1}{\theta}\Big). \tag{D.261}$$

Apparently the imaginary part of $x_{-\infty}$ is neither arbitrary nor unique, and depends on the parity of $k$ and the imaginary part of $\theta$. However, importantly, it turns out that we can always choose $x_{-\infty}$ to lie on one of the special WKB lines, though the precise choice doesn't matter.

On the other hand, we can also see this from a different perspective. Recall that our system only depends on the $g_{\text{eff}}$, a particular combination of $g$ and $\theta$, given by

$$e^{-\frac{1}{g_{\text{eff}}(\theta)}}g_{\text{eff}}(\theta)^{\frac{k}{2}} \equiv e^{-\frac{1}{g}}g^{\frac{k}{2}}e^{\theta}. \tag{D.262}$$

It is not hard to see that this is indeed the same equation as the one for $x_{-\infty}$ once we

[9]Note that the naive solution

$$x_{-\infty} = -\frac{1}{g} + \frac{k}{2}W\left(\frac{2}{kg}e^{\frac{2}{k}(\frac{1}{g}-\theta)}\right) \sim -\frac{\theta}{1+\frac{gk}{2}} + \frac{2k}{(2+gk)^3}(g\theta)^2 - \frac{4k(4-gk)}{3(2+gk)^5}(g\theta)^3 + \dots \tag{D.260}$$

is not the one we want, since $0 > x_{-\infty} > -\frac{1}{g}$, and $0 \ll \theta < \frac{1}{g}$

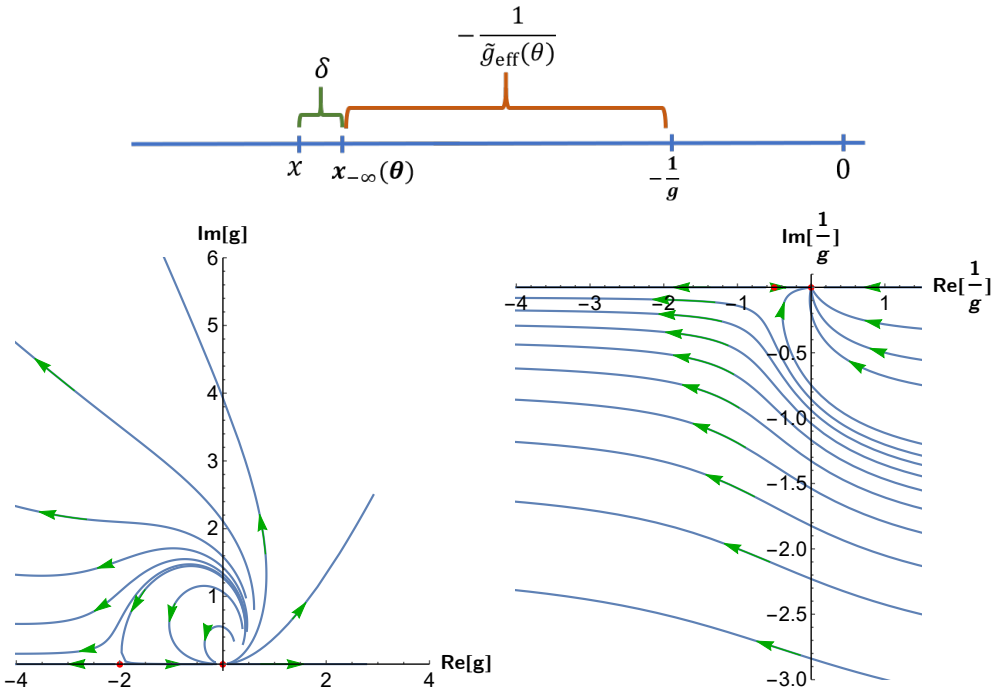


Figure D.9: In the top figure, $g$ is assumed to be a some order 1 constant, independent of $\theta$. $x_{-\infty}(\theta)$ is farther away from $-\frac{1}{g}$ as $\theta \to \infty$. $\delta$ is the local variation around $x_{-\infty}(\theta)$ that is complex. So it doesn't have to be on the real axis. In the bottom figures, the red line is an example of $g_{\text{eff}}$ discussed in this section, namely an example of circular RG flow.

identify

$$x_{-\infty}(\theta) = \frac{1}{g_{\text{eff}}(\theta)} - \frac{1}{g} \tag{D.263}$$

that satisfy

$$\frac{dx_{-\infty}(\theta)}{d\theta} = -\frac{1}{1+\frac{k}{2}\frac{1}{x_{-\infty}+\frac{1}{g}}}, \quad \left.\frac{dx_{-\infty}(\theta)}{d\theta}\right|_{\theta=\infty} = -1, \quad x_{-\infty}(\infty) = -\infty. \tag{D.264}$$

Or in terms of $g_{\text{eff}}(\theta)$, it starts with $g = g_{\text{eff}}(\theta = 0)$ that has some small imaginary part, and circles around in the complex $g_{\text{eff}}(\theta)$ plane and goes back to the zero $g_{\text{eff}}(\theta \to +\infty) \to 0^-$. Therefore the careful solution we found in (D.261), especially the imaginary part of $x_{-\infty}$ is just to make sure we choose this circular type of RG flow, depicted as red lines in Fig. D.9.

Using the definition (D.263), our quadratic differential is actually just

$$P(x) = e^{2\delta} \left(1 + g_{\text{eff}}(\theta)\delta\right)^k . \tag{D.265}$$

And with the above solution of $x_{-\infty}$ and $g_{\text{eff}}(\theta)$, we have $g_{\text{eff}}(\theta \to +\infty) \to 0^-$, therefore the perturbation in $g_{\text{eff}}$ is valid in the IR.[10] Note that $g_{\text{eff}}(\theta)$ expands in large $\theta$ as

$$-\frac{1}{\theta} + \frac{-2 + gk\log(-g\theta)}{2g\theta^2} + \dots \tag{D.267}$$

## D.6 Review of the standard ODE/IM correspondance

For completeness, we review the standard formulation of ODE/IM correspondence, though the details are not relevant to this thesis. Let's illustrate the idea in a simple example.

$$\partial_x^2 \psi = \left(x^{2M} - E\right)\psi, \quad 2M \in \mathbb{Z} \tag{D.268}$$

There are $2M+2$ Stokes line extending to $\infty$. The corresponding $2M+2$ Stokes sectors are given by

$$\mathcal{S}_k = \left|\arg x - k\frac{2\pi}{2M+2}\right| < \frac{\pi}{2M+2} \tag{D.269}$$

The ODE (D.268) is a second order differential equation and therefore has a unique solution (up to an overall normalization), denoted as $y_0(x, E)$, satisfying the following

- $y_0(x, E)$ is an entire function of $x$ and $E$
- $y_0(x, E)$ has the large $|x|$ asymptotics in sectors $\mathcal{S}_{-1} \cup \mathcal{S}_0 \cup \mathcal{S}_1$ given by the WKB approximation

$$y_0 \sim \frac{1}{\sqrt{2i}} x^{-M/2} \exp\left[-\frac{1}{M+1}x^{M+1}\right] \tag{D.270}$$

  More precisely, $y_0(x, E)$ is subdominant in $\mathcal{S}_0$ and dominant in $\mathcal{S}_{-1}$ and $\mathcal{S}_1$

[10] Of course we also have to make sure

$$|\delta| \ll -\frac{1}{g_{\text{eff}}}. \tag{D.266}$$

One can easily find solutions that decays in other sectors. One choice is to use the so-called Symanzik rotation

$$y_k(x,E) := \omega^{k/2} y_0\left(\omega^{-k}x, \omega^{2k}E\right), \quad k \in \mathbb{Z} \tag{D.271}$$

with

$$\omega = \exp\left(\frac{2\pi i}{2M+2}\right) \tag{D.272}$$

It is easy to see that for $k \in \mathbb{Z}$, $y_k(x,E)$ is solutions to (D.268) that decays exponentially in the sector $\mathcal{S}_k$.

Define the Wronskian between two solutions as

$$W_{k,j}(E) = y_k y_j' - y_k' y_j \tag{D.273}$$

which is independent of $x$. Then with the normalization in (D.270) and (D.271), we have

$$W_{0,1}(E) = 1, \quad W_{k_1+1,k_2+1}(E) = W_{k_1,k_2}(\omega^2 E) \tag{D.274}$$

Since the space of solutions to (D.268) is two dimensional, any solution $y_k$ is a linear combination of two other solutions that are linearly independent. In particular, we have

$$y_{-1}(x,E) = C(E) y_0(x,E) + \widetilde{C}(E) y_1(x,E) \tag{D.275}$$

where the coefficients can be given in terms of Wronskians

$$C(E) = \frac{W_{-1,1}(E)}{W_{0,1}(E)}, \quad \widetilde{C}(E) = -\frac{W_{-1,0}(E)}{W_{0,1}} = -1 \tag{D.276}$$

We can rewrite (D.275) as

$$C(E) y_0(x,E) = y_{-1}(x,E) + y_1(x,E) \tag{D.277}$$

or equivalently

$$C(E) D_\mp(E) = \omega^{\mp 1/2} D_\mp\left(\omega^{-2}E\right) + \omega^{\pm 1/2} D_\mp\left(\omega^2 E\right) \tag{D.278}$$

where

$$D_-(E) := y(0,E), \quad D_+(E) := y'(0,E) \tag{D.279}$$

Surprisingly, this turns out to take the same form as the TQ equation

$$T(s)Q_{\pm}(s) = e^{\mp 2\pi i p} Q_{\pm}\left(q^{-2}s\right) + e^{\pm 2\pi i p} Q_{\pm}\left(q^{2}s\right) \tag{D.280}$$

upon identifying $M = -1 + \beta^{-2}$, where $\beta$ is to parametrize the central charge

$$c = 1 - 6\left(\beta - \beta^{-1}\right)^2 \tag{D.281}$$

Note that this identification is only true for a specific highest weight state with momentum $p = \frac{\beta^2}{4}$. For other states, we need to modify the ODE (D.268) by adding regular singularities of trivial monodromy [39, 40].

Clearly, the idea underlying the standard formalism described in this section is very similar to the one we describe in section 3 and 4. The precise relation between these two is an intriguing question for the future.

Note that from the perspective of (D.268) as a Schrodinger equation, $D_{\pm}(E)$ are also interesting on their own. Consider the value of energy $E_n^{\pm}$ corresponding to even and odd eigenfunctions. They are precisely the zeros of $D_{\pm}(E) = 0$, so we must have $D_{\pm}(E)$ is the same as the spectral derminant

$$\prod_{n=1}^{\infty}\left(1 - \frac{E}{E_n^{\pm}}\right) \tag{D.282}$$

up to an entire function without zeros.

# Appendix E

# Boundary QFT

## E.1 Method of Images

In this appendix we show how to compute the two-point function of $F_{\mu\nu}$ in the free theory using the method of images.

Reflections about the boundary are implemented by the matrix

$$R_\mu{}^\nu = \delta_\mu{}^\nu - 2n_\mu n^\nu \ , \tag{E.1}$$

where $n^\mu$ is the inward pointing vector normal to the boundary. Note that the reflection of the field strength

$$F^R_{\mu\nu}(x) \equiv R_\mu{}^{\mu'} R_\nu{}^{\nu'} F_{\mu'\nu'}(R\,x) \tag{E.2}$$

has components $(F^R_{ya}(x),\ \widetilde{F^R_{ya}}(x)) = (-F_{ya}(R\,x),\ \tilde{F}_{ya}(R\,x))$. Hence, the combination

$$\langle F_{\mu\nu}(x_1)F_{\rho\sigma}(x_2)\rangle_{\mathbb{R}^3\times\mathbb{R}_+} \equiv \langle F_{\mu\nu}(x_1)F_{\rho\sigma}(x_2)\rangle_{\mathbb{R}^4} - s\langle F_{\mu\nu}(x_1)F^R_{\rho\sigma}(x_2)\rangle_{\mathbb{R}^4} \ , \tag{E.3}$$

satisfies the equation of motion and Bianchi identity for $y \geq 0$, and also satisfies the Dirichlet (Neumann with $\gamma = 0$) boundary condition upon choosing the sign $s = 1$ ($s = -1$, respectively). Even though Bose symmetry is not manifest in (E.3), it is satisfied because $\langle F_{\mu\nu}(x_1)F^R_{\rho\sigma}(x_2)\rangle_{\mathbb{R}^4} = \langle F^R_{\mu\nu}(x_1)F_{\rho\sigma}(x_2)\rangle_{\mathbb{R}^4}$. We can then rewrite the image term using the cross-ratio $\xi$ and the vectors $X_{i\,\mu}$ by means of the following identity

$$R_\rho{}^{\rho'} I_{\mu\rho'}(x_1 - Rx_2) = I_{\mu\rho}(x_{12}) - 2X_{1\,\mu}X_{2\,\rho} \ . \tag{E.4}$$

In this way we find (6.19).

In the more general case of Neumann boundary condition with $\gamma \neq 0$, consider the combination

$$F'_{\mu\nu} = F_{\mu\nu} + i\gamma\tilde{F}_{\mu\nu} = \mathcal{M}_{\mu\nu}{}^{\mu'\nu'}F_{\mu'\nu'} \tag{E.5}$$

$$\mathcal{M}_{\mu\nu}{}^{\mu'\nu'} = \delta^{\mu'}_{[\mu}\delta^{\nu'}_{\nu]} + i\frac{\gamma}{2}\epsilon_{\mu\nu}{}^{\mu'\nu'} \ . \tag{E.6}$$

For $F'_{\mu\nu}$ the problem is reduced to the Neumann boundary condition with $\gamma = 0$, so we have

$$\langle F'_{\mu\nu}(x_1)F'_{\rho\sigma}(x_2)\rangle_{\mathbb{R}^3\times\mathbb{R}_+} \equiv \langle F'_{\mu\nu}(x_1)F'_{\rho\sigma}(x_2)\rangle_{\mathbb{R}^4} + \langle F'_{\mu\nu}(x_1)(F')^R_{\rho\sigma}(x_2)\rangle_{\mathbb{R}^4} \ . \tag{E.7}$$

Note that

$$(F')^R_{\rho\sigma}(x) = \overline{\mathcal{M}}_{\mu\nu}{}^{\mu'\nu'}F^R_{\mu'\nu'} \ , \tag{E.8}$$

$$\overline{\mathcal{M}}_{\mu\nu}{}^{\mu'\nu'} = \delta^{\mu'}_{[\mu}\delta^{\nu'}_{\nu]} - i\frac{\gamma}{2}\epsilon_{\mu\nu}{}^{\mu'\nu'} \ . \tag{E.9}$$

Multiplying both sides of (E.7) by $\mathcal{M}^{-1}\otimes\mathcal{M}^{-1}$ we obtain

$$\langle F_{\mu\nu}(x_1)F_{\rho\sigma}(x_2)\rangle_{\mathbb{R}^3\times\mathbb{R}_+} = \langle F_{\mu\nu}(x_1)F_{\rho\sigma}(x_2)\rangle_{\mathbb{R}^4} + (\mathcal{M}^{-1}\overline{\mathcal{M}})_{\rho\sigma}{}^{\rho'\sigma'}\langle F_{\mu\nu}(x_1)F^R_{\rho'\sigma'}(x_2)\rangle_{\mathbb{R}^4} \ . \tag{E.10}$$

Finally we use that

$$(\mathcal{M}^{-1}\overline{\mathcal{M}})_{\rho\sigma}{}^{\rho'\sigma'} = \frac{1-\gamma^2}{1+\gamma^2}\delta^{\rho'}_{[\rho}\delta^{\sigma'}_{\sigma]} - i\frac{\gamma}{1+\gamma^2}\epsilon_{\rho\sigma}{}^{\rho'\sigma'} \ , \tag{E.11}$$

to write the final result for the two-point function in terms of the parameter $\gamma$ and the covariant structures $G$ and $H$, thus obtaining (6.23).

## E.2 Defect OPE of $F_{\mu\nu}$

Let us consider what can appear as a primary inside the bulk-to-boundary OPE of the field strength $F_{\mu\nu}$. By spin selection rules only vectors are admitted, with two possible

structures, namely

$$F_{\mu\nu}(\vec{x},y) \underset{y\to 0}{\sim} \frac{1}{y^{2-\widehat{\Delta}_1}}\hat{V}_1^a(\vec{x})2\delta_{a[\mu}\delta_{\nu]y} - \frac{1}{y^{2-\widehat{\Delta}_2}}i\epsilon^{abc}\hat{V}_{2\,c}(\vec{x})\delta_{a[\mu}\delta_{\nu]b} + \dots \tag{E.12}$$

and the ellipsis denotes contributions from descendants. Using the bulk eom and Bianchi identity, we have that

$$\begin{aligned}\partial_y F_{ya} &\sim \frac{(\widehat{\Delta}_1-2)}{y^{3-\widehat{\Delta}_1}}\hat{V}_{1\,a}(\vec{x}) + \dots\ , \\ \partial_y \tilde{F}_{ya} &\sim -i\frac{(\widehat{\Delta}_2-2)}{y^{3-\widehat{\Delta}_1}}\hat{V}_{2\,a}(\vec{x}) + \dots\ ,\end{aligned} \tag{E.13}$$

must be boundary descendants. This requires $\widehat{\Delta}_1 = \widehat{\Delta}_2 = 2$. We conclude that the only allowed boundary primaries are conserved currents.

To obtain the complete form of the bulk-to-boundary OPE of $F$ (including all the descendants) we first need the exact $\langle F\hat{V}\rangle$ correlator. This can be easily computed using the techniques of [230] to find

$$\begin{aligned}\langle F_{ya}(x)\hat{V}_{i\,c}(0)\rangle &= \frac{1}{x^4}\left[\left(\frac{2y^2\delta_{ac}}{x^2} - I_{ac}(x)\right)c_{1i}(\tau) - 2i\,c_{2i}(\tau)\frac{y}{x^2}\epsilon_{acd}x^d\right]\ , \\ \langle F_{ab}(x)\hat{V}_{i\,c}(0)\rangle &= \frac{1}{x^4}\left[i\left(\frac{2y^2\epsilon_{abc}}{x^2} - \epsilon_{abd}I_c^d(x)\right)c_{2i}(\tau) - 2c_{1i}(\tau)\frac{y}{x^2}(\delta_{ac}x_b - \delta_{bc}x_a)\right]\ ,\end{aligned} \tag{E.14}$$

where $c_{ij}(\tau)$ are defined in eq. (6.57). The bulk-to-boundary OPE of $F$ can now be obtained by expanding both sides of (E.14) to find

$$\begin{aligned}F_{ab}(\vec{x},y) &= \sum_{n=0}^{\infty}(-1)^n\left[(\delta_{ac}\delta_{bd}-\delta_{ad}\delta_{bc})y\partial^d\frac{(y^2\vec{\partial}^2)^n}{(2n+1)!}\hat{V}_1^c(\vec{x}) - i\epsilon_{abc}\frac{(y^2\vec{\partial}^2)^n}{2n!}\hat{V}_2^c(\vec{x})\right]\ , \\ F_{ya}(\vec{x},y) &= \sum_{n=0}^{\infty}(-1)^n\left[-\frac{(y^2\vec{\partial}^2)^n}{2n!}\hat{V}_{1\,a}(\vec{x}) + i\epsilon_{abd}\,y\partial^d\frac{(y^2\vec{\partial}^2)^n}{(2n+1)!}\hat{V}_2^b(\vec{x})\right]\ .\end{aligned} \tag{E.15}$$

With the bulk-to-boundary OPE above, it is straightforward to obtain the $\langle FF\rangle$ 2-point function in terms of the defect CFT data as in (6.55).

## E.3 Bulk OPE Limit of $\langle F_{\mu\nu}F_{\rho\sigma}\rangle$

Here we present some details of the bootstrap analysis presented in Section 6.1.7. To simplify computations, it is convenient to start from a configuration where the two bulk operators lie at the same parallel distance from the defect, i.e. $\vec{x}_{12}=0$. In this case some expressions in (6.55) simplify considerably, e.g.

$$G_{ay,by}(\vec{x}_{12}=0,y_1-y_2)=-\frac{\delta_{ab}}{(y_1-y_2)^4}\ , \tag{E.16}$$

$$H_{ay,by}(\vec{x}_{12}=0,y_1,y_2)=\frac{2X_{1\,y}X_{2\,y}\delta_{ab}}{(y_1-y_2)^4}\underset{y_1\to y_2}{\sim}-\frac{2\delta_{ab}}{(y_1-y_2)^4}\ , \tag{E.17}$$

$$G_{ab,cy}(\vec{x}_{12}=0,y_1-y_2)=0=H_{ab,cy}(\vec{x}_{12}=0,y_1,y_2)\ , \tag{E.18}$$

$$v^4|_{\vec{x}_{12}=0}=\frac{(y_1-y_2)^4}{(y_1+y_2)^4}\underset{y_1\to y_2}{\sim}\frac{(y_1-y_2)^4}{16y_2^4}\ . \tag{E.19}$$

It is now a simple exercise to derive the bulk OPE limit of (6.55)

$$\begin{aligned}\langle F_{ab}(\vec{x},y_1)F_{cy}(\vec{x},y_2)\rangle&\underset{y_1\to y_2}{\sim}-\frac{i\alpha_3}{16y_2^4}\epsilon_{abc}+\dots,\\ \langle F_{ay}(\vec{x},y_1)F_{by}(\vec{x},y_2)\rangle&\underset{y_1\to y_2}{\sim}-\left(\frac{\alpha_1}{(y_1-y_2)^4}+\frac{\alpha_2}{16y_2^4}\right)\delta_{ab}+\dots\end{aligned} \tag{E.20}$$

where the ellipsis denote contributions from descendants. On the other hand from (6.66) one finds

$$\begin{aligned}\langle F_{ab}(\vec{x},y_1)F_{cy}(\vec{x},y_2)\rangle&\underset{y_1\to y_2}{\sim}\frac{1}{12}\frac{a_{F\tilde{F}}(\tau,\bar{\tau})}{y_2^4}\epsilon_{abc}+\dots\ ,\\ \langle F_{ay}(\vec{x},y_1)F_{by}(\vec{x},y_2)\rangle&\underset{y_1\to y_2}{\sim}-\left(\frac{g^2}{\pi^2}\frac{1}{(y_1-y_2)^4}-\frac{1}{12}\frac{a_F^2(\tau,\bar{\tau})}{y_2^4}\right)\delta_{ab}+\dots\ .\end{aligned} \tag{E.21}$$

Crossing symmetry now implies that (E.21) and (E.20) must match, therefore

$$\alpha_1=\frac{g^2}{\pi^2},\quad a_{F^2}(\tau,\bar{\tau})=-\frac{3}{4}\alpha_2,\quad a_{F\tilde{F}}(\tau,\bar{\tau})=-i\frac{3}{4}\alpha_3. \tag{E.22}$$

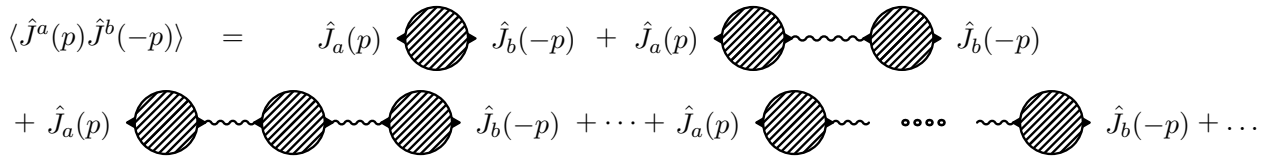


Figure E.1: The two-point function of the boundary current $\hat{J}$. The shaded blob represents the one-photon irreducible two-point function $\Sigma(p)$, by which we mean the sum of all the diagrams that cannot be disconnected by cutting a photon line. The full two-point function can be obtained in terms of $\Sigma$, via the geometric sum shown in the figure.

From the solution above, upon using (6.56) one obtains

$$c_{11}(\tau,\bar{\tau})+c_{22}(\tau,\bar{\tau})=\frac{2g^2}{\pi^2},\quad a_{F^2}(\tau,\bar{\tau})=\frac{3}{8}(c_{22}(\tau,\bar{\tau})-c_{11}(\tau,\bar{\tau})),\quad a_{F\tilde{F}}(\tau,\bar{\tau})=i\frac{3}{4}c_{12}(\tau,\bar{\tau}). \tag{E.23}$$

## E.4 Current Two-Point Functions

In this appendix derive some useful relations between the two-point functions of the conserved boundary currents. The two-point functions of the currents $\hat{V}_i^a$ – see (6.52) – in momentum space are

$$\langle \hat{V}_i^a(p)\hat{V}_j^b(-p)\rangle=-\frac{\pi^2}{2}c_{ij}p\left(\delta^{ab}-\frac{p^a p^b}{p^2}\right)+\frac{\kappa_{ij}}{2\pi}\epsilon^{abc}p_c\ . \tag{E.24}$$

The main goal is to express the coefficients $c_{ij}$ –that enter directly in the expression of the bulk two-point and one-point functions– in terms of the two-point correlator of the current $\hat{J}^a$, which is more natural to compute in perturbation theory at large $\tau$.

In perturbation theory it is convenient to define a two-point function of $\hat{J}^a$ that cannot be disconnected by cutting a photon line, which we will call one-photon irreducible and denote with the symbol $\Sigma$

$$\langle \hat{J}^a(p)\hat{J}^b(-p)\rangle|_{\text{one-photon irr.}}\equiv\Sigma^{ab}(p)=-\frac{\pi^2}{2}c_\Sigma(\tau,\bar{\tau})p\left(\delta^{ab}-\frac{p^a p^b}{p^2}\right)+\frac{\kappa_\Sigma(\tau,\bar{\tau})}{2\pi}\epsilon^{abc}p_c\ . \tag{E.25}$$

Clearly this two-point function reduces to the two-point function of the current of the 3d CFT as $\tau\to\infty$. By resumming the diagrams in fig. E.1 we obtain

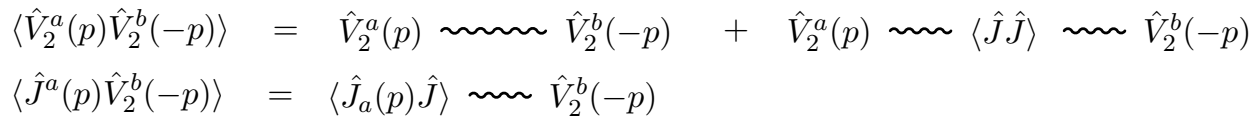


Figure E.2: Relations between the two-point functions involving the current $V_2$ and the two-point function $\langle JJ\rangle$. The relation in the second line is only true up to a contact term.

$$\langle \hat{J}^a(p)\hat{J}^b(-p)\rangle = \left(\Sigma(p)\cdot(\mathbb{1}-\Pi(p)\cdot\Sigma(p))^{-1}\right)^{ab} \tag{E.26}$$

$$= -\frac{\pi^2}{2}c_J(\tau,\bar{\tau})p\left(\delta^{ab}-\frac{p^a p^b}{p^2}\right)+\frac{\kappa_J(\tau,\bar{\tau})}{2\pi}\epsilon^{abc}p_c\ , \tag{E.27}$$

where $\Pi$ is the boundary propagator of the photon (see eq. (6.46)) and

$$\frac{\pi^2}{2}c_J = \frac{\frac{\pi^2}{2}c_\Sigma\left(\frac{\pi^2}{2}c_\Sigma g^2+\gamma^2+1\right)+\frac{g^2\kappa_\Sigma^2}{4\pi^2}}{\left(\frac{\pi^2}{2}c_\Sigma g^2+1\right)^2+\left(\gamma+\frac{g^2\kappa_\Sigma}{2\pi}\right)^2}\ , \tag{E.28}$$

$$\frac{\kappa_J}{2\pi} = \frac{\frac{\gamma}{g^2}\left(\frac{\pi^2}{2}c_\Sigma g^2\right)^2+\frac{\kappa_\Sigma}{2\pi}\left(\gamma^2+\gamma\frac{g^2\kappa_\Sigma}{2\pi}+1\right)}{\left(\frac{\pi^2}{2}c_\Sigma g^2+1\right)^2+\left(\gamma+\frac{g^2\kappa_\Sigma}{2\pi}\right)^2}\ . \tag{E.29}$$

We will also need the mixed two-point function $\langle \hat{J}\hat{V}_2\rangle$ which similarly can be parametrized as

$$\langle \hat{J}^a(p)\hat{V}_2^b(-p)\rangle = -\frac{\pi^2}{2}c_{J2}p\left(\delta^{ab}-\frac{p^a p^b}{p^2}\right)+\frac{\kappa_{J2}}{2\pi}\epsilon^{abc}p_c\ . \tag{E.30}$$

Since $\hat{V}_2^a = \frac{i}{2}\epsilon^{abc}F_{bc}|_{y=0}$, we can readily express the two-point function of $\hat{V}_2$ and the mixed two-point function of $\hat{V}_2$ and $\hat{J}$ in terms of the two-point function of $\hat{J}$ and the boundary propagator of the photon, using the relations depicted in fig. E.2. We obtain

$$\frac{\pi^2}{2}c_{22} = \frac{g^2}{1+\gamma^2} + \left(\frac{g^2}{1+\gamma^2}\right)^2 \left(\left(\gamma^2-1\right)\frac{\pi^2}{2}c_J - 2\gamma\frac{\kappa_J}{2\pi}\right) \ , \tag{E.31}$$

$$\frac{\kappa_{22}}{2\pi} = -\frac{g^2}{1+\gamma^2}\gamma + \left(\frac{g^2}{1+\gamma^2}\right)^2 \left(\gamma\pi^2 c_J + \left(\gamma^2-1\right)\frac{\kappa_J}{2\pi}\right) \ , \tag{E.32}$$

$$\frac{\pi^2}{2}c_{J2} = \frac{g^2}{1+\gamma^2}\left(-\gamma\frac{\pi^2}{2}c_J + \frac{\kappa_J}{2\pi}\right) \ , \tag{E.33}$$

$$\frac{\kappa_{J2}}{2\pi} = 1 - \frac{g^2}{1+\gamma^2}\left(\frac{\pi^2}{2}c_J + \gamma\frac{\kappa_J}{2\pi}\right) \ . \tag{E.34}$$

Finally, using that $\hat{V}_1 = -g^2\hat{J} - \gamma\hat{V}_2$, we obtain that

$$\begin{aligned}\frac{\pi^2}{2}c_{11} &= \frac{\pi^2}{2}\left(g^4 c_J + 2g^2\gamma c_{J2} + \gamma^2 c_{22}\right) \\ &= \frac{g^2}{1+\gamma^2}\gamma^2 - \left(\frac{g^2}{1+\gamma^2}\right)^2 \left(\left(\gamma^2-1\right)\frac{\pi^2}{2}c_J - 2\gamma\frac{\kappa_J}{2\pi}\right) \ , \end{aligned} \tag{E.35}$$

$$\begin{aligned}\frac{\kappa_{11}}{2\pi} &= g^4\frac{\kappa_J}{2\pi} + 2g^2\gamma\frac{\kappa_{J2}}{2\pi} + \gamma^2\frac{\kappa_{22}}{2\pi} \\ &= \frac{g^2}{1+\gamma^2}\gamma\left(\gamma^2+2\right) - \left(\frac{g^2}{1+\gamma^2}\right)^2 \left(\gamma\pi^2 c_J + \left(\gamma^2-1\right)\frac{\kappa_J}{2\pi}\right) \ , \end{aligned} \tag{E.36}$$

$$\begin{aligned}\frac{\pi^2}{2}c_{12} &= -\frac{\pi^2}{2}\left(g^2 c_{J2} + \gamma c_{22}\right) \\ &= -\frac{g^2}{1+\gamma^2}\gamma + \left(\frac{g^2}{1+\gamma^2}\right)^2 \left(\gamma\pi^2 c_J + \left(\gamma^2-1\right)\frac{\kappa_J}{2\pi}\right) \ , \end{aligned} \tag{E.37}$$

$$\begin{aligned}\frac{\kappa_{12}}{2\pi} &= -g^2\frac{\kappa_{J2}}{2\pi} - \gamma\frac{\kappa_{22}}{2\pi} \\ &= -\frac{g^2}{1+\gamma^2} - \left(\frac{g^2}{1+\gamma^2}\right)^2 \left(\left(\gamma^2-1\right)\frac{\pi^2}{2}c_J - 2\gamma\frac{\kappa_J}{2\pi}\right) \ . \end{aligned} \tag{E.38}$$

We see that all the coefficients $c_{ij}$ can be expressed in terms of the functions of the coupling $c_J$ and $\kappa_J$ (or equivalently $c_\Sigma$ and $\kappa_\Sigma$). As a check, note that the first identity in (6.69), that was derived from the contribution of the identity in the bulk OPE and relates $c_{11}$ and $c_{22}$, is identically satisfied.

## E.5 Calculation of $\langle \hat{V}_i \hat{V}_j \hat{D} \rangle$

We start by computing the three-point function

$$\langle F_{\mu\nu}(x_1) F_{\rho\sigma}(x_2) \hat{D}(\vec{x}_3) \rangle \ . \tag{E.39}$$

using the boundary channel. At leading order in the boundary OPE limit the three-point function becomes

$$\langle \hat{V}_i^a(\vec{x}_1) \hat{V}_j^b(\vec{x}_2) \hat{D}(\vec{x}_3) \rangle \ , \tag{E.40}$$

which upon placing the displacement operator at infinity simplifies to [176, 177]

$$\langle \hat{V}_i^a(\vec{x}_1) \hat{V}_j^b(\vec{x}_2) \hat{D}(\infty) \rangle \equiv \lim_{\vec{x}_3 \to \infty} |\vec{x}_3|^8 \langle \hat{V}_i^a(\vec{x}_1) \hat{V}_j^b(\vec{x}_2) \hat{D}(\vec{x}_3) \rangle = \lambda^{(1)}_{ij\hat{D}_+} \, \delta^{ab} + \lambda^{(1)}_{ij\hat{D}_-} \, \hat{x}_{12}^c \epsilon^{abc} \ . \tag{E.41}$$

From the boundary OPE-channel we find

$$\langle F_{ay}(x_1) F_{by}(x_2) \hat{D}(\infty) \rangle = \lambda^{(1)}_{11\hat{D}_+} \, \delta_{ab} + \lambda^{(1)}_{11\hat{D}_-} \, (\hat{x}_{12}^f \epsilon_{abf} + \dots) \ , \tag{E.42}$$

$$\langle F_{ay}(x_1) F_{bc}(x_2) \hat{D}(\infty) \rangle = -i \, \epsilon_{bc}{}^e (\lambda^{(1)}_{12\hat{D}_+} \, \delta_{ae} + \lambda^{(1)}_{12\hat{D}_-} \, (\hat{x}_{12}^f \epsilon_{aef} + \dots)) \ , \tag{E.43}$$

$$\langle F_{ab}(x_1) F_{cd}(x_2) \hat{D}(\infty) \rangle = -\epsilon_{ab}{}^e \epsilon_{cd}{}^g (\lambda^{(1)}_{22D_+} \delta_{eg} + \lambda^{(1)}_{22D_-} \, (\hat{x}_{12}^f \epsilon_{egf} + \dots)) \ , \tag{E.44}$$

where the ellipses denote the descendant contributions from the second term of (E.41), which are proportional to $\lambda^{(1)}_{ij\hat{D}_-}$ and will not play any role in the following.

Next, we compute the three-point function using the bulk OPE channel. The Lorentz spin and scaling dimensions of the full set of operators appearing in the OPE of two $F$'s can be found in [231] – see eq. (2.12) therein – where they are discussed in the context of the so-called minimal type-C higher spin theory on $AdS_5$, the bulk dual to the free Maxwell $CFT_4$. All the operators with scaling dimension $\Delta > 4$ in this OPE are higher-spin conserved currents (there is both a family of symmetric traceless tensors and a family of mixed-symmetry ones), and in addition there is the identity operator and a few operators of scaling dimension $\Delta = 4$: the scalar operators $F^2$ and $F\tilde{F}$, the stress tensor $T_{\mu\nu} = (\frac{1}{g^2} F_{\mu\rho} F_\nu{}^\rho - \text{trace})$, and a non-conserved operator in the representation $(2,0) \oplus (0,2)$ of rotations, i.e. a tensor with four indices and the same symmetry and trace properties of a Weyl tensor, for this reason we will denote it as $W_{\mu\nu\rho\sigma}$. The three-point function in the bulk OPE channel is written as a sum of the bulk-boundary two-point functions between

these operators and the displacement operator. Let us analyze which of these two-point functions can contribute. First of all, it is easy to see that two-point function between the conserved higher-spin currents and the displacement operator must vanish. This is an instance of the more general statement that in boundary CFTs bulk conserved currents $J$ can only have non-zero two-point functions with a scalar boundary operator $\hat{O}$ that has the same scaling dimension. The latter statement can be easily proved by placing the boundary operator at infinity, because in this case invariance under scaling and parallel translations force the two-point function to take the schematic form

$$\langle J(y,\vec{x})\hat{O}(\infty)\rangle = b_{J\hat{O}}\frac{1}{y^{\Delta_J-\Delta_{\hat{O}}}}\ (\text{structure})\ , \tag{E.45}$$

where "structure" denotes an appropriate tensor built out of the $\delta^{\mu\nu}$, the unit normal vector $n^\mu$ and possibly epsilon tensors. Clearly when $\Delta_J \neq \Delta_{\hat{O}}$ this two-point function cannot be compatible with current conservation unless the coefficient $b_{J\hat{O}}$ vanishes. Moreover, rotational invariance (6.77) implies that also the operator $W_{\mu\nu\rho\sigma}$ has vanishing two-point function with the displacement.[1] Therefore, the only bulk operators that can contribute to the three-point function are the scalar operators and the stress-tensor. When the displacement is placed at infinity, the corresponding two-point functions are

$$\langle F^2(x)\hat{D}(\infty)\rangle = b_{F^2,\hat{D}}\ , \tag{E.47}$$

$$\langle F\tilde{F}(x)\hat{D}(\infty)\rangle = b_{F\tilde{F},\hat{D}}\ , \tag{E.48}$$

$$\langle T_{\mu\nu}(x)\hat{D}(\infty)\rangle = b_{T,\hat{D}}\left(\delta_{\mu y}\delta_{\nu y}-\frac{1}{4}\delta_{\mu\nu}\right)\ . \tag{E.49}$$

Using the OPE (6.76) and the Ward identity (6.77) we can express the above two-point function coefficients in terms of the one-point function of the scalar operators, and of the

[1] To see this, consider the projector on the $(2,0)$ representation

$$(P^{(2,0)})_{\mu\nu\rho\sigma}^{\ \ \mu'\nu'\rho'\sigma'} \equiv \frac{1}{2}P^{+\ \mu'\nu'}_{\mu\nu}P^{+\ \rho'\sigma'}_{\rho\sigma}+\frac{1}{2}P^{+\ \mu'\nu'}_{\rho\sigma}P^{+\ \rho'\sigma'}_{\mu\nu}-\frac{1}{3}P^{+}_{\mu\nu,\rho\sigma}P^{+\,\mu'\nu',\rho'\sigma'}\ . \tag{E.46}$$

Since the two-point function between $W_{\mu\nu\rho\sigma}(x)$ and $\hat{D}(\infty)$ is a constant, the allowed structures are obtained by acting with this projector on constant four-tensors built out of $\delta$ and $\epsilon$, such as: $\delta_{\mu'\rho'}\delta_{\nu'\sigma'}$, $\delta_{\mu'\rho'}\delta_{\nu'y}\delta_{\sigma'y}$, $\epsilon_{\mu'\nu'\rho'\sigma'}$, $\epsilon_{\mu'\nu'\rho'y}\delta_{\sigma'y}$. Applying the projector to any of these structures we find 0.

coefficient $C_{\hat{D}}$ in the two-point function of the displacement, namely [169, 232, 233]

$$b_{F^2,\hat{D}} = -\frac{32 a_{F^2}}{\pi^2} \ , \tag{E.50}$$

$$b_{F\tilde{F},\hat{D}} = -\frac{32 a_{F\tilde{F}}}{\pi^2} \ , \tag{E.51}$$

$$b_{T,\hat{D}} = \frac{4\, C_{\hat{D}}}{3} \ . \tag{E.52}$$

Since the two-point functions are constant, we can simply plug in the three-point function the leading bulk OPE, ignoring the descendants (and also ignoring the singular contribution from the identity that drops from the three-point function)

$$F_{\mu\nu}(x) F^{\rho\sigma}(0) \underset{x\to 0}{\sim} \frac{1}{12}(\delta^\rho_\mu \delta^\sigma_\nu - \delta^\rho_\nu \delta^\sigma_\mu) F^2(0) + \frac{1}{12}\epsilon^{\rho\sigma}_{\mu\nu} F\tilde{F}\,(0) + 2 g^2 \delta^{[\rho}_{[\mu} T^{\sigma]}_{\nu]}(0) \ . \tag{E.53}$$

Using eq.s (E.50)-(E.51) in the two-point functions, we find

$$\langle F_{ay}(x_1) F_{by}(x_2) \hat{D}(\infty)\rangle = -\left(\frac{8}{3\pi^2} a_{F^2} - \frac{g^2}{3} C_{\hat{D}}\right) \delta_{ab} \ , \tag{E.54}$$

$$\langle F_{ab}(x_1) F_{cd}(x_2) \hat{D}(\infty)\rangle = -\left(\frac{8}{3\pi^2} a_{F^2} + \frac{g^2}{3} C_{\hat{D}}\right) \epsilon_{abe}\epsilon_{cde} \ , \tag{E.55}$$

$$\langle F_{ay}(x_1) F_{bc}(x_2) \hat{D}(\infty)\rangle = -\frac{8}{3\pi^2} a_{F\tilde{F}}\ \epsilon_{abc} \ . \tag{E.56}$$

Finally, by comparing (E.54) with (E.42) we find (6.84).

## E.6 Dimension of the Boundary Pseudo Stress Tensor

In section 6.3 we mentioned that the conservation of the stress tensor of the 3d CFT is violated at $g \neq 0$ due to multiplet recombination. At $g \neq 0$ we will call this operator boundary pseudo stress tensor. This is expected from the Ward identities derived in [233]. In this Appendix we exploit this idea, to reproduce the one loop result of (6.121). We start from the boundary Lagrangian of a 3d Dirac fermion $\psi$

$$\mathcal{L} = i\,\bar{\psi} \not{D}_A \psi, \tag{E.57}$$

where $D_a\psi = (\partial_a - iA_a)\psi$ and $D_a\bar{\psi} = (\partial_a + iA_a)\bar{\psi}$. The algebra of gamma matrices is $\{\gamma_a, \gamma_b\} = 2\delta_{ab}$. The pseudo boundary stress tensor is

$$(O_2)_{ab} = \frac{i}{2}[\bar{\psi}\gamma_{(a}D_{b)}\psi - D_{(a}\bar{\psi}\gamma_{b)}\psi], \tag{E.58}$$

where the symmetrization includes a factor of $1/2$. Note that the above operator is traceless as a consequence of the equations of motion:

$$\gamma^a D_a\psi = 0 \quad D_a\bar{\psi}\gamma^a = 0. \tag{E.59}$$

Using $[D_a, D_b]\psi = -iF_{ab}$ we obtain

$$\partial_a O_2^{ab} = F^{ab}\bar{\psi}\gamma_a\psi, \tag{E.60}$$

In the decoupling limit $g \to 0$ the two-point function of $F_{ab}$ vanishes, hence effectively the right-hand side of (E.60) is 0 and the operator $O_2^{ab}$ becomes a proper stress tensor for the boundary theory, with conformal dimension $\Delta_2 = 3$. Upon turning on $g$, this dimension must be lifted from the unitarity bound, i.e. $\Delta_2(g) = 3 + g^2\Delta_2^{(2)} + O(g^4)$. The two-point function of $O_2$ is fixed by 3d conformal invariance to be

$$\begin{aligned} \langle {O_2}^{ab}(\vec{x}){O_2}^{cd}(0)\rangle &= \frac{C_2(g)}{|\vec{x}|^{2\Delta_2(g)}} I^{ab,cd}(\vec{x}) \ , \\ I^{ab,cd}(\vec{x}) &= \frac{1}{2}[I^{3\,\mathrm{d}\,\mathrm{ac}}(\vec{x})I^{3\,\mathrm{d}\,\mathrm{bd}}(\vec{x}) + I^{3\,\mathrm{d}\,\mathrm{ad}}(\vec{x})I^{3\,\mathrm{d}\,\mathrm{bc}}(\vec{x})] - \frac{1}{3}\delta_{ab}\delta_{cd} \ , \end{aligned} \tag{E.61}$$

with $I^{3\,\mathrm{d}\,\mathrm{ac}}(\vec{x})$ defined in (6.42) and $C_2(g) = c_2^{(0)} + g^2 c_2^{(2)} + O(g^4)$, being $c_2^{(0)} = \frac{3}{16\pi^2}$ the central charge for a single free 3d Dirac fermion [234]. Furthermore the recombination rule (E.60) tells us

$$\langle \partial_a {O_2}^{ab}(\vec{x})\, \partial_c O_2^{cd}(0)\rangle = \langle (F^{ab}\bar{\psi}\gamma_a\psi)(\vec{x})(F^{cd}\bar{\psi}\gamma_c\psi)(0)\rangle. \tag{E.62}$$

On one hand, the r.h.s. of (E.62) can be computed at three level using (6.43) with the result

$$\langle (F^{ca}\bar{\psi}\gamma_c\psi)(\vec{x})(F^{db}\bar{\psi}\gamma_d\psi)(0)\rangle = \frac{4g^2 c_J^{(0)}}{\pi^2}\frac{I^{3\,\mathrm{d}\,\mathrm{ab}}(\vec{x})}{|\vec{x}|^8} + O(g^4), \tag{E.63}$$

where $c_J^{(0)} = \frac{1}{8\pi^2}$ is the central charge for the $U(1)$ conserved current $\hat{J}_a = \bar{\psi}\gamma_a\psi$ of a free 3d Dirac fermion [234].

On the other hand, taking two derivatives of (E.61) and expanding to the lowest non trivial order in $g$ gives

$$\langle \partial_c O_2{}^{ca}(\vec{x})\, \partial_d O_2{}^{db}(0)\rangle = \frac{10}{3} g^2 c_2^{(0)} \Delta_2^{(2)} \frac{I^{3\mathrm{d\,ab}}(\vec{x})}{|\vec{x}|^8} + O(g^4). \tag{E.64}$$

Hence the above result, together with (E.62) and (E.64) fixes the anomalous dimension of $O_2$ up to $O(g^4)$ terms to be

$$\Delta_2(g) = 3 + \frac{6}{5\pi^2}\frac{c_J^{(0)}}{c_2^{(0)}} g^2 + O(g^4) = 3 + \frac{4}{5\pi^2} g^2 + O(g^4), \tag{E.65}$$

in agreement with (6.121).

## E.7 Two-loop Integrals

In the perturbative calculations of anomalous dimensions we encountered two-loop diagrams with operator insertions at zero-momentum and two external legs. After performing tensor reduction to get rid of the numerators, the resulting integrals always take the form of a two-loop massless two-point integral, namely

$$\begin{aligned} G(n_1,n_2,n_3,n_4,n_5) &\equiv (4\pi)^d (k^2)^{n_1+n_2+n_3+n_4+n_5-d} \\ &\times \int \frac{d^dp}{(2\pi)^d}\frac{d^dq}{(2\pi)^d} \frac{1}{(p^2)^{n_1}(q^2)^{n_2}((k+p)^2)^{n_3}((k+q)^2)^{n_4}((p-q)^2)^{n_5}} \,. \end{aligned} \tag{E.66}$$

$k$ here is the external momentum associated to the two external legs, and $p$ and $q$ are the loop momenta. The powers $n_i$ depend on the diagram we are considering (and in fact each diagrams will give rise to a linear combination of $G$'s with several different sets of $n_i$'s after reducing the numerators). In order to extract the two-loop renormalization constants we need to find the $1/\epsilon^2$ and $1/\epsilon$ poles in the $\epsilon \to 0$ expansion of the constants $G(n_1,n_2,n_3,n_4,n_5)$, evaluated at $d = 3-2\epsilon$. (The coefficient of $1/\epsilon^2$ are fixed by one-loop data, so they do not contain new information.)

The function $G(n_1,n_2,n_3,n_4,n_5)$ enjoys a large group of symmetries [235] that allows to relate its values at different sets of quintuples of powers. Some of the symmetries are manifest from the definition, e.g. $G(n_1,n_2,n_3,n_4,n_5) = G(n_2,n_1,n_4,n_3,n_5) = G(n_3,n_4,n_1,n_2,n_5) = G(n_4,n_3,n_2,n_1,n_5)$. When one or more of the $n_i$'s vanish, there is a closed expression for $G(n_1,n_2,n_3,n_4,n_5)$ in terms of gamma functions. When all of the $n_i$'s

are integer, the strategy to compute $G(n_1, n_2, n_3, n_4, n_5)$ is to use integration-by-parts identities [236, 237] to lower the positive $n_i$'s, until the result is reduced to a linear combination of $G$'s with at least one vanishing entry. However, due to the $1/|p|$ "non-local" propagator of the photon restricted to the boundary, in our setup we encounter diagrams in which two of the $n_i$'s are half-integer, and the remaining three are integer.[2] In this case it might be impossible to reduce to the case of a vanishing power using integration-by-parts, and a further input is needed. The paper [238] derived a closed formula for $G(n_1, n_2, n_3, 1, 1)$ (and symmetry-related cases), with generic real $n_1, n_2, n_3$, in terms of the generalized hypergeometric function ${}_3F_2$. To recover the $1/\epsilon^2$ and $1/\epsilon$ poles from the result of [238], one needs to perform a Taylor expansion of the ${}_3F_2$ in its parameters. This is typically hard to do analytically, but the algorithm of [239] can be used to expand numerically to very high precision.

The strategy that we used is then to reduce all of the integrals that we encountered to a small number of "master integrals" using integration-by-parts identities. These master integrals have the property that they can be evaluated with the formula in [238], and that using the numerical expansion we can easily recognize the values of the coefficients. To compute anomalous dimensions in the fermion theory of section 6.3 we used the following two master integrals

$$G(1, \tfrac{1}{2}, \tfrac{1}{2}, 1, 1) \underset{\epsilon\to 0}{\sim} \frac{0}{\epsilon^2} + \frac{0}{\epsilon} + \mathcal{O}(1) \ , \tag{E.67}$$

$$G(1, \tfrac{3}{2}, \tfrac{1}{2}, 1, 1) \underset{\epsilon\to 0}{\sim} \frac{0}{\epsilon^2} + \frac{4}{\pi\epsilon} + \mathcal{O}(1) \ . \tag{E.68}$$

We never needed the $1/\epsilon$ coefficient of the master integral in the second line, and the only case in which we needed its $1/\epsilon^2$ coefficient is in the check that the gauged current does not get any anomalous dimension. So all of our non-trivial results only depend on the master integral in the first line. In the scalar theory of section 6.4.2 we also encountered the integral $G(1, \frac{1}{2}, \frac{1}{2}, 1, 2)$, which we were not able to compute with this strategy.

We will now give the result that we found for the contribution of each diagram to the renormalization constants. We make reference to the labeling of the diagrams in figure 6.8. In the two-loop calculation we also need to consider the one-loop diagram with the insertions of one-loop counterterms for the vertex or for the internal fermion lines, and

[2] Specifically, this happens for the diagrams that compute the coefficient of $\frac{(\mathrm{Im}\tau)^2}{|\tau|^2}$ in the two-loop anomalous dimensions. The diagrams that compute the coefficient of $\frac{(\mathrm{Re}\tau)^2}{|\tau|^2}$ do have only integer powers, and in fact they are the same as the diagrams in large-$k$ perturbation theory of CS-matter theories that compute the leading corrections to parity-even observables.

we refer to this contribution as "c.t.". We denote $L \equiv \log(\pi\mu^2) - \gamma_E$ where $\gamma_E$ is the Euler constant and $\mu$ is the scale introduced by dimensional regularization. Locality of counterterms requires that the $L$-dependence must cancel from the coefficient of the $1/\epsilon$ pole when all the diagrams are summed up, but generically it will be present in single diagrams. The cancelation of the $L$-dependence (and also the cancelation of $\xi$ in the gauge-invariant quantities) in the sum of all the diagrams is a check of the calculation.

- Wavefunction renormalization of the fermion: denoting the external momentum running on the fermion line with $k$, all the diagrams are proportional to $\not{k}$, with coefficients

$$(a) = \frac{g^2}{1+\gamma^2}\frac{(2-3\xi)}{12\pi^2\epsilon} \ , \tag{E.69}$$

$$(b.1) = \frac{g^4}{(1+\gamma^2)^2}\left(\frac{(2-3\xi)^2}{288\pi^4\epsilon^2}(1+2\epsilon L) + \frac{63\xi^2-90\xi+32}{432\pi^4\epsilon} + \frac{\gamma^2}{96\pi^2\epsilon}\right) \ , \tag{E.70}$$

$$(b.2) = \frac{g^4}{(1+\gamma^2)^2}\left(-\frac{(2-3\xi)^2}{144\pi^4\epsilon^2}(1+2\epsilon L) - \frac{117\xi^2-168\xi+64}{432\pi^4\epsilon} - \frac{\gamma^2}{192\pi^2\epsilon}\right) \ , \tag{E.71}$$

$$(b.3) = -\frac{g^4}{(1+\gamma^2)^2}\frac{1-\gamma^2}{192\pi^2\epsilon} \ , \tag{E.72}$$

$$\text{c.t.} = \frac{g^4}{(1+\gamma^2)^2}\left(\frac{(2-3\xi)^2}{144\pi^4\epsilon^2}(1+\epsilon L) + \frac{54\xi^2-78\xi+28}{432\pi^4\epsilon}\right) \ . \tag{E.73}$$

  Requiring the divergence to cancel with $-\delta((Z_\psi)^2)\not{k}$, we obtain eq. (6.117).

- Anomalous dimension of $O_0$: summing over all possible insertions in the given topol-

ogy, the diagrams give

$$(a) = \frac{g^2}{1+\gamma^2}\frac{2+\xi}{4\pi^2\epsilon} \ , \tag{E.74}$$

$$(b.1) = \frac{g^4}{(\gamma^2+1)^2}\left(\frac{(2+\xi)(10-3\xi)}{96\pi^4\epsilon^2}(1+2\epsilon L) - \frac{27\xi^2-86\xi-232}{144\pi^4\epsilon} + \frac{\gamma^2}{32\pi^2\epsilon}\right) \ , \tag{E.75}$$

$$(b.2) = \frac{g^4}{(\gamma^2+1)^2}\left(-\frac{(2+\xi)(2-3\xi)}{48\pi^4\epsilon^2}(1+2\epsilon L) + \frac{63\xi^2+40\xi-112}{144\pi^4\epsilon} + \frac{3\gamma^2}{64\pi^2\epsilon}\right) \ , \tag{E.76}$$

$$(b.3) = -\frac{g^4}{(\gamma^2+1)^2}\frac{5-5\gamma^2}{64\pi^2\epsilon} \ , \tag{E.77}$$

$$\text{c.t.} = \frac{g^4}{(1+\gamma^2)^2}\left(-\frac{(2+\xi)^2}{16\pi^4\epsilon^2}(1+\epsilon L) - \frac{2\xi^2+7\xi+6}{8\pi^4\epsilon}\right) \ . \tag{E.78}$$

Requiring the divergence to cancel with $\delta((Z_\psi)^2 Z_0)$, we obtain eq. (6.118).

- Anomalous dimension of $O_2$: we sum over all possible insertions in the given topology. The diagrams are proportional to the tree-level insertion of $O_2$ (see fig. 6.7) with the

following coefficients

$$(a) = -\frac{g^2}{1+\gamma^2}\frac{34-15\xi}{60\pi^2\epsilon} \ , \tag{E.79}$$

$$(b.1) = \frac{g^4}{(1+\gamma^2)^2}\left(-\frac{225\xi^2-300\xi+4}{7200\pi^4\epsilon^2}(1+2\epsilon L) - \frac{5175\xi^2-12690\xi+4096}{54000\pi^4\epsilon} - \frac{\gamma^2}{240\pi^2\epsilon}\right) \ , \tag{E.80}$$

$$(b.2) = \frac{g^4}{(1+\gamma^2)^2}\left(\frac{45\xi^2-132\xi+116}{720\pi^4\epsilon^2}(1+2\epsilon L) + \frac{1305\xi^2-6432\xi+8416}{10800\pi^4\epsilon} - \frac{\gamma^2}{960\pi^2\epsilon}\right) \ , \tag{E.81}$$

$$(b.3) = \frac{g^4}{(1+\gamma^2)^2}\frac{29-5\gamma^2}{960\pi^2\epsilon} \ , \tag{E.82}$$

$$\text{c.t.} = \frac{g^4}{(1+\gamma^2)^2}\left(-\frac{(15\xi-34)^2}{3600\pi^4\epsilon^2}(1+\epsilon L) - \frac{675\xi^2-9735\xi+18598}{27000\pi^4\epsilon}\right) \ . \tag{E.83}$$

Requiring the divergence to cancel with $\delta((Z_\psi)^2 Z_2)$, we obtain eq. (6.119).